United States
Environmental Protection
Agency

Robert S. Kerr Environmental
Research Laboratory
Ada, OK 74820

EPA/600/2-90/002
January 1990

Research and Development

EPA

# A New Approach and Methodologies for Characterizing the Hydrogeologic Properties of Aquifers

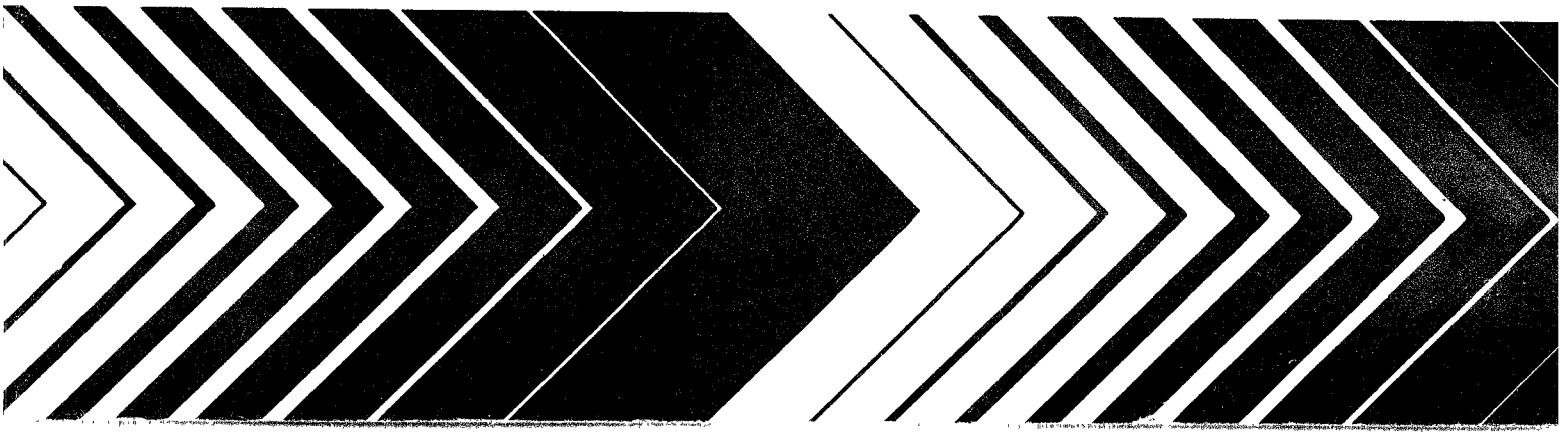

# A NEW APPROACH AND METHODOLOGIES FOR CHARACTERIZING THE HYDROGEOLOGIC PROPERTIES OF AQUIFERS

by

**FRED J. MOLZ; OKTAY GÜVEN; JOEL G. MELVILLE**
Civil Engineering Department
Auburn University, AL 36849

With Contributions By

**IRAJ JAVANDEL**
Earth Sciences Division
Lawrence Berkeley Laboratory
Berkeley, CA 94720

and

**ALFRED E. HESS; FREDERICK L. PAILLET**
United States Geological Survey
Denver Federal Center
Denver, CO 80225

CR-813647

Project Officer

**Lowell E. Leach**
Robert S. Kerr Environmental Research Laboratory
Ada, OK 74820

ROBERT S. KERR ENVIRONMENTAL RESEARCH LABORATORY
OFFICE OF RESEARCH AND DEVELOPMENT
U.S. ENVIRONMENTAL PROTECTION AGENCY
ADA, OK 74820

## DISCLAIMER

The information in this document has been funded wholly or in part by the United States Environmental Protection Agency under assistance agreement number CR-813647 to the Board of Trustees of Auburn University, Auburn, Alabama, subject to the Agency's peer and administrative review, and it has been approved for publication as an EPA document. Mention of trade names or commercial products does not constitute endorsement or recommendation for use.

# FOREWORD

EPA is charged by Congress to protect the Nation's land, air and water systems. Under a mandate of national environmental laws focused on air and water quality, solid waste management and the control of toxic substances, pesticides, noise and radiation, the Agency strives to formulate and implement actions which lead to a compatible balance between human activities and the ability of natural systems to support and nurture life.

The Robert S. Kerr Environmental Research Laboratory is the Agency's center of expertise for investigation of the soil and subsurface environment. Personnel at the laboratory are responsible for management of research programs to: (a) determine the fate, transport and transformation rates of pollutants in the soil, the unsaturated and the saturated zones of the subsurface environment; (b) define the processes to be used in characterizing the soil and subsurface environment as a receptor of pollutants; (c) develop techniques for predicting the effect of pollutants on ground water, soil, and indigenous organisms; and (d) define and demonstrate the applicability and limitations of using natural processes, indigenous to the soil and subsurface environment, for the protection of this resource.

This report presents techniques for field measurements of the vertical distribution of hydraulic conductivity in contaminated ground water at Superfund and other sites. These field techniques allow fully three-dimensional characterization of aquifer properties which can be used in advection-dominated transport models to significantly enhance our ability to understand and predict contaminant transport, reaction and degradation in the field.

Clinton W. Hall
Director
Robert S. Kerr Environmental
Research Laboratory

CONTENTS

# PREFACE

The decade of the eighties has seen the performance of several of the largest field hydrologic transport and dispersion experiments ever attempted. Included in this number are one or more studies performed at Base Borden, Ontario (University of Waterloo; Stanford University), Cape Cod, Massachusetts (U.S. Geological Survey; Massachusetts Institute of Technology), Chalk River, Ontario (Chalk River Nuclear Laboratories), Columbus, Mississippi (Tennessee Valley Authority; Massachusetts Institute of Technology), Mobile, Alabama (Auburn University), and Riverside, California (University of California at Riverside). Among other things, all of these experiments were able to gather three-dimensional information, on a relatively large scale, relating to parameters in the saturated zone or the unsaturated zone that control transport and dispersion.

It is the present authors' opinion that one of the more important conclusions supported by the studies mentioned above is that contaminant migration in both the saturated and unsaturated zones is commonly more of an advection-based than a hydrodynamic dispersion-based phenomenon. To understand what is going on in the subsurface, information is needed primarily about the hydraulic conductivity distribution not aquifer dispersivity. This is particularly true when one is attempting to understand or represent chemical and microbial processes that are sensitive to the degree of irreversible mixing that occurs among the components of a plume as it migrates downward or laterally away from its source. In aquifers, it is clearly not possible to represent these processes accurately in most situations with a model based on a two-dimensional (vertically-averaged) transmissivity field and large longitudinal and transverse dispersion coefficients. In the unsaturated zone, such processes are not represented well by a single downward flow velocity and a longitudinal dispersion coefficient, even when the downward flow is driven by a long-term, constant irrigation rate.

It is our conclusion that the overall results of the large field transport and dispersion experiments of the eighties, of which the present study is a member, have signaled an end to the brief era of the dispersion-dominated transport model and the resulting preoccupation of hydrologists with measurement, estimation, calibration, or otherwise divining a value for longitudinal dispersivity, whether based on deterministic or stochastic methodology. It appears likely that future models and regulations will increasingly be based on information about groundwater or soil water flow patterns, flow rates and flow distributions, that are measured directly or calculated based upon Darcy's law and a field-measured hydraulic conductivity distribution. It may be that another type of model will come into use in unsaturated zone problems because of the virtual impossibility of measuring accurate unsaturated hydraulic conductivity and water retention distributions in the field using technology that is presently available.

This report presents and summarizes most of the information and experience gained from six years of field experimental and theoretical studies by Auburn University that were funded by the U.S. Environmental Protection Agency through the Robert S. Kerr Laboratory. In one way or another, most of this work dealt with the understanding and measurement of hydraulic conductivity distributions in the field, with all measurements made in the saturated zone. However, the title of the present report, "A New Approach and Methodologies for Characterizing the Hydrogeologic Properties of Aquifers", implies more than the measurement of horizontal hydraulic conductivity as a function of vertical position in a granular aquifer. The additional information needed to make this report a more complete and useful document,

especially for individuals working in the field, was kindly supplied by colleagues at the Lawrence Berkeley Laboratory and the U.S. Geological Survey in Denver.

The report itself is divided into seven chapters, four appendices and a list of references. Chapter I, entitled "Why a New Approach is Needed", describes what the authors see as the basis for the next logical step to be taken in the quest for improved hydrogeologic property measurement in the field. An attempt is made also to place the needed changes within their proper historical context. The next three chapters entitled "The Borehole Flowmeter Method for Measuring Hydraulic Conductivity Distributions"; "Multi-Level Slug Tests for Measuring Hydraulic Conductivity Distributions"; and "Characterizing Flow Paths and Permeability Distributions in Fractured Rock Aquifers" are devoted to the better devices and techniques for measuring vertical distributions of horizontal hydraulic conductivity in both granular and fractured rock aquifers. These three chapters along with their two related and supporting appendices ("Overview and Evaluation of Methods for Determining the Distribution of Horizontal Hydraulic Conductivity in the Vertical Dimension", and "Analysis of Partially Penetrating Slug Tests Considering Radial and Vertical Flow and Anisotropy") form the core of this report. Most of the existing and emerging methodologies associated with our suggested new approach are described in these sections of the report.

The final three chapters, entitled "Measurement of Hydraulic Conductivity in the Vertical Direction", "Field Measurement of Effective Porosity, Storativity and Head", and "Mathematical Modeling of Advection-Dominated Transport in Aquifers", make the overall report more complete by defining and describing the measurement of related hydrogeologic properties, and how these properties may be incorporated in mathematical models of advection-dominated transport. Whenever applicable, we tried to remain consistent with the overall theme of measuring vertically distributed rather than vertically-averaged quantities.

For those individuals not comfortable with the concepts of hydrodynamic dispersion or for those wishing a review, we have included a third appendix entitled "The Physical Processes of Advection and Hydrodynamic Dispersion".

Most individuals attempting to deal with subsurface contamination problems in the field are well aware that more information is needed than that resulting from the measurement of hydrogeologic properties as they are defined herein. Measurement of chemical and biochemical subsurface properties, input from geologists, geophysicists, biologists and other scientists, measurement of subsurface geometry, and information concerning the interplay of field measurements and regulations are all important, but beyond the scope of this report. In order to compensate for this shortcoming, a national conference entitled "New Field Techniques for Quantifying the Physical and Chemical Properties of Heterogeneous Aquifers" was convened in Dallas, Texas on March 20-23, 1989. Similar to this report, the conference was motivated by the need to enhance field measurement capabilities if, as a nation, we are to solve the many site-specific problems being addressed by the Superfund and other programs. The meeting provided a much needed forum for professionals from government regulatory agencies, universities, and private industry to discuss, describe or display the best and most applicable techniques or equipment for measuring aquifer properties that have an important influence on contaminant migration. The conference featured a broad spectrum of invited and submitted papers and displays dealing with the most important topics facing ground water scientists, engineers and consultants in this field of inquiry. Approximately 50 papers were presented and the 883 page proceedings is available from the Water Resources Research Institute, 202 Hargis Hall, Auburn University, AL 36849 at a moderate cost. The proceedings is intended to serve as a broad-based supplement to this report, and the Table of Contents is included herein as Appendix IV.

Given the current level of understanding concerning contaminant migration in porous media, it was necessary for the authors of this report, and also for the participants in the aforementioned conference, to attempt to identify practical and useful measurement techniques and equipment while recognizing that we are working within a framework of basic understanding that is far from perfect. This is a classical example of a situation that requires innovative engineering solutions. Within this context, it is hoped that the work described in the present report will serve as part of the basis for the "next step" in field measurements that must be taken if we are to improve significantly our ability to characterize, evaluate and reclaim contaminated aquifers.

# ABSTRACT

In the authors' opinion, the ability of hydrologists to perform field measurements of aquifer hydraulic properties must be enhanced if we are to improve significantly our capacity to solve ground water contamination problems at Superfund and other sites. Therefore, the primary purpose of this report is to provide motivation and new methodology for measuring K(z), the distribution of horizontal hydraulic conductivity in the vertical direction in the vicinity of a test well. Measurements in nearby wells can then be used to build up three-dimensional distributions. For completeness, and to enhance the usefulness of this report as a field manual, existing methodology for the measurement of effective porosity, vertical hydraulic conductivity, storativity and hydraulic head, are presented also. It is argued that dispersion-dominated models, particularly two-dimensional, vertically-averaged (areal) models, have been pushed about as far as they can go, and that two-dimensional vertical profile or fully three-dimensional advection-dominated transport models are necessary if we are to increase significantly our ability to understand and predict contaminant transport, reaction, and degradation in the field. Such models require the measurement of hydraulic conductivity distributions, K(z), rather than vertically averaged values in the form of transmissivities.

Three devices for measuring K(z) distributions (the impeller flowmeter, the heat-pulse flowmeter, and a multi-level slug test apparatus) are described in detail, along with application and data reduction procedures. Results of the various methods are compared with each other and with the results of tracer studies performed previously. The flowmeter approach emerged as the best candidate for routine K(z) measurements. Impeller meters are now available commercially, and the more sensitive flowmeters (heat pulse and electromagnetic) are expected to be available in the near future.

Three-dimensional transport models tend to be advection-dominated rather than dispersion-dominated, and most of the standard finite-difference and finite-element algorithms produce excessive amounts of numerical dispersion when applied to advection-dominated models. Therefore this report closes by providing an introductory review of some newer numerical methods that by tracking the flow produce a minimum of numerical dispersion.

FIGURES

# TABLES

# LIST OF ABBREVIATIONS AND SYMBOLS

## Abbreviations

| | |
|---|---|
| Br | Bromide |
| CPM | counts per minute |
| EFLOW | computer code name |
| ELM | Eulerian-Lagrangian Methods |
| EPA | Environmental Protection Agency |
| IGWMC | International Ground Water Modeling Center |
| NWWA | National Water Well Association |
| OTA | Office of Technology Assessment |
| SWADM | Single Well Advection-Dispersion Model |
| TWAM | Two-Well Advection Model |
| USGS | United States Geological Survey |

## Symbols (Chapters 1, 2, 3, 4, 7, and appendices)*

| | |
|---|---|
| A | screen area per unit length, (L) |
| $A_c$ | open cross-sectional area of casing, ($L^2$) |
| B | slope of semi-log plot, ($T^{-1}$) |
| B,b | aquifer thickness, (L) |
| C | solute concentration, ($M/L^3$) |
| $C_o$ | Courant number, (-) |
| D | aquifer thickness, (L) |
| $\underline{\underline{D}}$ | dispersivity matrix, ($L^2/T$) |
| $D_d$ | molecular diffusion coefficient, ($L^2/T$) |
| $D_m$ | mechanical dispersion coefficient, ($L^2/T$) |
| $D_{ss}$ | longitudinal component of dispersion matrix, ($L^2/T$) |
| H | distance from confining layer to straddle packer, (L) |
| h | hydraulic head, (L) |
| $h_o$ | initial head, (L) |
| i | counting index, (-) |
| K | hydraulic conductivity, (L/T) |
| $K_r$ | hydraulic conductivity in radial direction, (L/T) |
| $K_z$ | hydraulic conductivity in vertical direction, (L/T) |
| $\underline{\underline{K}}$ | hydraulic conductivity matrix, (L/T) |
| $\overline{K}$ | vertically-averaged hydraulic conductivity, (L/T) |
| L | length, (L) |
| $O_{18}/O_{16}$ | Oxygen-18/Oxygen-16 isotope ratio, (-) |
| P | dimensionless flow parameter, (-) |
| $P_e$ | Peclet number, (-) |
| Q | discharge rate, ($L^3/T$) |
| QP | pumping rate, ($L^3/T$) |
| q | Darcy velocity, (L/T) |

---

* Generalized symbols for the dimensions of length, time and mass will be L, T, and M respectively. The symbol (-) indicates a dimensionless quantity.

| | |
|---|---|
| $r$ | radius, (L) |
| $r_c$ | casing radius, (L) |
| $R_e$ | radius of influence, (L) |
| $R_f$ | retardation factor, (-) |
| $r_p$ | plunger radius, (L) |
| $r_w$ | well radius, (L) |
| $S$ | storage coefficient, (-) |
| $S_i$ | volumetric sink of water, ($L^3/L^3/T$) |
| $S_o$ | volumetric source of water, ($L^3/L^3/T$) |
| $S_s$ | specific storage, ($L^{-1}$) |
| $T$ | transmissivity, ($L^2/T$) |
| $t$ | time, (T) |
| $U$ | Darcy velocity, (L/T) |
| $\underline{V}$ | pore or seepage velocity vector, (L/T) |
| $\overline{V}_r$ | radial seepage velocity, (L/T) |
| $x,y$ | horizontal coordinates, (L) |
| $y(t)$ | head change in slug test, (L) |
| $y_o$ | initial head change, (L) |
| $Z,z$ | vertical coordinates, (L) |
| $\alpha$ | type curve parameter for slug test, (-) |
| $\alpha_r$ | radial dispersivity, ($L^{-1}$) |
| $\alpha_v$ | vertical dispersivity, ($L^{-1}$) |
| $\Delta$ | prefix symbol indicating "change in", (-) |
| $\nabla$ | gradient operator, (-) |
| $\pi$ | 3.14159, (-) |
| $\theta$ | porosity, (-) |

Symbols (Chapters 5 and 6)

| | |
|---|---|
| $a$ | half the distance between recharge and discharge walls in the tracer test, (L) |
| $B$ | leakage factor, (L) |
| $b,b'$ | thickness of an aquifer and aquitard, respectively, (L) |
| $C$ | concentration of the tracer, ($ML^{-3}$) |
| $C_o$ | input concentration of the tracer, ($ML^{-3}$) |
| $c_w$ | compressibility of water, ($LT^2M^{-1}$) |
| $D_m$ | dispersion constant or dispersivity, (L) |
| $-Ei(-u)$ | well function, (-) |
| $E_w$ | bulk modulus of elasticity of water, ($ML^{-1}T^{-2}$) |
| $erfc(x)$ | complementary error function, (-) |
| $\vec{g}$ | acceleration of gravity vector, ($LT^{-2}$) |
| $h$ | hydraulic head, (L) |
| $K,K'$ | hydraulic conductivities of an aquifer and aquitard, respectively, ($LT^{-1}$) |
| $K_r,K_z$ | components of hydraulic conductivity in radial and vertical directions, respectively, ($LT^{-1}$) |
| $k$ | intrinsic permeability, ($L^2$) |
| $l$ | depth of penetration, (L) |
| $M,M'$ | thickness of an aquifer and aquitard, respectively, (L) |
| $P$ | Peclet number, (-) |
| $P_D$ | dimensionless pressure, (-) |

| | |
|---|---|
| $Q$ | rate of pumping, $(L^3T^{-1})$ |
| $q$ | pumping rate per unit aquifer thickness, $(L^2T^{-1})$ |
| $r$ | radial distance from a pumping well, (L) |
| $r_s$ | radius of well in the tested interval, (L) |
| $S,S'$ | storage coefficient of an aquifer and aquitard, respectively, (-) |
| $S_s,S'_s$ | specific storage of an aquifer and aquitard respectively, $(L^{-1})$ |
| $s,s'$ | drawdowns in an aquifer and aquitard, respectively, (L) |
| $s_D$ | dimensionless drawdown, (-) |
| $T$ | time for a water particle to travel along a particular streamline between two wells, (T) |
| $t$ | time, (T) |
| $t_D$ | dimensionless time, (-) |
| $\vec{V}$ | vector of apparent or Darcy's velocity, $(LT^{-1})$ |
| $V_f$ | sonic wave velocity of fluid filling the pores, $(LT^{-1})$ |
| $W(u,r/B)$ | well function of leaky aquifers, (-) |
| $x,y,z$ | coordinate system, (L) |
| $\alpha$ | effective porosity, (-) |
| $\gamma$ | specific weight of water, $(ML^{-2}T^{-2})$ |
| $\Phi$ | hydraulic potential, $(L^2T^{-2})$ |
| $\phi$ | porosity, (-) |
| $\rho$ | density of fluid, $(ML^{-3})$ |
| $\rho_b$ | bulk density, $(ML^{-3})$ |
| $\nabla$ | gradient operator, $(L^{-1})$ |
| $\mu$ | dynamic viscosity, $(ML^{-2}T^{-1})$ |
| $\psi$ | stream function, (-) |

## ACKNOWLEDGEMENTS

This work was supported in part by the U.S. Environmental Protection Agency (contract CR813647) through the Robert S. Kerr Environmental Research Laboratory. At Auburn University, the project was administered by the Water Resources Research Institute (Joseph F. Judkins, Director). The authors would like to acknowledge gratefully the support of both institutions. Thanks are due also to the U.S. Geological Survey and the Lawrence Berkeley Laboratory for indirect support.

The Alabama Power Company made their land available for the field experiments performed by Auburn University and along with Southern Company Services, provided well drilling services and materials free of charge. This help had a major positive impact on the outcome of the project and is acknowledged with thanks.

Many individuals whose names do not appear on this report made valuable contributions over the past four years. Those that come immediately to mind are Roger Morin of the USGS Denver Federal Center for providing his help and expertise with early impeller meter measurements, Ken Taylor and Joel Hayworth from the University of Nevada Desert Research Institute for help with various geophysical methods, Post-Doctoral Fellow Mark Widdowson of Auburn University (now an Assistant Professor at the University of South Carolina) for his work on the analysis of multi-level slug tests, AU Field Engineers Clay Cardone and Jerry Bowman for field work of various types, Daniel Ronen and Mordekai Magaritz of the Weizman Institute, Rehovot, Israel for performing and analyzing the dialysis cell experiments for measuring Darcy velocity, Lowell Leach of the R. S. Kerr Laboratory, U.S. Environmental Protection Agency, for help and encouragement throughout the project, and last but not least, AU Technical Secretary Kathy Seibel for her tireless typing of so many documents including this report.

# EXECUTIVE SUMMARY

## Introduction

The present writers are of the opinion that field measurement capability must increase if we are to improve significantly our ability to handle ground water contamination problems associated with Superfund and other sites. To this end, the single most important parameter concerning contaminant migration is the hydraulic conductivity distribution. If one can not predict where the water goes, how can one expect to predict the movement of a contaminant that is carried by the water? Most conventional flow analyses are based on fully-penetrating pumping tests to get a transmissivity field and large longitudinal dispersion coefficients to account for contaminant spreading in the direction of flow. We call such models dispersion-dominated. In the authors' opinion, the time has arrived to develop and apply aquifer tests for determining the horizontal hydraulic conductivity as a function of vertical position (K(z)) within a well or borehole. When this is done at a number of locations in the horizontal plane, the resulting data can serve as a basis for developing two-dimensional vertical cross-section, quasi three-dimensional or fully three-dimensional flow and transport models that do not require large, scale-dependent, dispersion coefficients.

Shown in Figure I-6 are dimensionless K(z) distributions obtained at four different scales of measurement in a single well using an impeller meter (Hufschmied, 1983; Morin et al., 1988a; Rehfeldt et al., 1988; Molz et al., 1989a). It is apparent that as the measurement interval varies from 10 ft (3.05 m) to 1 ft (0.305 m), the apparent variability of the hydraulic conductivity increases. This is the type of information that is lost when fully-penetrating pumping tests are used to obtain vertically-averaged hydraulic conductivities.

There are several techniques for making vertically-distributed measurements, including tracer tests, flowmeter tests, dilution tests and multi-level slug tests, that are described in this report. Such measurements should serve as the basis for an improved understanding and conceptualization of subsurface transport pathways, and may also allow the application of a new generation of contaminant transport models that are advection-dominated and largely free of the problems associated with large, scale-dependent, dispersion coefficients. All of this taken together constitutes what the authors are advocating as the new approach to characterizing the hydrogeologic properties of aquifers.

## Selected Methodology

After studying a number of methodologies for measuring K(z) distributions, two techniques, the flowmeter method and the multi-level slug test, emerged as the most practical methodologies for obtaining K(z) information, and were, therefore, studied in detail. Of the two, the flowmeter was more responsive, less sensitive to near-well disturbances due to drilling, and easier to apply. As illustrated in Figure II-2, a flowmeter test may be viewed as a natural generalization of a standard fully penetrating pumping test. In the latter application, only the steady pumping rate, QP, is measured, whereas the flow rate distribution along the borehole or well screen, Q(z), as well as QP is recorded during a flowmeter test.

Various types of flowmeters based on heat pulse or impeller technology have been devised for measuring Q(z), and a few groundwater applications have been described in the literature (Hada, 1977; Keys and Sullivan, 1978; Schimschal, 1981; Hufschmied, 1983; Hess, 1986; Morin et al., 1988a; Rehfeldt et al., 1988; Molz et al., 1989a,b). The most low-flow-sensitive types of meters are based on heat-pulse, electromagnetic, or tracer-release technology

(Keys and MacCary, 1971; Hess, 1986), but to the authors' knowledge such instruments are not presently available commercially, although several are nearing commercial availability. Impeller meters (commonly called spinners) have been used for several decades in the petroleum industry, and a few such instruments suitable for groundwater applications are now available for purchase (Further information available upon request). A meter of this type was applied at the Mobile site to produce the kind of hydraulic conductivity data shown in Figure I-6.

Impeller Meter Tests

Once the necessary equipment is obtained, impeller meter tests can be a relatively quick and convenient method for obtaining information about the vertical variation of horizontal hydraulic conductivity in an aquifer. The idea and methodology behind the impeller meter test are illustrated in Figure II-2. One first runs a caliper log to ascertain that the screen diameter is known and constant. If it is not constant, the variations must be taken into account when calculating discharge. A small pump is placed in a well and operated at a constant flow rate, QP. After pseudo steady-state behavior is obtained, the flowmeter, which when calibrated measures vertical flow within the screen, is lowered to near the bottom of the well, and a measurement of discharge rate is obtained in terms of impeller-generated electrical pulses over a selected period of time. The meter is then raised a few feet, another reading taken, raised another few feet--and so on. As illustrated in the lower portion of Figure II-2, the result is a series of data points giving vertical discharge, Q, within the well screen as a function of vertical position z. Just above the top of the screen the meter reading should be equal to QP, the steady pumping rate that is measured independently on the surface with a water meter. The procedure may be repeated several times to ascertain that readings are stable.

While Figure II-2 applies explicitly to a confined aquifer, which was the type of aquifer studied at the Mobile site, application to an unconfined aquifer is similar. Most impeller meters are capable of measuring upward or downward flow, so if the selected pumping rate, QP, causes excessive drawdown, one can employ an injection procedure as an alternative. In either case, there will be unavoidable errors near the water table due to the deviation from horizontal flow. It is desirable in unconfined aquifers to keep QP as small as possible, consistent with the stall velocity of the meter. Thus more sensitive meters will have an advantage.

The basic analysis procedure for flowmeter data is quite straightforward. One assumes that the aquifer is composed of a series of n horizontal layers and takes the difference between two successive meter readings, which yields the net flow, $\Delta Q_i$, entering the screen segment between the elevations where the readings were taken, which is assumed to bound layer $i(i=1,2,...,n)$. One then employs the Cooper-Jacob (1946) formula for horizontal flow to a well or an alternative procedure to obtain K(z) values.

Heat-Pulse Flowmeter Tests

Application of impeller meter technology will be limited at many sites due to the presence of low permeability materials that will preclude the pumping of test wells at a rate sufficient to operate an impeller meter. Another type of flowmeter that is in the prototype stage, the heat-pulse flowmeter, can be used as an alternative to an impeller meter in virtually any application, and it has the advantage of greater sensitivity. Spinner flowmeters measure a minimum velocity ranging from about 3 to 10 ft/min (1 to 3 m/min), which limits their usefulness in many boreholes having slower water movement. Flow volumes of as much as 4 gal/min (15 L/min) may go undetected in a 4-in (10 cm) diameter borehole when flow is measured with a spinner flowmeter, and much larger volumes may go undetected in larger

diameter holes. Heat-pulse flowmeters are particularly useful for application to fractured rock aquifers where flows are often small and contaminant transport pathways difficult to visualize. Such meters may be used to located productive fracture zones and to characterize apparent hydraulic conductivity distributions.

The urgent need for a reliable, slow-velocity flowmeter prompted the U.S. Geological Survey to develop a small-diameter, sensitive, thermal flowmeter. This meter has interchangeable flow-sensors, 1.63 and 2.5 in. (4.1 and 6.4 cm) in diameters, and has flow sensitivity from 0.1 to 20 ft/min (0.03 to 6.1 m/min) in boreholes with diameters that range from 2 to 5 in. (5 to 12.5 cm). Vertical discharge in a borehole is measured with the thermal flowmeter by noting the time-of-travel of the heat pulse and determining water volume flow from calibration charts developed in the laboratory using a tube with a diameter similar to that of the borehole under investigation (Hess, 1986).

The basic measurement principle of the USGS meter is to create a thin horizontal disc of heated water within the well screen at a known time and a known distance from two thermocouple heat sensors, one above and one below the heating element. One then assumes that the heat moves with the upward or downward water flow and records the time required for the temperature peak to arrive at one of the heat sensors. The apparent velocity is then given by the known travel distance divided by the recorded travel time. Thermal buoyancy effects are eliminated by raising the water temperature by only a small fraction of a centigrade degree. The geometry associated with the flowmeter is shown in Figure IV-2.

The USGS heat-pulse meter has been applied to the granular aquifer at the Mobile site and several fracture flow systems. In the present report the authors describe applications to fractured dolomite in northeastern Illinois, fractured Gneiss in southeastern New York, and a granitic fracture zone on the Canadian shield in Manitoba. In these applications, supplemental information was obtained from acoustic-televiewer logs, temperature logs, and caliper logs. Information similar to that shown in Figure IV-8 was obtained. The case studies illustrate potential application of the thermal flowmeter in the interpretation of slow flow in fractured aquifers. The relative ease and simplicity of thermal-flowmeter measurements permits reconnaissance of naturally occurring flows priors to hydraulic testing, and identification of transient pumping effects, which may occur during logging. In making thermal flowmeter measurements, one needs to take advantage of those flows that occur under natural hydraulic-head conditions as well as the flows that are induced by pumping or injection. However, thermal-flowmeter measurements interfere with attempts to control borehole conditions during testing, because the flowmeter and wire-line prevent isolation of individual zones with packers. In spite of this limitation, the simplicity and rapidity of thermal-flowmeter measurements constitute a valuable means by which to eliminate many possible fracture interconnections and identify contaminant plume pathways during planning for much more time consuming packer and solute studies. The thermal flowmeter is especially useful at sites similar to the site in northeastern Illinois, where boreholes are intersected by permeable horizontal fractures or bedding planes. Under these conditions, naturally occurring hydraulic-head differences between individual fracture zones are decreased greatly by the presence of open boreholes at the study site. These hydraulic-head differences could only have been studied by the expensive and time consuming process of closing off all connections between fracture zones in all of the boreholes with packers. The simple and direct measurements of vertical flows being caused by these hydraulic-head differences obtained with the thermal flowmeter provided information pertaining to the relative size and vertical extent of naturally occurring hydraulic-head differences in a few hours of measurements. Additional improvement of the thermal-flowmeter/packer system and refinement of techniques for flowmeter interpretation may decrease greatly the time and effort

required to characterize fractured-rock aquifers by means of conventional hydraulic testing.

While the case studies described in the present report did not all involve contaminated groundwater, the potential application to plume migration problems and sampling well screen locating is obvious. The relationship of flowmeter measurements to more standard tests such as caliper and televiewer logs is indicated also. Hopefully, thermal flowmeters and other sensitive devices, such as the electromagnetic flowmeter being developed by the Tennessee Valley Authority, will be available commercially in the near future.

Multilevel Slug Tests

The flowmeter testing procedure is generally superior to the multilevel slug test approach, because the latter procedure depends on one's ability to isolate hydraulically a portion of the test aquifer using a straddle packer. However, if reasonable isolation can be achieved, which was the case at the Mobile test site, then the multi-level slug test is a viable procedure for measuring K(z). All equipment needed for such testing is available commercially, and the test procedure has the added advantage of not requiring any water to be injected into or withdrawn from the test well if a water displacement technique is used to cause a sudden head change.

The testing apparatus used in the applications reported herein is illustrated schematically in Figure III-1 for the aquifer geometry at the Mobile site. Two inflatable packers separated by a length of perforated, galvanized steel pipe comprised the straddle packer assembly. Aquifer test length defined by the straddle packer was L=3.63 ft (1.1 m). A larger packer, referred to as the reservoir packer, was attached to the straddle packer with 2" (2.54 cm) Triloc PVC pipe, creating a unit of fixed length of approximately 100 ft (30.5 m) which could be moved with the attached cable to desired positions in the well. When inflated, the straddle packer isolated the desired test region of the aquifer and the reservoir packer isolated a reservoir in the 6" (15.2 cm) casing above the multilevel slug test unit and below the potentiometric surface of the confined aquifer.

In a typical test, water was displaced in the reservoir above the packer. The head increase then induced a flow down through the central core of the reservoir packer and down the Triloc pipe to the straddle packer assembly. In the assembly, water flowed from the perforated pipe, through the slotted well screen, and into the test region of the aquifer.

The multilevel unit described was used for slug tests by inserting the plunger, displacing a volume of water in the reservoir and then recording the depth variation, y=y(t), relative to the initial potentiometric surface (falling head test). Plunger withdrawal was used to generate a rising head test. Head measurements were made with a manually operated digital recorder (Level Head model LH10, with a 10 psig pressure transducer, In Situ, Inc.).

Three methods of analysis have been applied to the collected slug test data. In the first and second methods, it is assumed that the flow from the test section is horizontal and radially symmetric about the axis of the well. In the first method the quasi-steady state assumption is made. In the second, a transient analysis is applied. In the third analysis, also quasi-steady state, the possibility of vertical flow and anisotropy are considered using curves generated by a finite element model.

Typical results of a series of tests at different elevations are shown for well E6 in Figure III-3. The data shown are from plunger insertion tests where a sudden reservoir depth increase to approximately $y_o$=3 ft was imposed. The depth variation, y=y(t), which is nearly an

exponential decay, is a result of flow into the aquifer test section adjacent to the straddle packer. The different slopes of the straight line approximations (least squares fits) are due to the variability of the hydraulic conductivity in the aquifer at the different test section elevations. Tests repeated at a given elevation were generally reproducible, with the maximum difference in slopes of the straight line fits to the data being less than 11%. From this data it is easy to calculate hydraulic conductivity distributions as described in the report.

Modeling of Advection-Dominated Flows

There are a variety of ways in which vertically-distributed hydraulic conductivity distributions can be used to understand and assess problems involving contaminated ground water. A significant amount of insight will be obtained simply by observing and discussing the implications of such information on patterns of contaminant migration. However, use of the vertically-distributed data in three-dimensional mathematical models will be a common procedure for developing quantitative assessments of a variety of possible activities such as evaluation of site remediation plans. Thus it is worthwhile to devote part of this report to a discussion of the relationship between vertically-distributed hydraulic conductivity data and mathematical modeling.

As pointed out previously, once one moves from the use of vertically-averaged aquifer properties in two-dimensional mathematical models to the use of vertically-distributed aquifer properties in three-dimensional models, the nature of the physical process represented by the model changes dramatically. In many situations, the model changes from one being largely dominated by dispersion (low Peclet number flows) to one largely dominated by advection (high Peclet number flows). Unfortunately, most of the standard finite-difference and finite-element algorithms for solving mathematical models do not work well when applied to advection-dominated flows, especially those that involve chemical or microbial reactions. The necessary evolution from dispersion-dominated to advection-dominated numerical algorithms for solving the flow and transport equations is far from trivial, so it is important to call attention to some of the newer numerical methods, particularly those that produce a minimum of numerical dispersion when used to solve the transport equation.

A complete numerical analysis of contaminant migration in the subsurface usually involves solution of the ground water flow equation and the transport (advection/dispersion) equation. The latter equation is the more complicated due primarily to the existence of the advective transport term which gives the transport equation a hyperbolic character and makes its solution subject to numerical dispersion. In general, the techniques for solving such an equation can be grouped into three classes; namely, Eulerian, Lagrangian, and Eulerian-Lagrangian methods. Eulerian methods are more suited to dispersion-dominated systems while Lagrangian methods are most suited to advection dominated systems. Eulerian-Lagrangian methods have been introduced to deal efficiently and accurately with situations in which both advection and dispersion are important.

The Eulerian methods are based on the discretization of the transport equation on a numerical solution grid that is fixed in space, and all of the terms of the equation, including the advective transport term, are discretized together and the resulting algebraic equations are solved simultaneously in one solution step. As discussed by Cady and Neuman (1987), while Eulerian methods are fairly straightforward and generally perform well when dispersion dominates the problem and the concentration distribution is relatively smooth, they are usually constrained to small local grid Peclet numbers.

Methods which are based on solutions of the transport equation on a moving grid, or

grids, defined by the advection field, or methods which do not rely on a direct solution of the Eulerian transport equation but which are based on an analysis of the transport, deformation and transformation of identified material volumes, surfaces, lines or particles by tracking their motion in the flow field are generally called Lagrangian methods (Cady and Neuman, 1987). In the present report, we reserve this term only for methods which are based on tracking alone and will consider the moving-grid methods which have been called Lagrangian before by some authors simply as special cases of the Eulerian-Lagrangian methods.

Reviews of Eulerian-Lagrangian methods (ELM) have also been presented recently by Cady and Neuman (1987). These methods combine the advantageous aspects of the Lagrangian and the Eulerian methods by treating the advective transport using a Lagrangian approach and the dispersive transport and chemical reactions using an Eulerian approach. According to how the advective transport is taken into account, these methods can be generally grouped into three classes; one class makes use of particle tracking and relates the concentration at a grid node to the solute mass associated with each particle and the particle density around that node, while the second class treats concentration directly as a primary variable throughout the calculations without resorting to the use of any particles, and the third class consists of models in which the first and second approaches are used together in an adaptive manner depending on the steepness of the concentration gradients.

It may be useful to point out that Eulerian-Lagrangian methods have been developed extensively for the numerical modeling of complex three-dimensional industrial and environmental flows and for the solution of various fluid mechanics problems particularly over the last decade (Orin and Boris, 1987). These methods are now becoming popular also in the area of subsurface contaminant migration modeling.

Availability of Computer Codes

Several well documented computer codes for three-dimensional flow and solute transport modeling as well as parameter identification and uncertainty analysis are available in the public domain. These codes have been developed by universities, various government agencies and government supported laboratories. There are also several proprietary codes developed by private consulting firms and research organizations such as the Electric Power Research Institute. Many of these codes have been listed in the recent monographs by Javandel et al. (1984) and van der Heijde et al. (1985). In this regard, the International Ground Water Modeling Center (IGWMC) serves as an information, education, and research center for groundwater modeling with offices in Indianapolis, Indiana (IGWMC, Holcomb Research Institute, Butler University, 4600 Sunset Avenue, Indianapolis, Indiana 46208) and Delft, the Netherlands. IGWMC operates as a clearinghouse for groundwater modeling codes and organizes an annual series of short courses on the use of various codes. Similar specialized short courses are also organized by various universities as well as professional organizations such as the National Water Well Association (NWWA, 6375 Riverside Dr., Dublin, Ohio 43017). The aforementioned references and organizations may be consulted for the availability of various modeling codes.

Supplemental Information

This report is devoted mainly to a presentation of the information and experience gained from six years of field experimental and theoretical studies by Auburn University that were funded by the U.S. Environmental Protection Agency through the Robert S. Kerr Laboratory. In one way or another, most of this work dealt with the understanding and measurement of

hydraulic conductivity distributions in the field, with all measurements made in the saturated zone. However, the title of the present report, "A New Approach and Methodologies for Characterizing the Hydrogeologic Properties of Aquifers", implies more than the measurement of horizontal hydraulic conductivity as a function of vertical position in a granular aquifer. The additional information, including methodology for measuring specific storage, porosity, hydraulic head, and hydraulic conductivity in the vertical direction, was kindly supplied by a colleague at the Lawrence Berkeley Laboratory and is included in the report in two separate chapters.

Most individuals attempting to deal with subsurface contamination problems in the field are well aware that more information is needed than that resulting from the measurement of hydrogeologic properties as they are defined herein. Measurement of chemical and biochemical subsurface properties, input from geologists, geophysicists, biologists and other scientists, measurement of subsurface geometry, and information concerning the interplay of field measurements and regulation are all important, but beyond the scope of this report. In order to compensate for this shortcoming, a national conference entitled "New Field Techniques for Quantifying the Physical and Chemical Properties of Heterogeneous Aquifers" was convened in Dallas, Texas on March 20-23, 1989. Similar to this report, the conference was motivated by the need to enhance field measurement capabilities if, as a nation, we are to solve the many site-specific problems being addressed by the Superfund and other programs. The meeting provided a much needed forum for professionals from government regulatory agencies, universities, and private industry to discuss, describe or display the best and most applicable techniques or equipment for measuring aquifer properties that have an important influence on contaminant migration. The conference featured a broad spectrum of invited and submitted papers and displays dealing with the most important topics facing ground water scientists, engineers and consultants in this field of inquiry. Approximately 50 papers were presented and the 883 page proceedings is available from the Water Resources Research Institute, 202 Hargis Hall, Auburn University, AL 36849 at a moderate cost. The proceedings is intended to serve as a broad-based supplement to this report.

Given the current level of understanding concerning contaminant migration in porous media, it was necessary for the authors of this report, and also for the participants in the aforementioned conference, to attempt to identify practical and useful measurement techniques and equipment while recognizing the fact that we are working within a framework of basic understanding that is far from perfect. This is a classical example of a situation that requires innovative engineering solutions. Within this context, it is hoped that the work described in the present report will serve as part of the basis for the "next step" in field measurements that must be taken if we are to improve significantly out ability to characterize, evaluate and reclaim contaminated aquifers.

# CHAPTER I

# WHY A NEW APPROACH IS NEEDED

## I-1 Introduction

In a recent evaluation of the Superfund program, the Office of Technology Assessment (OTA) asked the question "Are we cleaning up the mess or messing up the cleanup?" (U.S. Congress, OTA, 1988). Their study suggested that in a significant number of cases the reclamation technologies selected did not offer a permanent solution to the problem at hand. Many surface and subsurface natural processes contribute to the difficulty in selecting the best remediation report for each Superfund site, and no one technical paper can deal in depth with all of them. However, significant concern at many sites relates to the diverse problems caused by polluted groundwater. Groundwater is often the primary medium through which contaminants are transported off site. Uncertainties concerning how fast, how far, in what amounts and in what direction contaminants are expected to move can contribute greatly to potential remediation, liability and monitoring costs.

The OTA suggests several reasons for its perceived problems with the Superfund program including "too much flexibility, lack of central management control, and too much preoccupation with site uniqueness." However, the fact that many of the very best existing tools for evaluating groundwater contamination problems are not adequate for the problems at hand is not emphasized. If the necessary tools are simply not available, no amount of management wizardry will solve the problem.

It has never been easy and still is not easy to obtain good physical and chemical information about the subsurface. An immense amount of basic research will be necessary for years to come before our understanding approaches a satisfactory level. We have been relatively successful in the modeling/computational area, which has resulted computer models and other computational tools being developed far beyond our ability to measure the physical and chemical parameters upon which they are based. Thus, it is not easy for individuals working directly with Superfund problems to obtain the direct, specific and seemingly straightforward information that is needed. In many cases the techniques for obtaining such information either do not exist or are not developed sufficiently to be useful.

The present writers are of the opinion that field measurement capability must increase if we are to improve significantly our ability to handle groundwater problems associated with Superfund and other sites. Fortunately, it appears that such an increase is about to take place. Therefore, the purpose of this introductory chapter is to describe what we see as the basis for the next logical step to be taken in the quest for improved hydrogeological property measurement procedures. We also wish to place the motivation for this change within its proper historical context.

## I-2 What's Wrong With Existing Procedures?

Most hydrologists will agree that the single most important parameter concerning contaminant migration in groundwater is the hydraulic conductivity. If one can't predict where the water goes, how can one expect to predict the movement of a contaminant that is carried by the water? Recent studies have emphasized the importance of understanding the pattern of groundwater movement, because in most situations contaminant migration is advection

dominated (Molz et al., 1983; Osiensky et al., 1984; Fogg, 1986; Güven et al., 1986; Molz et al., 1986a, 1986b; Ronen et al., 1987a, 1987b; Güven and Molz, 1988; Molz and Widdowson, 1988; Molz et al., 1988; Lehr, 1988).

As illustrated in Figure I-1, the conventional field measurement of hydraulic conductivity is almost always based on some variant of a fully penetrating pumping test, which results in a vertically-averaged value for hydraulic conductivity ($\overline{K}$). This parameter is an excellent index to the water supply capability of an aquifer; certainly not surprising because the basics of subsurface hydrology were developed during the 20th century in response to water supply problems. Conceptual and computational tools based on vertically-averaged aquifer parameters, such as transmissivity and storativity, work well in water supply situations because no one cares where, from within an aquifer, the water comes. Everyone is happy as long as there is an abundant and dependable supply.

This is not the situation, however, when one is dealing with groundwater quality problems. In most situations, the essence of such problems is to determine from where the contaminated water came and where it is going. As illustrated in the paper by Osiensky et al. (1984) and also in Figure I-2, practically all natural aquifers are highly heterogeneous. On the scale of most contaminant plumes, there are usually irregular but non-random high hydraulic conductivity pathways along which contaminated water moves preferentially. Therefore, plumes often assume complicated shapes with certain portions moving more rapidly than other portions as illustrated schematically in Figure I-2. At least some understanding of this type of groundwater motion is required in order to determine where a contaminant is coming from and where it is going.

### I-2.1 First Attempt to Adapt Water "Quantity" Tools to Water "Quality" Problems.

Beginning about 25 years ago, the concern of various citizens and federal regulatory agencies began to include, to a greater and greater extent, groundwater quality problems. The natural "first effort" of groundwater hydrologists to deal with such problems was to adapt the existing water quantity tools to water quality problems. The most straightforward way to accomplish this was to neglect the vertical hydraulic structure of aquifers and assume that contaminants spread by a diffusion-like process called hydrodynamic dispersion. (For a definition and brief discussion of hydrodynamic dispersion see Appendix III.) This resulted in what was assumed to be a new aquifer property called full aquifer dispersivity. In principle, dispersivity was supposed to be a tensorial quantity, but as a practical matter subsurface hydrologists were satisfied to determine the principal longitudinal component which seemed to dominate the field dispersion process. The principal transverse component was then estimated as some fraction of the longitudinal component. Both components were assumed to apply over the full-aquifer thickness, so in principle fully penetrating pumping tests and tracer tests would be adequate to support the theory. The two-dimensional lateral-flow and transport models that most commonly resulted from these concepts were called areal dispersion or areal transport models.

To apply the areal dispersion models one would ideally determine the vertically-averaged hydraulic conductivity distribution $\overline{K}(x,y)$ ((x,y) = horizontal, principal Cartesian coordinates) using a series of fully penetrating pumping tests. Then the longitudinal and transverse components of full-aquifer dispersivity could be determined from fully-penetrating tracer tests. It was much more common, however, to use the principal dispersivity components as calibration parameters for fitting the overall concentration distribution coming out of the model to some measured distribution in the field. When areal dispersion models were

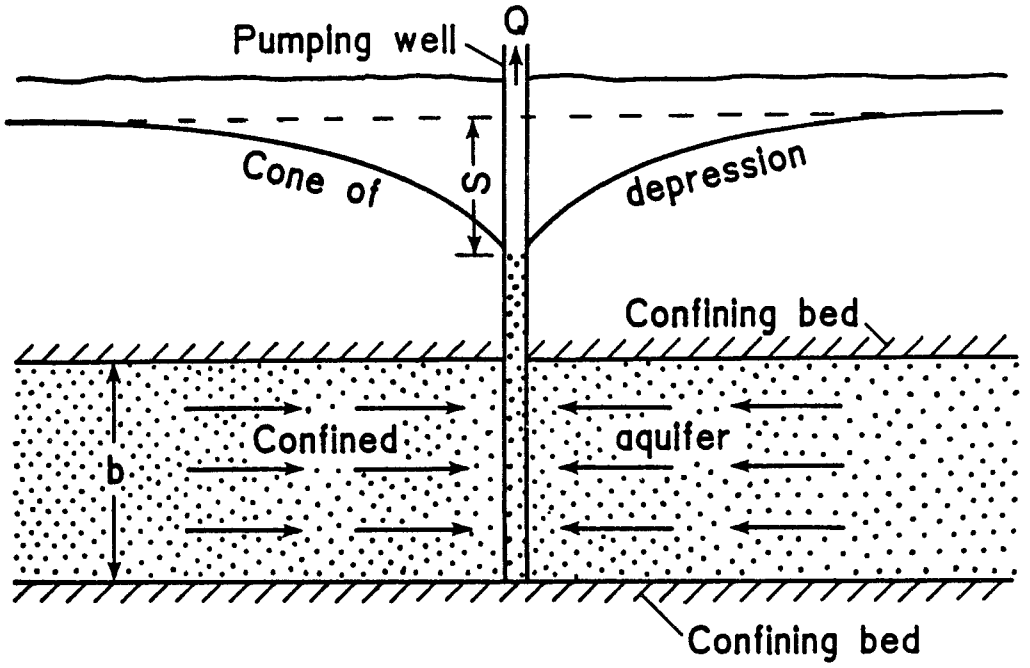


Figure I-1. Diagram illustrating the concept of a fully-penetrating pumping test to determine $\bar{K}$, the vertically-averaged hydraulic conductivity. Conventional pumping tests, however, do not use the pumping well as an observation well for measuring the drawdowns.

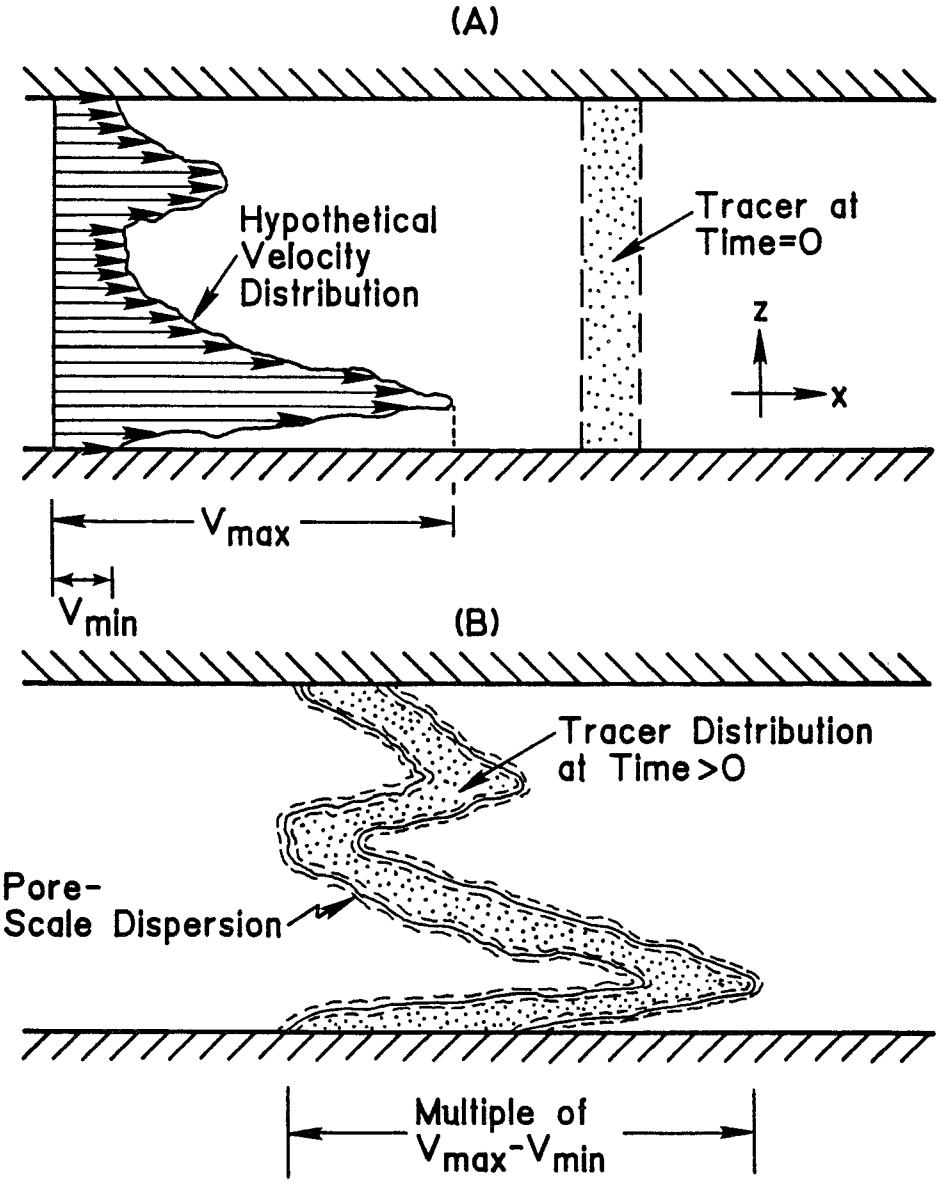


Figure I-2. Drawing providing a more realistic illustration of how water actually moves in an aquifer. Variation of horizontal groundwater velocity with vertical position is called differential advection. It is an example of a shearing type of flow or simply shear flow.

first developed, and for some time thereafter, this was reasonable because even fully penetrating pumping test data were scarce, and tracer tests are tedious, time consuming, expensive and therefore seldom performed.

Regardless of the manner in which dispersivity values were measured, calibrated, estimated, or otherwise divined, it gradually became apparent that something was seriously wrong. By the early seventies, various investigators were questioning the meaning of the huge longitudinal dispersivities that were resulting from field tracer tests and plume calibrations (Cherry et al., 1975; Anderson, 1979). It also became apparent that field-measured dispersivity values were scale-dependent (Robson, 1974; Anderson, 1979, 1984). This means that the value one obtains for longitudinal dispersivity will increase as the size of the experiment used to measure dispersivity is increased. Thus when one plots many values of longitudinal dispersivity versus the scales of the experiments or natural processes used to obtain those values, one produces a scatter diagram similar to that shown schematically in Figure I-3. (For plots of actual data see Anderson, 1984 and Gelhar, 1986.)

The controversy and confusion resulting from attempts to rationalize full aquifer dispersion, which still have not abated completely, led the EPA Kerr Laboratory to fund a combined experimental/theoretical study of contaminant dispersion in groundwater. The results of this study (Molz et al., 1983; Güven et al., 1984, 1985, 1986; Güven and Molz, 1986; Huyakorn et al., 1986; Molz et al., 1985, 1986a, 1986b, 1988) led to the following working conclusions relating to the concept of longitudinal dispersivity.

A. Local longitudinal hydrodynamic dispersion plays a relatively unimportant role in the transport of contaminants in most aquifers. As illustrated in Figure I-2, differential advection (shear flow) in the horizontal direction is much more important in determining the overall extent and structure of most contaminant plumes.

B. The concept of full-aquifer dispersivity used in vertically-averaged (areal) models will not be applicable over distances of interest in most contamination problems. If one has no choice but to apply a full-aquifer dispersion concept, the resulting dispersivity will not represent a physical property of the aquifer. Instead, it will be a scale-dependent quantity that will depend on the size and type of experiment used for its supposed measurement.

C. Because of conclusion B, it makes no sense to perform tracer tests or any other tests aimed at measuring full-aquifer dispersivity. If an areal model is used, the modeler will end up adjusting the dispersivity during the calibration process anyway, independent of the measured value.

Other theoretical studies and field experiments performed more recently support the above conclusions and indicate further that local dispersivities, especially transverse dispersivities, are very small in natural systems. (Moltyaner, 1987; Taylor and Howard, 1987, 1988; Güven and Molz, 1988; Molz and Widdowson, 1988; Moltyaner and Killey, 1988a,b).

One does not have to be trained technically in order to grasp the idea that full aquifer dispersion is a concept that has very limited physical meaning. One merely has to realize that the use of the concept in a stratified aquifer flow system is equivalent to attempting to represent a transport process analogous to that shown in Figure I-2 with a model having the inherent

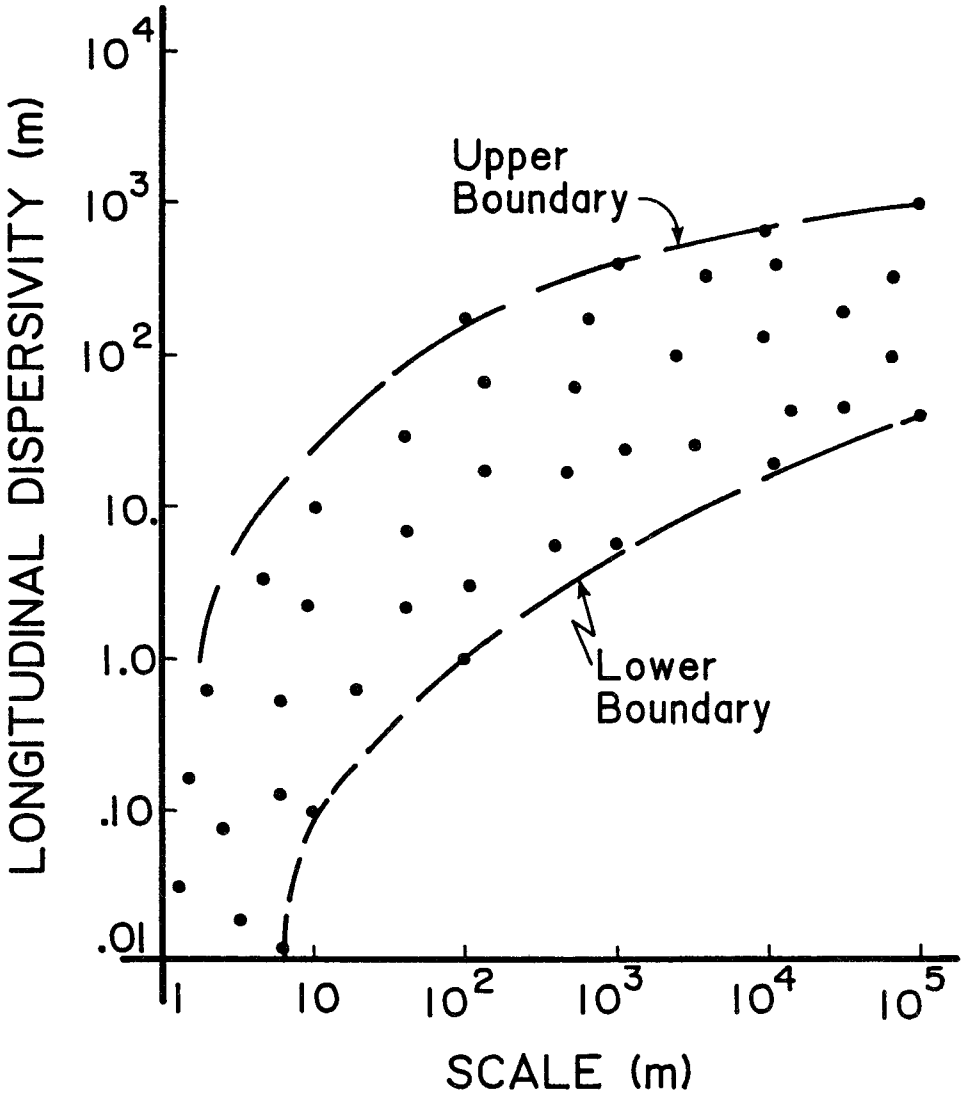


Figure I-3. Schematic plot showing what happens when one assumes that contaminants spread predominantly by a diffusion-like process called hydrodynamic dispersion and attempts to measure dispersivity. The dispersivity value depends on the size (scale) of the measurement process.

limitations illustrated in Figure I-4. Obviously, the horizontal velocity variations that are actually present will cause the plume to elongate dramatically in the horizontal direction. The larger the value of $V_{max}$ - $V_{min}$ the larger the degree of spreading at a given time. To assume, as the areal dispersion model does, that this spreading is proportional to the concentration gradients illustrated in Figure I-4 requires an increasing value for the constant of proportionality (dispersion coefficient) to make up for the decreasing value of the concentration gradients calculated by the vertically-averaged model.

## I-3 What's The New Approach?

In the authors' opinion, the time has arrived to develop and apply aquifer tests for determining the horizontal hydraulic conductivity as a function of vertical position (K(z)) within a well or borehole. When this is done at a number of locations in the horizontal plane, the resulting data can serve as a basis for developing two-dimensional vertical cross-section, quasi three-dimensional or fully three-dimensional flow and transport models that do not require large, scale-dependent dispersion coefficients. There are several methodologies for obtaining K(z) distributions, and a major purpose of this report is to describe the methodologies associated with the various field techniques, emphasizing those that are most promising. Shown in Figure I-5 are dimensionless K(z) distributions in three mutually perpendicular directions based on results of single-well tracer tests (Molz et al., 1988). These distributions show that K(z) varies with direction as well as with vertical position. Shown in Figure I-6 are dimensionless K(z) distributions obtained at five different scales of measurement in a single well using an impeller meter (Hufschmied, 1983; Morin et al., 1988a; Rehfeldt et al., 1988; Molz et al., 1989a). These differ from the tracer test results because at each measurement elevation, the K value is averaged over the $360^0$ polar angle, so that directional information is lost. It is apparent that as the measurement interval varies from 10 ft (3.05 m) to 1 ft (0.3 m), the apparent variability of the hydraulic conductivity increases, and there is every reason to expect that it would increase further if the measurement interval were decreased below 1 ft (0.3 m). This is the type of information that is lost when fully-penetrating pumping tests are used to obtain vertically-averaged hydraulic conductivities. Of course, it is unlikely that information as detailed as the 1 ft. data will be needed for practical purposes.

There are several techniques for making such measurements including tracer tests, impeller meter tests, dilution tests and multi-level slug tests that are described in this report. Such measurements should serve as the basis for an improved understanding and conceptualization of subsurface transport processes, and may also allow the application of a new generation of contaminant transport models that are advection-dominated and largely free of the problems associated with large, scale-dependent, dispersion coefficients. All of this taken together constitutes what the authors are advocating as the new approach to characterizing the hydrogeologic properties of aquifers.

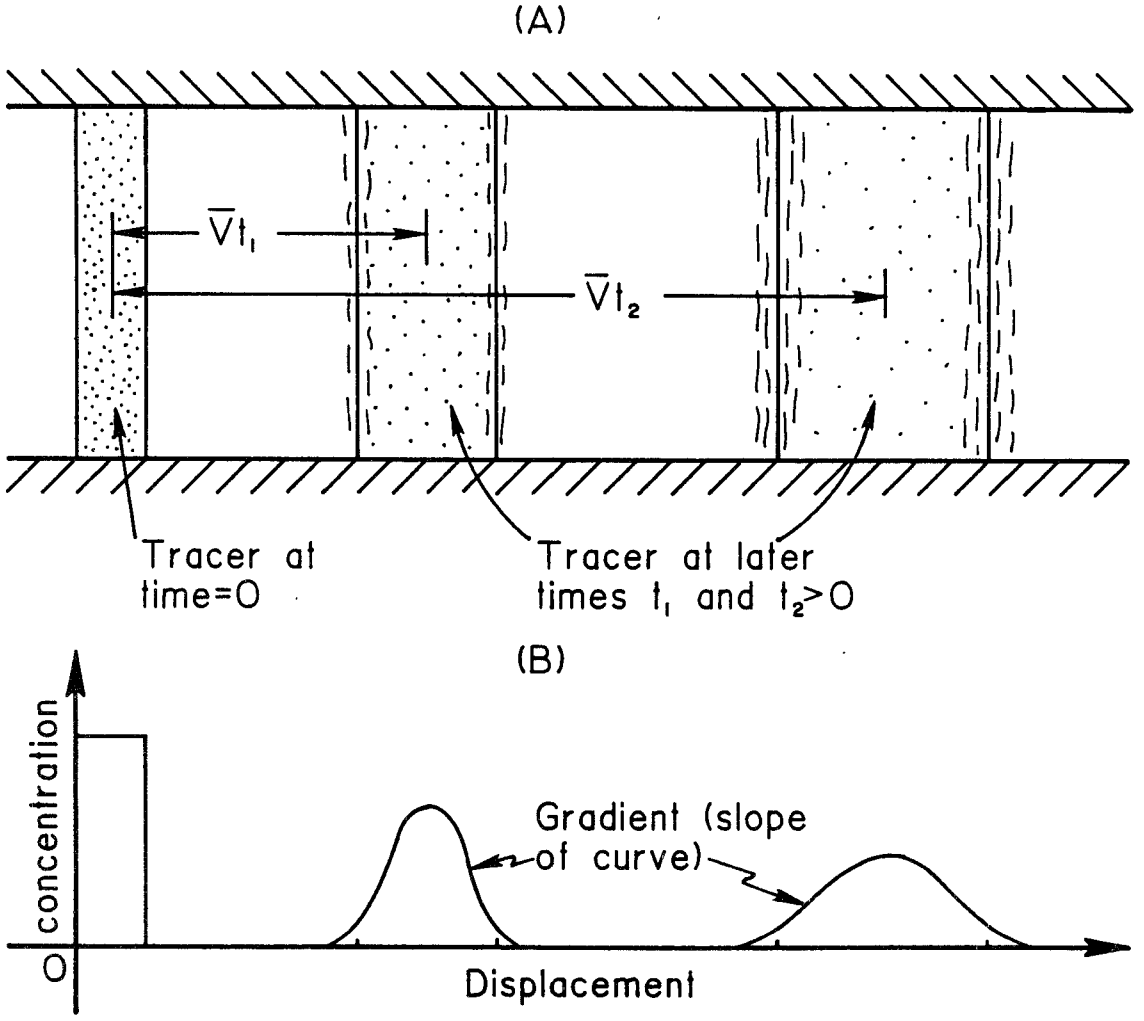


Figure I-4. Schematic diagram showing the inherent lack of vertical contaminant concentration structure that results from the solution of vertically-averaged transport models.

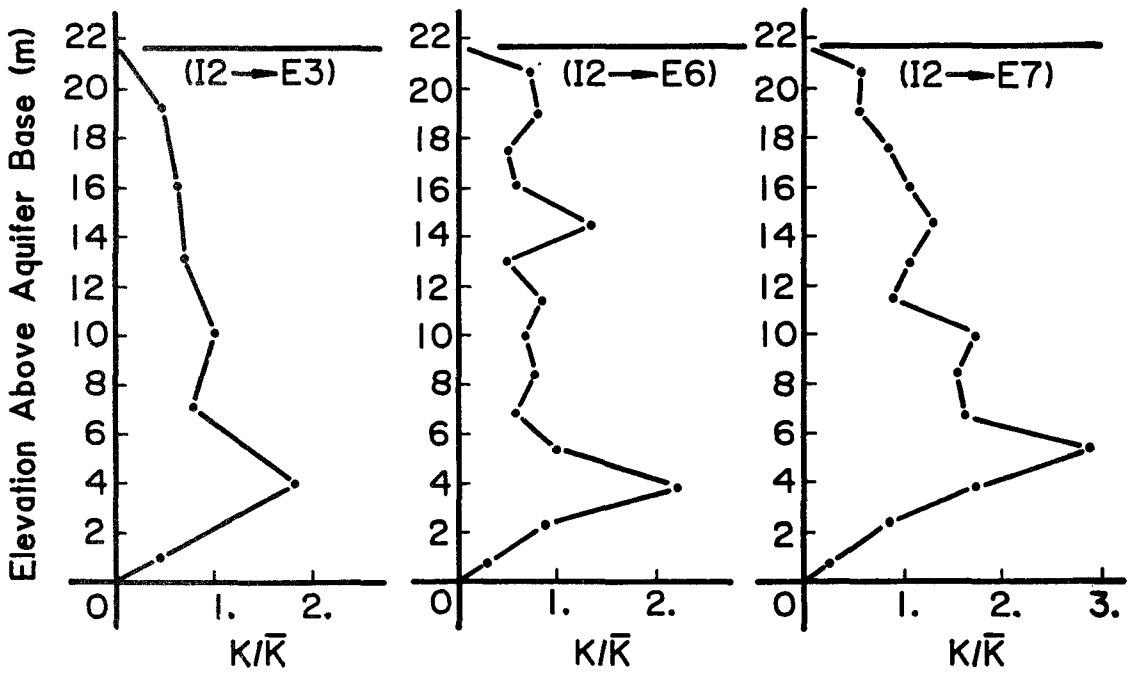


Figure I-5. Plots of dimensionless horizontal hydraulic conductivity versus elevation in three mutually perpendicular directions from well I2. The basic data were obtained from single-well tracer tests.

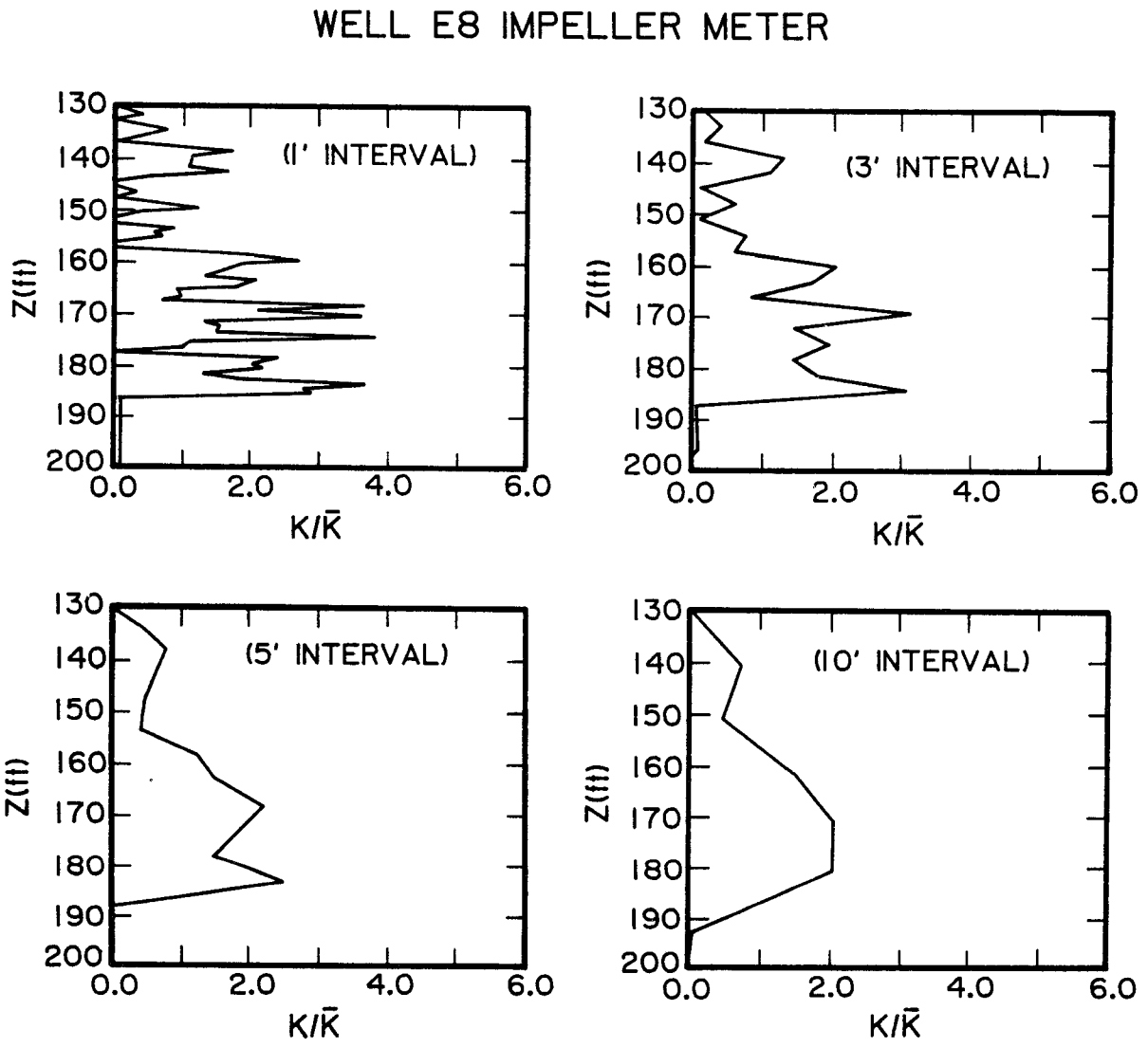


Figure I-6. Dimensionless horizontal hydraulic conductivity distributions based on impeller meter readings taken at the various measurement intervals indicated on the figure.

# CHAPTER II

# THE IMPELLER METER METHOD FOR MEASURING HYDRAULIC CONDUCTIVITY DISTRIBUTIONS

## II-1 Introduction

As outlined in Appendix I, one the best existing methodologies for obtaining vertically distributed hydraulic conductivity information is the borehole impeller meter test. Such a test may be viewed as a natural generalization of a standard fully penetrating pumping test. In the latter application, only the steady pumping rate, QP, is measured, whereas the flow rate distribution along the borehole or well screen, Q(z), as well as QP is recorded during an impeller meter test.

Various types of flowmeters based on heat-pulse or impeller technology have been devised for measuring Q(z), and a few groundwater applications have been described in the literature (Hada, 1977; Keys and Sullivan, 1978; Schimschal, 1981; Hufschmied, 1983; Hess, 1986; Morin et al., 1988a; Rehfeldt et al., 1988; Molz et al., 1989a,b). The most low-flow-sensitive types of meters are based on heat-pulse, electromagnetic or tracer-release technology (Keys and MacCary, 1971; Hess, 1986), but to the authors' knowledge such instruments are not presently available commercially, although several are nearing commercial availability. Impeller meters (commonly called spinners) have been used for several decades in the petroleum industry, and a few such instruments suitable for groundwater applications are now available for purchase (Further information available upon request.). A meter of this type was calibrated, applied, and the resulting data analyzed by Hufschmied (1983). A similar meter was applied in the field and analyzed further by Rehfeldt et al. (1988). This latter study is probably the most detailed to date regarding the analysis of assumptions one makes when using the borehole impeller meter to measure formation hydraulic conductivity as a function of vertical position.

The main purpose of this chapter is to describe the application of an impeller meter to measure K(z), at various locations in the horizontal plane, at a field site near Mobile, Alabama. Identical or similar methodology should be applicable at many sites. The project site is located in a soil borrow area at the Barry Steam Plant of the Alabama Power Company, about 32 km (20 mi) north of Mobile, Alabama. The surface zone is composed of a low-terrace formation of Quaternary age consisting of interbedded sands and clays deposited along the western edge of the Mobile River. These sand and clay deposits extend to a depth of approximately 61 m (200 ft) where the contact between the Tertiary and Quaternary deposits is located. The water table is about 3 m (9.84 ft) below the land surface. Below the contact, Miocene deposits are found that consist of undifferentiated sands, silty clays and thin-bedded limestones extending to an approximate depth of 305 m (1000 ft). The study formation is a sandy confined aquifer approximately 21.3 m (70 ft) thick which rests on the Tertiary-Quaternary contact as illustrated in Figure II-1.

## II-2 Performance and Analysis of Impeller Meter Tests

### II-2.1 Background Information

The idea and methodology behind the impeller meter test are illustrated in Figure II-2. One first runs a caliper log to ascertain that the screen diameter is known and constant. If it is not constant, the variations must be taken into account when calculating discharge. A small pump is placed in a well and operated at a constant flow rate; QP. After pseudo steady-state

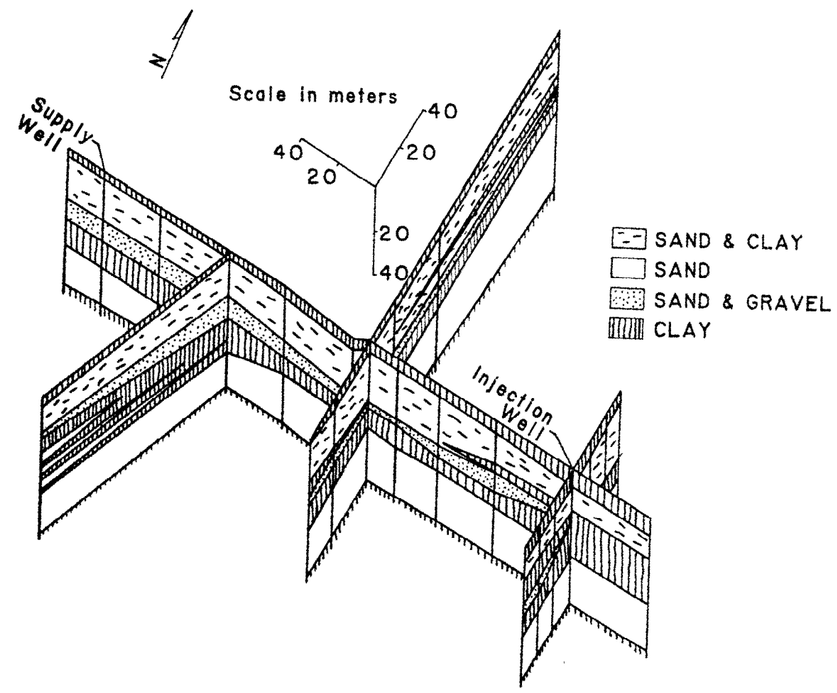


**Figure II-1.** Subsurface Hydrologic System at the Mobile site.

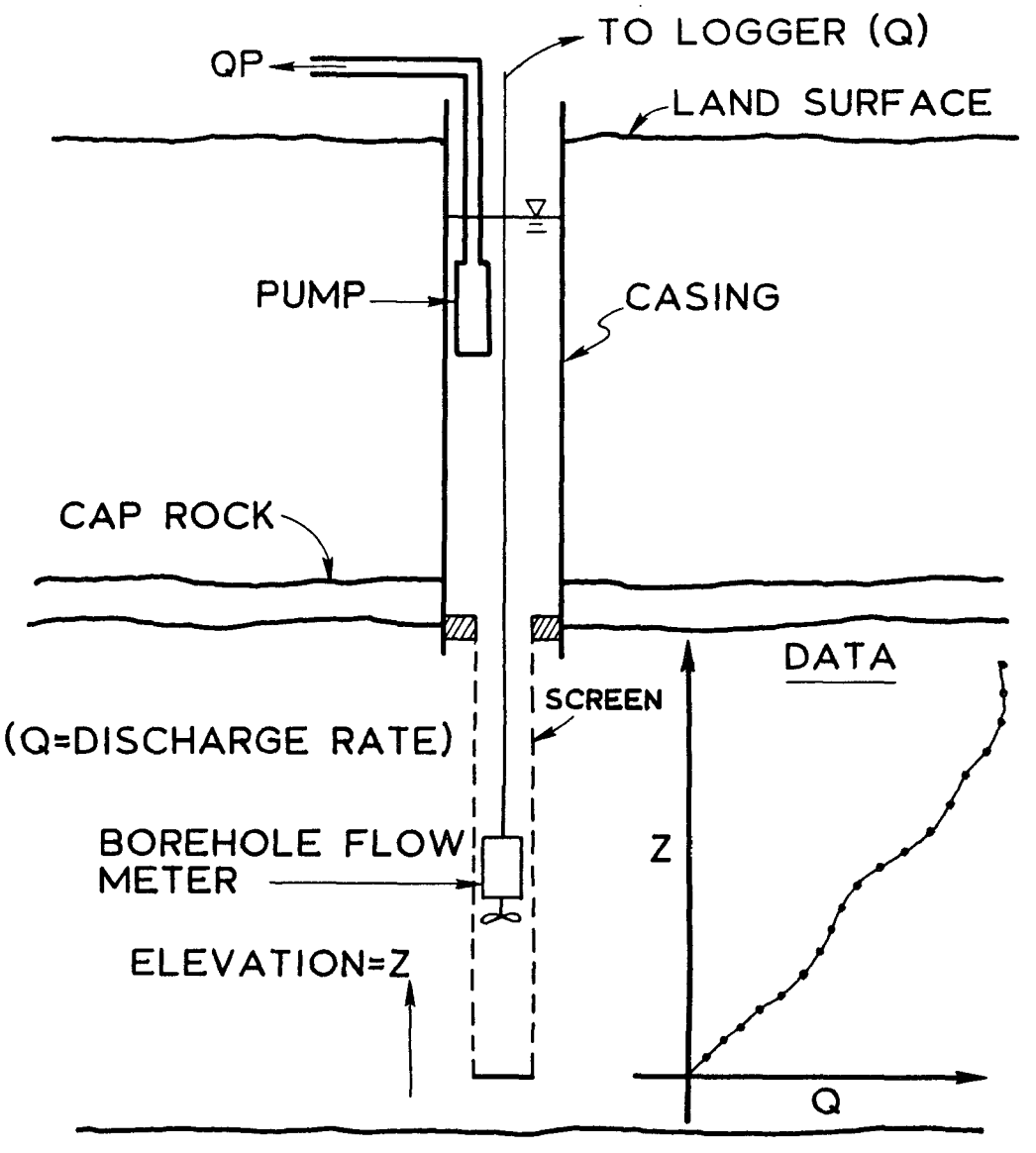


Figure II-2. Apparatus and geometry associated with a borehole flowmeter test.

behavior is obtained, the flowmeter, which when calibrated measures vertical flow within the screen, is lowered to near the bottom of the well, and a measurement of discharge rate is obtained in terms of impeller-generated electrical pulses over a selected period of time. The meter is then raised a few feet, another reading taken, raised another few feet--and so on. As illustrated in the lower portion of Figure II-2, the result is a series of data points giving vertical discharge, Q, within the well screen as a function of vertical position z. Just above the top of the screen the meter reading should be equal to QP, the steady pumping rate that is measured independently on the surface with a water meter. The procedure may be repeated several times to ascertain that readings are stable.

While Figure II-2 applies explicitly to a confined aquifer, which was the type of aquifer studied at the Mobile site, application to an unconfined aquifer is similar. Most impeller meters are capable of measuring upward or downward flow, so if the selected pumping rate, QP, causes excessive drawdown, one can employ an injection procedure as an alternative. In either case, there will be unavoidable errors near the water table due to the deviation from horizontal flow. It is desirable in unconfined aquifers to keep QP as small as possible consistent with the stall velocity of the meter. Thus more sensitive meters will have an advantage.

As shown in Figure II-3, the basic data analysis procedure is quite easy. One assumes that the aquifer is composed of a series of n horizontal layers and takes the difference between two successive meter readings, which yields the net flow, $\Delta Q_i$, entering the screen segment between the elevations where the readings were taken, which is assumed to bound layer i(i = 1,2,...,n). One then employs the Cooper-Jacob [1946] formula for horizontal flow to a well from a layer, i, of thickness $\Delta z_i$, given by

$$\Delta H_i(r_w,t) = \frac{\Delta Q_i}{2\pi K_i \Delta z_i} \ln \left[\frac{1.5}{r_w}\sqrt{\frac{K_i(\Delta z_i)t}{S_i}}\right] \qquad \text{(II-1)}$$

where $\Delta H_i$ = drawdown in ith layer, $\Delta Q_i$ = flow from ith layer into the well, $K_i$ = horizontal hydraulic conductivity of the ith layer, $\Delta z_i$ = ith layer thickness, $r_w$ = effective well radius, t = time since pumping started, and $S_i$ = storage coefficient for the ith layer. Solving equation (II-1) for the $K_i$ outside of the log term yields

$$K_i = \frac{\Delta Q_i}{2\pi \Delta H_i \Delta z_i} \ln \left[\frac{1.5}{r_w}\sqrt{\frac{K_i(\Delta z_i)t}{S_i}}\right] \qquad \text{(II-2)}$$

which can be solved iteratively to obtain a value for $K_i$. Further details may be found in Morin et al. [1988a] or Rehfeldt et al. [1988].

A convenient alternative method for obtaining a K distribution is based on the study of flow in a layered, stratified aquifer by Javandel and Witherspoon [1969]. Their work showed that in idealized, layered aquifers, flow at the well bore radius, $r_w$, rapidly becomes horizontal even for relatively large permeability contrasts between layers. As the writers point out, under such conditions the radial gradients along the well bore are constant and uniform, and flow into the well from a given layer is proportional to the transmissivity of that layer, that is:

$$\Delta Q_i = \alpha \Delta z_i K_i \qquad \text{(II-3)}$$

where $\alpha$ is a constant of proportionality. This condition occurs when the dimensionless time $t_D = \bar{K}t/S_s r^2_w$ is $\geq 100$. (In this expression $\bar{K}$ is the average horizontal aquifer hydraulic conductivity defined as $\Sigma K_i \Delta z_i/b$, where b is aquifer thickness, $S_s$ is the aquifer specific storage, t is time since pumping started and $r_w$ is well bore radius.)

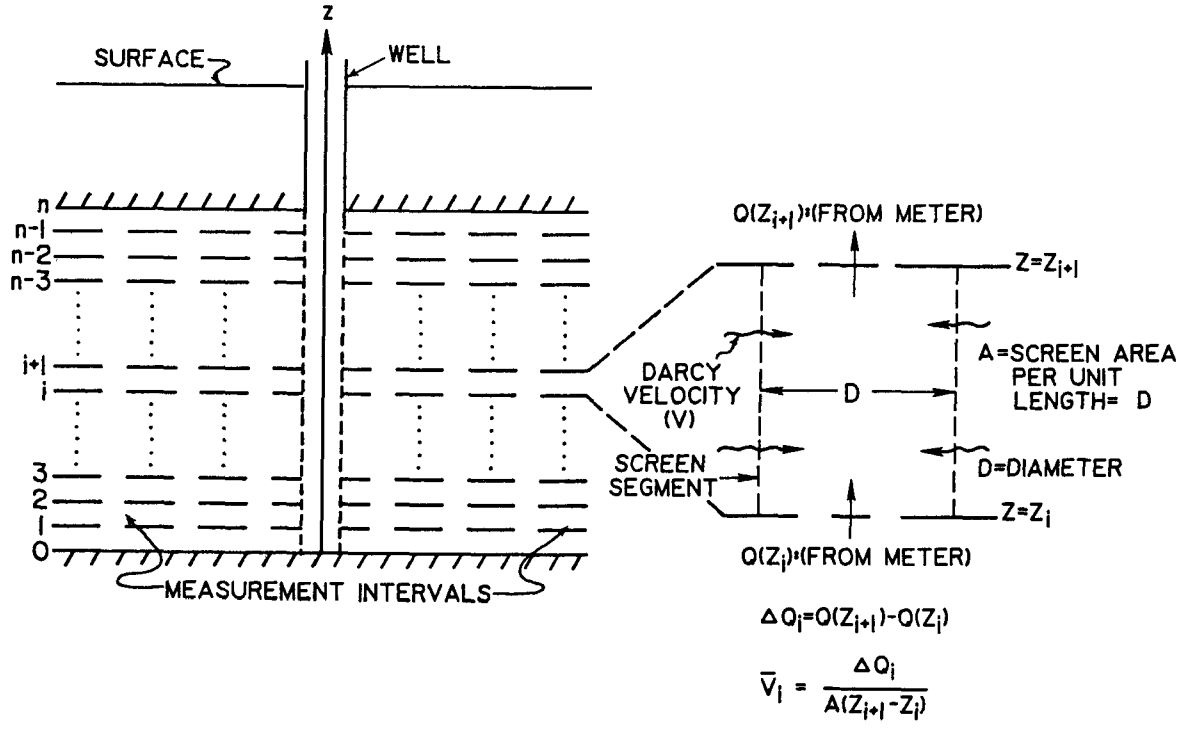


Figure II-3. Assumed layered geometry within which impeller meter data are collected and analyzed. (Q(z) is discharge measured at elevation z.)

To solve for $\alpha$, sum the $\Delta Q_i$ over the aquifer thickness, to get

$$\sum_{i=1}^{n} \Delta Q_i = QP = \alpha \sum_{i=1}^{n} \Delta z_i K_i \qquad \text{(II-4)}$$

Multiplying the right-hand side of equation (II.4) by b/b and solving for $\alpha$ yields

$$\alpha = \frac{QP}{b\overline{K}} \qquad \text{(II-5)}$$

Finally, substituting for $\alpha$ in equation (II.4) and solving for $K_i/\overline{K}$ gives

$$\frac{K_i}{\overline{K}} = \frac{\Delta Q_i/\Delta z_i}{QP/b} \; ; \; i = 1, 2, \ldots n \qquad \text{(II-6)}$$

To obtain equation (II-6) it was assumed that $\Delta Q_i$ and QP do not change with time (i.e. pseudo-steady-state conditions apply). This will occur when $r^2_w S/4Tt < 0.01$, where S and T are aquifer storage coefficient and transmissivity, respectively. Thus, from the basic data it is quite easy to get a plot of $K/\overline{K}$ versus elevation. If one then has the value of $\overline{K}$ from a fully penetrating pumping test, one can easily obtain dimensional values for K. At the Mobile site, the theoretical time for $t_D \geq 100$ is a fraction of a second, and after about 3 min. of pumping, pseudo-steady-state conditions are reached. The $K/\overline{K}$ approach has practical appeal because one does not have to know values for $r_w$ or $S_i$, which are impossible to specify precisely. Also, multiplicative errors in flowmeter readings are cancelled out, and the meter does not have to be calibrated. All that is needed is a linear response. However, a fully penetrating pumping test or slug test must be performed along with each flowmeter test.

While the basic data analysis involved in the flowmeter method is quite simple, care must be taken to come as close as possible to meeting all assumptions and measuring only the actual flow caused by the pumping (Rehfeldt et al., 1988). For example, if there is ambient flow in the well, this must be measured prior to any pumping so that the initial flow condition is known. Alternatively, a two step pumping procedure can be used (Rehfeldt et al., 1988). In addition, the basic data analysis procedure assumes horizontal flow in the aquifer and that measured head loss in the well is due only to water flow through the undisturbed formation. However, there are screen losses and head losses within the well. In general, hydraulic losses can be minimized by pumping at the lowest rate consistent with the stall velocity of the impeller meter. For a much more detailed discussion of well head losses and their possible correction see Rehfeldt et al. (1988). Local deviations from horizontal flow will exist in most aquifers, but the effects should be of second order compared to those of the average flow field as long as the measurement intervals are not too small. As the $\Delta z_i$ get smaller, one can expect errors due to deviations from horizontal flow to get larger. Among other things, such errors will lead to poor repeatability of flowmeter readings obtained from multiple tests performed in the same well.

### II.2.2 Example Application at the Mobile Site

Testing began at the Mobile site with a mild redevelopment and cleaning of the test well screens (Fig. II-4) with air. Ambient flow measurements were then made using a heat-pulse flow meter developed by the U.S. Geological Survey, which has a measurement range of 0.1 to 20 ft./min (0.03 to 6.1 m/min.) (Hess, 1986), which is about 10 times more sensitive than any impeller meter. Even at this sensitivity, however, no ambient vertical flow within the screen could be detected. This is consistent with the study aquifer being relatively permeable and well

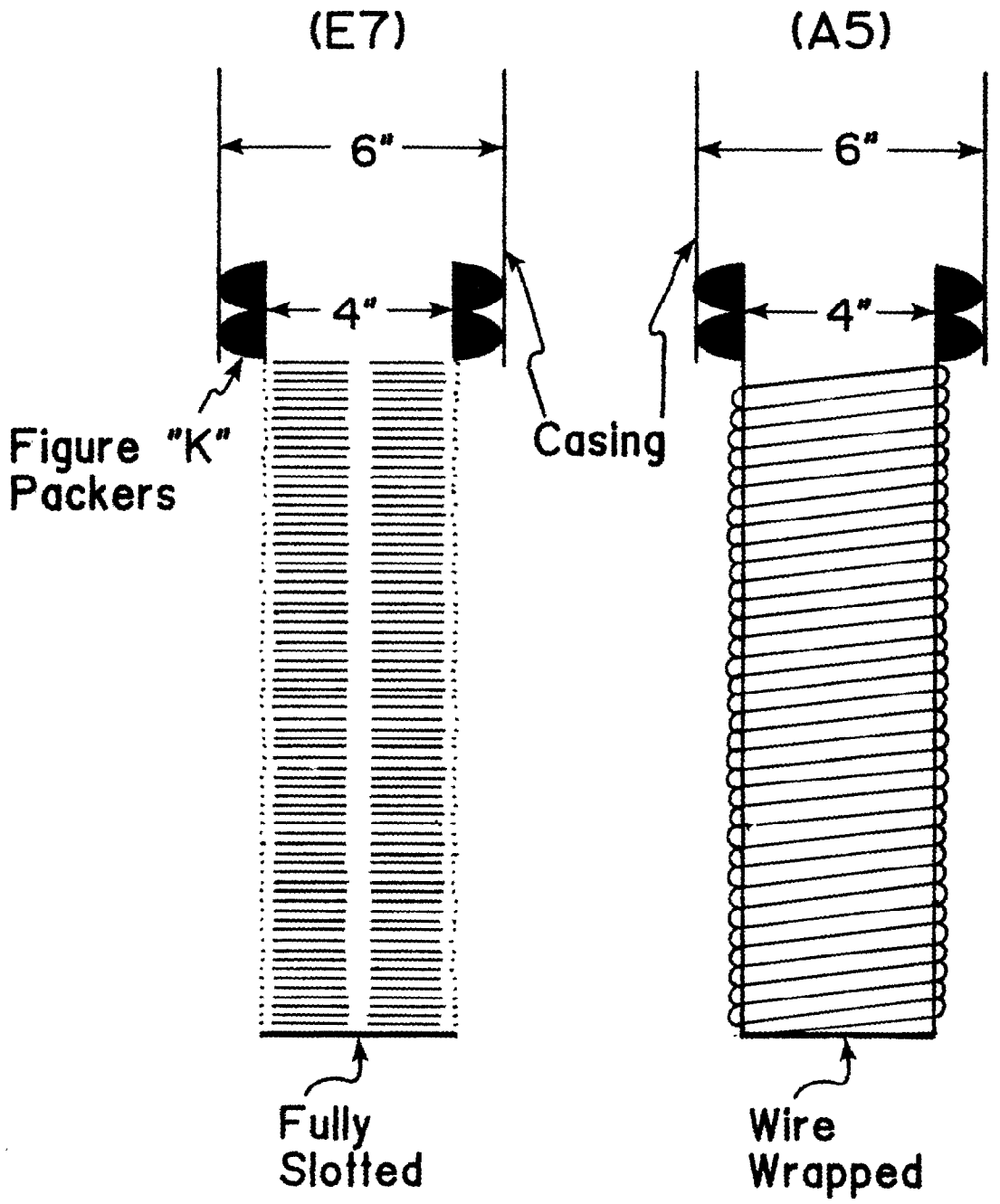


Figure II-4. Details of well construction and screen types in wells E7 and A5.

confined in an area of low horizontal hydraulic gradient. If there had been a significant ambient flow, the ambient flow at any measurement level $z_i$ would have been subtracted from the impeller meter reading at that level prior to data analysis.

The test well geometry shown in Figure II-2 is similar to that at the Mobile site, with the 4 in (10 cm) ID well screen (0.01 inch slotted plastic or plastic wire-wrap, see Fig. II-4) extending from about 130 ft (39.6 m) to 200 ft (61 m) below the land surface. None of the screens had a sand pack. To prepare for a test, the well screens were cleaned with air (clean and open screens are important), and caliper and ambient pressure logs were run. Data obtained from the caliper log were used to verify and compute the cross-sectional area of the well, and the hydraulic-head distribution derived from the pressure log served as a calibration reference for evaluating $\Delta H_i$ produced by pumping. Subsequently, a pressure transducer and an impeller meter with centralizer were lowered into the well, followed by a small submersible pump capable of pumping about 60 gpm (227 liter/min). The pump was started and allowed to run for about an hour prior to taking pressure and impeller meter readings, more than adequate time for drawdown to reach a pseudo-steady-state as defined by the Cooper-Jacob criterion discussed in a following section. Data analysis showed that $\Delta H_i$ varied only slightly over the length of the screens.

An impeller meter can function in either a stationary or a trolling mode. In the stationary mode, the meter is held at a series of set elevations and readings are taken in the form of pulses per unit time with the aid of an electronic pulse counter. In the trolling mode, the meter is raised or lowered at a constant known rate, and the reading reflects a superposition of the trolling and water flow velocities. For fine-scale groundwater applications, the stationary mode seems better suited; however, both methods of data acquisition were used during this study.

Listed in Table II-1 are the basic impeller meter data obtained in wells E7, and A5, along with the corresponding head difference between static and dynamic (pumping) conditions derived from the pressure logs. In order to convert impeller meter readings into discharge, the meter was calibrated in-situ by placing it in the top unslotted extension of the well screens (Fig. II-4) and then pumping at three different rates which were measured independently at the surface. In all cases the response was quite linear, and a straight line approximation was drawn through the calibration points. For wells E7 and A5, the calibration equation was $Q = 0.00428(CPM)$ in both cases, where Q is in $ft^3/min$ and CPM represents impeller "counts per minute." Applying this equation to the data listed in Table II-1 resulted in the discharge profiles presented in Table II-2.

## II-2.3 Data Analysis

As discussed previously, we visualize two procedures for inferring a hydraulic conductivity function, K(z), from impeller meter data. One approach involves the application of equation (II-2) to each depth interval. This was done for wells A5 and E7 using a storage coefficient $S_i = 10^{-5} \cdot \Delta z_i$, where the average specific storage of $10^{-5} ft^{-1}$ ($3.05 \times 10^{-6} m^{-1}$) was determined from a pumping test performed previously (Parr et al., 1983). The results of this computation are presented in Table II-3 as K1(z), with depth values corresponding to the midpoint (of the assumed layers) between impeller meter readings. Also shown in Table II-3 as K2(z) are the results of applying equation (II-6) to each measurement interval in wells A5 and E7. To obtain these results, values of the dimensionless function $K_i/\overline{K}$ were calculated, where $\overline{K}$ is average hydraulic conductivity. Knowing $\overline{K}$ from the analysis of a standard, fully penetrating pumping test enables us to solve for each $K_i$. For a $\overline{K}$ of 0.121 ft/min ($3.69 \times 10^{-2} m/min$), a

Table II-1. Impeller meter (discrete mode) and differential head data obtained in Wells E7, and A5 at the Mobile Site. (z=depth, CPM=counts per minute, and ΔH=head difference between static and dynamic conditions.)

| Well #E7 | | | Well #A5 | | |
|---|---|---|---|---|---|
| z(ft) | CPM | ΔH(ft) | z(ft) | CPM | ΔH(ft) |
| 130 | 1983 | 1.218 | 132.5 | 2024 | 1.210 |
| 135 | 1933 | 1.202 | 137.5 | 1968 | 1.201 |
| 140 | 1886 | 1.189 | 142.5 | 1885 | 1.170 |
| 145 | 1764 | 1.177 | 147.5 | 1799 | 1.147 |
| 150 | 1705 | 1.166 | 152.5 | 1652 | 1.136 |
| 155 | 1607 | 1.157 | 157.5 | 1488 | 1.132 |
| 160 | 1561 | 1.149 | 162.5 | 1362 | 1.132 |
| 165 | 1468 | 1.143 | 167.5 | 1106 | 1.132 |
| 170 | 1118 | 1.139 | 172.5 | 882 | 1.138 |
| 175 | 994 | 1.138 | 177.5 | 740 | 1.156 |
| 180 | 911 | 1.138 | 182.5 | 506 | 1.173 |
| 185 | 638 | 1.138 | 187.5 | 293 | 1.186 |
| 190 | 277 | 1.138 | 190.0 | 57 | 1.193 |

Table II-2. Well screen discharge as a function of vertical position in wells E7 and A5 at the Mobile site. (z=depth, Q=discharge rate in well screen.)

| Well #E7 | | Well #A5 | |
|---|---|---|---|
| z(ft) | Q($ft^3$/min) | z(ft) | Q($ft^3$/min) |
| 130 | 8.49 | 132.5 | 8.66 |
| 135 | 8.27 | 137.5 | 8.42 |
| 140 | 8.07 | 142.5 | 8.07 |
| 145 | 7.55 | 147.5 | 7.70 |
| 150 | 7.30 | 152.5 | 7.07 |
| 155 | 6.88 | 157.5 | 6.37 |
| 160 | 6.68 | 162.5 | 5.83 |
| 165 | 6.28 | 167.5 | 4.73 |
| 170 | 4.79 | 172.5 | 3.77 |
| 175 | 4.25 | 177.5 | 3.17 |
| 180 | 3.90 | 182.5 | 2.17 |
| 185 | 2.73 | 187.5 | 1.25 |
| 190 | 1.19 | 190.00 | 0.244 |

Table II-3. Hydraulic conductivity distributions inferred from impeller meter data using two different approaches described herein. (Depth z is in ft. and K(z) is in ft./min.)

| Well #E7 | | | Well #A5 | | |
|---|---|---|---|---|---|
| z | K1(z) | K2(z) | z | K1(z) | K2(z) |
| 132.5 | 0.050 | 0.042 | 135 | 0.055 | 0.043 |
| 137.5 | 0.046 | 0.038 | 140 | 0.083 | 0.063 |
| 142.5 | 0.128 | 0.100 | 145 | 0.091 | 0.069 |
| 147.5 | 0.059 | 0.049 | 150 | 0.163 | 0.119 |
| 152.5 | 0.104 | 0.083 | 155 | 0.184 | 0.134 |
| 157.5 | 0.048 | 0.040 | 160 | 0.140 | 0.104 |
| 162.5 | 0.100 | 0.080 | 165 | 0.297 | 0.212 |
| 167.5 | 0.405 | 0.299 | 170 | 0.257 | 0.185 |
| 172.5 | 0.139 | 0.109 | 175 | 0.156 | 0.115 |
| 177.5 | 0.088 | 0.071 | 180 | 0.263 | 0.189 |
| 182.5 | 0.315 | 0.236 | 185 | 0.237 | 0.171 |
| 187.5 | 0.421 | 0.310 | 189 | 0.536 | 0.371 |
| 195.0 | 0.154 | 0.120 | 195 | 0.027 | 0.022 |

value obtained from a pumping test performed in the vicinity of E7 and A5, corresponding values of K2(z) are listed in Table II-3. These hydraulic conductivity profiles are plotted also in Figure II-5.

### II-2.4 Comparison of Impeller Meter Tests With Tracer Tests

Examination of Figure II-5 shows that the trends in the data are virtually identical for wells A5 and E7. There is also fairly good agreement between the absolute (dimensional) values calculated for the hydraulic conductivity.

It is of interest to compare the hydraulic conductivity distributions inferred from the impeller meter data with those obtained previously using single well tracer tests (Molz et al., 1988). These tests involved one fully penetrating tracer injection well and one multilevel sampling/observation well located about 20 ft (6.1 m) away. A bromide tracer solution was injected at a constant rate through the injection well, while water samples were collected periodically from up to 14 different elevations of the multilevel sampling well. Analysis of the samples for Br concentration allowed one to determine the travel time distribution between the injection and sampling wells as a function of elevation. From this information it is possible to infer a relative hydraulic conductivity distribution (Molz et al., 1988). There is no reason to expect detailed agreement between the impeller meter results and the single-well tracer test results because the latter data reflect an average hydraulic conductivity value inferred over a travel distance of approximately 20 ft (6.1 m). However, as shown in Figure II-6, the agreement is reasonably good, indicating that the overall trend in K(z) persists over the 20 ft (6.1 m) travel distance of the tracer test (Molz et al., 1988).

## II-3 Measurement of Hydraulic Conductivity at Difference Scales Using Impeller Meter Tests and Pumping Tests

The main purpose of this section is to describe the application of impeller meter tests and pumping tests so that the reader will develop an appreciation for the type and extent of hydraulic information that can be assembled at a particular site. Once again, the site chosen for this detailed application was the Mobile site. Vertical scale information was obtained using the impeller meter, while fully penetrating pumping tests were employed for obtaining information at various lateral scales. The testing procedures where those described in the previous sections. The fully penetrating pumping tests were analyzed using the Cooper-Jacob Method (Freeze and Cherry, 1970 (or almost any contemporary groundwater text)).

### II-3.1 Results of Tests

Shown in Figure II-7 is a plan view of the Mobile study site where the pumping tests and impeller meter tests were performed. The various wells are designated as I2, E6, A3, etc. The number in parentheses next to each well designation is the vertically-averaged hydraulic conductivity in meters per day, $\overline{K}(x,y)$, that resulted from one or more small-scale pumping tests in which the designated well was the pumping well. Arrows indicate the pattern of the observation well/pumping-well arrangement in Figure II-7. They point from the observation well towards the pumping well. Each arrow represents a single test with a pumping rate of about 0.22 $m^3$/min (58 gpm). The repeatability of any one test was good with the drawdown data falling within 5% of each other.

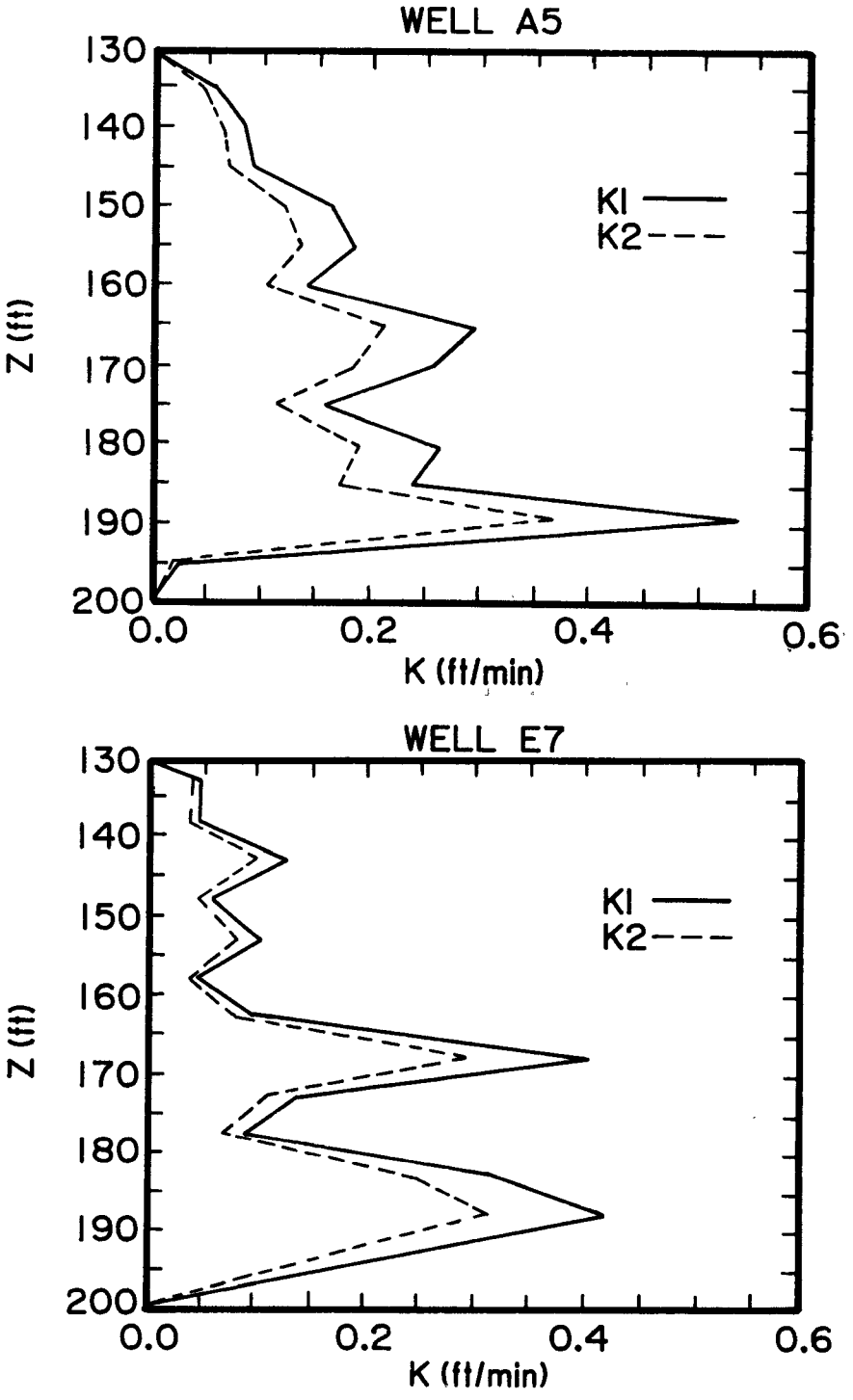


Figure II-5. Hydraulic conductivity distributions calculated from flowmeter data using two different methods.

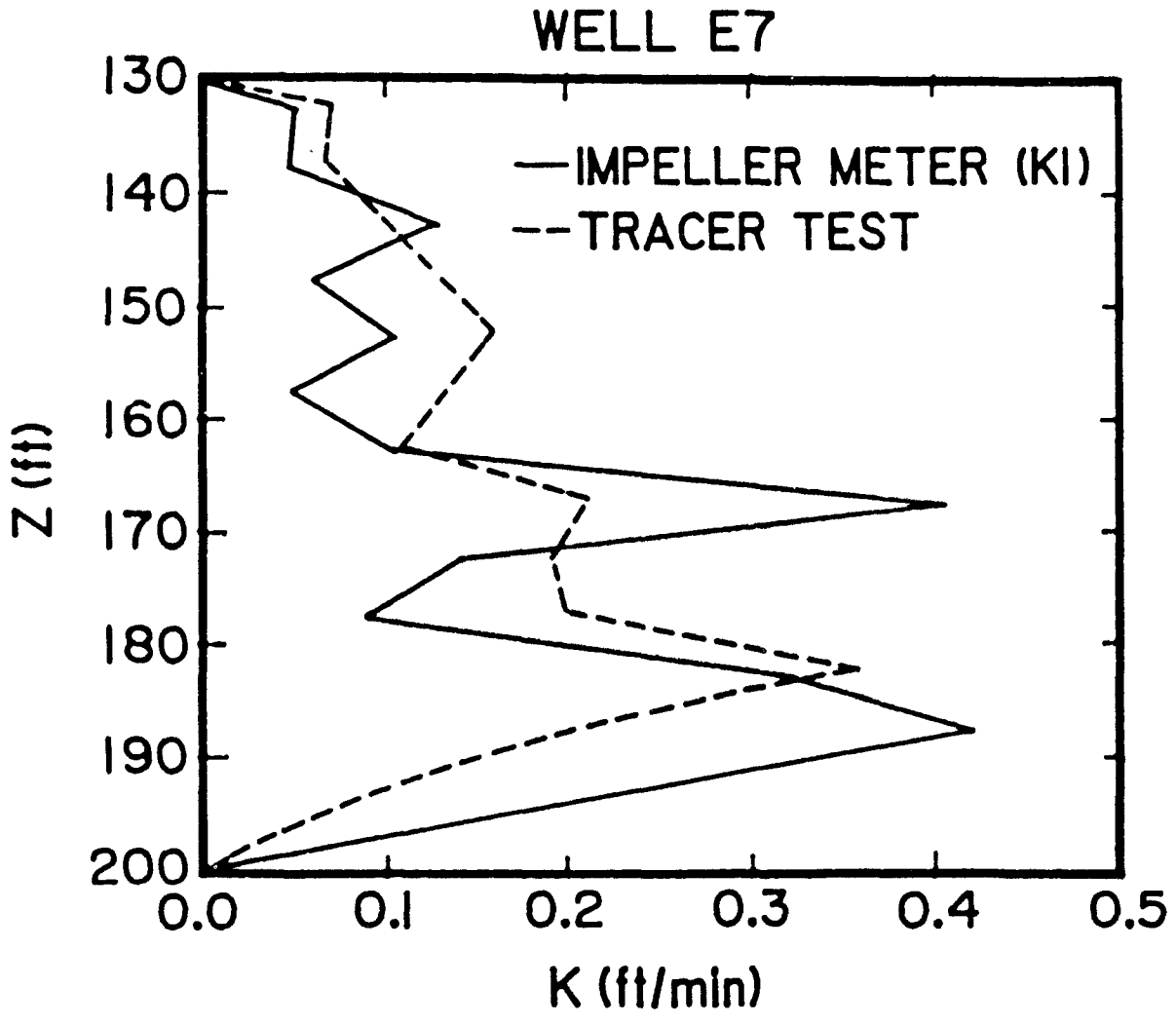


Figure II-6. Comparison of hydraulic conductivity distributions for well E7 based on tracer test data and impeller meter data.

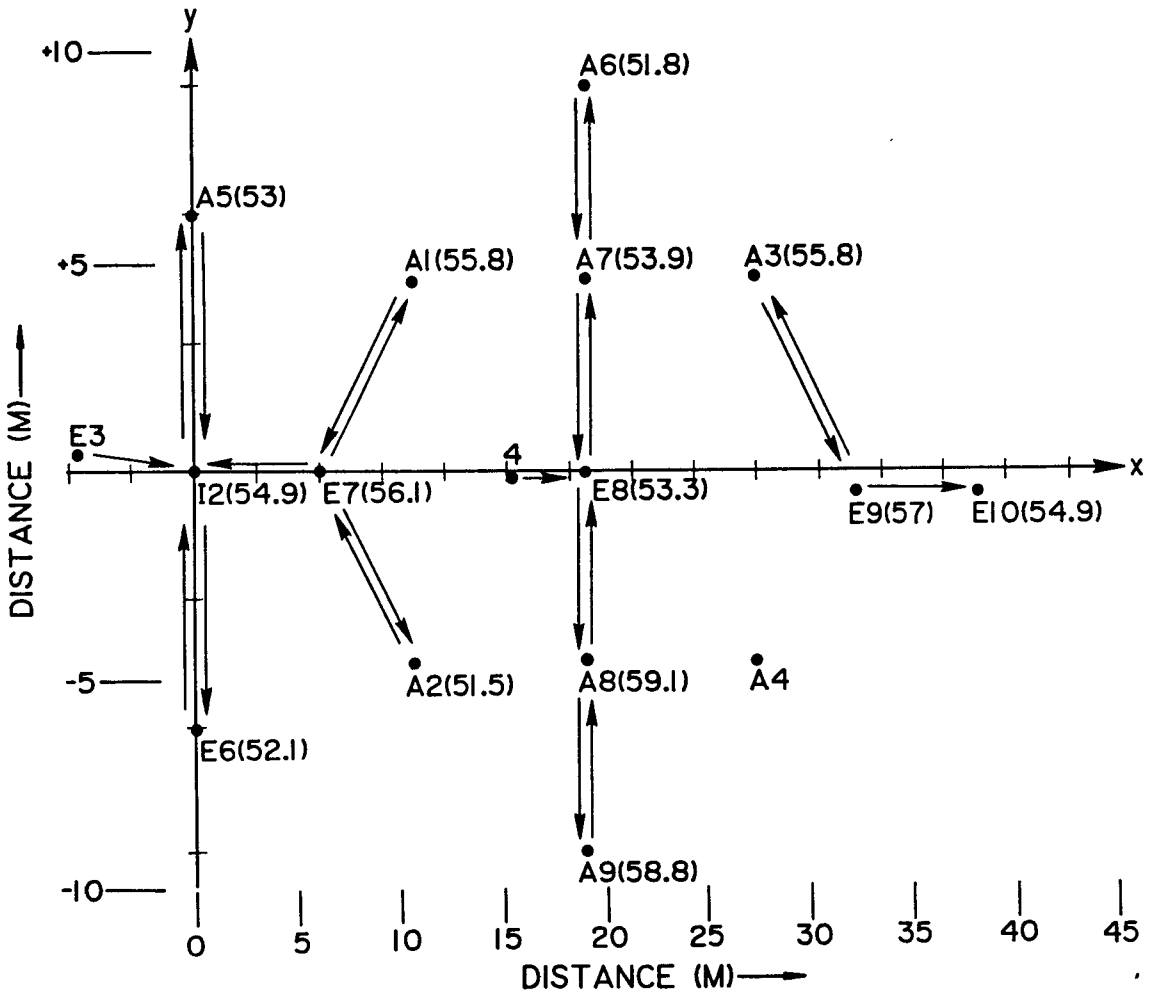


Figure II-7. Plan view of the field site where small-scale pumping tests were performed. The numbers next to the dots are well designations, while the values in parentheses are the average hydraulic conductivities (m/day) assigned to the vicinity of each pumping well. Each arrow represents a test and points from the observation well to the pumping well. Wells with more than one arrow pointing toward them were assigned average values.

A series of pumping tests in which the pumped wells were used as observation wells were performed also. Once again the pumping rate was approximately 0.22 $m^3$/min (58 gpm). The results of these tests are shown in Figure II-8.

$K/\overline{K}$ distributions based on impeller meter tests performed in wells E7, E8, E9, A6, A7, A8, and A9 are shown in Figures II-9 through II-15, respectively. Each figure was obtained with the use of equation II-6 applied to impeller meter data from measurement intervals of 0.3 m (1 ft), 0.91 m (3 ft), 1.52 m (5 ft), and 3.108 m (10 ft), as illustrated in Figure II-3.

As with the fully penetrating pumping tests, repeatability of the impeller meter tests was good. Evidence for this is shown in Figure II-16 which documents the results of repeated impeller meter tests in well E7.

II-3.2 Discussion of Results

The vertically-averaged hydraulic conductivity, $\overline{K}(x,y)$, shown in Figure II-7 seems to imply that the study aquifer is fairly homogeneous. The mean value of hydraulic conductivity is 54.9 m/day with a standard deviation of only 2.4 m/day*. The mean value agrees well with the result of a large-scale pumping test (53.4 m/day) performed previously using I2 as the pumping well and pumping at the rate of 1.48 $m^3$/min (390 gpm) (Parr et al., 1983).

As one would expect, the results shown in Figure II-8 are more variable because a pumping test using the pumping well as an observation well will sample a smaller volume of the aquifer. Here the mean value is only 3.5% smaller at 53.0 m/day, but the standard deviation has increased by a factor of 4.75 to 11.4 m/day.

In the authors' judgement, no distinct pattern emerges from Figure II-7 or Figure II-8. It is probable that $\overline{K}(x,y)$ will show lateral trends over distances in excess of 38 m, which is the approximate distance between wells I2 and E10. However, over the lateral distances representative of Figures II-7 and II-8 the $\overline{K}(x,y)$ variations appear more or less random.

Given the generally layered nature of geologic deposits in a fluvial environment, one would expect much more variability of horizontal hydraulic conductivity as a function of vertical position, K(z), than of vertically-averaged horizontal hydraulic conductivity as a function of lateral position, $\overline{K}(x,y)$. Examination of Figures II-9 through II-15 shows this to be the case. (Note that K(z) at any particular z is still averaged over the $360^0$ polar angle, so that the impeller meter test gives no information about lateral heterogeneity or anisotropy around a given well.) Different degrees of heterogeneity are apparent at the various measurement scales common to each figure. As the measurement scale varies from 10 ft (3.05 m) to 1 ft (0.3 m), the measured variation in hydraulic conductivity increases, and there is every reason to expect that it would increase further if the measurement scale were decreased to 0.5 ft, 0.25 ft. etc. Obviously, this type of heterogeneity is not reflected in the results of fully penetrating pumping tests.

---

* Since the data are correlated, the standard deviation is not well defined in a statistical sense. We are using it here just as a convenient measure of variation.

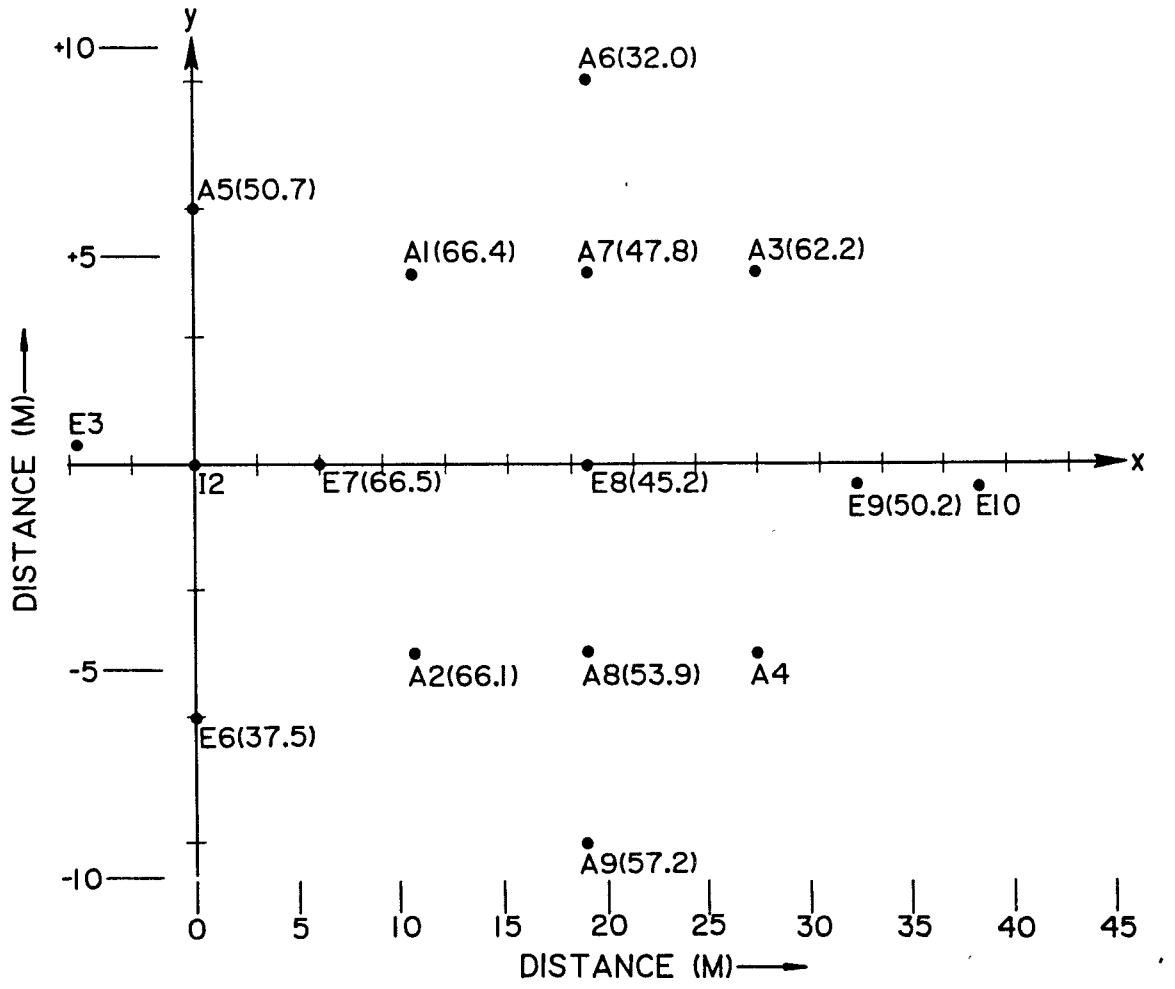


Figure II-8. Results of small-scale pumping tests (m/day) wherein the pumping wells were used as observation wells.

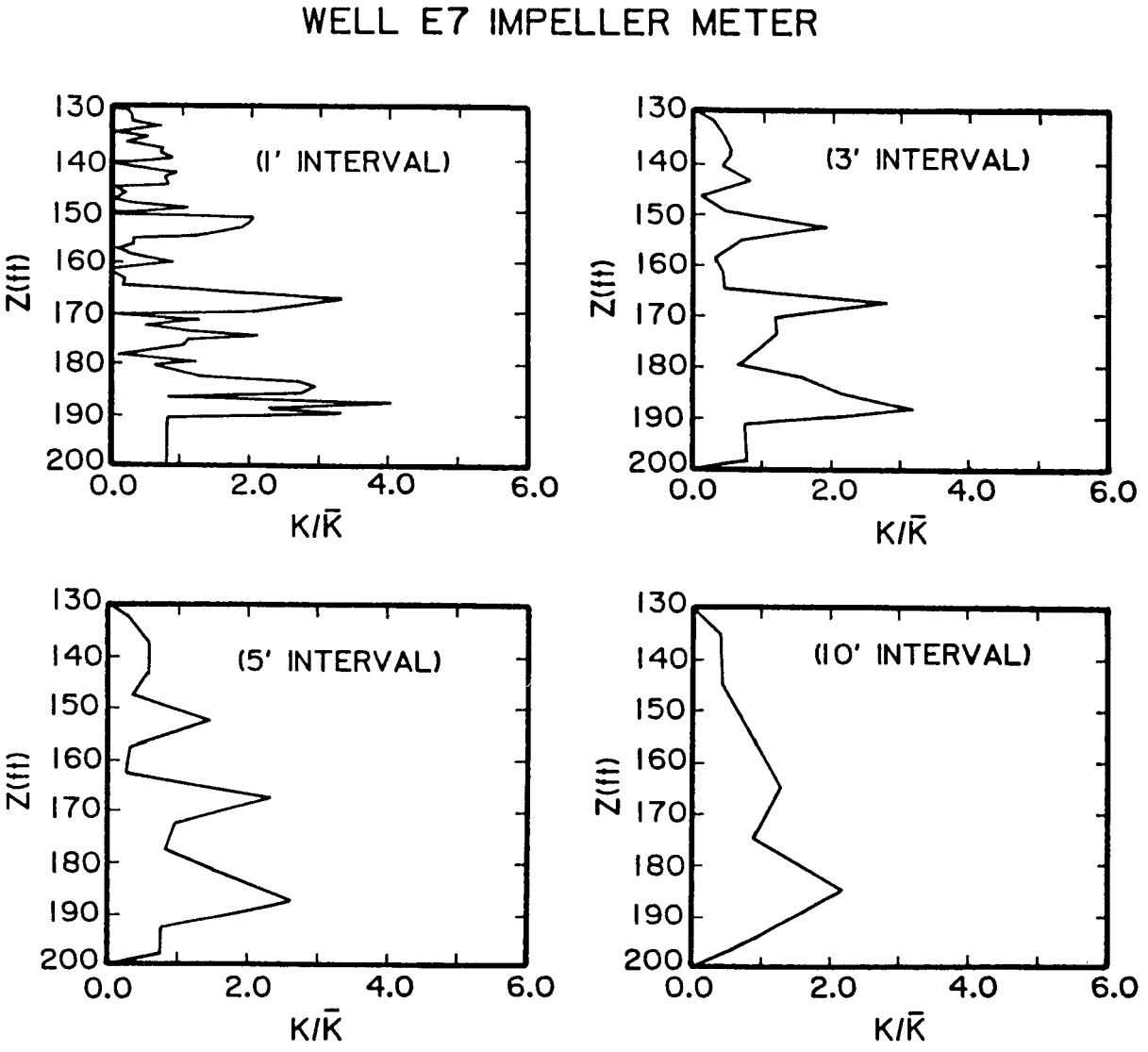


Figure II-9. Dimensionless horizontal hydraulic conductivity distributions based on impeller meter readings taken at the various measurement intervals indicated on the figure.

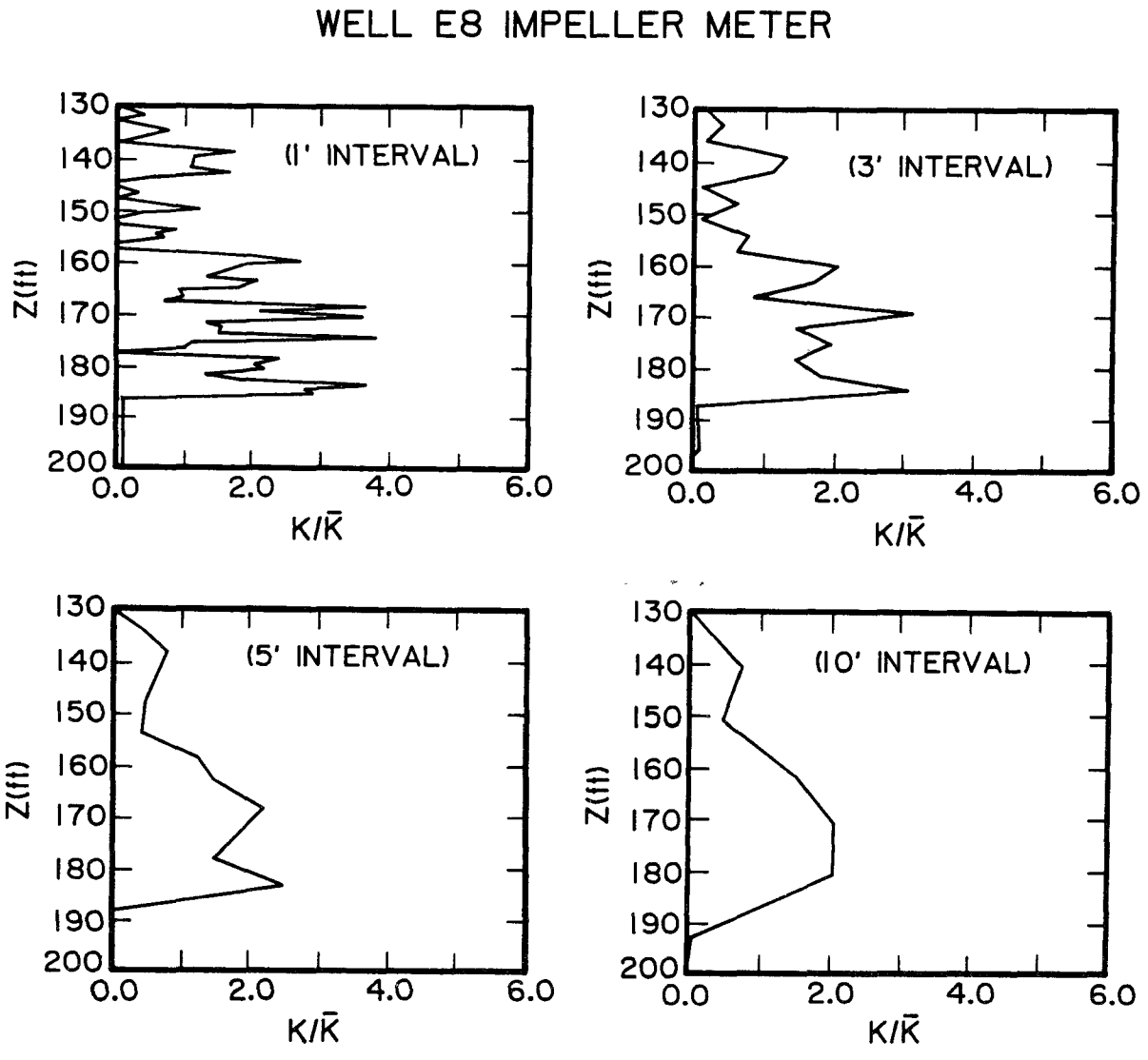


Figure II-10. Dimensionless horizontal hydraulic conductivity distributions based on impeller meter readings taken at the various measurement intervals indicated on the figure.

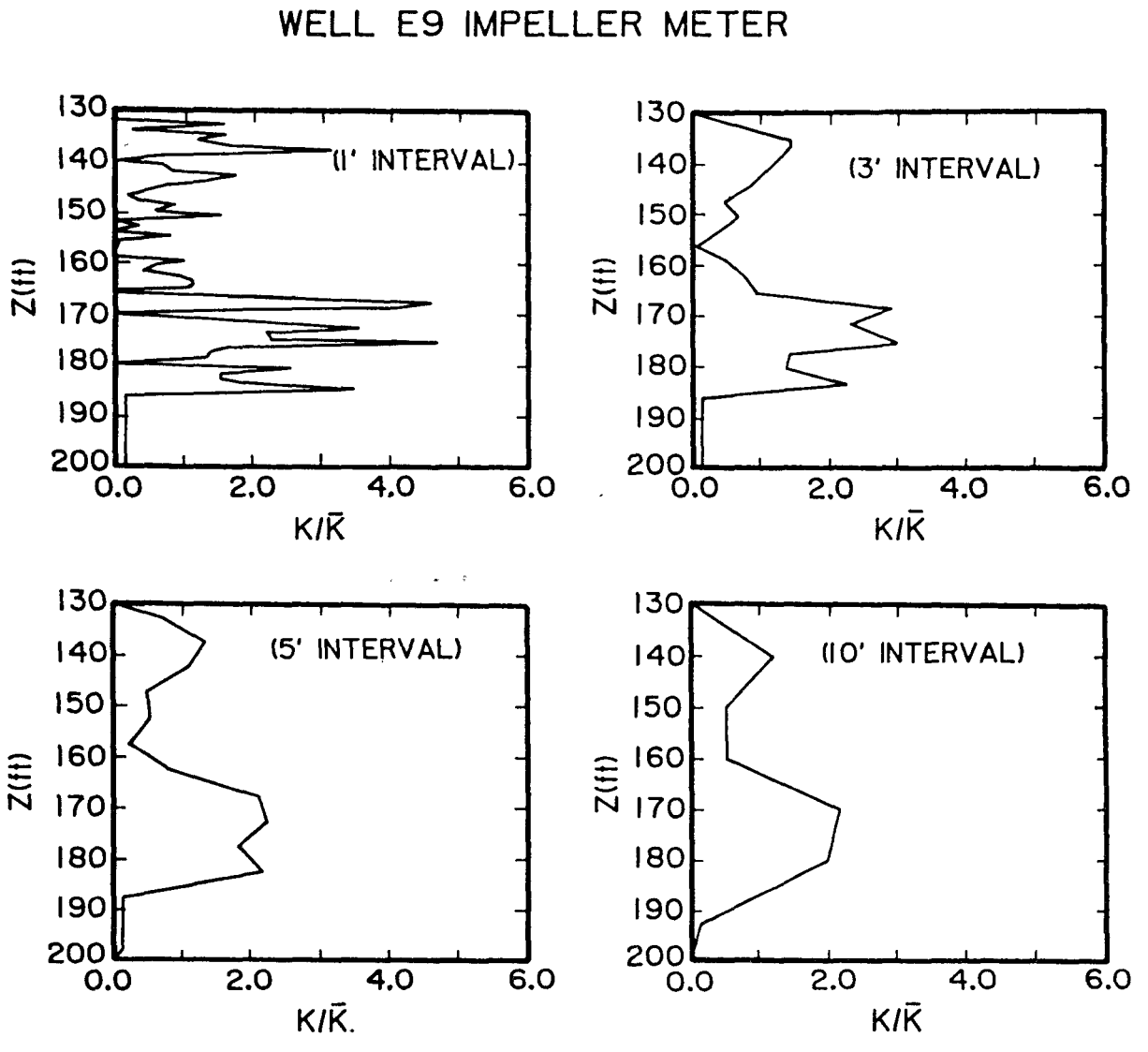


Figure II-11. Dimensionless horizontal hydraulic conductivity distributions based on impeller meter readings taken at the various measurement intervals indicated on the figure.

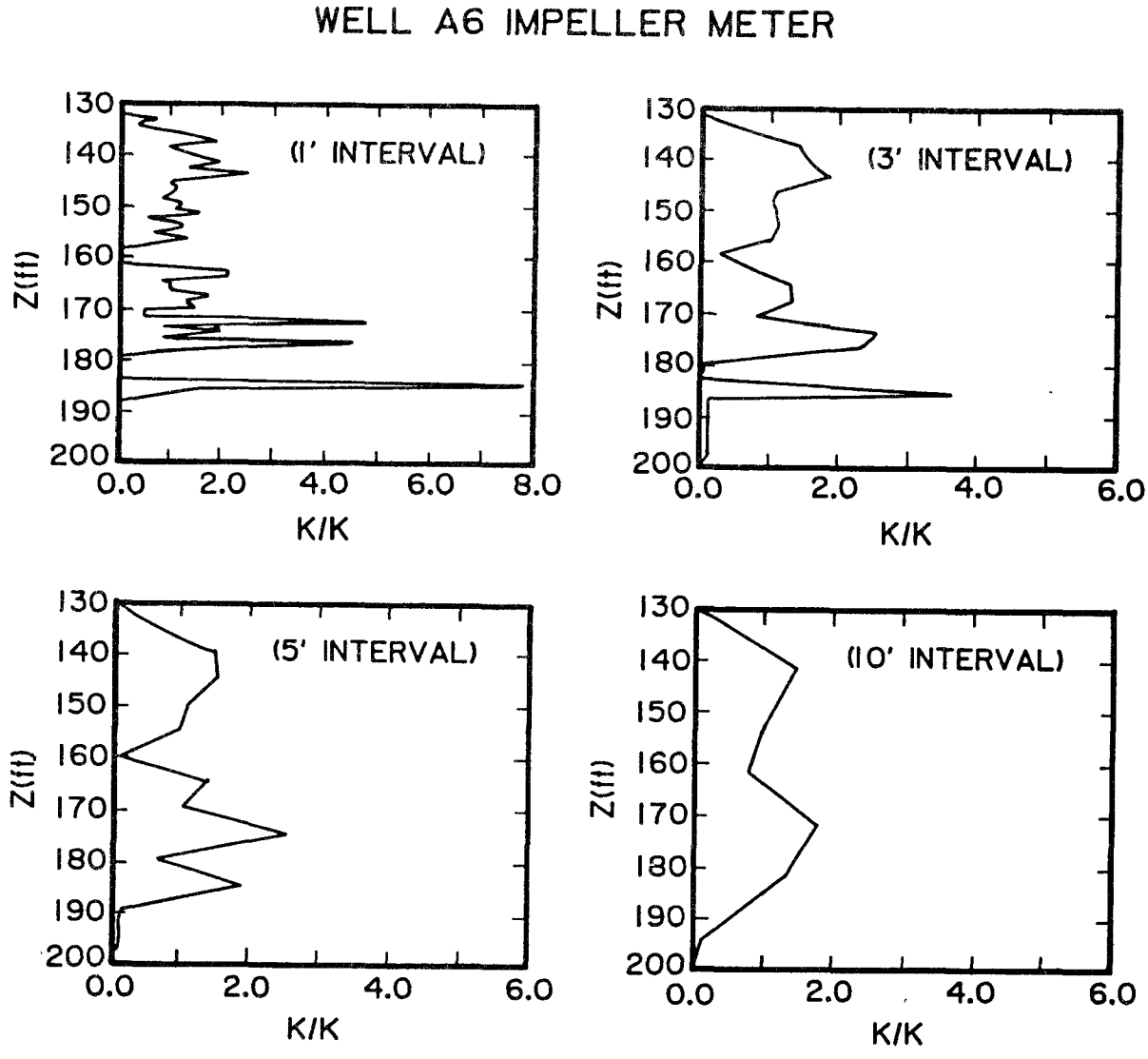


Figure II-12. Dimensionless horizontal hydraulic conductivity distributions based on impeller meter readings taken at the various measurement intervals indicated on the figure.

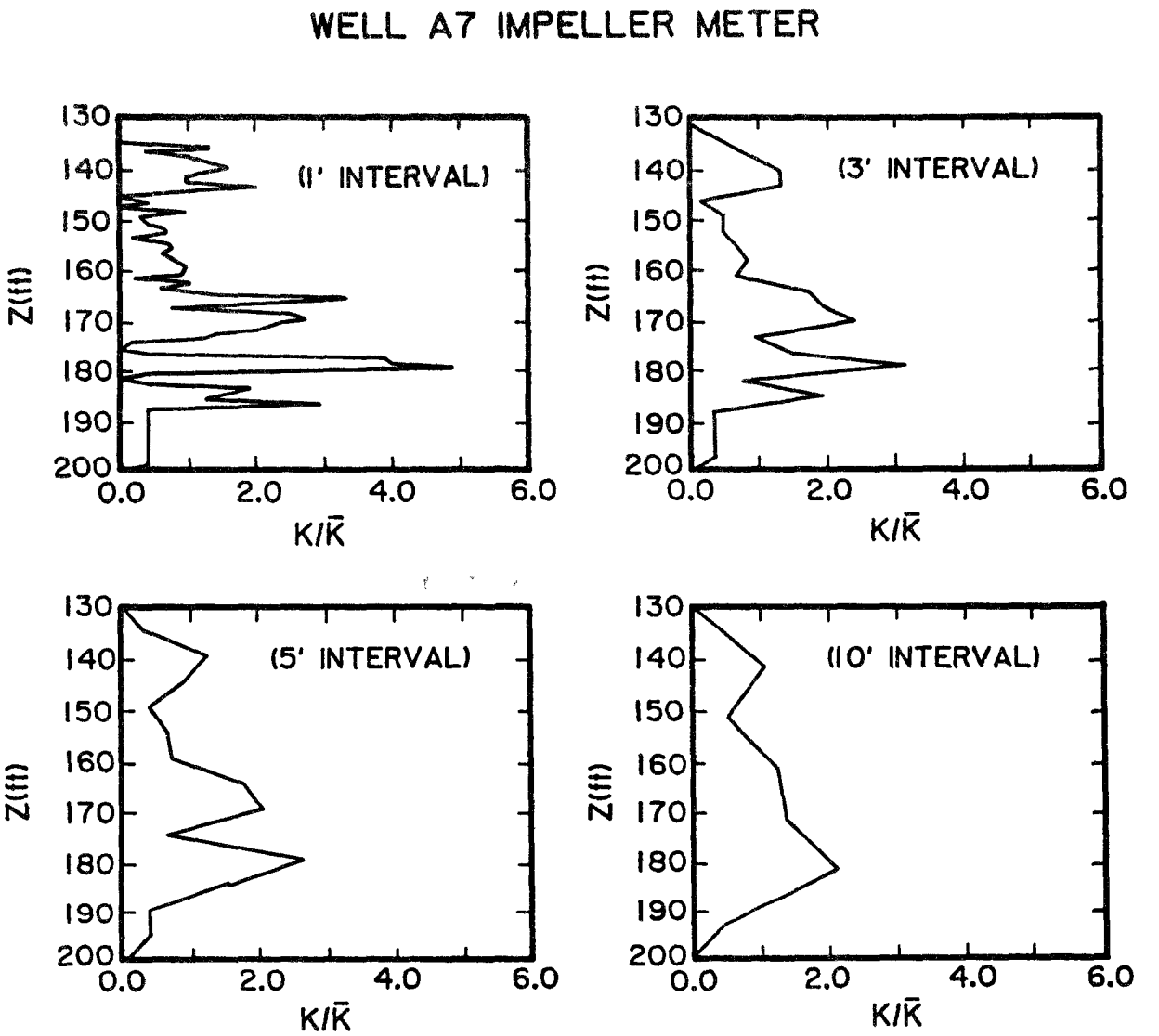


Figure II-13. Dimensionless horizontal hydraulic conductivity distributions based on impeller meter readings taken at the various measurement intervals indicated on the figure.

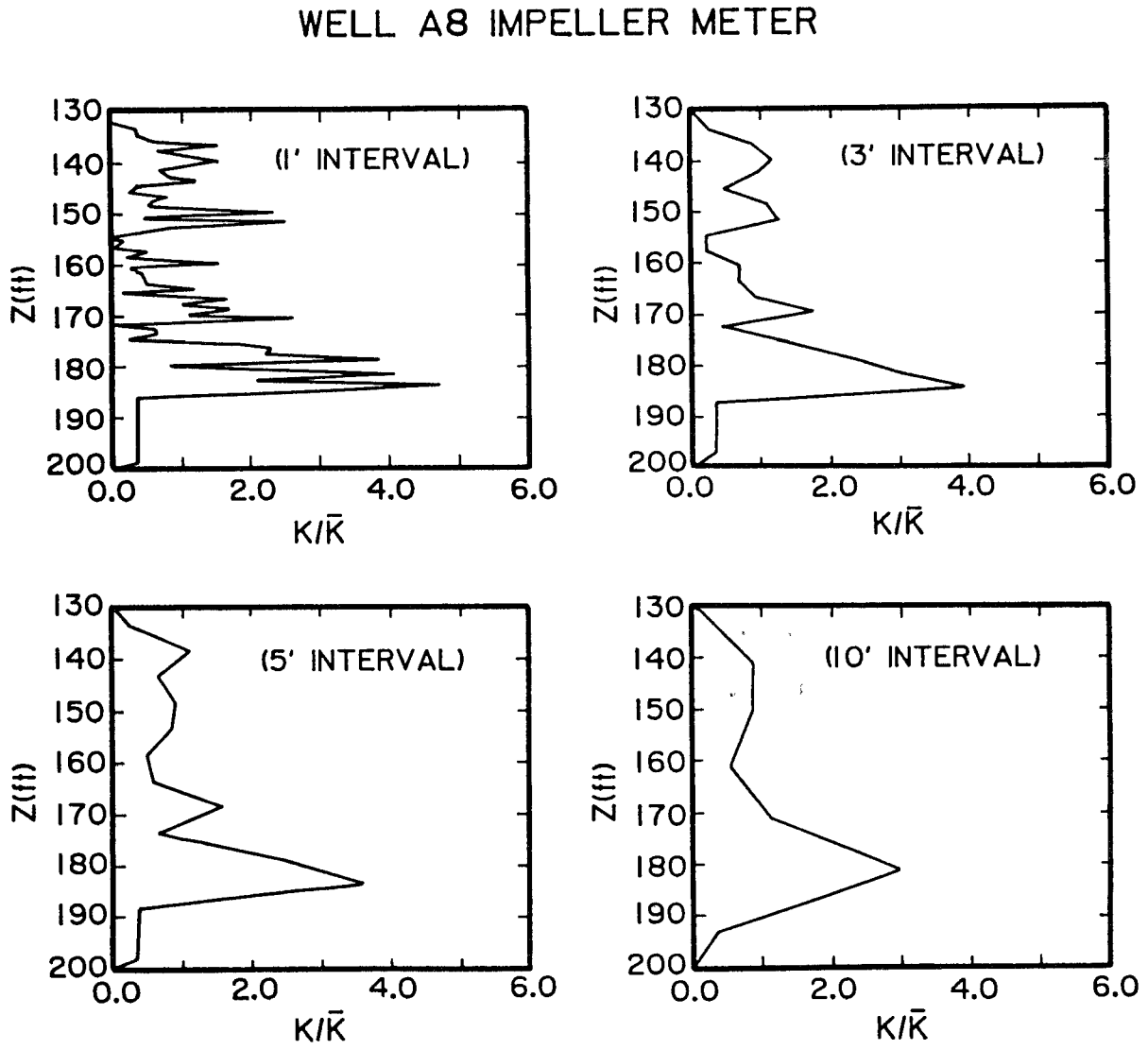


Figure II-14. Dimensionless horizontal hydraulic conductivity distributions based on impeller meter readings taken at the various measurement intervals indicated on the figure.

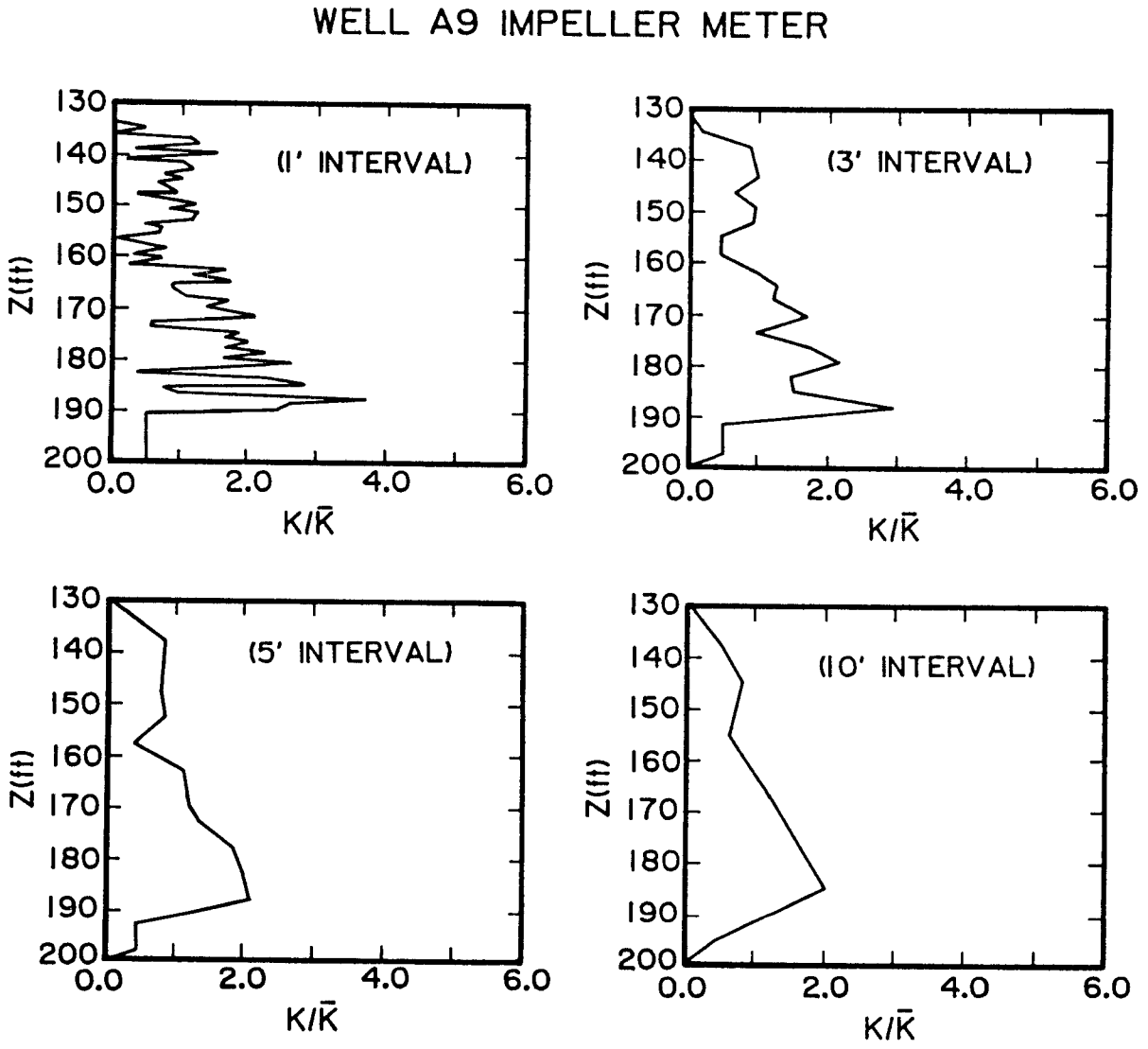


Figure II-15. Dimensionless horizontal hydraulic conductivity distributions based on impeller meter readings taken at the various measurement intervals indicated on the figure.

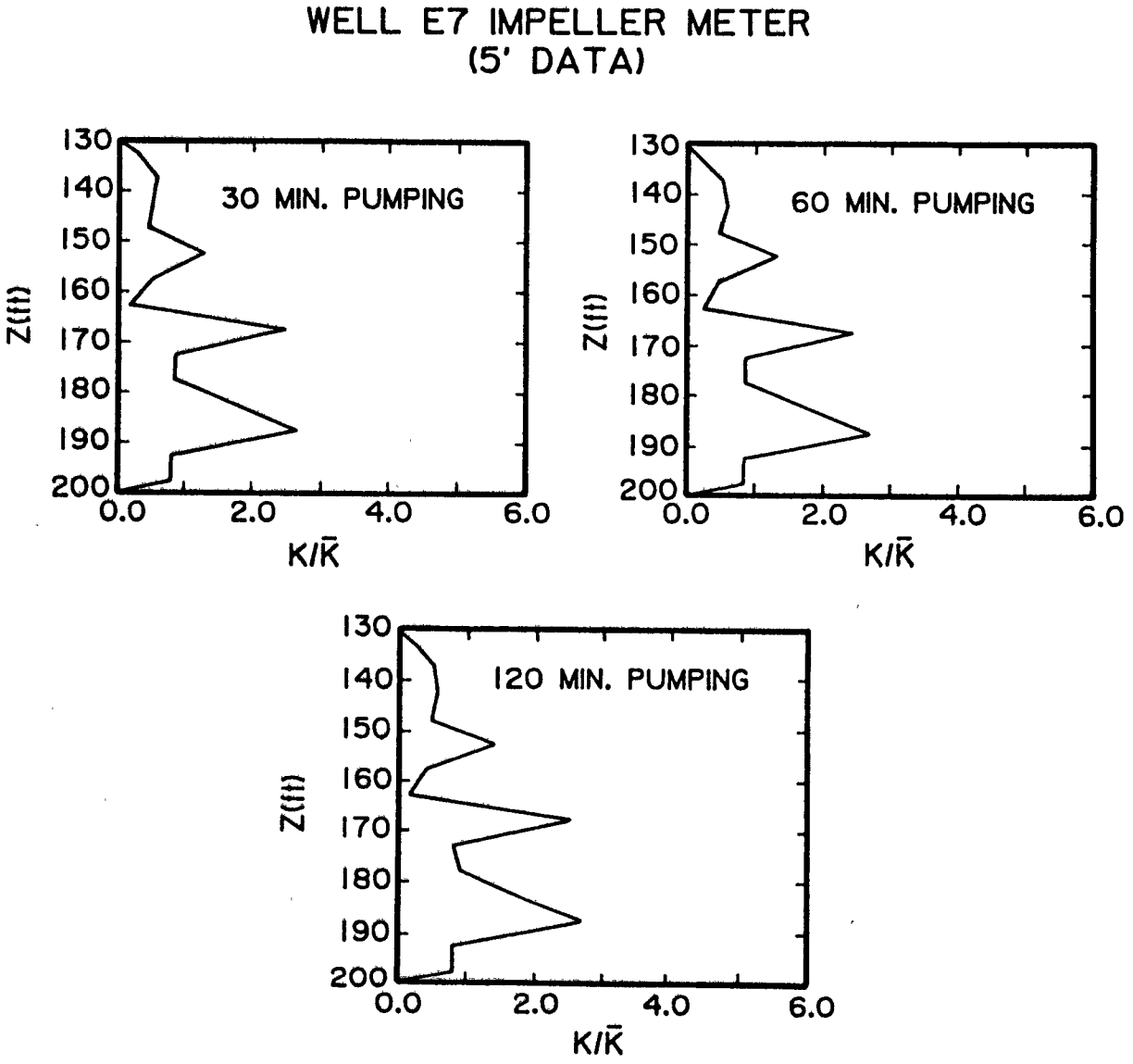


Figure II-16. Dimensionless hydraulic conductivity distributions at five-foot intervals in well E7 taken 30 min., 60 min. and 120 min. after the start of pumping. The results show good repeatability of the impeller meter method.

As shown in Figure II-8, wells E7, E8 and E9 are located along a common line, which runs approximately in an east-west direction. As the measurement scale gets larger, all three wells begin to approximate something like a triangular distribution with a peak in the bottom third of the aquifer. In the perpendicular direction, the same general behavior is demonstrated by wells A7, A8, A9 and to a lesser extent by A6. Thus, with respect to the vertical coordinate, the mean horizontal hydraulic conductivity is not constant with depth. There is a definite trend toward a hydraulic conductivity peak in the bottom third of the aquifer, and a smaller, less consistent peak in the top third. In the language of stochastic hydrology, one would say that the K(z) distribution is nonstationary (Russo and Jury, 1987a,b).

## II-4 Summary and Conclusions Concerning Impeller Meter Applications

Once the necessary equipment is obtained, impeller meter tests can be a relatively quick and convenient method for obtaining information about the vertical variation of horizontal hydraulic conductivity K(z) in an aquifer. This information can be used in a variety of ways including the design of sampling/monitoring wells or pump and treat systems. It can also be used as the basis for the development of three-dimensional flow and transport models which will be far more realistic than their vertically-averaged forerunners. (Applications to fractured rock hydrology are described in Chapter IV.)

Over the past several years at the Mobile site, a fairly large amount of hydraulic conductivity data have been developed based in part on fully penetrating pumping tests, both large and small scale, and impeller meter tests. As far as contaminant transport predictions are concerned, the pumping tests alone are of limited use because by their nature they fail to show the large amount of vertically-distributed heterogeneity that is apparent to varying degrees in the impeller meter tests. This may be obvious, but merits emphasis because fully penetrating tests and vertically-averaged properties are still the mainstay for dealing with contaminant migration problems in the field. Obviously, this has to change. Vertically distributed information is vital to successful remediation design and meaningful simulation of contaminant transport in aquifers.

Although much less restrictive than the assumption of a vertically homogeneous aquifer, the assumption of a layered, stratified aquifer in the vicinity of a test well is still limiting to complete characterization of the unknown three-dimensional variations that actually exist. Thus errors will be made in analyzing a given test, and discrepancies will arise when different types of tests are compared, or even when the same test is analyzed using different methods. Our data suggest that the best strategy for suppressing such errors or discrepancies may consist of using an impeller meter to obtain a dimensionless $K/\overline{K}$ distribution and then a standard pumping test, or a slug test, to compute $\overline{K}$. Combining both types of information enables one to "fit" an impeller meter test to a given aquifer and to obtain dimensional values for K(z). Shown in Figure II-5 is the type of information that results when the two testing procedures are combined.

In the flowmeter applications at Mobile, a different $K(z)/\overline{K}$ distribution was obtained at every vertical scale of measurement at each of seven different wells. As one would expect, the smaller the vertical scale of measurement the larger the degree of heterogeneity that becomes apparent.

In such a system that shows increasing heterogeneity at decreasing scales of measurement, one is led to ask the question: "What scale of measurement is appropriate for a given application?" Although there are some promising approaches in the area of geostatistics for answering this question, the authors have left this question largely unanswered in a general sense. However, based on our studies at the Mobile site, a rule of thumb would be to use measurement intervals of about one tenth of the aquifer thickness [Molz et al., 1989b]. However, once the equipment is set up, one foot measurement intervals would be practical in most aquifers. If at a later time less detailed data is desirable, one could use every other data point, or every third data point, etc.

# CHAPTER III

# MULTI-LEVEL SLUG TESTS FOR MEASURING HYDRAULIC CONDUCTIVITY DISTRIBUTIONS

## III-1 Introduction

As discussed in Appendix I, the impeller meter test procedure is generally superior to the multilevel slug test approach, because the latter procedure depends on one's ability to isolate hydraulically a portion of the test aquifer using a straddle packer. However, if reasonable isolation can be achieved, which was the case at the Mobile test site, then the multi-level slug test is a viable procedure for measuring K(z). All equipment needed for such testing is available commercially, and the test procedure has the added advantage of not requiring any water to be injected into or withdrawn from the test well if a water displacement technique is used to cause a sudden head change.

The testing apparatus used in the applications reported herein is illustrated schematically in Figure III-1 for the aquifer geometry at the Mobile site. Two inflatable packers separated by a length of perforated, galvanized steel pipe comprised the straddle packer assembly. The test length of aquifer defined by the straddle packer was L=3.63 ft. (1.1 m). A larger packer, referred to as the reservoir packer, was attached to the straddle packer with 2" (5.08 cm) Triloc PVC pipe, creating a unit of fixed length of approximately 100 ft (30.5 m) which could be moved with the attached cable to desired positions in the well. When inflated, the straddle packer isolated the desired test region of the aquifer and the reservoir packer isolated a reservoir in the 6" (15.2 cm) casing above the multilevel slug test unit and below the potentiometric surface of the confined aquifer.

An advantage of this unit design was that the length of 2 in (5.08 cm) connecting pipe and other geometric factors contributing to frictional losses remained unchanged regardless of packer elevation in the well. (This was possible at the Mobile site because the piezometric surface was approximately 120 ft (36.6 m) above the top of the 70 ft (21.3 m) thick aquifer.) For the straddle packers, the inflatable lengths were 24.5 in. (62.2 cm) (model 36, pneumatic packer, Tigre Tierra, Inc.) and for the reservoir packer the inflatable length was 39.0 in. (99.1 cm) (model 610, pneumatic packer, Tigre Tierra, Inc.)

## III-2 Performance of Multi-Level Slug Tests

Multilevel slug tests are described for three wells (E3,E6,E7) at the Mobile, Alabama site shown in the plan view of Figure III-2. The wells, formerly used as multilevel tracer sampling wells (Molz, et al. 1988), were constructed of 6 in (15.2 cm) PVC casing down 130 ft (39.6 m) to the top of the medium sand aquifer. Fully slotted 4 in (10.2 cm) PVC pipe extended an additional 70 ft (21.3 m) through the aquifer as shown in Figure III-1. Well E3 was an exception, having 3 ft (0.91 m) slotted pipe sections separated by 7 ft (2.13 m) solid sections through the aquifer.

In a typical test, water was displaced in the reservoir above the packer. The head increase then induced a flow down through the central core of the reservoir packer and down the TriLoc pipe to the straddle packer assembly. In the assembly, water flowed from the perforated pipe, through the slotted well screen, and into the test region of the aquifer.

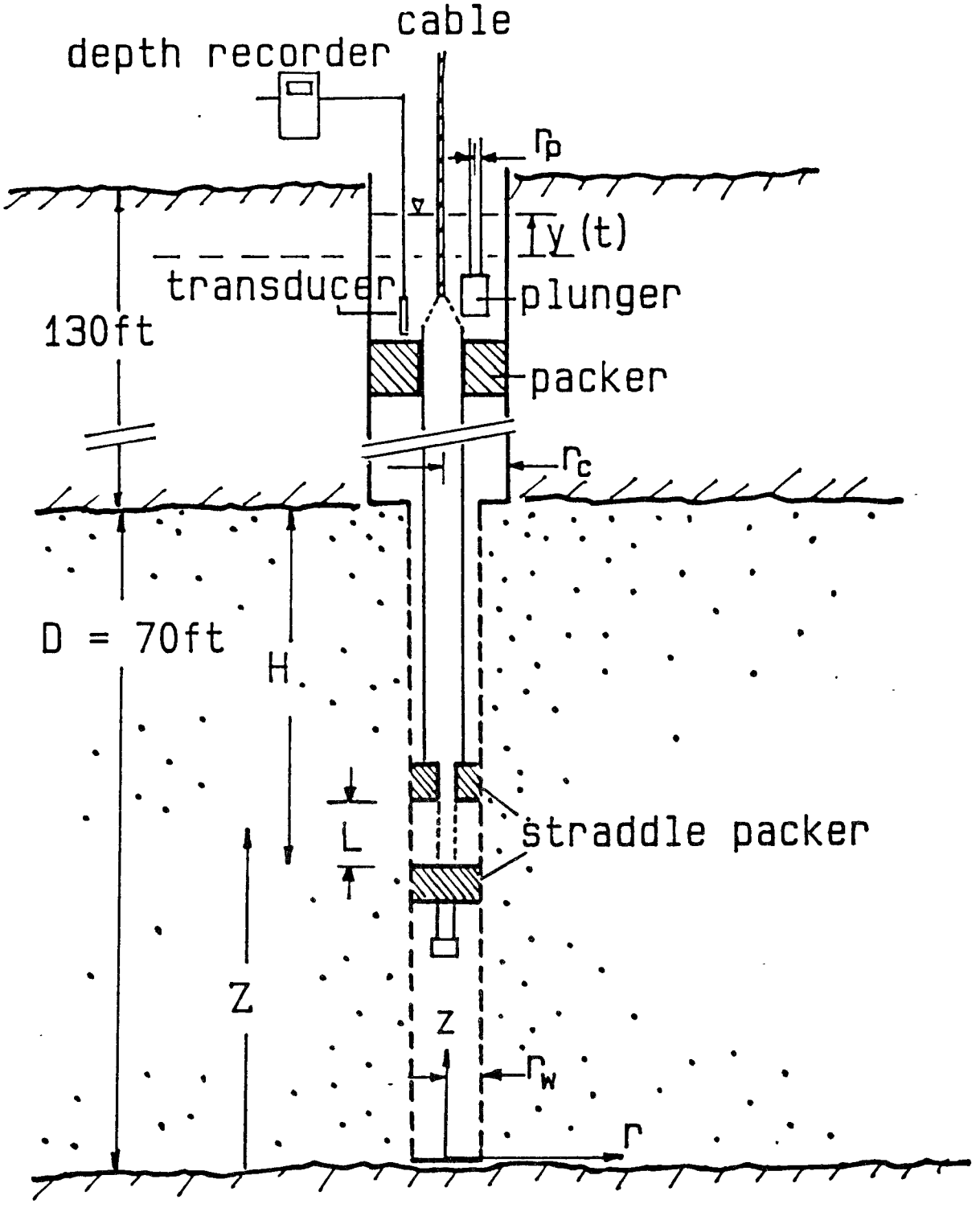


Figure III-1. Schematic diagram of the apparatus for performing a multi-level slug test.

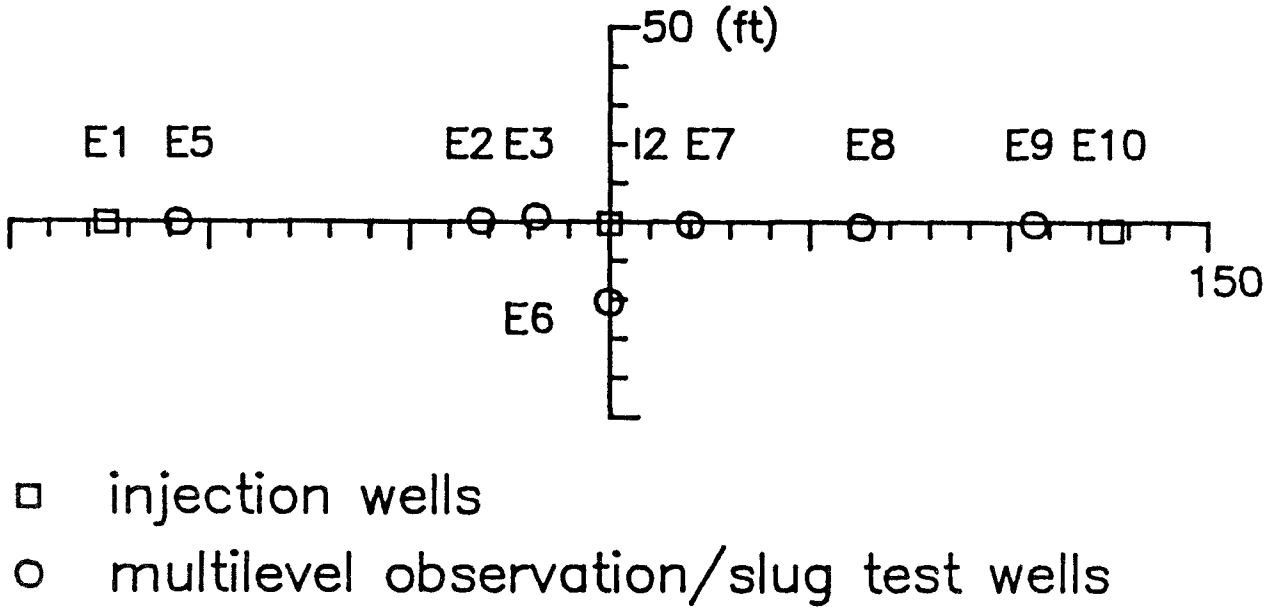


Figure III-2. Plan view of part of the well field at the Mobile site.

The multilevel unit described was used for slug tests by inserting the plunger, displacing a volume of water in the reservoir and then recording the depth variation, y=y(t), relative to the initial potentiometric surface (falling head test). Plunger withdrawal was used to generate a rising head test. Head measurements were made with a manually operated digital recorder (Level Head model LH10, with a 10 psig pressure transducer, In Situ, Inc.).

Typical results of a series of tests at different elevations are shown for well E6 in Figure III-3. The data shown are from plunger insertion tests where a sudden reservoir depth increase to approximately $y_o$=3 ft (0.91 m) was imposed. The depth variation, y=y(t), which is nearly an exponential decay, is a result of flow into the aquifer test section adjacent to the straddle packer. The different slopes of the straight line approximations (least squares fits) are due to the variability of the hydraulic conductivity in the aquifer at the different test section elevations. Tests repeated at a given elevation were generally reproducible, as shown in Figure III-4, with the maximum difference in slopes of the straight line fits to the data being 10% or less.

An initial exception to the general rule of reproducible behavior was observed in well E6. Shown in Figure III-5 are the results of tests at two elevations conducted on three different days in well E6. For the tests of July 20, 1987, the well had been undisturbed for approximately 40 days. For the repeated tests on July 21, 1987, the well was developed by repeated air injection and flushing prior to the slug testing. Noting the significant change, particularly for the curves having larger slope (higher hydraulic conductivity), the tests were repeated on July 30, 1988 after more extensive development with an air jetting tool at the bottom of the well. With this third set of data in close agreement with the second set, it was decided that the development was sufficient. This behavior was not observed at the other test wells; however, all tests were done after a small amount of well re-development. The well construction, originally done for tracer observations (Molz, et al., 1986a, 1986b), was intended to minimally disturb the aquifer close to the screen. Particularly after the passage of several months, some minor redevelopment is important prior to hydraulic testing. It seems that clay and silt materials tend to migrate into the well, coat the screen and often collect at the well bottom.

Multilevel slug testing will be meaningful only if the straddle packer system isolates hydraulically the segment of the screen and the adjacent aquifer. Channels, which will negate the packer seal, may be present in the well screen structure or can be caused by failure of the formation or backfill material to fill the annulus between the screen and the borehole. Similarly, any backfill material of greater permeability than the formation can allow flow to bypass the packers rather than having outward flow into the test section. Additional pressure monitoring above and below the straddle packer assembly may be desireable if nonisolation problems are suspected (Taylor et al., 1989).

## III-3 Analysis of Multilevel Data

Three methods of analysis have been applied to the collected data. In the first and second methods, it is assumed that the flow from the test section is horizontal and radially symmetric about the axis of the well. In the first method the quasi-steady state assumption is made. In the second, a transient analysis is applied. In the third analysis, also quasi-steady state, the possibility of vertical flow and anisotropy are considered using a finite element model.

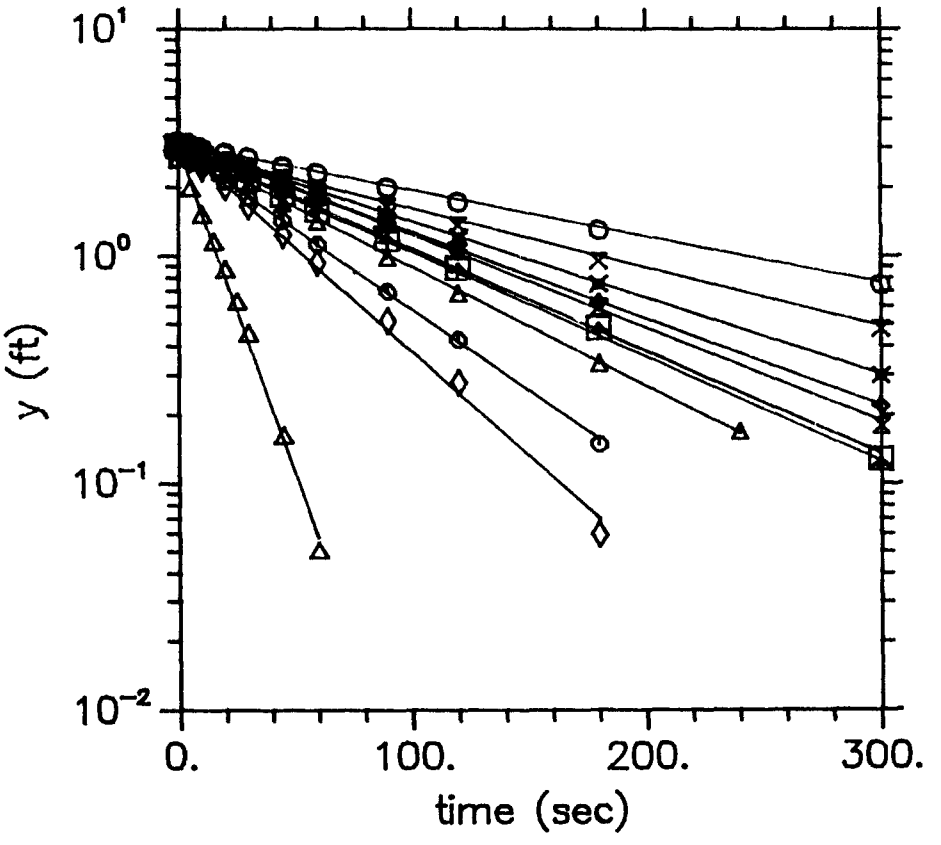


log(y)=−0.0280t+0.47 Z=11.2 ft
log(y)=−0.0045t+0.49 Z=17.2 ft
log(y)=−0.0020t+0.50 Z=23.2 ft
log(y)=−0.0038t+0.49 Z= 5.2 ft
log(y)=−0.0041t+0.51 Z=29.2 ft
log(y)=−0.0034t+0.49 Z=35.2 ft
log(y)=−0.0026t+0.47 Z=41.2 ft
log(y)=−0.0046t+0.48 Z=47.2 ft
log(y)=−0.0053t+0.48 Z=53.2 ft
log(y)=−0.0071t+0.47 Z=59.2 ft
log(y)=−0.0092t+0.50 Z=65.2 ft

Figure III-3. Multilevel slug test data from well E6. $B=\log(y_1/y_2)/(t_2-t_1)$ = magnitude of the slope of the log y(t) response.

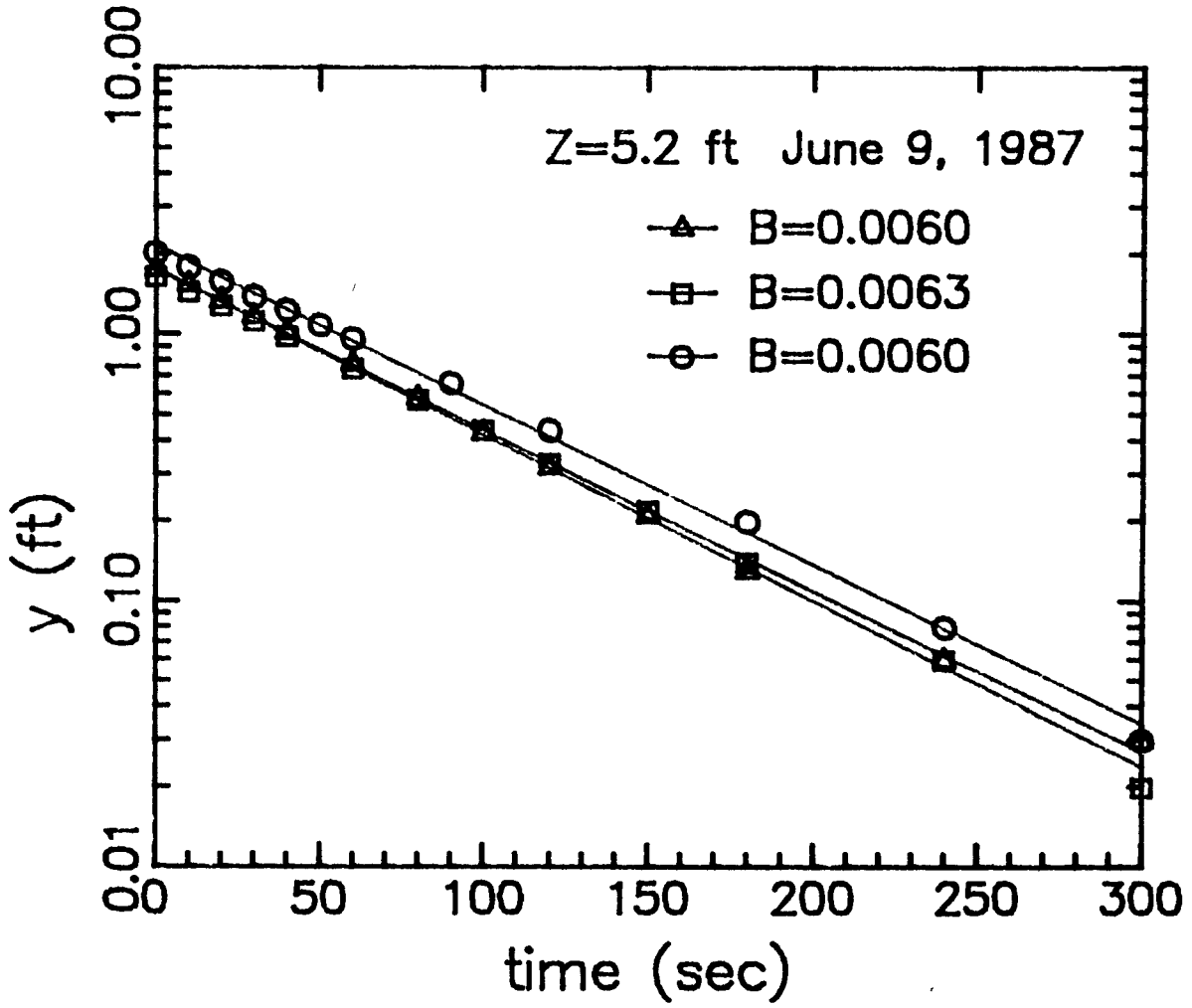


Figure III-4. Plot showing the reproducibility of data collected at well E6.

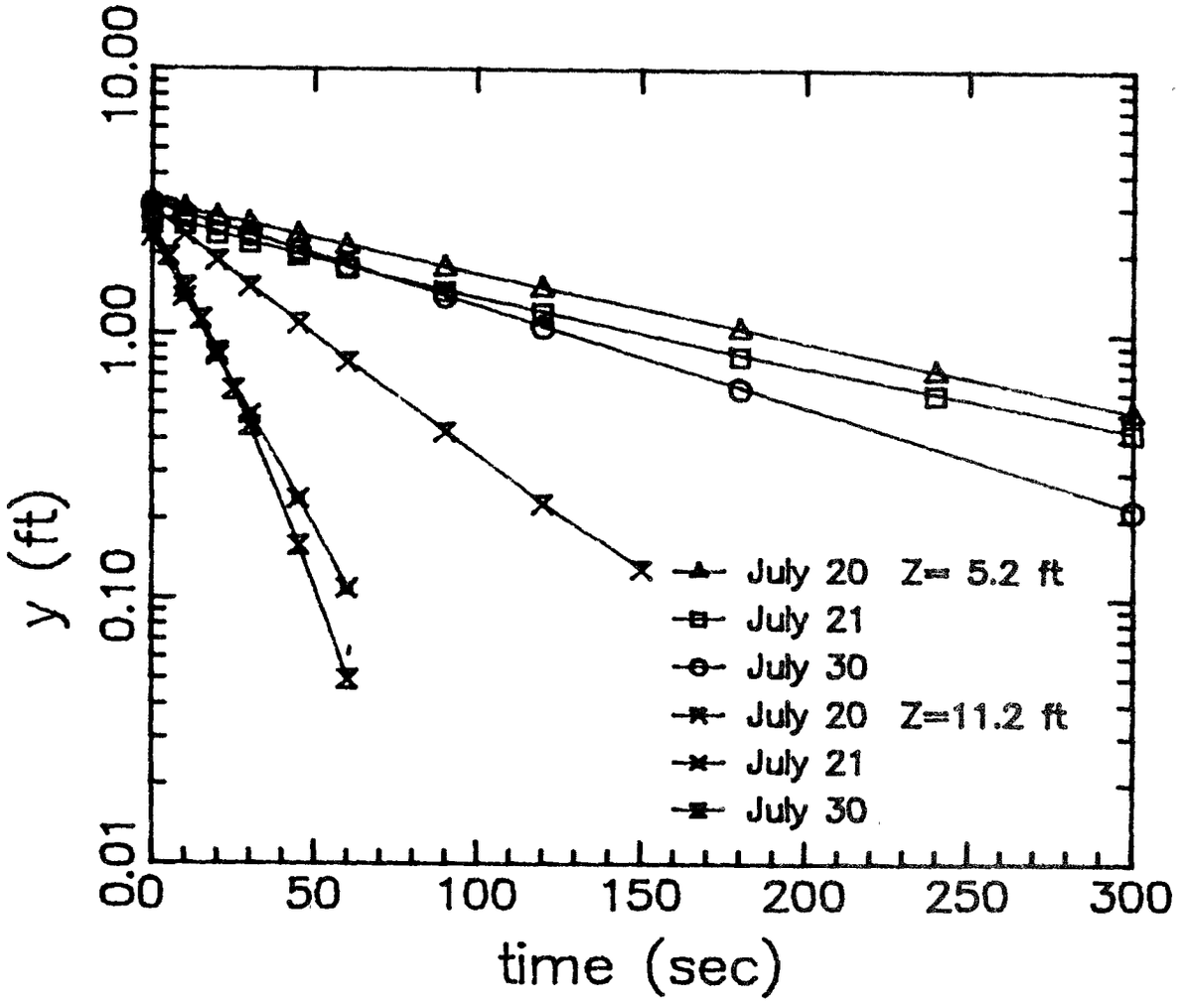


Figure III-5. Plots showing the influence of well development at two elevations in well E6.

III-3.1 Quasi-Steady Radial Flow Assumption

A very common analysis of slug test data (Hvorslev, 1951) assumes that the radial seepage is steady state (no aquifer storage effects) and that the head increase induced during the test is zero at the radius of influence, $r=r_e$. If B is the magnitude of the slope of the log y(t) response (Figure III-3), the hydraulic conductivity, based on this radial, quasi-steady analysis is

$$K = 2.30B(r_c^2 - r_p^2)\ln(r_e/r_w)/2L \qquad \text{(III-1)}$$

where K = hydraulic conductivity, $r_c$ = casing radius, $r_p$ = plunger radius, B = magnitude of the slope of log [y(t)], $r_e$ = radius of influence, $r_w$ = well screen effective radius, and L = separation length of straddle packers. If the plunger is not used, or in the case of plunger withdrawal (rising head test), then $r_p = 0$ in equation (III-1). This method of interpretation is somewhat arbitrary since $r_e$ is not measured and is basically an adjustable parameter in the Hvorslev (1951) method. Chirlin (1989) pointed out that $r_e$ should be interpreted as a storage-effect parameter. For this study, $r_e$ = 60 ft (18.29 m) was chosen. This value of $r_e$ results in K(z) values similar to those calculated in the transient analysis which follows. This similarity of K(z) values and dependence on $r_e$ is consistent with Figure 4 of the critique by Chirlin (1989). For well E6, the slopes from Figure III-3 and the K(z) values calculated using equation (III-1) are shown in Table III-1.

III-3.2 Radial, Transient Flow Assumption

With the radial flow assumption, the slug test interpretation is equivalent to the fully-penetrating analysis of Cooper, et al. (1967) and the extension of the analysis by Papadopulos et al. (1973). In these analyses, the response of a finite diameter well to an instantaneously injected or withdrawn volume of water is considered, and a set of type curves, Figure III-6, is presented which permit the matching of slug test data to determine the transmissivity of the aquifer. The storage coefficient of the aquifer can, in theory, also be determined with this matching method, but the accuracy is poor as discussed in the two original papers. In this transient model, there is no need for a $r_e$ parameter.

Previous full-aquifer pumping tests at the Mobile site (Parr et al., 1983) have indicated a specific storage of $7.14 \times 10^{-6}$ ($ft^{-1}$) ($2.18 \times 10^{-6}$ m). If it is assumed that the full-aquifer result applies on the smaller scale of the multilevel tests described here, then the storage coefficient for the test length of L = 3.63 ft (1.1 m) is $S = 2.6 \times 10^{-5}$.

For slug testing with the plunger in place the parameter defined by Cooper et al., (1967) is modified to $\alpha = Sr_w^2/(r_c^2 - r_p^2)$. Thus, for the match point, (t,T) the hydraulic conductivity is determined from

$$K = T(r_c^2 - r_p^2)/Lt. \qquad \text{(III-2)}$$

Slug test data taken at 11 elevations in well E6 as shown in Figure III-7 are plotted on a log-linear scale. Determination of storage coefficients from these data, which has questionable reliability using this method (Cooper et al. 1967), was not done since the value of S determined from full aquifer tests was available. These points for the data and type curves are shown in Table III-1. The match points were obtained by visual inspection in the attempt to best fit the data between the $\alpha=10^{-4}$ and the $\alpha=10^{-5}$ curves of Figure III-6. These bounds were obtained based on our measured values for S. Match points for the curves of Figure III-7 are shown in Table III-1, with the corresponding calculations for hydraulic conductivity at each elevation. Repeated independent visual fits using this method provided reproducibility within

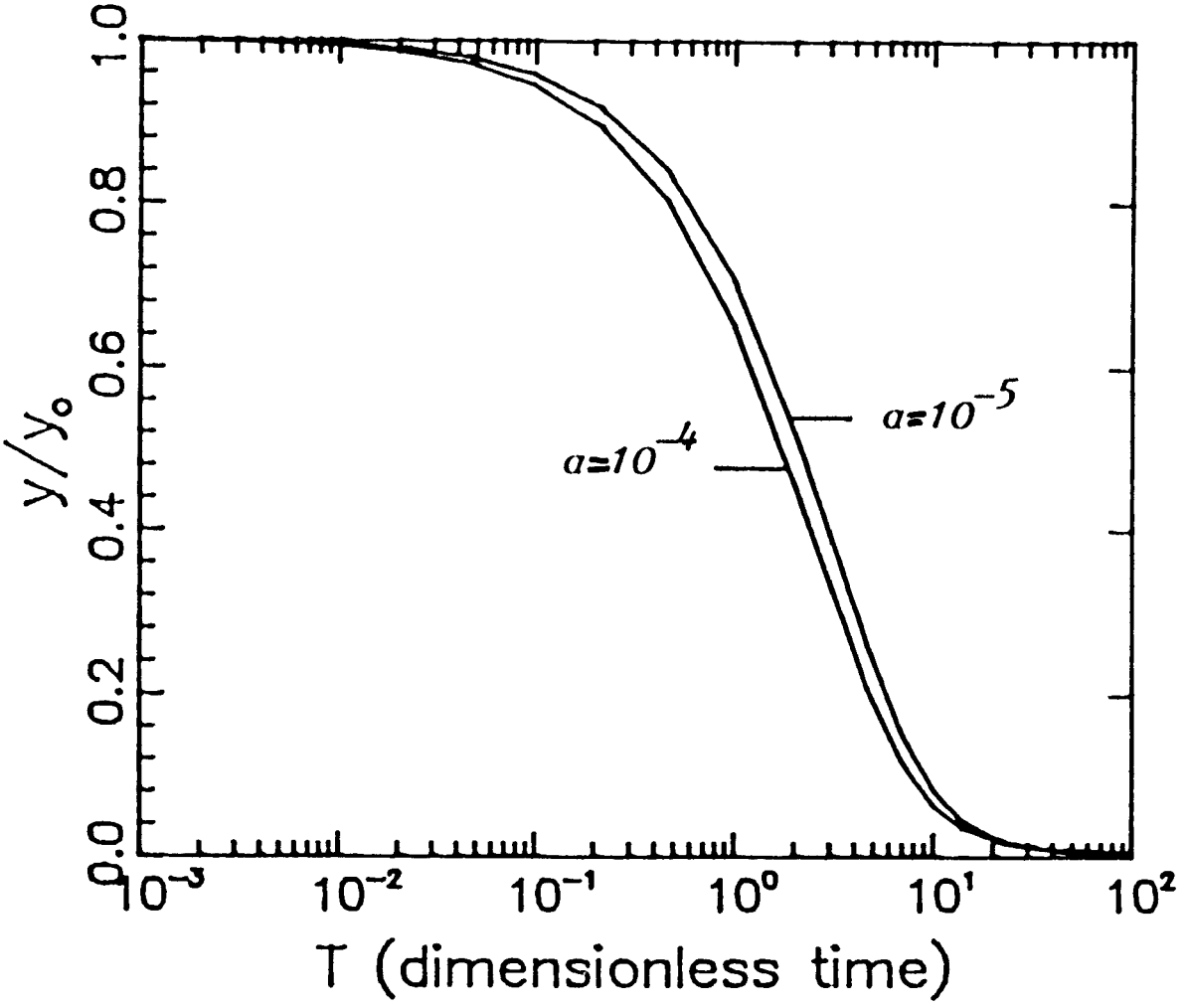


Figure III-6. Example type curves from Cooper, Bredehoeft and Papadopulos (1967).

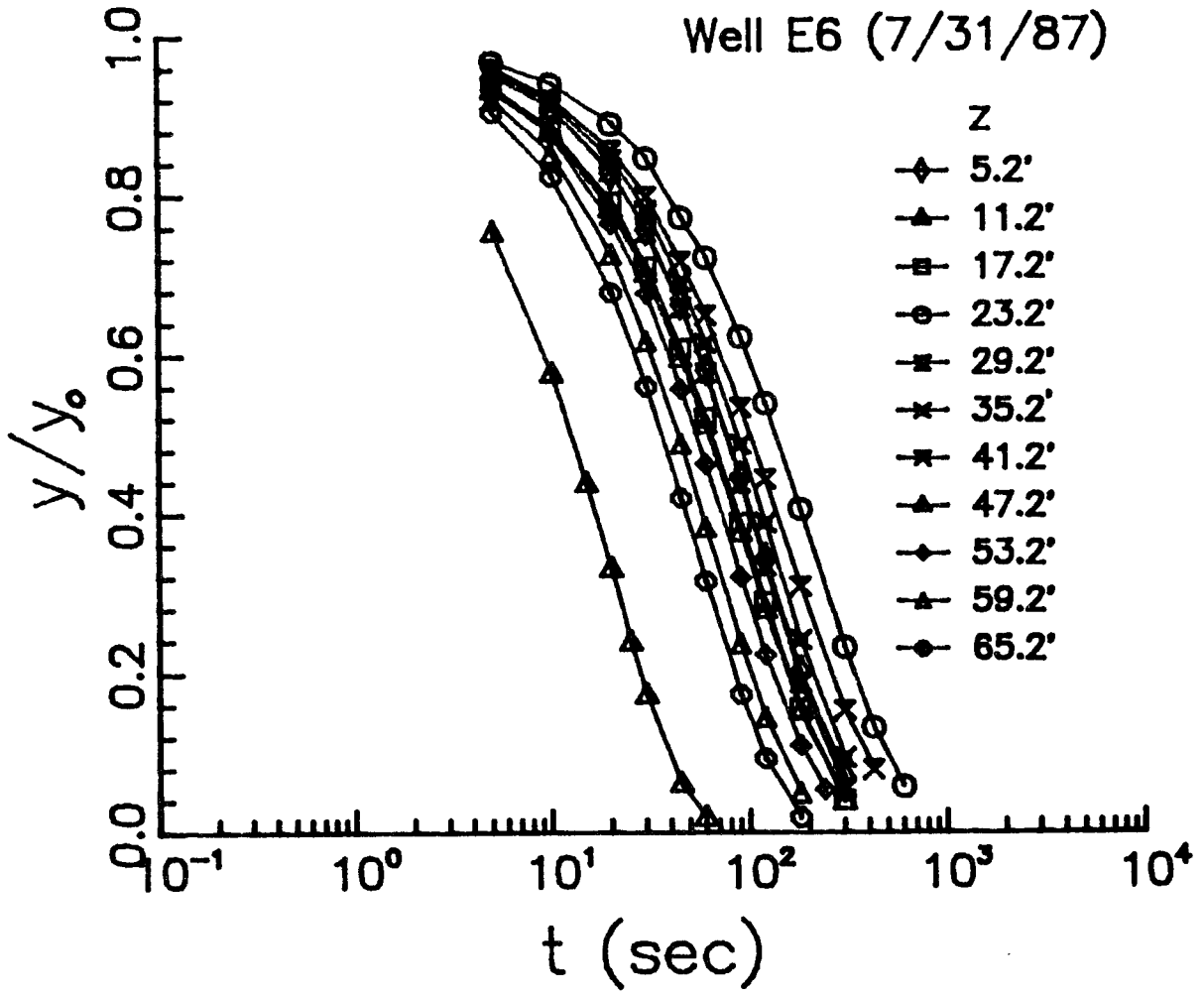


Figure III-7. Slug test data from different elevations in well E6.

Table III-1. Multilevel Slug Test Data and Calculated Hydraulic Conductivities at Well E6 (6/31/87 data)

| Elevation Z (ft) | Slope (Figure III-3) B (1/sec) | Eq. (III-1) K (ft/day) | T | Match Point t(sec) | Eq. (III-2) K (ft/day) | Eq. (III-8) K (ft/day) |
|---|---|---|---|---|---|---|
| 5.2 | 0.00383 | 34.8 | 1.0 | 40 | 33.6 | 22.3 |
| 11.2 | 0.0284 | 258.2 | 1.0 | 6 | 223.7 | 162.4 |
| 17.2 | 0.00453 | 41.1 | 3.0 | 100 | 40.3 | 25.9 |
| 23.2 | 0.00205 | 18.6 | 1.0 | 70 | 19.2 | 11.7 |
| 29.2 | 0.00411 | 37.4 | 1.0 | 40 | 33.6 | 23.4 |
| 35.2 | 0.00339 | 30.8 | 9.2 | 400 | 30.9 | 19.3 |
| 41.2 | 0.00261 | 23.7 | 1.0 | 50 | 26.9 | 14.9 |
| 47.2 | 0.00463 | 42.1 | 2.9 | 90 | 43.4 | 26.4 |
| 53.2 | 0.00525 | 47.7 | 3.0 | 80 | 50.4 | 30.0 |
| 59.2 | 0.00712 | 64.7 | 9.0 | 200 | 60.5 | 40.7 |
| 65.2 | 0.00918 | 83.4 | 5.0 | 90 | 74.6 | 54.5 |
| | | $\bar{K}$ = 57.6 | | | $\bar{K}$ = 53.8 | $\bar{K}$ = 36.4 |

approximately 10% which is consistent with field data accuracy. Numerical fitting procedures have also been applied but did not yield a significant change in the K(z) values calculated.

The variation of horizontal hydraulic conductivity with respect to elevation, K(z), is shown in Figure III-8 for well E6. This K(z) profile is based on one slug test at each of the 11 elevations. The length of the aquifer isolated by the straddle packers, L=3.63 ft (1.1 m), is shown in the figure. Short sampling lengths and/or more sampling elevations would produce K(z) profiles of more detail.

III-3.3 Quasi-Steady State Radial and Vertical Flow Assumption

Dagan's (1978) partially-penetrating well test analysis considers the double packer configuration for determining hydraulic conductivity in unconfined aquifers. The effects of vertical as well as radial components to the aquifer flow are included in the analysis. However, the analytical solution presented and the resulting dimensionless curves apply to an unconfined aquifer and are valid only if the distance between the packers (L) is at least 50 times greater than the well screen radius ($r_w$). Braester and Thunvik (1984) simulated double packer tests by solving an equation for axisymmetric flow in cylindrical coordinates by the Galerkin method and were able to produce results consistent with those derived from Dagan's solution. While the study considered the effects of anisotropy and inhomogeneity on interpretation of double packer slug test data, a general solution technique to extract a value for hydraulic conductivity from experimental data was not offered.

The analysis developed is an extension of Dagan's dimensionless-curve approach (1978) using a method similar to Braester and Thunvik (1984). A finite element model (EFLOW, licensed through the Electric Power Research Institute) was modified to simulate multilevel slug tests for a variety of flow configurations and aquifer conditions. Using EFLOW simulation results for a generic confined aquifer, a family of curves was developed and a procedure by which hydraulic conductivity is determined was derived.

Mathematically, the aquifer head distribution is described by the equation,

$$0 = \frac{1}{r}\left(\frac{\partial}{\partial r} rK\left(\frac{\partial h}{\partial r}\right)\right) + K_z\left(\frac{\partial^2 h}{\partial z^2}\right) \qquad \text{(III-3)}$$

Where r = radial coordinate, z = vertical coordinate (as shown in Figure III-2), h = head in the aquifer, K = hydraulic conductivity in the horizontal, radial direction, and $K_z$ = hydraulic conductivity in the vertical direction. Equation (III-3) is independent of time but will be subjected to a time-dependent boundary condition at $r=r_w$. Thus the transient slug test is approximated by a succession of steady states (quasi-steady state model). The boundary conditions are:

$$\frac{\partial h}{\partial z}(r, o) = \frac{\partial h}{\partial z}(r, D) = 0, \text{ for } r_w \le r \le r_e$$

$$\frac{\partial h}{\partial r}(r_w, z) = 0, \text{ for } 0 \le z \le (D\text{-}H) \text{ and } (D\text{-}H+L) \le z \le D$$

and

$$h(r_e, z) = h_o, \text{ for } 0 \le z \le D$$

$$h(r_w, z, t) = h_o + y(t), \text{ for } (D - H) \le z \le (D - H + L)$$

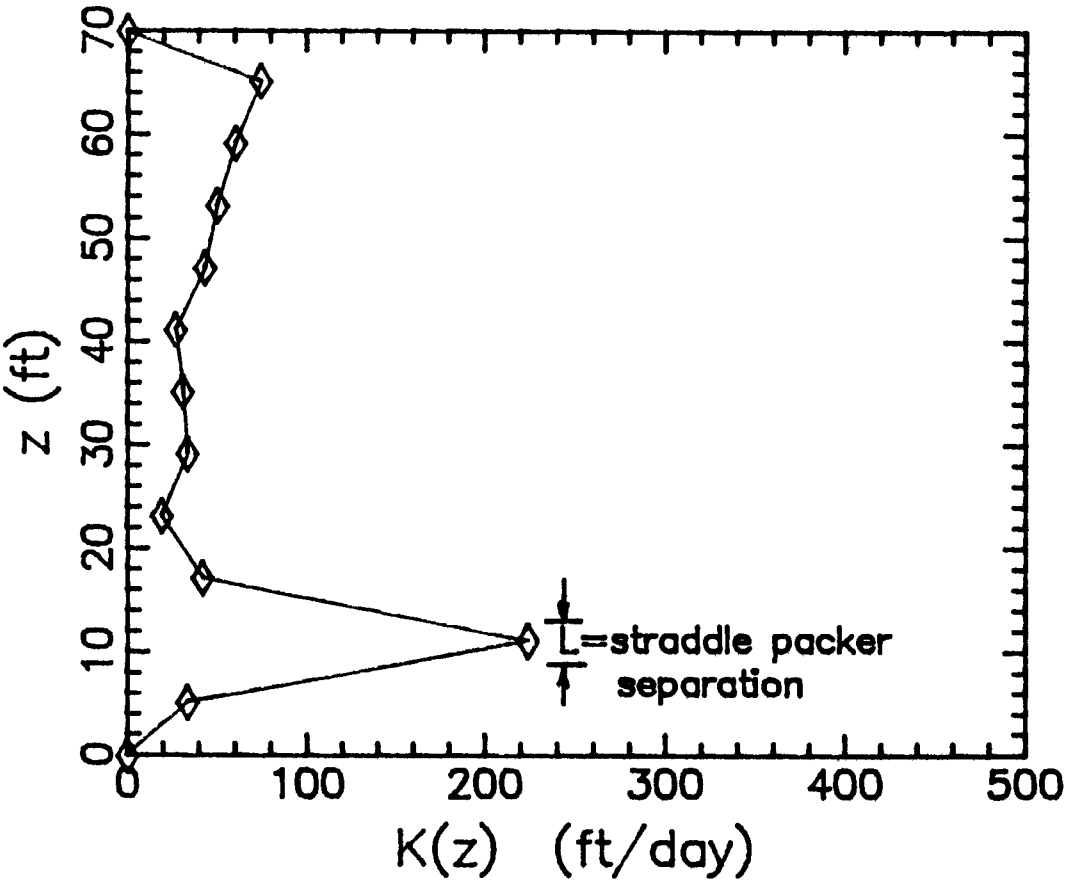


Figure III-8. K(z) profile at well E6 based on the radial transient analysis (Cooper et al., 1967).

where y is the depth increase in the well casing reservoir, $r_w$ = the screen radius, D = the aquifer thickness, $h_o$ = the undisturbed head in the aquifer, and H = the vertical depth to the lower packer (Figure III-2).

By conservation, the change of the reservoir head with respect to time, dy/dt, is related to the volumetric flow rate into the aquifer, Q, by

$$- \pi(r_c^2 - r_p^2)dy/dt = Q \qquad \text{(III-4)}$$

For the succession of steady states and a given aquifer geometry, the flow into the aquifer at any instant of time is proportional to y, i.e. because of the steady-state flow distribution at each time instant, doubling y will double the flow into the aquifer. More precisely,

$$Q = \beta y \qquad \text{(III-5)}$$

where $\beta$ is the constant of proportionality. Combining equations (III-4) and (III-5) and rearranging yields

$$(1/y)dy/dt = d(\ln(y))/dt = - \beta/(\pi(r_c^2 - r_p^2)) \qquad \text{(III-6)}$$

Since the right-hand side of (III-6) is constant, this shows that a plot of ln(y) versus t will yield a straight line.

Through the use of Darcy's law the flow into the aquifer may also be written as

$$Q = 2\pi r_w K \int_{D-H}^{D-H+L} \frac{\partial h(r_w, z)}{\partial r} dz \qquad \text{(III-7)}$$

One may now define a dimensionless flow parameter, P, given by

$$P = \frac{Q}{2\pi KLy} = \left(\frac{r_w}{Ly}\right) \int_{D-H}^{D-H+L} \frac{\partial h(r_w, z)}{\partial r} dz \qquad \text{(III-8)}$$

The parameter, P, depends only on the geometry of a particular slug test. From numerical solutions of equation (III-3) for different geometries and using equation (III-8), Figure III-9 was generated showing the dependence of P on H/L and $L/r_w$. The anisotropy considered here was $K_z/K$ = 0.1 (Parr et al., 1983), which is approximately that which applies at the Mobile site.

Once Figure III-9 is developed for a given anisotropy ratio, it may be used in combination with a semi-log plot of slug test data to calculate the hydraulic conductivity. The procedure is to enter Figure III-9 with the appropriate values of L, $r_w$, and H and obtain the corresponding number for P (call it $P_n$). Then using equation (III-4) one notes that

$$Q = 2\pi KLyP_n = - \pi(r_c^2 - r_p^2)dy/dt \qquad \text{(III-9)}$$

Employing the fact that $(1/y)dy/dt = d(\ln(y))/dt$ and solving equation (III-9) for K yields

$$K = \frac{(r_c^2 - r_p^2)}{2LP_n} \left(\frac{d(\ln(y))}{dt}\right) = \frac{(r_c^2 - r_p^2)}{2LP_n} \quad (2.3B) \qquad \text{(III-10)}$$

where B is the slope of a semi-log plot (base 10 logs) of y versus t as shown in Figure III-3. An example calculation of K using equation (III-10) is shown in Appendix II.

The radius of influence for this study was chosen as $r_e$ = 60 ft (18.3 m) to be consistent with that used in method 1. For the geometries of the slug tests described here, the dependence of K on $r_e$ is not so strong as it is in equation (III-1). For example, if $r_e$ is

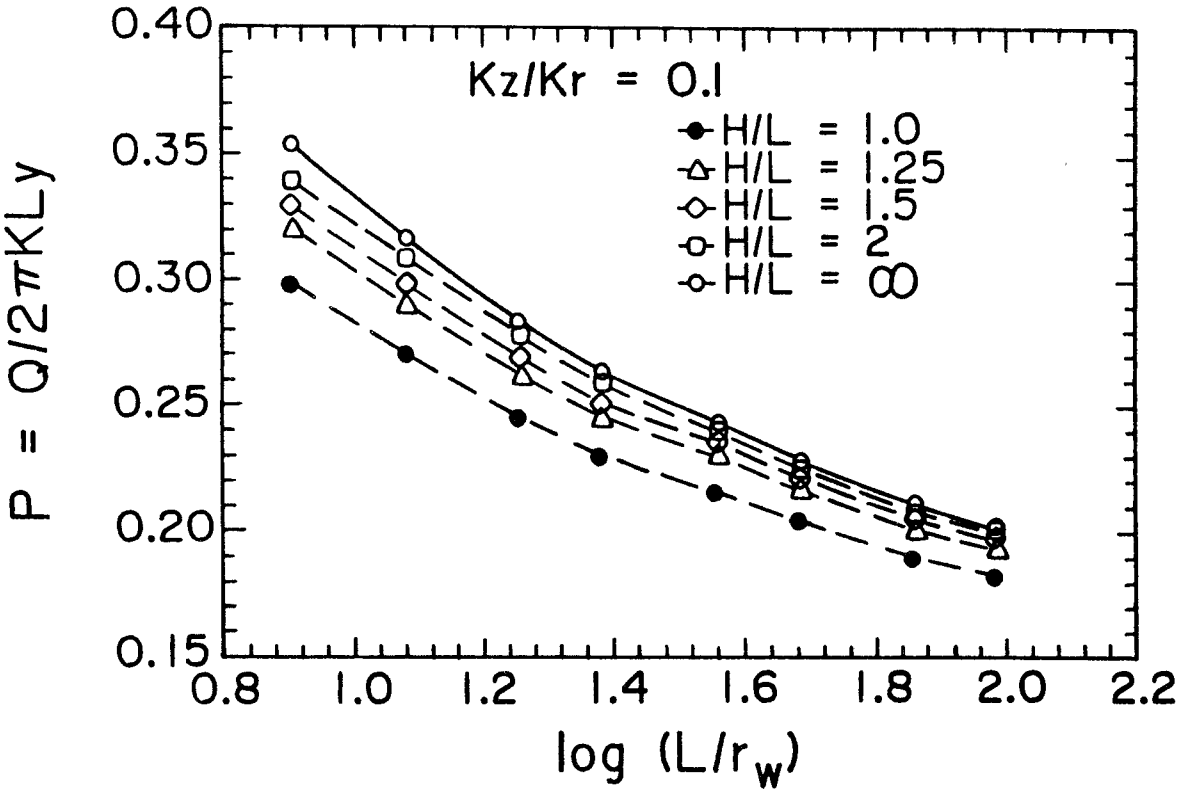


Figure III-9. Dimensionless flow parameter for consideration of vertical flow and anisotropy. These curves apply for D/H > 2, i.e. effects of the far boundary are not considered. For test interpretation when D/H <2, the same curves can be applied if H is redefined as the distance from the lower confining layer to the top of the straddle packer. (Widdowson et al., 1989).

increased from 60 ft (10.3 m) to 600 ft (182.9 m), the increase in K is less than 5%. (For equation (III-1) the increase in K would be by a factor of 2.3). The matter of K dependence on $r_e$ and $S_s$ as studied by Chirlin (1989) deserves further investigation for the geometry of the multilevel slug tests.

The influence of the confining layer boundaries is nearly negligible for the tests considered here. For the tests completed adjacent to the boundary, P = 0.26 is found from Figure III-8. For all the other tests, P = 0.27. When P = 0.27 the values of K calculated from equations (III-10) (method 3) and (III-1) (method 1) are related by

$$K_{(3)} = K_{(1)} / P \ln(r_e/r_w)$$
$$= 0.63 K_{(1)} \qquad \text{(III-11)}$$

Thus, the K(z) profile shapes calculated using equation (III-10) of method 3 are the same as those calculated using equation (III-1). Thus methods 1 and 3 give proportional but not identical results.

## III-4 Results, Discussion and Conclusions

Well E6 slug data, Figure III-3, and the corresponding hydraulic conductivity calculations, Table III-1, are summarized in the K(z) profiles shown in Figure III-10. Based on similar field tests and analyses, K(z) profiles for wells E7 and E3 are shown in Figures III-11 and III-12. For all three wells, the K(z) values calculated using methods 1 and 2 are very similar. Of course, as discussed earlier, the magnitude of K(z) for method 1 is strongly dependent on the choice of $r_e$. The profiles for method 3 are 63% of those calculated using method 1 (with small deviation for those slug tests conducted adjacent to the confining layer boundary).

Although method 3 is under further investigation, it is probable that the magnitudes of the K values based on this method are improved approximations of the aquifer values compared with the K values based on the horizontal, radial flow models. For a slug test in the configuration of Figure III-2, it is obvious that the seepage to or from the aquifer test section is not horizontal only. The vertical component of seepage contributes to the slug test response, y=y(t), and the resulting K values are smaller than those based on radial flow interpretations. Method 3 also allows one to consider the effects of anisotropy.

The similarity of profile shapes for the different methods of analysis is apparent in Figures III-10, III-11, and III-12. If an average of K(z) is calculated for each profile

$$\bar{K} = (1/D)\int_0^D K(z)dz \qquad \text{(III-12)}$$

where the trapezoidal rule is applied to approximate the integral (the values of $\bar{K}$ are shown in Figure III-10, III-11, and III-12), then nondimensional profiles can be generated. These profiles of $K(z)/\bar{K}$ are shown in Figure III-13, III-14, and III-15. The collapse to nearly identical profiles, regardless of the method of data analysis, is evident.

If an average hydraulic conductivity, $\bar{K}$, is available from full aquifer pumping tests, multilevel tests like those described here could be used to develop $K(z)/\bar{K}$ profiles. Then, the full aquifer $\bar{K}$ could be applied to generate the dimensional K(z) profile. For the characterization of contaminant transport, this method of obtaining K(z) profiles would appear

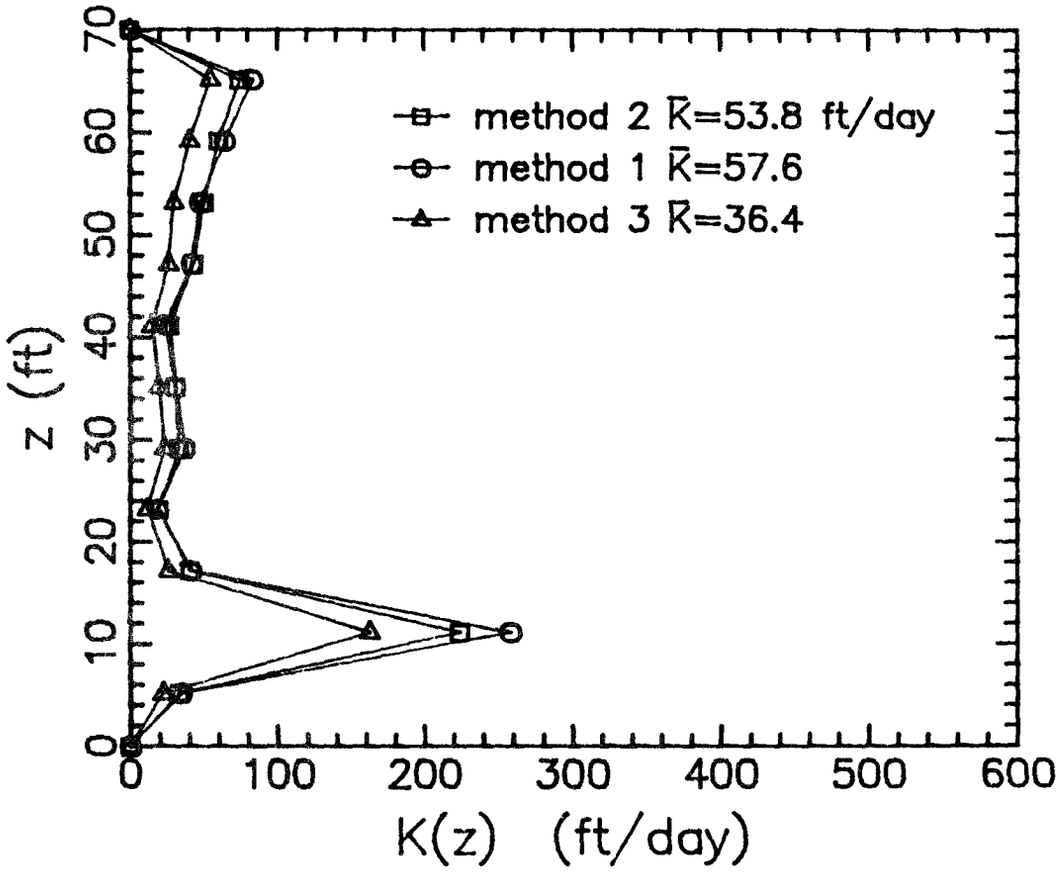


Figure III-10. K(z) profiles for the three different methods of analysis at well E6.

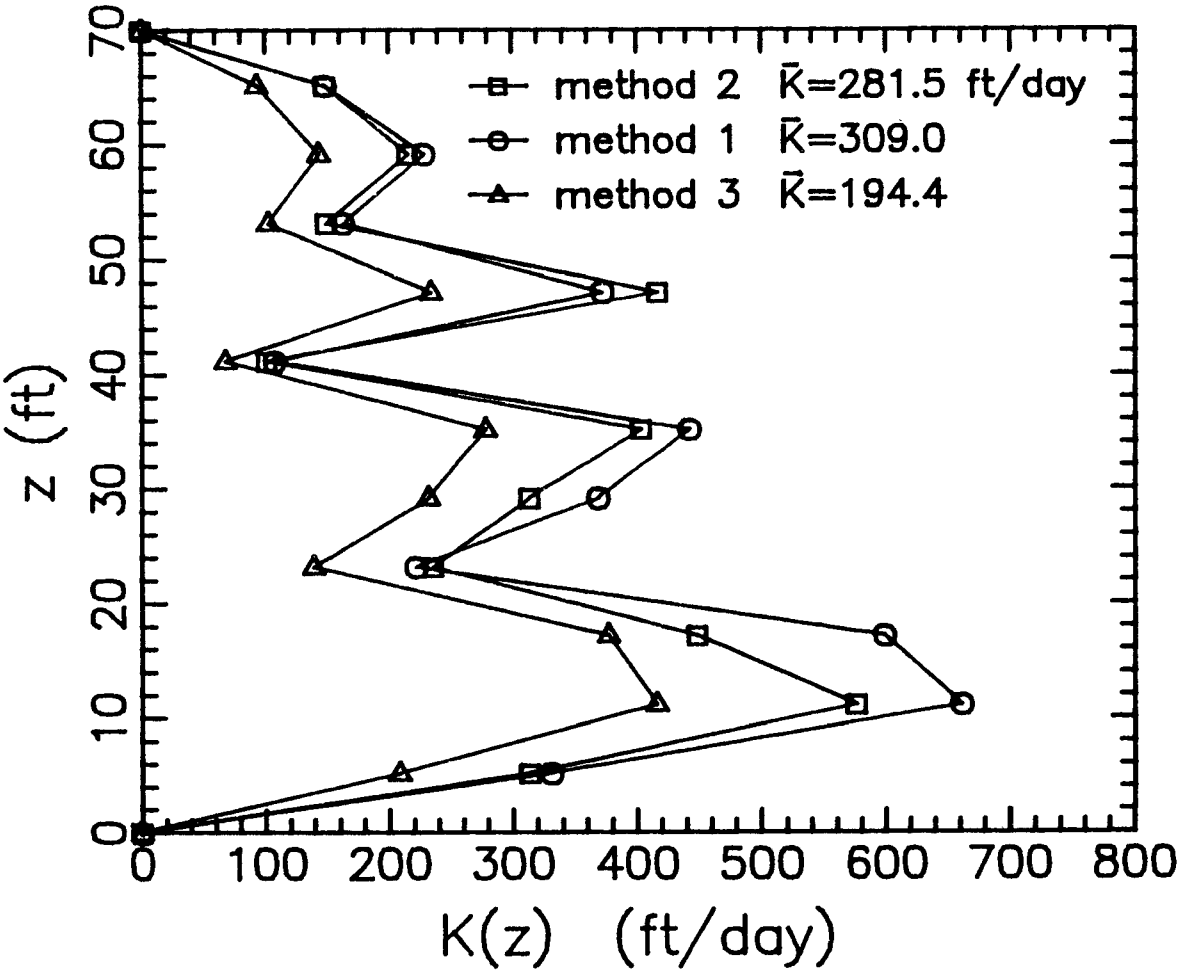


Figure III-11. K(z) profiles for the three different methods of analysis at well E7.

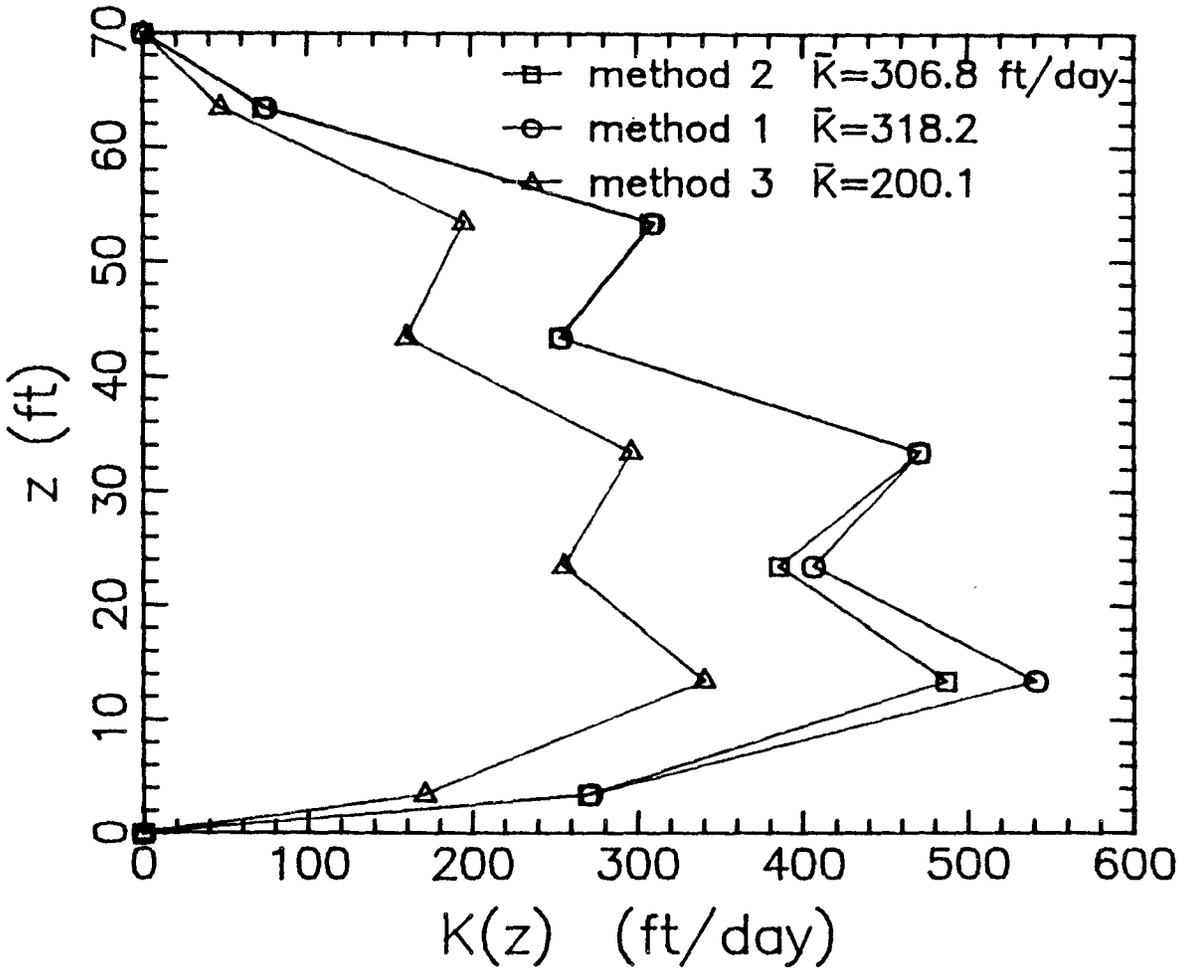


Figure III-12. K(z) profiles for the three different methods of analysis at well E3.

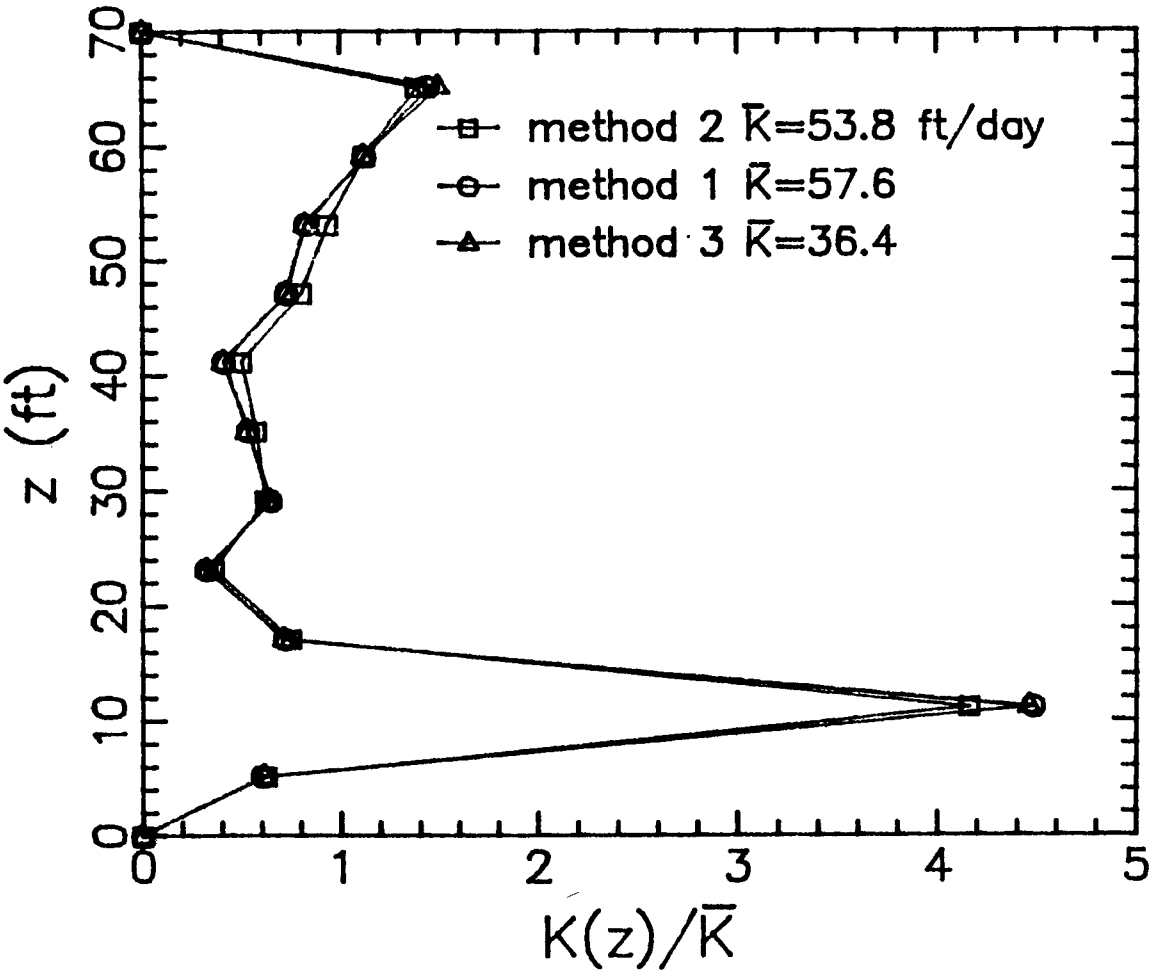


Figure III-13. Dimensionless hydraulic conductivity profiles at well E6.

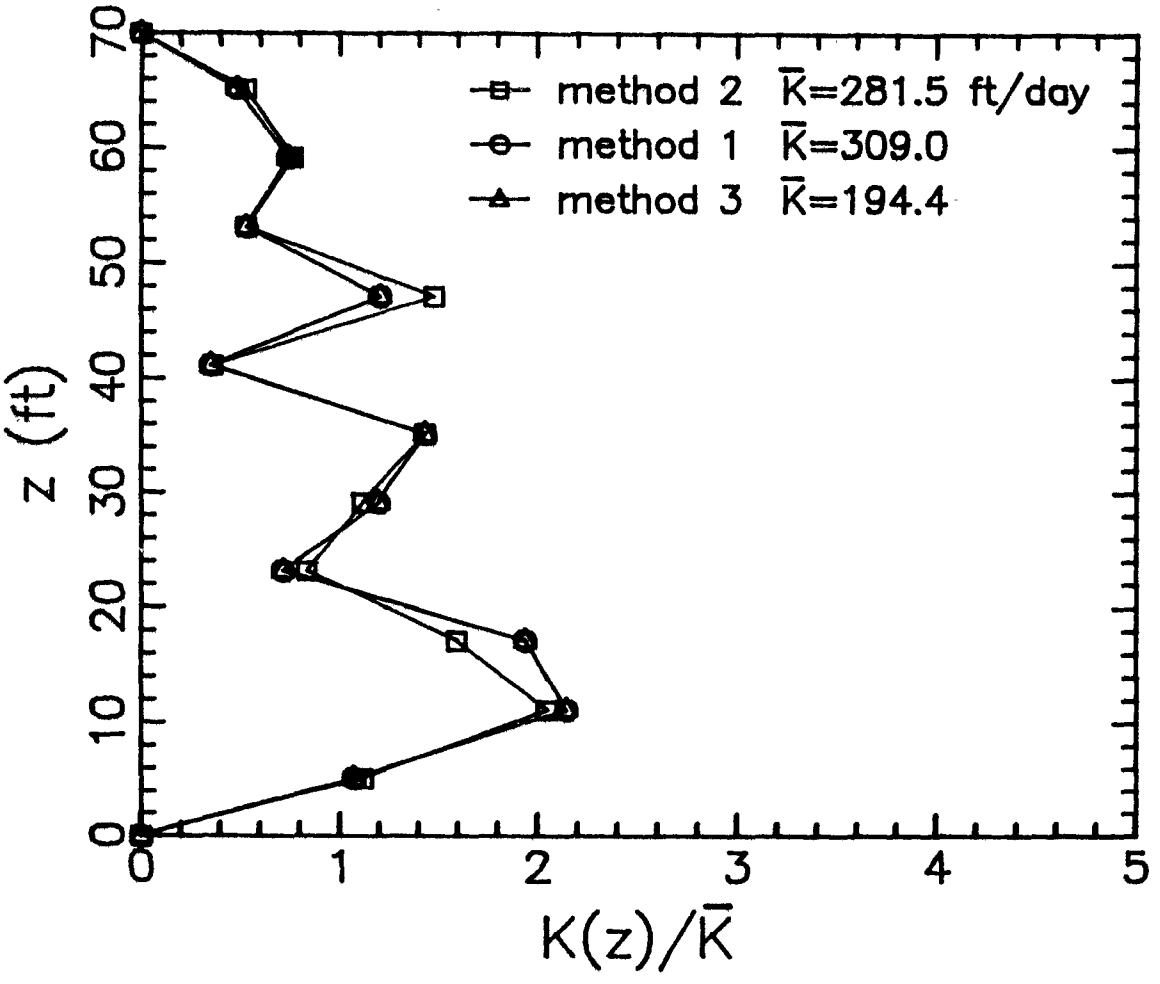


Figure III-14. Dimensionless hydraulic conductivity profiles at well E7.

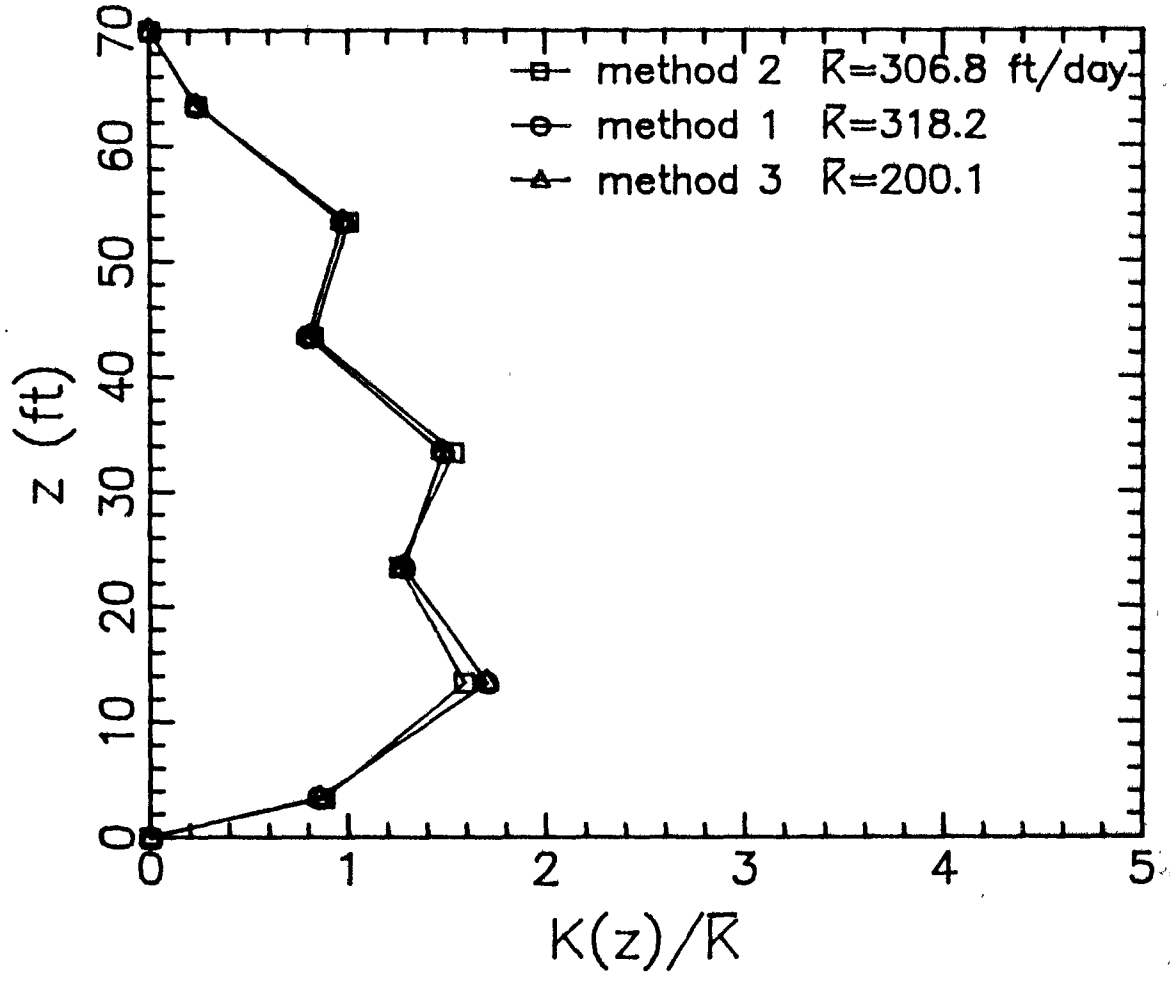


Figure III-15. Dimensionless hydraulic conductivity profiles at well E3.

practical until more confidence in the magnitudes from the multilevel tests can be developed. This point is made also in Chapter I dealing with the impeller meter test.

The K(z) profiles at wells E7 and E3 (Figure III-11 and III-12) are quite similar. A full-aquifer pumping test at well E7, using observation of drawdown at E7, resulted in $\bar{K}$ = 218 ft/day (66.4 m/day) which supports the validity of the slug tests and analysis completed for well E7. Full aquifer pumping test data at E3 are not available. A full aquifer pumping test at E6 resulted in $\bar{K}$ = 123 ft/day (37.5 m/day). This value of $\bar{K}$ does suggest a heterogeneity of low permeability, but is not so small as the K values calculated from the multilevel slug tests at well E6.

Several colleagues have expressed serious reservations about the reliability of slug test data. We are sure that the slug tests performed in wells having slotted screens at the Mobile site are reasonably accurate. However, we were unable to perform slug tests in wells having wire-wrapped screens because of vertical water leakage in the screen structure that could not be prevented with packers. As discussed in Braester and Thunvik (1984), partially-penetrating slug tests are very sensitive to cylindrical annuli of high or low permeability surrounding a well. Thus test wells must be prepared and developed very carefully if they are going to be used for slug tests. Gravel or sand packs must never be used. Tests in unscreened boreholes are questionable because the surface of the formation can become coated with low permeability materials. It must be admitted that all of these considerations make multi-level slug testing much more problematical than impeller meter testing. However, if the formation permeability is sufficiently low, an impeller meter can not be used because of stall speed problems, and multilevel slug testing may be a viable alternative.

# CHAPTER IV

# CHARACTERIZING FLOW PATHS AND PERMEABILITY DISTRIBUTIONS IN FRACTURED ROCK AQUIFERS*

## IV-1 Introduction

In chapters II and III, the impeller meter test and the multi-level slug test were described as a means for measuring hydraulic conductivity distributions in the vertical. This chapter deals with the application of another type of borehole flowmeter called the heat-pulse flowmeter. This meter can be used as an alternative to an impeller meter in virtually any application, and it has the advantage of greater sensitivity. Increased sensitivity is needed near the bottom of almost any test well where flow velocities are small. Spinner flowmeters measure a minimum velocity ranging from about 3 to 10 ft/min (1 to 3 m/min), which limits their usefulness in many boreholes having slower water movement. Flow volumes of as much as 4 gal/min (15 l/min) may go undetected in a 4-in (10 cm) diameter borehole when flow is measured with a spinner flowmeter, and much larger volumes may go undetected in larger diameter holes. However, impeller flowmeters are available commercially and to the authors' knowledge, heat-pulse flowmeters of the type described herein are not.

Analysis of data obtained with a heat-pulse flowmeter in granular aquifers is identical to that applied to impeller meter data. Therefore, the present chapter will be devoted to the application of flowmeters, particularly heat-pulse flowmeters, to fractured rock aquifers. Such meters may be used to locate productive fracture zones and to characterize apparent hydraulic conductivity distributions. Because flow from or to individual fractures is often small, flowmeters more sensitive than impeller meters are commonly needed.

Several thermal, flow-measuring techniques have been developed or considered for the measurement of slow borehole flow, including a thermal flowmeter described by Chapman and Robinson (1962) and an evaluation of hot-wire and hot-film anemometers in liquids by Morrow and Kline (1971). Dudgeon et al. (1975) reported the development of a heat-pulse flowmeter for boreholes that used a minimal-energy thermal pulse in a tag-trace, travel-time technique. This flowmeter had accurate slow-flow resolution and was only 1.63 in. (41 mm) in diameter, so it could be used in small-diameter boreholes. Although the other thermal flowmeters considered have not proved to be practical in a borehole environment, the commercial version of the Dudgeon-style, heat-pulse flowmeter was determined to be viable even though the instrument lacked features important for borehole use, such as seals which could withstand water pressures to at least 10,000 ft (3,048 m), insensitivity to changes in logging cable resistance and to stray electrical currents which exist in the ground, and integral centralizer (Hess, 1982).

The basic measurement principle of the USGS Meter is to create a thin horizontal disc of heated water within the well screen at a known time and a known distance from two thermocouple heat sensors, one above and one below the heating element. One then assumes that the heat moves with the upward or downward water flow and records the time required for the temperature peak to arrive at one of the heat sensors. The flow velocity is then given by

---

* Material in this chapter was prepared by Alfred E. Hess and Frederick L. Paillet under sponsorship of the Water Resources Division, U.S. Geological Survey, at the Denver Federal Center, Denver, CO 80225.

the known travel distance divided by the recorded travel time. Thermal buoyancy effects are eliminated by raising the water temperature only a small fraction of a centigrade degree.

This chapter describes three case studies where flow measurements were used to provide a quick survey of aquifer hydraulic response in fractured rock. This information then was made available for subsequent studies, which markedly decreased the time that would have been required to complete aquifer characterization by means of conventional hydraulic tests and tracer studies.

## IV-2 The U.S. Geological Survey's Thermal Flowmeter

The urgent need for a reliable, slow-velocity flowmeter prompted the U.S.G.S. to develop a small-diameter, sensitive, thermal flowmeter that would operate to depths of 10,000 ft (3,048 m) or more using 16,000 ft (5,000 m) or longer lengths of conventional four-conductor logging cable (Figure IV-1). The thermal flowmeter developed by the U.S.G.S. has interchangeable flow-sensors, 1.63 and 2.5 in. (41 and 64 mm) in diameters, and has flow sensitivity from 0.1 to 20 ft/min (0.03 to 6.1 m/min) in boreholes with diameters that range from 2 to 5 in. (50 to 125 mm). Vertical velocity in a borehole is measured with the thermal flowmeter by noting the time-of-travel of the heat pulse and determining water velocity (or volume flow) from calibration charts developed in the laboratory using a tube with a diameter similar to that of the borehole under investigation (Hess, 1986).

After the thermal flowmeter was tested at several sites, the U.S.G.S. developed an inflatable, flow-concentrating packer to decrease the measurement uncertainties caused by geothermally induced convection currents within the borehole fluid and to increase flow sensitivity in larger diameter holes. The thermal flowmeter and packer have been integrated into a single probe that operates on logging lines having four or more conductors (Figure IV-2). The packer system requires only a single conductor (plus the cable armor). The packer also can be used with other borehole probes, such as spinner flowmeters and pressure transducers, whose function would be enhanced with the use of an easily controlled packer (Hess, 1988). The thermal flowmeter, with or without packers, was used to measure natural or artificially induced flow distributions, or both, in boreholes with diameters ranging from 3 to 10 in. (75 to 250 mm), at temperatures from 6 to 60°C, and in a variety of lithologies including basalt, dolomite, gneiss, granite, limestone, sandstone, and shale. When the packer is used to direct all borehole flow through the measurement section, measured thermal travel-times correlate with borehole discharge, rather than average vertical velocity. With the flow-concentrating packer inflated, the thermal flowmeter measures borehole flows in the range of 0.02 to 2 gal/min (0.04 to 8 L/min). A representative flow calibration chart for the thermal flowmeter, with separate curves for operation when the concentrating packer is inflated, deflated, or not installed is shown in Figure IV-3. The inverse of the time-of-travel is used on the calibration chart for ease and accuracy of reading the calibration curves (Hess, 1982).

The thermal flowmeter was used initially to define naturally occurring flows in boreholes. However, the flowmeter has been used for additional applications, such as locating fractures that produce water during aquifer tests and identifying flows induced in adjacent boreholes during such tests. The capability of rapid measurement provided by the thermal flowmeter means that a few hours of flowmeter measurements have the potential for saving many days or weeks of investigation using conventional packer and tracer techniques.

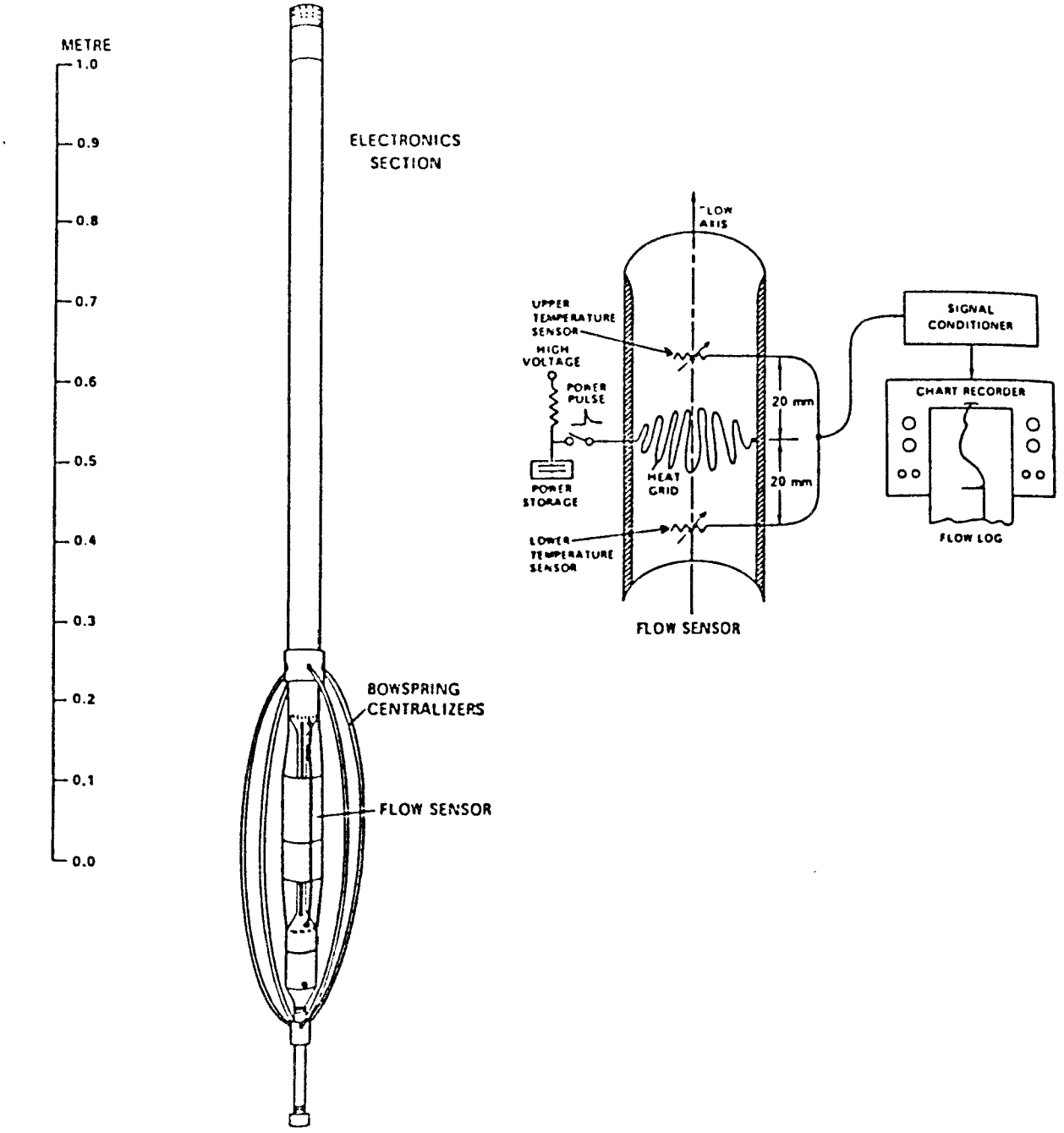


Figure IV-1. The U.S. Geological Survey's slow-velocity-sensitive thermal flowmeter (modified from Hess, 1986).

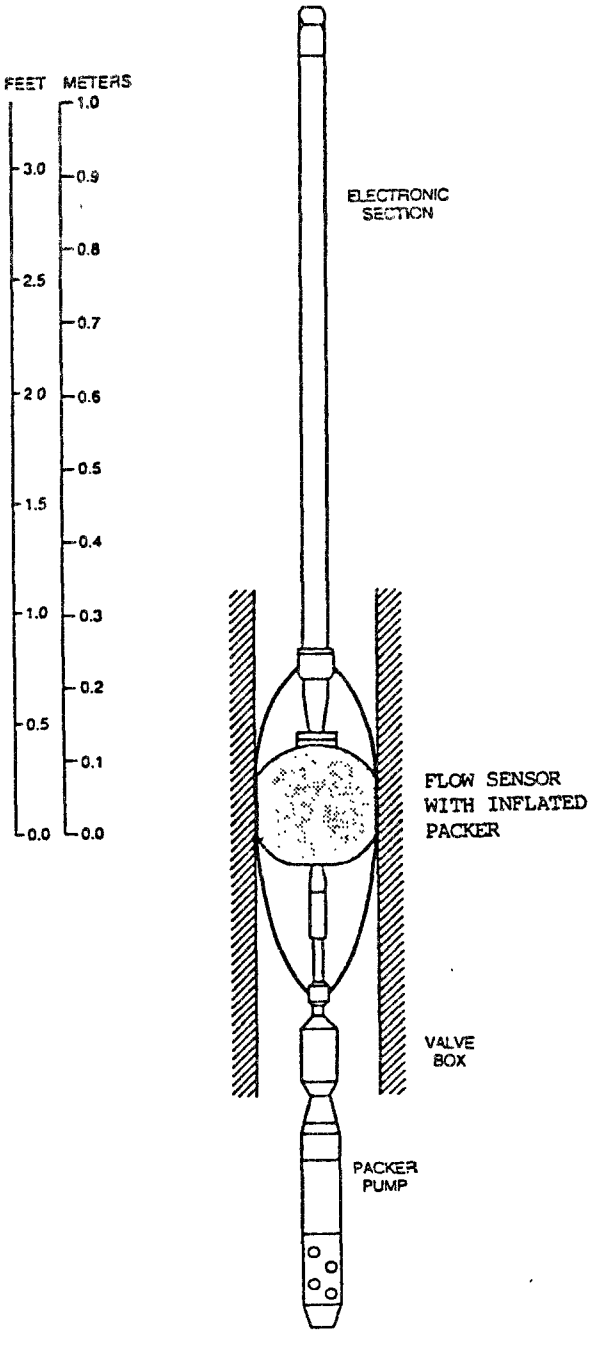


Figure IV-2. The U.S. Geological Survey's thermal flowmeter with inflated flow-concentrating packer (modified from Hess, 1988).

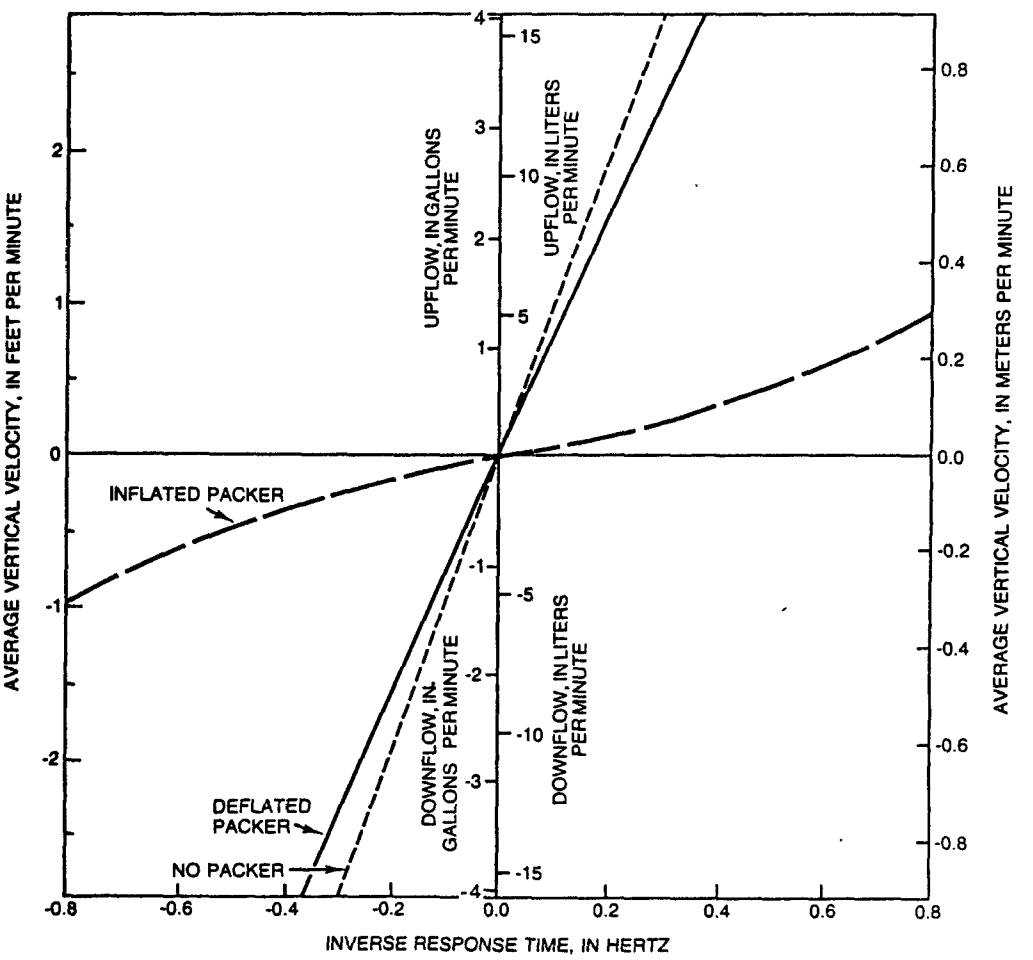


Figure IV-3. Example of a thermal flowmeter calibration in a 6-inch (15.2 cm) diameter calibration column.

## IV-2.1 Case Study 1--Fractured Dolomite in Northeastern Illinois

Acoustic-televiewer, caliper, single-point-resistance and flowmeter logs were obtained in a 210 ft (64 m) deep borehole in northeastern Illinois as part of a study of contaminant migration in fractured dolomite (Figure IV-4). The acoustic-televiewer log is a magnetically orientated, television-like image of the borehole wall, which is produced with a short-range sonar probe (Zemanek and others, 1970). Irregularities in the borehole wall, such as fracture and vugular openings absorb or scatter the incident acoustic energy, and result in dark features on the recorded image. Such televiewer logs may be used to determine the strike and dip of observed features (Paillet and others, 1985). The acoustic-televiewer and caliper logs for borehole DH-14 indicate a number of nearly horizontal fractures that seem to be associated with bedding-lanes. The largest of these fractures are designated A, B, C, and D in Figure IV-4. The caliper log indicates that the major planar features on the televiewer log are large fractures or solution openings associated with substantial borehole diameter enlargements. The large but irregular features on the televiewer log between fractures B and C also are associated with borehole enlargements, but these are interpreted as vugular cavities within the dolomite rather than fractures. The single-point-resistance log indicates abrupt shifts in resistance, at depths of about 130 and 185 ft (40 and 56 m). These shifts may reflect differences in the dissolved-solids concentration of the water in the borehole.

The pattern of vertical flow determined by the flowmeter measurements indicated the probable origin for the inferred water-quality contrasts in the borehole (Figure IV-4). The flowmeter log indicated downflow, which probably was associated with naturally occurring hydraulic-head differences, causing water to enter at the uppermost fracture, A, and exit at fracture B. A much smaller flow of water with the same electrical conductivity and dissolved-solids concentration continued down the borehole to fracture C. At this fracture, the downflow increased and the water inflow apparently contained a greater concentration of dissolved solids, which accounts for the shift to greater electrical conductivity. This increased downflow exited the borehole at fracture D, where there was another, somewhat smaller shift in single-point-resistance. Although not rigorously proven from the geophysical logs, the second shift in resistance appears to be associated with the dissolved-solids concentration of the water entering at fracture C.

Subsequent water sampling confirmed that there were differences in the dissolved-solids concentration of the water at the different depths. Sample analysis indicated that the water entering at fracture A had a dissolved-solids concentration of about 750 mg/L; the water entering at fracture C had a dissolved-solids concentration of about 1,800 mg/L. In this instance, the geophysical data, especially the thermal-flowmeter data, were useful in planning subsequent packer testing of the aquifer and in interpreting the results of water-quality measurements. Identification of substantial natural differences in background water quality was useful in planning for modeling of conservative-solute transport. At the same time, measurements of vertical-velocity distributions in the borehole provided useful indications of hydraulic-head differences between different depth intervals. This information could not be obtained from conventional water-level measurements without the time-consuming installations of packers at multiple levels in all of the boreholes at the site.

## IV-2.2 Case Study 2--Fractured Gneiss in Southeastern New York

Conventional geophysical and televiewer logs were obtained in a 400 ft (123 m) deep borehole completed in fractured gneiss at a site with contaminated ground water in southeastern New York. This borehole was located about 200 ft (70 m) from Lake Mahopac. After a night

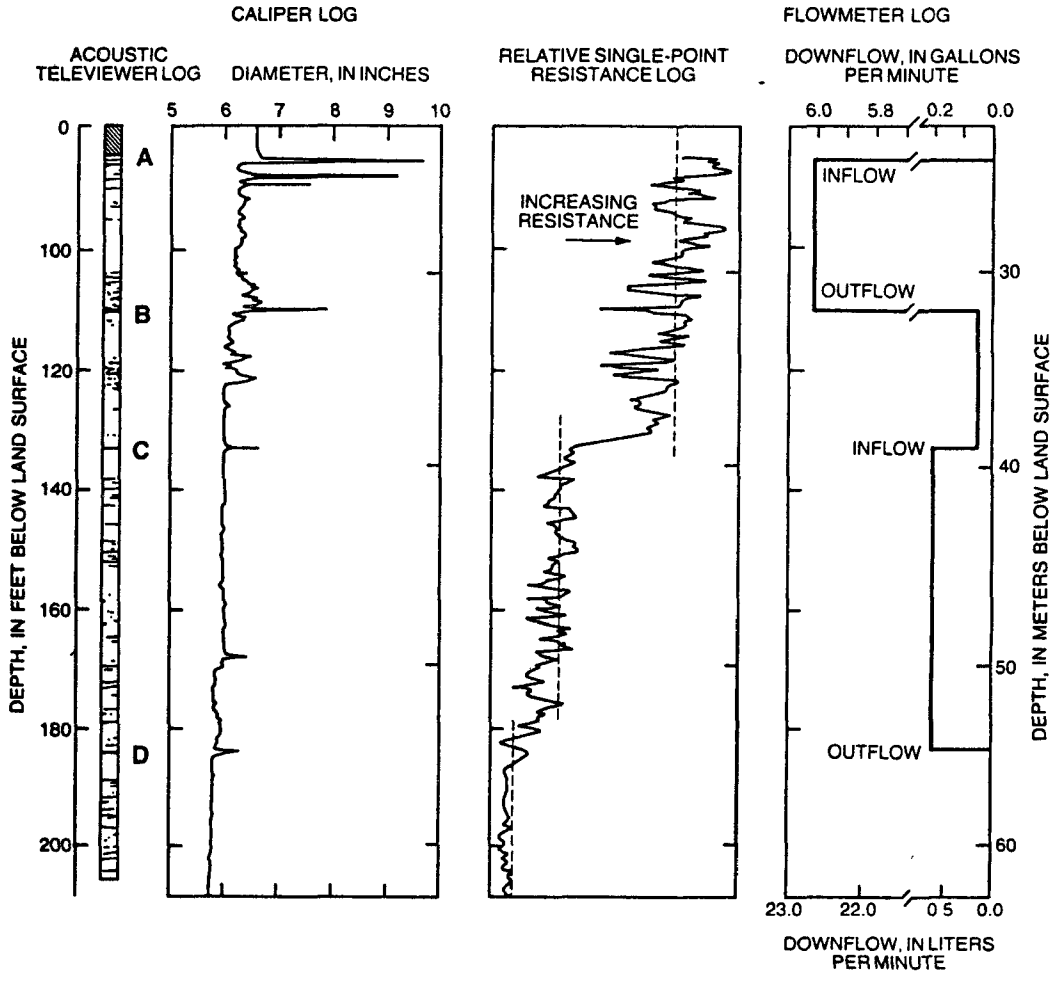


Figure IV-4. Acoustic-televiewer, caliper, single-point-resistance, and flowmeter logs for borehole DH-14 in northeastern Illinois.

of recovery from the effects of pumping nearby wells, the water level in the borehole appeared to be slightly higher than the lake level, but the lake level generally was higher than the water level in the borehole during the day. The acoustic-televiewer log indicated that fractures intersected almost every depth interval of this borehole. Brine-solution tracing had indicated that there was downflow within the borehole, but the locations of the fractures providing entry and exit points for the downflow were uncertain.

Acoustic-televiewer and caliper logs for selected intervals of the borehole are shown in Figure IV-5. The caliper log indicates several borehole enlargements at point A just below the bottom of the casing and other enlargements, B and C, near the bottom of the borehole. The selected intervals of the televiewer log indicate the large number of major fractures that could be entry and exit points for flow in the borehole.

The flowmeter logs obtained in the borehole indicated both the entry and exit points of the downflow (Figure IV-6). With just a few hours of flowmeter measurements, we learned that the entry points of the downflow were the uppermost fractures and most of the inflow was from fracture A. Consistent differences in the downflow indicated that about 20 percent of the flow exited at fracture B and that the rest of the downflow exited at fracture C.

The flowmeter measurements also indicated a series of transient fluctuations in downward flow in the borehole. These fluctuations were attributed to the effects of pumping in nearby water-supply wells. For example, the downward flow between fractures A and B was determined to vary from a maximum of about 0.7 gal/min (2.7 L/min) to a minimum of 0.4 gal/min (1.5 L/min). These transient changes occurred during periods ranging from a few minutes to an hour and were accompanied by changes in the water level in the borehole. The transient-flow changes probably represented the effects of pumping in one or more nearby water-supply wells on the local hydraulic-head differences between individual fractures intersected by the borehole. The transient changes in downflow may have been related to a pattern of changing hydraulic-head differences between shallow and deep fractures during pumping of nearby wells. Flowmeter measurements could not be made quickly enough to characterize the transient changes in the upper part of the borehole. However, several fractures just below fracture A in Figure IV-5 may have contributed flow during periods when the changes affected the flow distribution in the borehole. This preliminary conclusion provides information about possible fracture interconnections within the vicinity of fracture A that can be tested during future tests.

These results enabled the hydrologists studying the contamination problem to infer local flow conditions in the aquifer. The results of the flowmeter measurements provide useful information about the extent and characteristics of the hydraulic-head differences between the upper and lower permeable-fracture zones and the extent of interconnection between individual fracture sets within those two zones. Of special interest in this situation is the small proportion of the many large fractures indicated by the caliper log that actually produced or accepted flow under ambient hydraulic-head conditions. This conclusion agrees with conclusions reached in several other recent studies of fractured-rock aquifers (Paillet et al., 1987; Paillet and Hess, 1987).

### IV-2.3 Case Study 3--Water Movement In and Around a Fracture Zone on the Canadian Shield in Manitoba

This case study describes the flow in interconnected fractures inferred for an isolated fracture zone on the southeastern margin of the Canadian Shield in Manitoba, Canada. Two

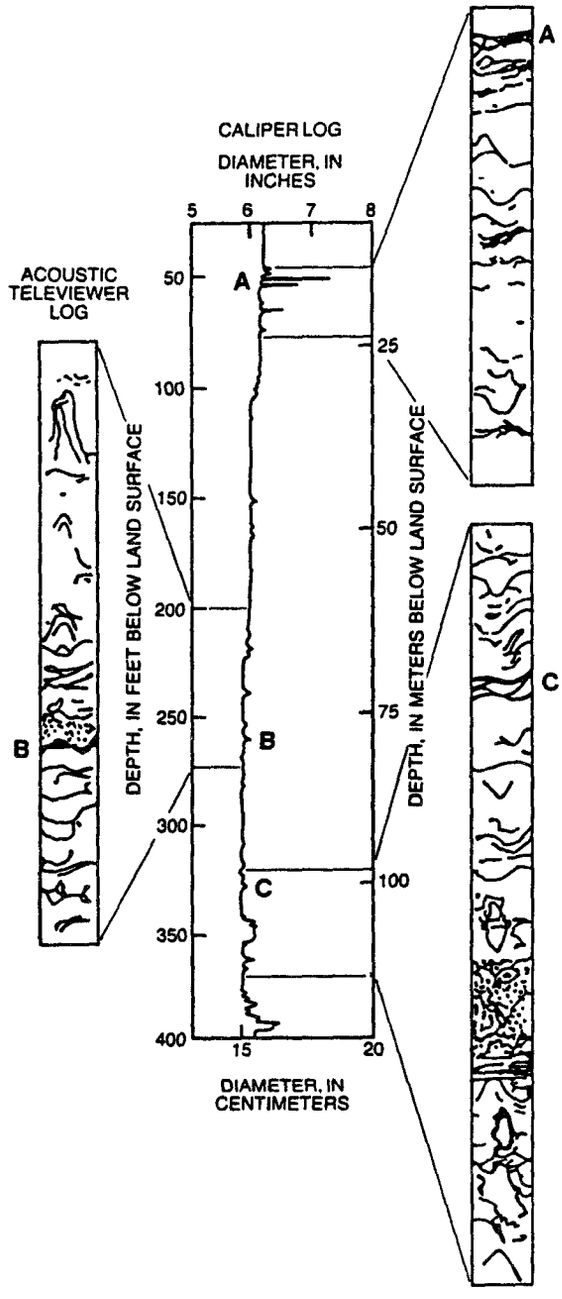


Figure IV-5. Acoustic-televiewer and caliper logs for selected intervals in a borehole in southeastern New York.

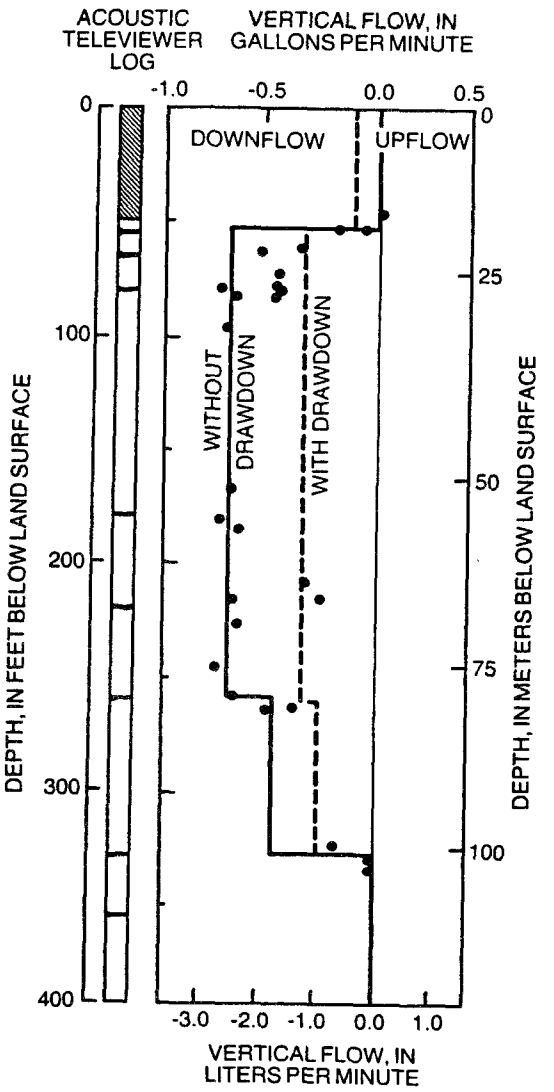


Figure IV-6. Profile of vertical flow in a borehole in southeastern New York, illustrating downflow with and without drawdown in the upper fracture zone.

boreholes spaced about 425 ft (130 m) apart intersected a fracture zone at a depth of about 870 ft (265 m). The nominal depths on the logs are somewhat greater than actual vertical depths because the boreholes had been angled deliberately from the vertical by about 20 degrees. The boreholes intersected almost no fractures except for those associated with the major zone (Figure IV-7). The results indicate substantial permeability in the main fracture zone and in several sets of fractures that appear to splay off from the main zone.

Flowmeter tests in these boreholes indicated that each borehole produced water from the vicinity of the fracture zone during pumping, but at markedly different rates. In borehole URL14, a pumping rate of only 0.07 gal/min (0.25 L/min) maintained a drawdown of more than 260 ft (80 m). In borehole URL15, a pumping rate of 5 gal/min (19 L/min) resulted in only 5 ft (1.5 m) of drawdown. All water production in borehole URL14 came from a minor fracture, far below the major fracture zone, whereas all of the water production in borehole URL15 came from the lower one-half of the major fracture zone.

The hydraulic connection between the two boreholes was investigated by measuring the flow in borehole URL15 while borehole URL14 was pumped. Flow was determined to enter borehole URL15 at the main fracture zone at a depth of 880 ft (270 m) and then flow downhole and exit at an apparently minor fracture about 50 ft (15 m) below. Flow entered borehole URL14 at a minor fracture about 130 ft (40 m) below the main fracture zone (Figure IV-8). Measured outflow from borehole URL15 was equal to measured inflow to URL14 to within the measurement uncertainty associated with the thermal flowmeter. Projection of the exit and entry fractures with respect to the plane connecting the two boreholes indicates that there was no direct planar connection between the exit point in borehole URL15 and the entry point in borehole URL14. This analysis indicates that the hydraulic connection between the boreholes occurred by means of irregular fracture intersections beneath the main fracture. Although the major fracture zone was the primary producer when borehole URL15 was pumped, that zone produced no inflow in borehole URL14 when it was pumped.

The apparent small size of the fracture conveying the flow between boreholes URL14 and URL15 raises questions about why fractures located away from the main fracture zone should provide the only hydraulic connection between the two boreholes. Other geophysical logs provided additional information pertaining to how this connection may have been achieved. Local stress concentrations inferred from borehole-wall breakouts identified on acoustic-televiewer logs, and later confirmed by hydraulic-fracturing stress measurements, may have caused local rock mass dilatency, accounting for the permeable pathway below the main fracture zone.

## IV-3 Conclusions

These case studies illustrate potential application of the thermal flowmeter in the interpretation of slow flow in fractured aquifers. The relative ease and simplicity of thermal-flowmeter measurements permits reconnaissance of naturally occurring flows prior to hydraulic testing, and identification of transient pumping effects, which may occur during logging. In making thermal flowmeter measurements, one needs to take advantage of those flows that occur under natural hydraulic-head conditions as well as the flows that are induced by pumping or injection. However, thermal-flowmeter measurements interfere with attempts to control borehole conditions during testing, because the flowmeter and wire-line prevent isolation of individual zones with packers. In spite of this limitation, the simplicity and rapidity of thermal-flowmeter measurements constitute a valuable means by which to eliminate many possible fracture interconnections and identify contaminant plume pathways during planning for much

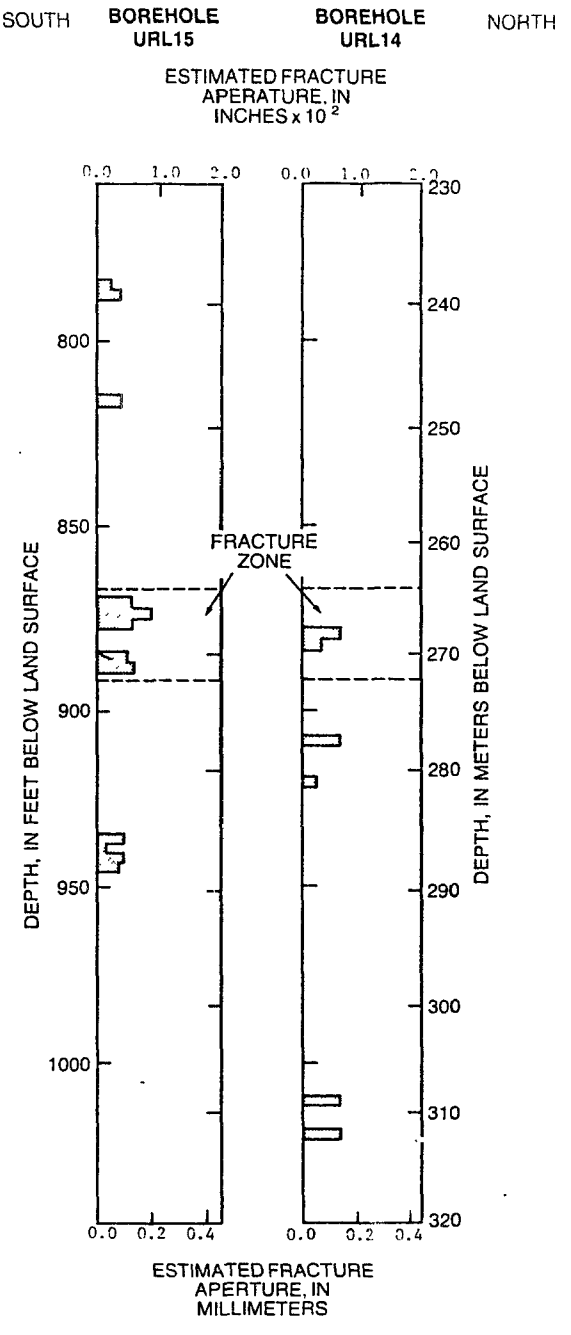


Figure IV-7. Distribution of fracture permeability in boreholes URL14 and URL15 in southeastern Manitoba determined from acoustic-waveform and other geophysical logs; fracture permeability is expressed as the aperture of a single, planar fracture capable of transmitting an equivalent volume of flow.

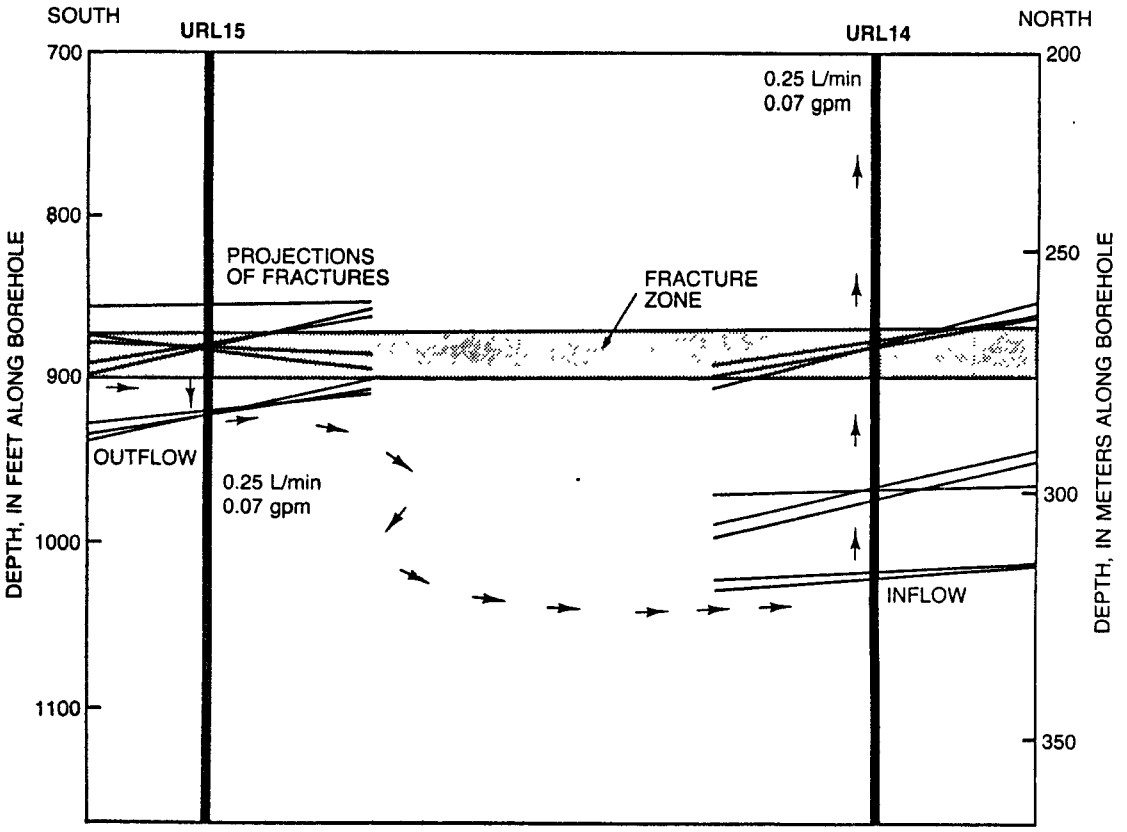


**Figure IV-8.** Distribution of vertical flow measured in boreholes URL14 and URL15 in southeastern Manitoba superimposed on the projection of fracture planes identified using the acoustic televiewer.

more time consuming packer and solute studies. The thermal flowmeter is especially useful at sites similar to the site in northeastern Illinois, where boreholes are intersected by permeable horizontal fractures or bedding planes. Under these conditions, naturally occurring hydraulic-head differences between individual fracture zones are decreased greatly by the presence of open boreholes at the study site. These hydraulic-head differences could only have been studied by the expensive and time consuming process of closing off all connections between fracture zones in all of the boreholes with packers. The simple and direct measurements of vertical flows being caused by these hydraulic-head differences obtained with the thermal flowmeter provided information pertaining to the relative size and vertical extent of naturally occurring hydraulic-head differences in a few hours of measurement. Additional improvement of the thermal-flowmeter/packer system and refinement of techniques for flowmeter interpretation may decrease greatly the time and effort required to characterize fractured-rock aquifers by means of conventional hydraulic testing.

While the case studies described in this chapter did not all involve contaminated groundwater, the potential application to plume migration problems and sampling well screen locating is obvious. The relationship of flowmeter measurements to more standard tests such as caliper and televiewer logs is indicated also. Hopefully, thermal flowmeters and other sensitive devices, such as the electromagnetic flowmeter being developed by the Tennessee Valley Authority, will be available commercially in the near future. Additional information is available in the proceedings discussed in the Preface (New Field Techniques for Quantifying the Physical and Chemical Properties of Heterogeneous Aquifers).

# CHAPTER V

## DEFINITION AND MEASUREMENT OF HYDRAULIC CONDUCTIVITY IN THE VERTICAL DIRECTION*

### V-1 Introduction

Chapters II and III dealt primarily with the measurement of hydraulic conductivity in the horizontal direction, while chapter IV was devoted to various types of borehole flowmeter measurements in fractured rock aquifers. Problems in the subsurface involving predominantly horizontal flow are common. Nevertheless, situations will often arise wherein one will need a value for hydraulic conductivity in the vertical direction. In general, a value will be needed whenever one wishes to determine how quickly contaminated water may move from one aquifer to another located at a different elevation.

One obvious method for obtaining vertical K values is to perform laboratory permeability tests on cores (Freeze and Cherry, 1979). This technique is well developed and applied often, but suffers from the usual problems of sample disturbance and non-representative sampling. In this chapter techniques will be presented that when successful will result in a vertical K value averaged over a volume of subsurface material much larger than that contained in a core. Of course, each of the techniques discussed has its own limitations and is not applicable in all situations. For each technique, such limitations are identified and discussed.

It is also convenient in this chapter to review some of the basic definitions and principles of Darcian flow in porous media. The remainder of this introduction will be devoted to that endeavor.

Hydraulic conductivity is the constant of proportionality in Darcy's law,

$$V = - K \frac{dh}{dx} \qquad \text{(V-1)}$$

where

| | | |
|---|---|---|
| K | = | hydraulic conductivity. |
| V | = | Darcy's velocity. |
| x | = | distance. |
| h | = | hydraulic head. |
| $\frac{dh}{dx}$ | = | hydraulic gradient. |

Hydraulic conductivity, which is sometimes called the coefficient of permeability, has been shown to be related to the fluid properties and the permeability of the porous medium by the following formula (Hubbert, 1940):

---

* Material in this chapter has been taken from the Lawrence Berkeley Laboratory Report No. LBL-15050 entitled "Field Determination of the Hydrologic Properties and Parameters that Control the Vertical Component of Groundwater Movement" by Iraj Javandel, prepared under sponsorship of the U.S. Nuclear Regulatory Commission.

$$K = \frac{k\rho g}{\mu}$$

where

| | | |
|---|---|---|
| k | = | specific or intrinsic permeability of the porous medium. |
| $\rho$ | = | density of fluid. |
| $\mu$ | = | dynamic viscosity of fluid. |
| g | = | gravitational acceleration. |

Intrinsic permeability k, which is a function of mean grain diameter, grain size distribution, sphericity, and roundness of the grains, is a measure of the ability of the medium to transfer fluids, independent of the density and viscosity of any particular fluid.

The hydraulic conductivity of geological materials varies from approximately 1 to $10^{-13}$ m/s. This is a very wide range of variation. There are very few physical parameters that take on values over 13 orders of magnitude (Freeze and Cherry, 1979). Values of hydraulic conductivity of a geological formation can vary in space. This property of the medium is called heterogeneity. They can also show variations with the direction of measurement at any given point. This property is called anisotropy and is quite common in sedimentary rocks. In such rocks, hydraulic conductivity along the layers is sometimes several orders of magnitude larger than across the layers. This property becomes especially important in layered formations where some thin layers of very low permeability appear within highly permeable sediments. Anisotropy is also quite common in fractured rocks where aperture and spacing of joints varies with direction.

As a result, in an anisotropic medium, hydraulic conductivity in its general form may be represented by a 3x3 symmetric matrix. The components of fluid velocity in an anisotropic medium may then be written by the following equations:

$$v_x = - K_{xx}\frac{\partial h}{\partial x} - K_{xy}\frac{\partial h}{\partial y} - K_{xz}\frac{\partial h}{\partial z} \qquad \text{(V-2)}$$

$$v_y = - K_{yx}\frac{\partial h}{\partial x} - K_{yy}\frac{\partial h}{\partial y} - K_{yz}\frac{\partial h}{\partial z} \qquad \text{(V-3)}$$

$$v_z = - K_{zx}\frac{\partial h}{\partial x} - K_{zy}\frac{\partial h}{\partial y} - K_{zz}\frac{\partial h}{\partial z} \qquad \text{(V-4)}$$

The values of K in the above equations are components of the hydraulic conductivity matrix (or tensor). It has been shown that an appropriate selection of coordinate system enables one to diagonalize a symmetric matrix. The necessary and sufficient condition that allows such a transformation is that the principal directions of anisotropy coincide with the x, y, and z coordinate axes. If the system allows such a simplification, then the three components of flow velocity may be represented by the following equations

$$v_x = -K_x\frac{\partial h}{\partial x} \qquad \text{(V-5)}$$

$$v_y = -K_y\frac{\partial h}{\partial y} \qquad \text{(V-6)}$$

$$v_z = -K_z\frac{\partial h}{\partial z} \qquad \text{(V-7)}$$

where $K_x$, $K_y$ and $K_z$ are principal values of hydraulic conductivity which are now in the direction of x,y, and z. Therefore, depending on the media, the vertical velocity of groundwater movement may be given by one of the two equations, (V-4) or (V-7). Equation (V-7) indicates that the vertical component of groundwater motion is controlled by $K_z$ alone. In cases where vertical velocity is given by equation (V-4), values of hydraulic conductivity in other directions are also required.

In this section some of the conventional, as opposed to multilevel, methods for determination of in situ hydraulic conductivity in geological materials will be discussed. Emphasis will be placed on the methods that lead also to determination of vertical hydraulic conductivity, which is the main motivation for this chapter. Some methods which have been recently developed for finding horizontal hydraulic conductivity in tight formations will also be examined.

In general these tests may be divided into two categories: those which are performed in a single well and those whose execution requires more than one well.

## V-2 Single-Well Tests

### V-2.1 Burns' Single-Well Test

Burns (1969) proposed a method of estimating vertical permeability of rocks. Following is a modification of that method.

#### A) Purpose

The purpose of this test is to find in-situ vertical permeability of geological material in the vicinity of the test well. Average horizontal permeability may also be estimated by this method.

#### B) Procedure

This test can be performed with several alternative arrangements of down-hole equipment. Two useful arrangements proposed by Burns are illustrated in Fig. V-1. Here the procedure for the more simple test (Fig. V-1A) is described. For further detail the reader is referred to Burns (1969).

- A well is drilled into the zone of interest. Assuming the well is cased, the annulus between the casing and the formation should be tightly cemented to prevent any sort of vertical flow. Arnold and Paap (1979) have presented a method for monitoring water flow behind a well casing. If the process of cementing fills up the voids in the vicinity of the well it may cause an artificial reduction of permeability. Then the casing and cement should be perforated at least at two different intervals separated from each other by a few feet.

- A packer is placed between these two perforated intervals to seal the hydraulic connection between them from inside the casing. Care should be taken that the change of pressure on one side does not transmit through the packer. Installation of two packers with about half a foot distance may achieve this goal.

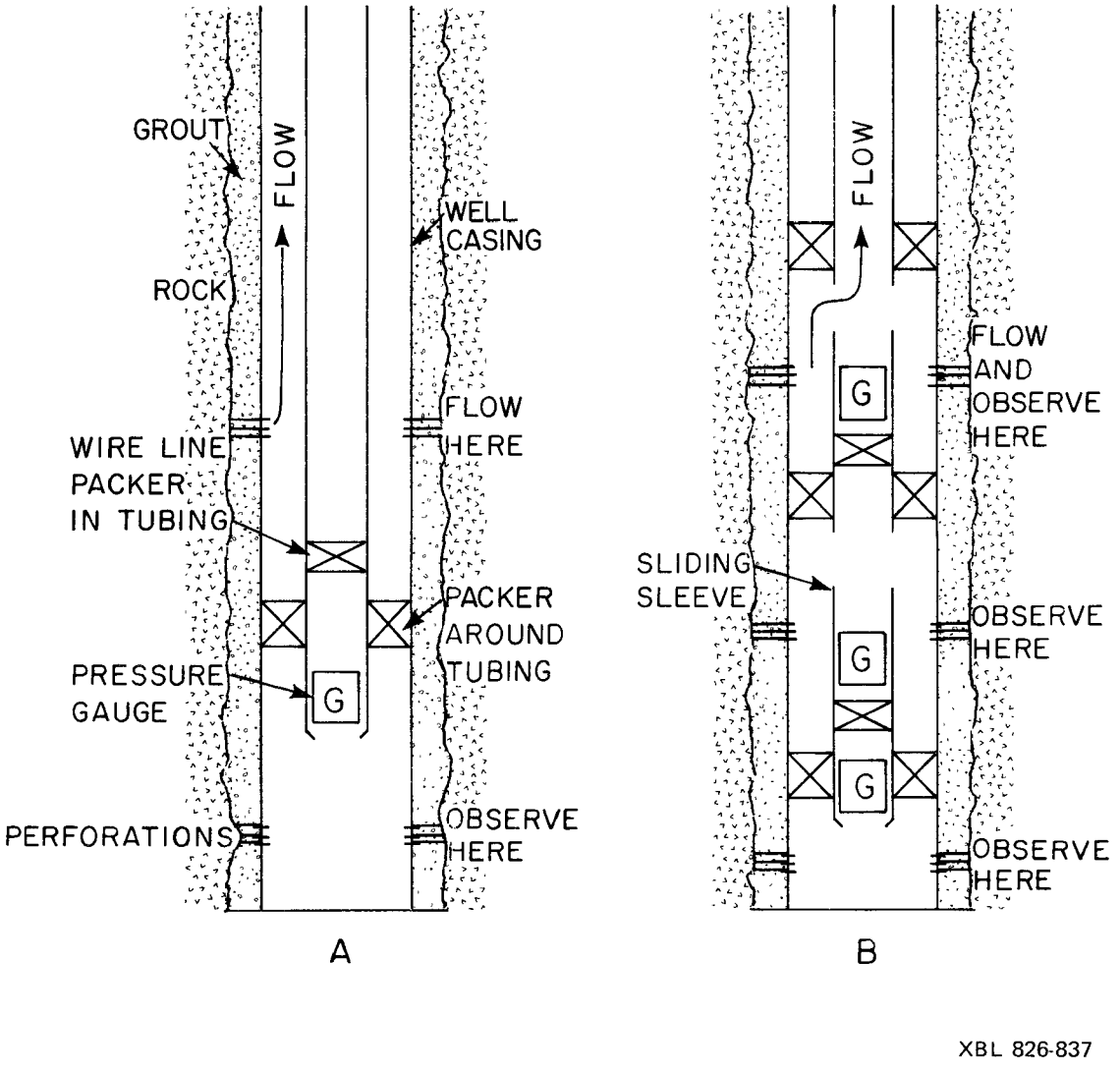


Figure V-1 Downhole equipment arrangements for vertical well tests; A) single interval test, and B) multiple interval test with sliding sleeve (after Burns, 1969).

- One pressure transducer is installed on each side of the packer. The ambient pressure trend is monitored by both of the transducers for some period before injection. To facilitate test data interpretation, the values of ambient pressure should either remain constant or change linearly during the trend monitoring period.

- Start injecting into or pumping from the upper perforated zone. The rate of flow should remain constant during this period. Flow rate should be monitored very accurately.

- Production or injection may be stopped after the pressure change recorded in the lower part reaches at least 10 times the sensitivity of the gauge.

- Recording of pressure at both intervals should continue throughout the producing or injection period and afterwards for a period equal to at least 20 percent of the elapsed flow period.

- Caution: extra packers may be used to minimize the effect of well bore storage.

C) Theory

The theory behind this method rests on the derivation of pressure changes due to a finite-length vertical line source in a homogeneous, anisotropic infinite aquifer bounded between two impermeable confining layers. The solution of this problem has been given by Hantush (1957), and Nisle (1958). See also Hantush (1964).

According to Hantush the change of hydraulic head or drawdown s(r,z,t) in a piezometer having a depth of penetration z and being at a distance r from a steadily discharging well (with infinitesimal diameter) that is screened between the penetration depths d and l in the anisotropic aquifer of Fig. V-2 is given by

$$s = (Q/4\pi K_r b)\{W(u_r) + f\} \qquad \text{(V-8)}$$

where

$$f = [2b/\pi(1-d)] \sum_{n=1}^{\infty} 1/n \left[\sin\frac{n\pi l}{b} - \sin\frac{n\pi d}{b}\right] \cdot \cos\frac{n\pi z}{b} \cdot$$

$$\cdot\, w\{u_r, \sqrt{\frac{K_z}{K_r}(\frac{n\pi r}{b})^2}\}, \text{ and } u_r = \frac{r^2 S}{4K_r bt} \qquad \text{(V-9)}$$

The two functions, $W(u_r)$ and $W\{u_r, \sqrt{\frac{K_z}{K_r}(\frac{n\pi r}{b})^2}\}$, have been tabulated and given by Hantush (1964). The solution presented by Burns is based on the more complicated form which Nisle (1958) presented.

Introducing the following dimensionless parameters

$$s_D = \frac{4\pi K_r bs}{Q} \quad \text{and} \quad t_D = \frac{bK_z t}{S r_w^2}, \qquad \text{(V-10)}$$

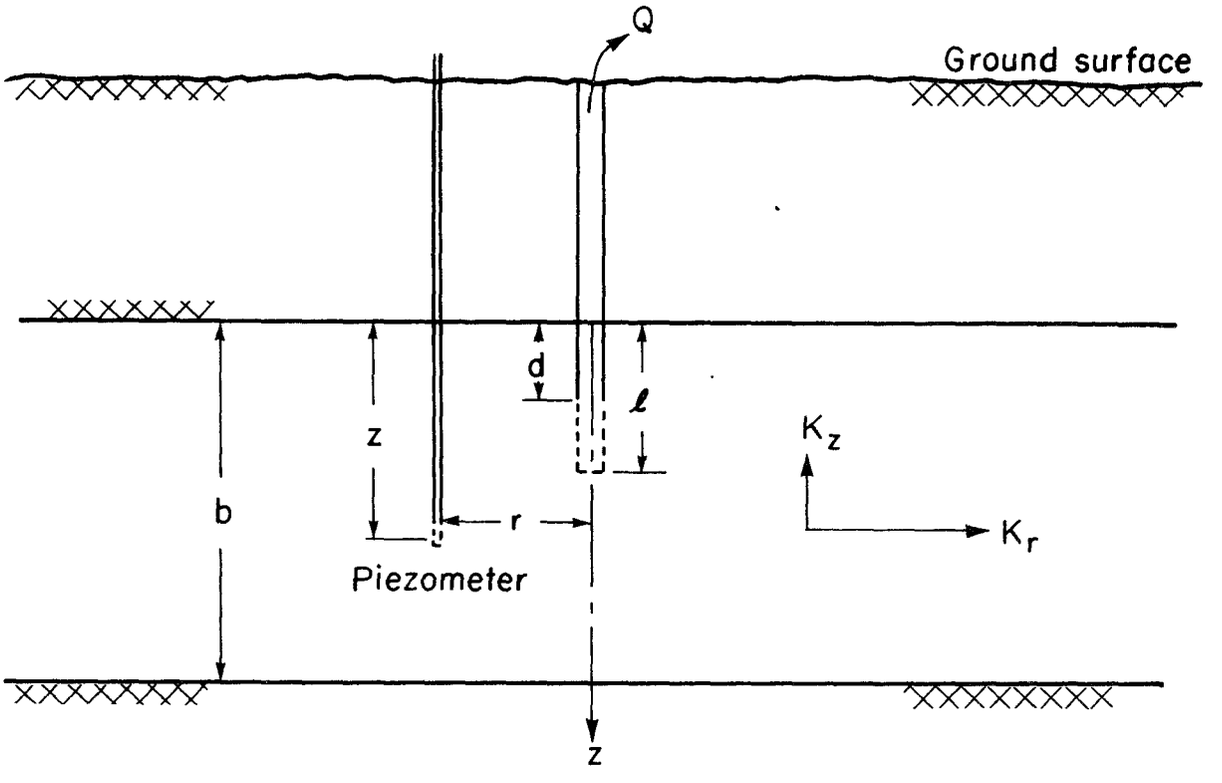


XBL 826-838

Figure V-2. Aquifer with a partially penetrating well.

one can compute families of type curves of $s_D$ versus $t_D$ for different dimensionless parameters such as $\frac{z}{b}$, $\frac{1}{b}$, $\frac{d}{b}$, and $\frac{r}{b}$.

D) Analysis of Field Data

- Plot observed values of pressure versus time on rectangular coordinates.
- Draw the best straight line through the pressure response measurements during the trend-monitoring period, and extend it to the end of the flow period.
- The difference between the measured pressures and the original trend, $\Delta p = \gamma s$, is determined as a function of time since initiation of flow.
- Knowing dimensionless parameters such as $\frac{z}{b}$, $\frac{1}{b}$, $\frac{d}{b}$, and $\frac{r_w}{b}$, a family of type curves (log-log plot of $s_D$ vs $t_D$) is prepared from equations (V-8) through (V-10), for different values of $\frac{K_z}{K_r}$.
- Variation of s versus time is plotted on another log-log paper with the same scale as the type curve plots.
- The observed plot is then compared with the type curves.
- Keeping the axes of the two plots parallel, find the position that the observed plot matches best with one of the type curves.
- Read the value of $\frac{K_z}{K_r}$ and pick up a point on the top paper and identify the corresponding point right beneath that on the other plot. Read the coordinates of the two points i.e. s,t,$s_D$ and $t_D$.
- Calculate the value of $K_r$ from the definition of $s_D$, and $K_z$ from the ratio of $\frac{K_z}{K_r}$.
- The value of S may now be computed from equation (V-10).

E) Multiple Tests in the Same Well

Several tests may be performed over different portions of a formation in the same well. In this case two or more packers may be used to isolate the testing portions of the well. Multiple tests can sometimes determine whether the response is characteristic of the formation or is a result of behind-casing leaks arising from poor cementing.

F) Uncertainties

- This test relies heavily on the assumption that the cementing behind the casing is not leaking. The existence of cement leaks behind the casing could result in abnormally high vertical permeability measurements. Sufficiently large values of leakage behind the casing could cause almost equal response at the transducers in the flow and measurement zones.

- If the well has skin damage or if discontinuous shale barriers are locally present in the tested interval, then the calculated vertical permeability would be lower than the actual regional value.

- Within low permeability materials, if proper instrumentation is not utilized, the period of time required to reach a stabilized pressure before beginning the test might be long. In this case linear extrapolation of test pressure trends might lead to errors.

- The value of the hydraulic conductivity calculated by this method corresponds to a small volume of rock located in the vicinity of the testing zone.

## V-2.2 Prats' Single-Well Test

Prats (1970) proposed a method for estimating in-situ vertical permeability of geological materials which we shall describe here. This test requires injection or production at a constant rate from a short perforated interval and measurement of the pressure response at another perforated interval that is isolated from the first by a packer.

The purpose of this test is estimating the in-situ vertical permeability of materials in the vicinity of a well. The test procedure is essentially the same as for the previously discussed Burns' test (1969), but probably less accurate.

A) Procedure

- Consider a single well with a casing cemented to the rock.

- Perforate two small intervals into the casing in the zone to be tested.

- Set a packer in the casing between the two perforations.

- Set one pressure transducer close to each perforation and monitor changes in pressure with time. As was discussed in the previous test, to avoid transfer of pressure through the packer, more than two packers may be used for separation of the flow and measurement zones.

- After pressure is almost stabilized, inject into the formation with a constant rate Q for some period of time until a reasonable amount of pressure response is picked up by the transducer at the other perforation zone. In order to minimize the time required for pressure to stabilize, isolate the injection and observation zones from the rest of the well.

- Stop injection and continue to monitor the change of pressure at both transducers until the original ambient condition is almost reached.

B) Theory

The supporting theory behind this method is based on the pressure response of a confined homogeneous, anisotropic infinite aquifer due to a continuous point source. Thus, not only is the well considered to be of zero radius, but the perforation length of both injection zone and pressure measurement zone are also assumed to be vanishingly small. Based on these assumptions, the pressure change at a point z due to the release of a constant rate of flow Q at the point z', both located on the axis of the well, may be given by

$$\Delta p = \frac{Q\gamma}{4\pi K_r b} \sum_{n=-\infty}^{+\infty} \frac{\operatorname{erfc}\left[\frac{|Z_D - Z_D' - 2n|}{2\sqrt{\tau}}\right]}{|Z_D - Z_D' - 2n|} + \frac{\operatorname{erfc}\left[\frac{|Z_D + Z_D' - 2n|}{2\sqrt{\tau}}\right]}{|Z_D + Z_D' - 2n|} \qquad \text{(V-11)}$$

where

erfc = complementary error function.

$Z_D = \frac{z}{b}$

$Z_D' = \frac{z'}{b}$

b = aquifer thickness.

$\tau = \frac{K_z t}{S b}$

$\gamma$ = unit weight of fluid.

z = vertical distance of the point of measurement from the base of the aquifer.

z' = vertical distance of the point of injection from the base of the aquifer.

For large times, equation (V-11) may be simplified to

$$\Delta P = \frac{Q\gamma}{4\pi K_r b}\left[\ln \frac{K_z t}{S b} + G(Z_D, Z_D') + \frac{b}{|z-z'|}\right] \qquad \text{(V-12)}$$

where $G(Z_D, Z_D')$ may be obtained from Table V-1.

C) Analysis of Field Data

- Calculate pressure changes at the measuring interval with the same procedure mentioned in the previous test.
- Plot pressure changes at the measuring interval versus time on a semi-logarithmic paper.
- If the test was run long enough, the above curve should become a straight line at large value of time. Measure the slope m of that portion as $\Delta P$/cycle.

Table V-1. Values of $G(Z_D,Z_D')$

| $Z_D'$ \ $Z_D$ | 0.1 | 0.2 | 0.3 | 0.4 | 0.5 | 0.6 | 0.7 | 0.8 | 0.9 | 0.10 |
|---|---|---|---|---|---|---|---|---|---|---|
| 0.1 | 4.188 | 2.511 | 1.685 | 1.210 | 0.919 | 0.743 | 0.648 | 0.617 | 0.644 | 0.729 |
| 0.2 | 2.542 | 1.701 | 1.210 | 0.904 | 0.712 | 0.600 | 0.550 | 0.555 | 0.613 | 0.729 |
| 0.3 | 1.742 | 1.237 | 0.916 | 0.709 | 0.582 | 0.517 | 0.505 | 0.544 | 0.638 | 0.796 |
| 0.4 | 1.289 | 0.953 | 0.732 | 0.591 | 0.512 | 0.485 | 0.509 | 0.586 | 0.725 | 0.944 |
| 0.5 | 1.017 | 0.781 | 0.625 | 0.532 | 0.492 | 0.502 | 0.565 | 0.689 | 0.891 | 1.207 |
| 0.6 | 0.857 | 0.685 | 0.577 | 0.523 | 0.520 | 0.569 | 0.680 | 0.868 | 1.169 | 1.653 |
| 0.7 | 0.777 | 0.651 | 0.581 | 0.563 | 0.599 | 0.696 | 0.872 | 1.159 | 1.629 | 2.446 |
| 0.8 | 0.759 | 0.669 | 0.634 | 0.655 | 0.738 | 0.900 | 1.174 | 1.631 | 2.435 | 4.086 |
| 0.9 | 0.797 | 0.740 | 0.741 | 0.807 | 0.954 | 1.214 | 1.657 | 2.488 | 4.087 | 9.072 |

- Calculate the radial hydraulic conductivity from $K_r = \frac{2.3Q\gamma}{4\pi bm}$

- Extrapolate the straight-line portion of the plot to a value of t = 1 hr, and read the pressure change at that time. This pressure change will be denoted as $\Delta P(1)$.

- Read the value of $G(Z_D, Z_D')$ from Table V-1.

- Determine $K_z$ from the following formula:

$$K_z = \frac{S\,b}{3600}\ \exp\left[\frac{4\pi K_r b}{Q\gamma}\ \Delta P(1) - G(Z_D, Z_D') - \frac{b}{|z-z'|}\right]. \qquad \text{(V-13)}$$

All dimensions in equation (V-13) are in SI units. Note that $K_z$ can be calculated only when S is known.

D) Advantages and Limitations

The advantage of this method over the Burns' method is its simplicity in application. No type curve is necessary and analysis may be carried out with a small calculator.

Major limitations are as follows:

- The injection and measuring intervals must be short compared with the distance between them, probably 10 percent or less.

- If the distance between the injection (production) interval and the measuring interval is relatively long and the net vertical permeability is low, the pressure response may not be measured even in weeks. If this distance is relatively short, then the assumptions of point recharge (discharge) and point measurement become questionable.

- The thickness of the aquifer and the coefficient of storage are assumed to be known from other sources of information.

- The method will probably produce representative results in sands containing shaly streaks of limited extent, say not more than a few feet in length. But its application is subject to question in the case of a reservoir with rather extended lenses of shale which could have significant local but not regional effects on vertical permeability.

- The method is rather sensitive to variations in the mass rate of fluid injection (production). The rate of flow is supposed to be constant.

- The method can only give the horizontal and vertical hydraulic conductivity of the materials immediately adjacent to the well being tested.

## V-2.3 Hirasaki's Single-Well Pulse Test

Hirasaki (1974) has proposed a pulse test technique for estimating in-situ vertical permeability. The test consists of pumping or injecting a small interval of a well for a short time, shutting in, and then measuring the time for the maximum pressure response to occur at

another small interval of the well. This method has been used to estimate the vertical permeability of a low-permeability zone in the Fahud field, Oman (Rijnders, 1973).

A) Purpose

The purpose of this technique is also to provide a simple means of estimating in-situ vertical permeability of an aquifer in the vicinity of the testing location.

B) Procedure

- Perforate the casing of the well over a short interval at the top of the aquifer just beneath the confining layer.
- Perforate another short interval at a distance z below the first interval.
- Isolate these two intervals with a packer.
- Pump water from or inject into the upper perforated interval for a short time and measure pressure changes at the lower interval.
- Stop pumping or injection and continue measuring pressure change at the lower interval until the major part of the pulse test curve is obtained. Figure V-3 shows a typical curve which may be obtained from such a pulse test. Note that the pumping or injection period should be short compared with the time required to reach the maximum pressure response (e.g., less than 10 percent) in the lower interval.

C) Theory

The theory of this technique rests on an approximation of the recovery equation for a continuous point source in a homogeneous anisotropic medium. Consider a continuous point source at z = 0 on the axis of the well, operating for a period t = $t_1$, as shown in Fig. V-4. The pressure response of a semi-infinite medium (b is so large that the lower boundary is not touched) to the source at the point z and at any time $t>t_1$ may be given by

$$P_D = \frac{2}{Z_D}\left[\operatorname{erfc}\left(\frac{Z_D}{2\sqrt{\tau}}\right) - \operatorname{erfc}\left(\frac{Z_D}{2\sqrt{\tau-\tau_1}}\right)\right] \qquad \text{(V-14)}$$

where

$$Z_D = \frac{z}{b}$$

$$\tau = \frac{K_z t}{S b}$$

$$\tau_1 = \frac{K_z t_1}{S b}$$

$$P_D = \frac{4\pi K_r b \Delta P}{Q\gamma}$$

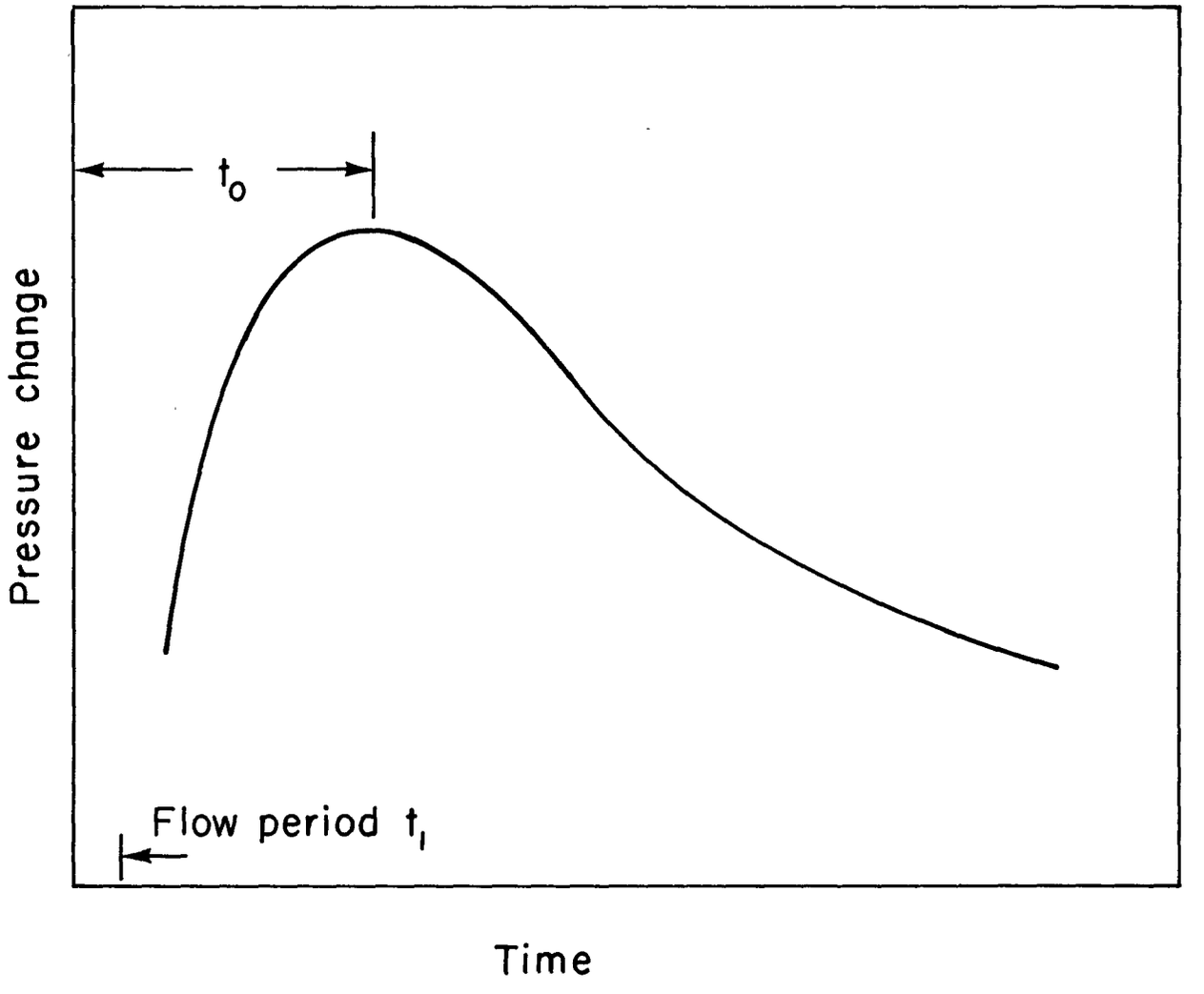


Figure V-3. A typical pulse test response in the lower perforated interval, (modified from Hirasaki, 1974).

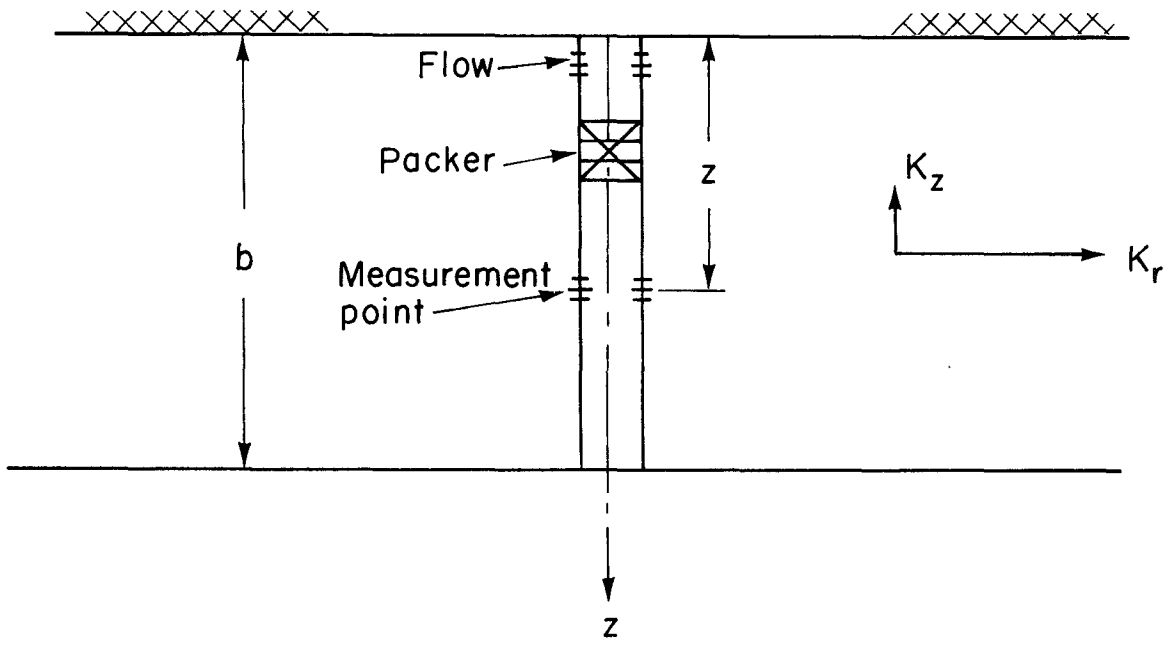


XBL 826-840

Figure V-4. Sketch of the Hirasaki's test configuration.

If $t_1$ is much less than t, then equation (V-14) may be approximated by

$$P_D = \frac{\tau_1}{\sqrt{\pi}} \frac{\exp - [Z_D^2/4\tau]}{\tau^{3/2}} \qquad \text{(V-15)}$$

Equation (V-15) represents the pulse-pressure curve. The arrival time of the peak of this curve may easily be obtained by setting its derivative equal to zero, which would give

$$\tau_o = \frac{Z_D^2}{6} \qquad \text{(V-16)}$$

Substituting for $\tau_o$ gives

$$K_z = \frac{SbZ_D^2}{6t_o} \qquad \text{(V-17)}$$

As was mentioned above, equations (V-14) through (V-17) apply to a semi-infinite medium. Two other cases have also been considered by this author. In one case the aquifer is considered to be finite in thickness, which is treated by the introduction of a no flow condition at the lower boundary. In the other case the lower boundary is assumed to remain at constant head. A family of curves has been presented in Fig. V-5, which gives the variation of $\tau_o$ versus $Z_D$ for all three cases. It is interesting to note that the equation (V-17) holds for all three cases as long as $Z_D \leq 0.6$.

D) Analysis of Field Data

- Plot the variation of $\Delta P$ versus time as measured at the lower interval. The same precautions for measuring $\Delta P$ apply here as were discussed in previous methods.
- If this curve shows a peak like that on Fig. V-3, then measure the time $t_o$ corresponding to the maximum pressure response.
- Modify the time $t_o$ by subtracting half of the flow period $t_1$

$$t_o' = t_o - \frac{1}{2} t_1 \qquad \text{(V-18)}$$

- If the distance z between the upper and lower intervals is relatively short with respect to the thickness of the aquifer ($z < 0.6b$), then calculate $K_z$ using equation (V-17) by employing $t_o'$ instead of $t_o$.
- If the distance z is larger than 0.6b, then calculate $Z_D = z/b$ and determine the type of lower boundary which best approximates field conditions.
- Determine the value of $\tau_o$ from the appropriate curve of Fig. V-5.
- Calculate vertical hydraulic conductivity $K_z$ from the following equation:

$$K_z = \frac{S_s b^2 \tau_o}{t_o'} \qquad \text{(V-19)}$$

Here again it is assumed that the specific storage $S_s$ is known from other information.

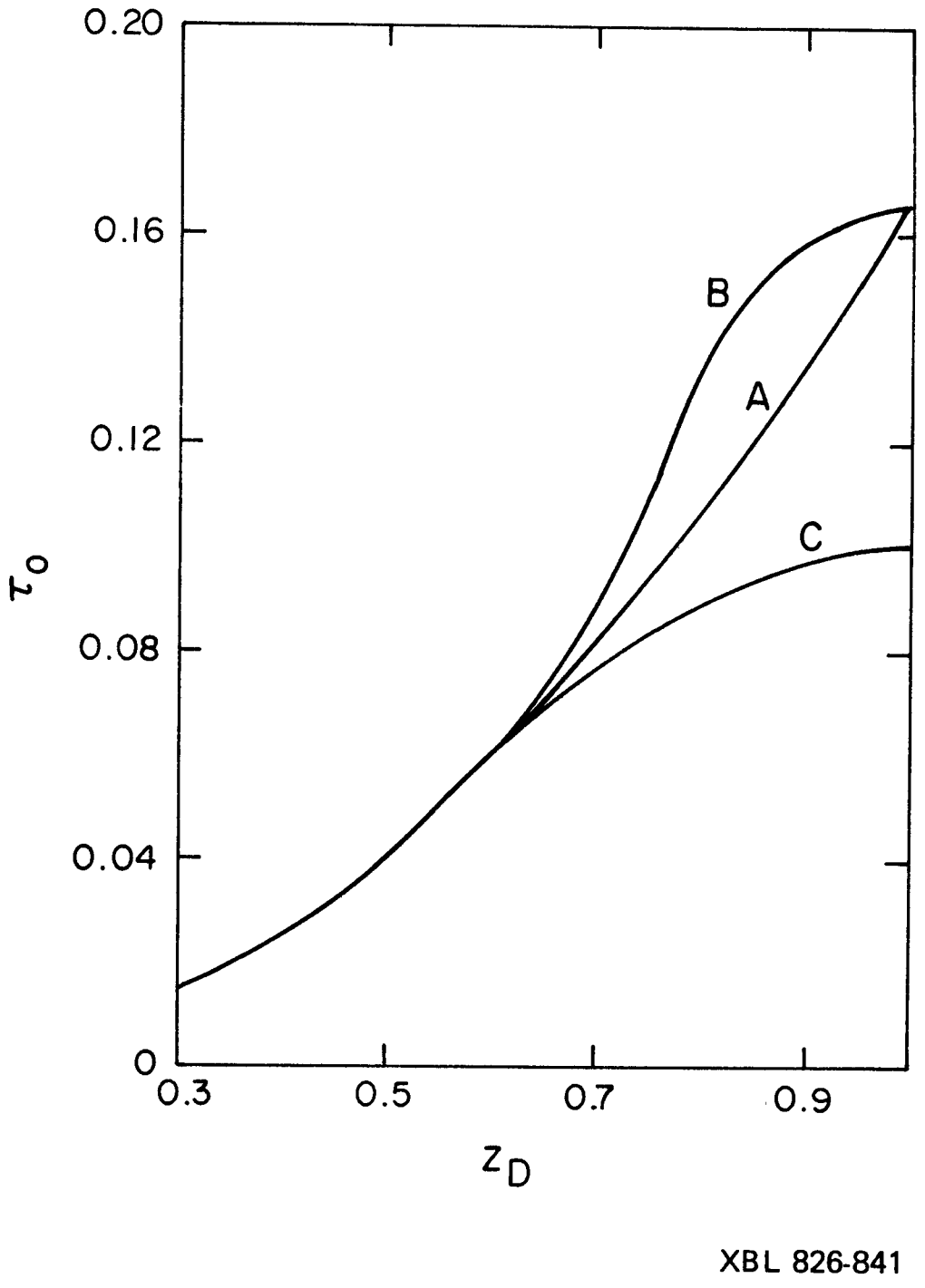


Figure V-5. Dimensionless response time for pulse test; A) for semi-infinite case, B) for a finite thickness layer with an impermeable lower boundary, and C) for a finite thickness layer and constant head at the lower boundary, (modified from Hirasaki, 1974).

E) Uncertainties

- This test is based on the assumption that the period of injection or pumping is almost negligible in comparison with the time to reach the maximum pressure response.

- Possible leaks behind the casing lead to erroneously high values of vertical hydraulic conductivity.

- The hydraulic conductivity measured by this method is representative of materials very close to the well.

V-2.4 Bredehoeft-Papadopulos Single-Well Test

Bredehoeft and Papadopulos (1980) have proposed a method of measuring permeability which is a modification of the conventional slug test. Although their method is designed for measuring horizontal rather than vertical hydraulic conductivity, we shall discuss it here because (1) the conventional methods for measuring vertical hydraulic conductivity in tight formations are associated with uncertainties, and the value of horizontal hydraulic conductivity could give an upper limit for the vertical component provided that major vertical fractures are absent, and (2) as we saw before, in some cases in addition to the vertical value one also needs horizontal hydraulic conductivity to evaluate the vertical component of fluid flow.

A) Purpose

The purpose of this test is to measure in-situ horizontal hydraulic conductivity of so called "tight formations", such as tightly compacted clays, rock units in which fractures, if they exist, are essentially closed or filled, or matrix rock between fractures.

B) Procedure

Figure V-6 depicts set-ups for the test in (a) an unconsolidated formation and (b) a consolidated formation. Depending on the time elapsed since the well has been drilled, the water level in the hole may or may not have stabilized to the ambient hydraulic head at the interval to be tested. To start the test, the test system is filled with water and, after a period of observing the water level for ambient conditions, the test interval is suddenly pressurized by injecting an additional amount of water with a high pressure pump. The test interval is then shut-in, and the head change $H_o$ caused by the pressurization is allowed to decay. As water slowly penetrates into the formation, $H_o$ will drop. The variation of $H_o$ with time is recorded.

C) Theory

Apart from the conventional initial-boundary value formulation which is generally adopted for simple radial flow in a confined and infinitely long aquifer, one specific constraint used in this development is as follows. The driving force governing the movement of water from the well into the formation is the expansion that the water stored within the pressurized system undergoes as the head, or the pressure within the system, declines. Thus, the rate at which water flows from the well is equal to the rate of expansion. In a conventional slug test the water flow into the formation comes directly from the volume of stored water in the system under normal hydrostatic pressure. The solution for the modified slug test has been presented in the form

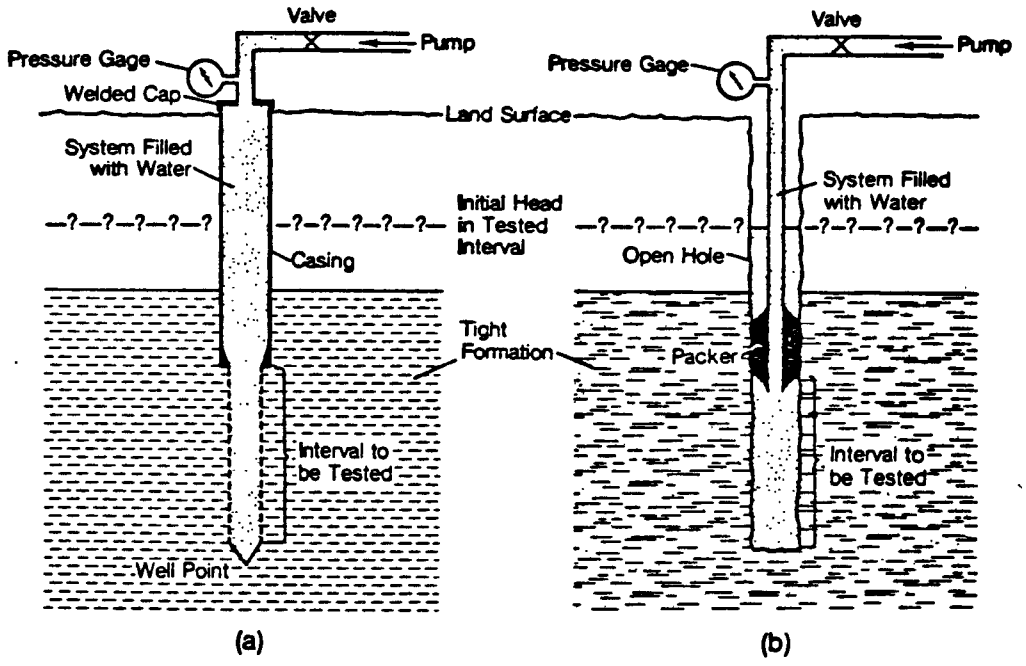


Figure V-6. Possible arrangements for conducting pressurized test (a) in unconsolidated formations and (b) in consolidated formations, (after Bredehoeft and Papadopulos, 1980).

$$\frac{H}{H_o} = F(\alpha,\beta) \qquad \text{(V-20)}$$

where $H_o$ and H are values of head measurement in the hole at the time of shut-in and following that with respect to the background head, respectively. $\alpha$ and $\beta$ are given by

$$\alpha = \frac{\pi r_s^2 S}{V_w C_w \rho_w g} \qquad \text{(V-21)}$$

$$\beta = \frac{\pi T\, t}{V_w C_w \rho_w g} \qquad \text{(V-22)}$$

where

$r_s$ = radius of well in the tested interval.

t = time.

S = storage coefficient of the tested interval.

$V_w$ = volume of water within the pressurized section of the system.

$C_w$ = compressibility of water.

$\rho_w$ = density of water.

T = transmissivity of the tested interval.

g = gravitational acceleration.

Tables of the function $F(\alpha,\beta)$ for a large range of variation of $\alpha$ and $\beta$ are given by the above authors as well as Cooper et al. [1967] and Papadopulos et al. [1973].

Major assumptions applied in development of this method are as follows:

- Flow in the tested interval is radial, which will also imply that the flow at any distance from the well is limited to the radial zone defined by the tested interval.
- Hydraulic properties of the formation remain constant throughout the test.
- The casing and the formation on the side of the borehole containing the water are rigid and do not expand or contract during the test.
- Before the system is pressurized, the water level in the well has come to a near equilibrium condition with the aquifer.

D) Analysis of Field Data

Bredehoeft and Papadopulos have proposed two different techniques, one for $\alpha < 0.1$ and the other for $\alpha > 0.1$. If $\alpha < 0.1$ the following steps should be taken.

- Prepare a family of type curves, one for each $\alpha$, of $F(\alpha,\beta)$ against $\beta$ on semilogarithmic paper. A table giving the value of $F(\alpha,\beta)$ as a function of $\alpha$ and $\beta$ is presented by Bredehoeft and Papadopulos (1980).

- Plot observed values of $H/H_o$ versus time t on another semilog paper of the same scale as the type curves.

- Match the observed curve with one of the type curves keeping the $\beta$ and taxes coincident and moving the plots horizontally.

- Note the value of $\alpha$ of the matched type curve, and the values of $\beta$ and t from the match point.

- Calculate values of S and T from the definitions of $\alpha$ and $\beta$ given by equations (V-21) and (V-22).

The above method is not suitable for $\alpha > 0.1$. In this range of $\alpha$, this method can only give the product of transmissivity and storage coefficient, TS. This product may be calculated by matching the field curve of $H/H_o$ versus time t with a type curve family of $F(\alpha,\beta)$ versus the product $\alpha\beta$ (Fig. V-7).

E) Merits of the Method

As the authors have shown in one example, a conventional slug test in a formation with hydraulic conductivity of $K = 10^{-12}$ m/s may last more than one year whereas the modified slug test method as discussed here may take only a few hours.

F) Uncertainties

- The major assumption employed in this method is that "volumetric changes due to expansion and contraction of other components of the system are negligible." In other words, expansion of the pipes and contraction of the rock in the test zone is negligible relative to that of water. This assumption may introduce large errors into the calculation of hydraulic conductivity. Neuzil (1982) has referred to a test in which the compressibility in the shut-in well was approximately six times larger than the compressibility of water.

- The other major assumption which was employed in this method was that before the system was pressurized, either the water level in the well had come to a near equilibrium condition with the aquifer or that the observed trend could be extended throughout the test. Neuzil (1982) has pointed out that this assumption may also lead to erroneous results. He argues that the pressure changes due to nonequilibrium conditions before shut-in become much more rapid after the well is pressurized. Neuzil (1982) has proposed the following modifications in the setup and procedure for performing the test.

- Modify the test equipment to that shown on Fig. V-8.

- Fill the borehole with water and set two packers near each other.

- Set up two pressure transducers as shown in the figure.

- Close the valve, shutting in the test section, and monitor the pressures in both sections until they are changing very slowly.

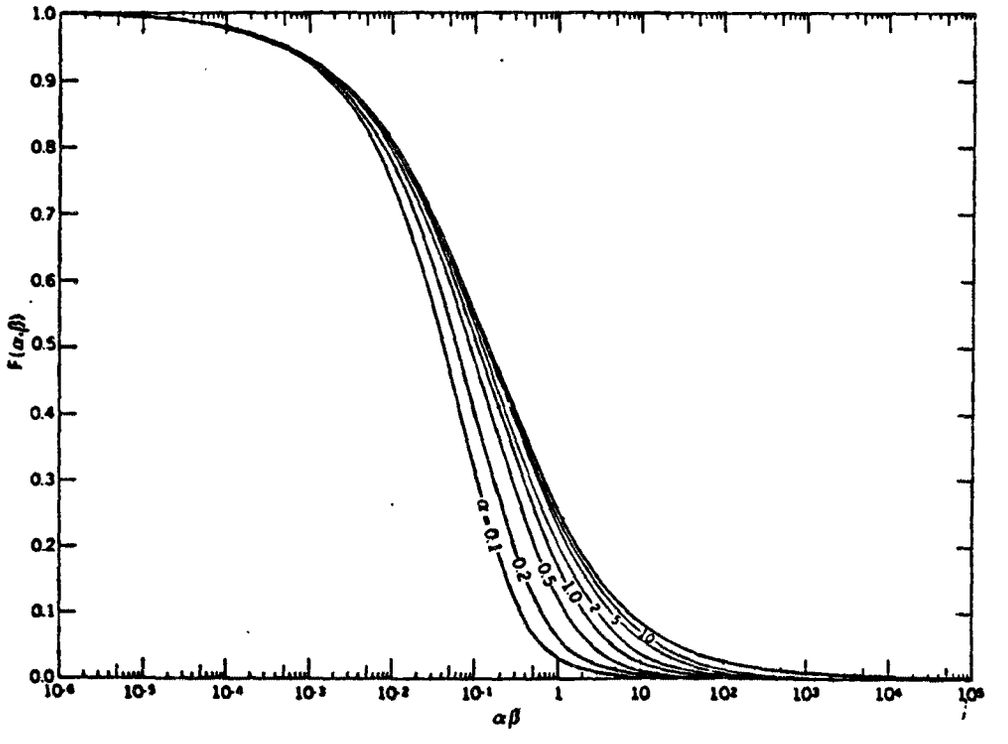


Figure V-7. Type curves of the function $F(\alpha,\beta)$ against the product parameter $\alpha\beta$, (after, Bredehoeft and Papadopulos, 1980).

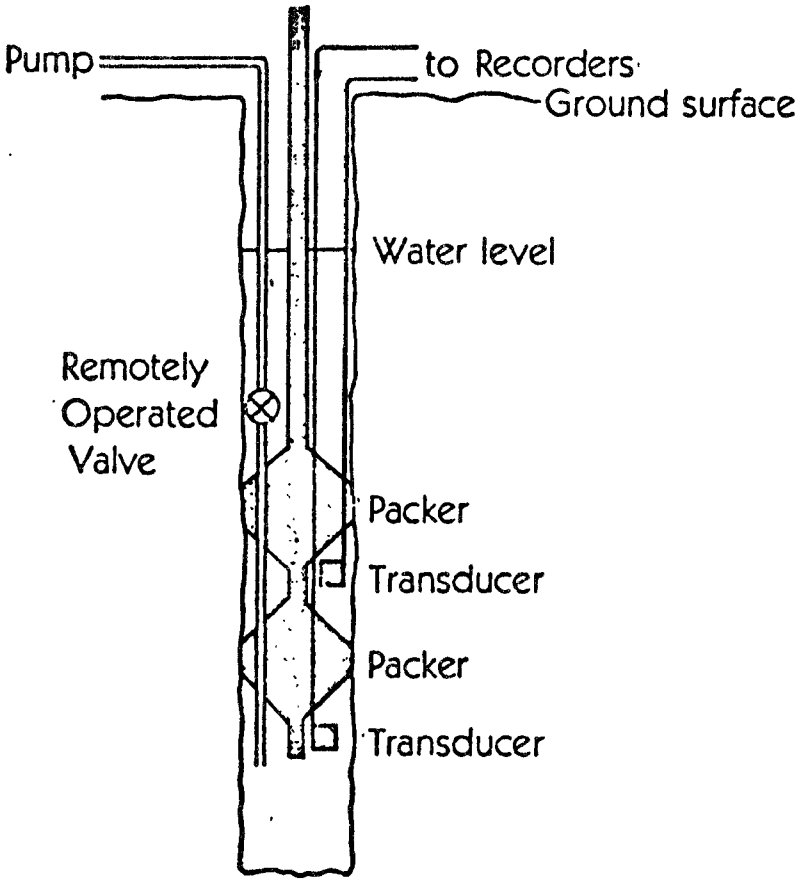


Figure V-8. Arrangement of the borehole instrumentation as suggested by Neuzil (1982).

- Open the valve, pressurize the test section by pumping in a known volume of water, and reclose the valve.

- Measure the net pressure decay (slug) by subtracting the decline due to transient flow prior to the test from the measured total pressure.

- Analyze data using the technique prepared by Bredehoeft and Papadopulos (1980) as was mentioned before, except that the term for the compressibility of water $c_w$ is replaced by the ratio c, defined as

$$c = (\Delta V/v)/\Delta P \qquad \text{(V-23)}$$

where v is the volume of the shut-in section, and $\Delta v$ is the volume of water added to generate a pressure change of $\Delta p$. Neuzil (1982) indicates that a rise in pressure measured by the transducer between the two packers may indicate leakage upward from the test section. However, two other phenomena may cause some rise of pressure in the middle section. One is increase of pressure inside the formation adjacent to the test section, which may or may not be significant. The other reason is the possibility of transfer of pressure by the packer itself, from the test section to the middle section.

## V-2.5 General Comments About Single-Well Tests

The following problems are inherent in all single well tests.

- The hydraulic conductivity measured by these tests is only representative of a small zone around the testing interval. A thin lens of very small permeability located between injection and measuring zones could lead to an erroneously low vertical hydraulic conductivity, even if it is only locally present. This problem may be overcome by conducting several tests within the total thickness of a given formation. However, the lateral variation of vertical hydraulic conductivity could be another problem which requires either other types of testing or performance of a number of single-well tests.

- Because the horizontal permeability of sedimentary materials is usually much larger than the vertical permeability, flow lines generated by either injection or pumping in these tests are predominantly horizontal. Therefore, a long time may be required to have significant pressure disturbances in measuring intervals located vertically above or below the flow zone. A small pressure change together with the possibility of leakage behind the casing due to poor cementing will result in an increased degree of uncertainty in the credibility of these tests in tight formations.

- Measurement of change of pressure due to pumping or injection in single-well tests is another source of uncertainty. This is because the test may often start before the pressure at the measuring interval has stabilized. One way to handle this problem is to minimize the volume of the measurement cavity in the well with the help of extra packers. This will shorten the time required for pressure stabilization.

- In a single-well test, injection is preferred over pumping unless the well will flow without artificial lift (Earlougher, 1980). In a tight formation, indeed, injection is the only feasible way to test.

- The injection or pumping zone should be packed off to minimize well bore storage.

## V-3 Tests with Two or More Wells

Tests involving two or more wells measure the response of a much larger volume of rocks than tests from a single well. Therefore, the value of hydraulic conductivity obtained from multiple well tests is usually more representative of the large scale behavior of the formation. The only problem with these tests is that they cannot be directly used within the formation of interest, once the permeability of that formation becomes very low. Wells completed in very low permeability materials are unable to produce fluid for the required test period. Fluid could be injected in these wells; however, it may take years before any useful response can be measured in observation wells at a distance of 5 to 10 m.

In the following discussions readers are assumed to be familiar with general pump test design and operation. For more information on this subject readers are referred to Stallman (1971).

### V-3.1 Weeks' Method

Weeks (1964) proposed a method of calculating vertical hydraulic conductivity of higher conductivity aquifers. A brief description of his method is given here.

#### A) Purpose

The purpose of this method is to determine in-situ vertical and horizontal hydraulic conductivity of anisotropic aquifers.

#### B) Procedure

- Consider a pumping well which is only partially penetrating an anisotropic aquifer. The well is open to the aquifer over a length of (1-d), (see Fig. V-2).

- Also consider one or more piezometers at distances $r_i$, from the axis of the pumping well, such that each $r_i$ is smaller than half of the thickness of the aquifer.

- Pump the well with a constant rate of discharge Q, for a period of time.

- Measure water level variations in the piezometers and record these variations against the time of measurement.

#### C) Theory

The solution for the drawdown around a partially penetrating well in an anisotropic aquifer has been given by Hantush (1957, 1964).

$$s = (Q/4\pi K_r b)\{w(u) + f\} \qquad \text{(V-8)}$$

where

$$f = [2b/(\pi(1-d))] \sum_{n=1}^{\infty} (1/n)[\sin\frac{n\pi 1}{b} - \sin\frac{n\pi d}{b}]\cdot\cos\frac{n\pi z}{b}\cdot$$

$$\cdot\, W\{u_r, \sqrt{\frac{K_z}{K_r}(\frac{n\pi r}{b})^2}\} \qquad \text{(V-9)}$$

This equation was presented in a slightly different context in section V-2.1.

Hantush (1961) has given another form for f which is valid at large values of time. Weeks (1964) has modified this solution for anisotropic aquifers.

$$f = \frac{4b}{\pi(1-d)} \sum_{n=1}^{\infty} \frac{1}{n}(\sin\frac{n\pi 1}{b} - \sin\frac{n\pi d}{b})\cos\frac{n\pi z}{b}\cdot K_o\cdot[\frac{n\pi r}{b}(\frac{K_z}{K_r})^{1/2}] \qquad \text{(V-24)}$$

where $K_o$ is a modified Bessel function of the second kind and zero order. Equation (V-24) is valid for large values of time when

$$u_r < (\frac{\pi r}{b})^2 \frac{K_z}{20K_r} \qquad \text{(V-25)}$$

$$\text{or } t > \frac{b\,S}{2K_z} \qquad \text{(V-26)}$$

Let us introduce the following dimensionless terms:

$$s_D = \frac{4\pi K_r b s}{Q} \qquad \text{(V-27)}$$

$$t_D = \frac{t\,T}{r^2 S} \qquad \text{(V-28)}$$

where T and S are transmissivity and storage coefficient of the aquifer, respectively.

Given the geometry of the system, one can calculate r/b, z/b, l/b, and d/b. Assuming different values for $K_z/K_r$, a family of type curves showing the variation of $s_D$ against $t_D$ can be prepared for the above known dimensionless parameters.

One may have noticed that the methods proposed by Weeks and Burns are both based on the same theory. Burns' method applies the theory to a single well, and Weeks' method applies it to multiple wells. Saad (1967) and Weeks (1969) have proposed other methods for calculating the ratio of horizontal to vertical permeability in aquifers. Both of those methods are also based on the theory of the Partially Penetrating Wells which was discussed above.

D) Analysis of Field Data

- Plot $s_D$ versus $t_D$ calculated from equation (V-8), (V-9), (V-27), and (V-28) for the dimensionless parameters of the system and for different values of $K_z/K_r$ on log-log paper. Note that equation (V-24) is independent of time. Therefore, it is much simpler to use equation (V-24) in place of equation (V-9) for those times

when $t > \frac{bS}{2K_z}$. This means that the order of magnitude of S and $K_z$ should be estimated in advance. An extensive table evaluating equation (V-8) for the simple case of $d=0$ and $K_z/K_r=1$ is given by Witherspoon et al. (1967), which could be easily modified for the case of $d\neq0$ and an anisotropic medium.

- Plot values of drawdown versus time as measured by each piezometer on another log-log paper with the same scale as the type curves.

- Using the superposition technique, find the best match between the observed data and one of the type curves.

- When the best match is achieved read the $K_z/K_r$ corresponding to the type curve and the coordinates of a match point on both graphs.

- Calculate the radial hydraulic conductivity and the storage coefficient of the aquifer from the following equations.

$$K_r = \frac{S_D Q}{4\pi bs} \qquad \text{(V-29)}$$

$$S = \frac{tbK_r}{t_D r^2} \qquad \text{(V-30)}$$

where s, t, $t_D$ and $s_D$ are coordinates of the match point.

- Calculate the vertical hydraulic conductivity of the aquifer from

$$K_z = \left(\frac{K_z}{K_r}\right)K_r \qquad \text{(V-31)}$$

## V-3.2 Tests Based on the Theory of Leaky Aquifers

The term leaky aquifer generally refers to a system in which an aquifer is overlain and/or underlain by much less permeable layers. Once the pressure in the aquifer drops while being pumped, water from saturated less permeable layers lying above or below leaks into the aquifer. Sometimes the amount of leakage is so great that its effect can be detected in the aquifer being pumped. In this case the confining beds are called "aquitards" and the aquifer is referred to as being 'leaky'. When the amount of leakage is so little that its effect cannot be easily detected in the aquifer, then the confining beds are called "aquicludes" and the aquifer is termed 'slightly leaky' (Neuman and Witherspoon, 1968).

Much work has been done on the theory of leaky aquifers. The first group of papers appeared before 1960 (Jacob, 1946, Hantush and Jacob, 1955, Hantush, 1956) and were based on the assumption that the storage capacity of the aquitard was negligible. Later, Hantush (1960a,b) introduced a new solution for leaky aquifers in which he had considered the effect of storage capacity on the confining bed. Neuman and Witherspoon (1969, 1972) evaluated the significance of the assumptions applied in the earlier work and provided more generalized solutions. A brief description of these methods will be given in the following sections.

One may ask what the relation is between leaky aquifers and the subject of field determination of vertical hydraulic conductivity. Why should we study the leaky aquifer pump

test techniques? As we shall see later, all of the leaky aquifer solutions which are discussed here are based on the assumption that the flow in the less permeable layer, above or below an aquifer, is essentially vertical. Therefore, application of these methods should give an overall vertical hydraulic conductivity for the confining layer.

A) Hantush and Jacob Solution

Jacob (1946) developed a partial differential equation for a leaky aquifer and solved it for a bounded reservoir. Hantush and Jacob (1955) solved the same problem for a radially infinite aquifer. Because of its simplicity, in spite of the fact that in some cases it leads to erroneous results, these solutions have been widely used by groundwater hydrologists.

Purpose

The purpose of this section is to evaluate the possibility of determining the vertical hydraulic conductivity of the confining layer and discuss the assumptions and limitations encompassing the method of approach.

Procedure

The procedure for conducting the test is similar to that for a standard pump test within a simple aquifer. From such a test one obtains a table of observed drawdown in an observation well or a piezometer against the time elapsed from the start of pumping.

Theory

Figure V-9 depicts the arrangement of the system to be studied. A semi-permeable layer (aquitard) with a constant thickness of b' is overlying an aquifer with much higher hydraulic conductivity. The aquitard is overlain by another highly permeable extensive aquifer. The lower aquifer is being pumped with a constant rate of discharge Q. Hantush and Jacob (1955) obtained an expression which gives the drawdown distribution in the pumped aquifer as a function of time. Derivation of this solution was based on the following major assumptions: (1) flow is essentially horizontal in the aquifer and vertical in the aquitard, (2) no drawdown is permitted in the upper aquifer because of pumping in the lower aquifer, (3) leakage into the pumped aquifer is proportional to the potential drop across the aquitard. This last assumption is equivalent to assuming that the storage capacity of the confining bed is negligible, and all the water leaking into the pumped aquifer comes directly from the upper aquifer; thus the aquitard behaves only as a conduit between the two aquifers. The solution to this problem as given by Hantush and Jacob (1955), sometimes referred to as the (r/B solution) is

$$s = \frac{Q}{4\pi Kb} W(u, r/B) \qquad \text{(V-32)}$$

where

$$u = \frac{r^2 S_s}{4tK}$$

$$B = \frac{Kbb'}{K'}, \text{ called the leakage factor.}$$

K, K' = hydraulic conductivity of the aquifer and aquitard, respectively.

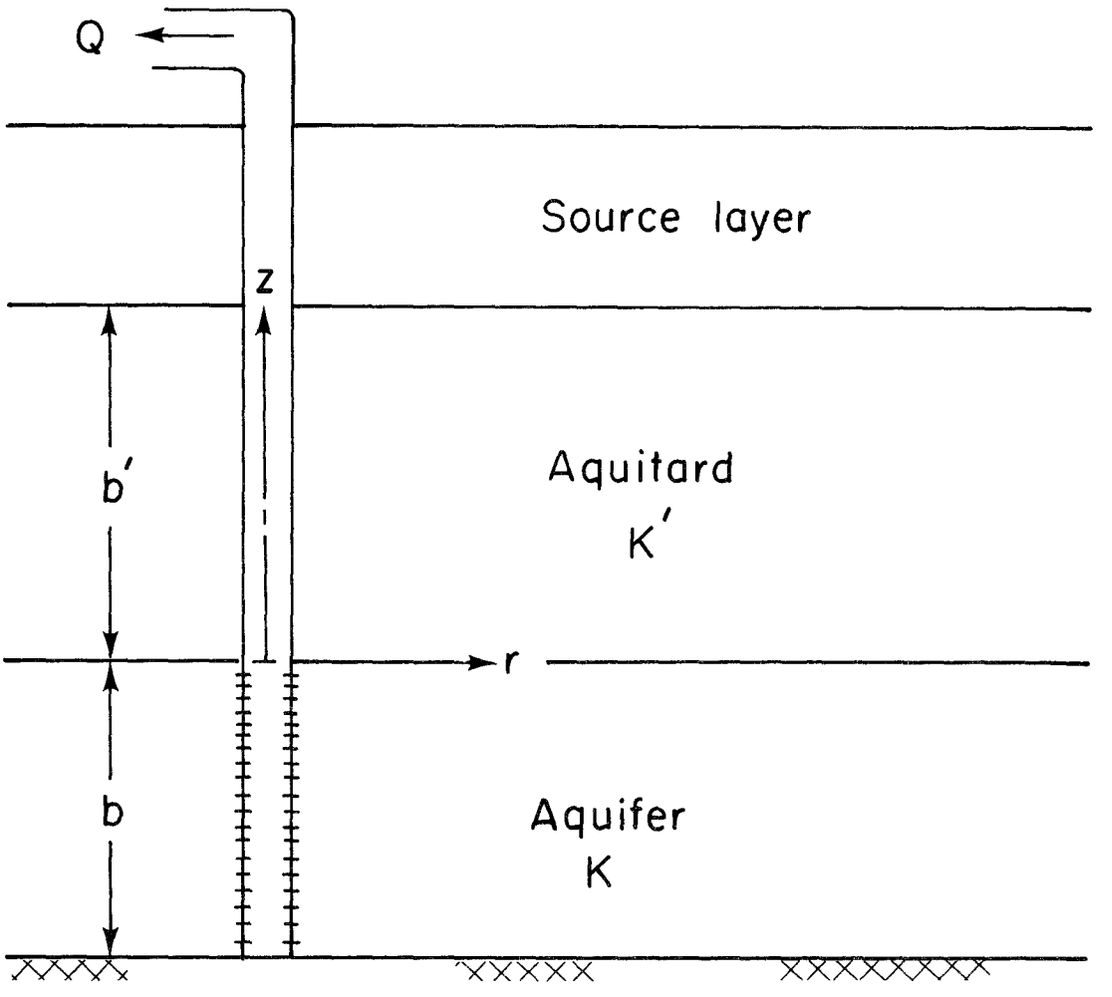


Figure V-9. Leaky aquifer with a constant head boundary at the top of the aquitard.

$S_s$ = specific storage.

s = drawdown in the aquifer.

b, b' = thickness of the aquifer and the aquitard, respectively.

$$W(u, r/B) = \int_u^{\infty} \exp(-y - \frac{r^2}{4yB^2}) \frac{dy}{y}$$

This last term is called the well function of leaky aquifers and has been extensively tabulated (Hantush, 1956).

Analysis of Field Test Data

Several methods based on the r/B solution are conventionally used for interpretation of leaky aquifer pump test data. Here we shall discuss two of these methods.

Walton's Type-Curve Method (1960)

- Prepare a family of type curves by plotting on a log-log paper the values of the function W(u,r/B) versus 1/u with r/B as the running parameter of the curves. Note that the curve with r/B = 0 is the Theis curve.
- Plot the drawdowns versus time as were recorded within an observation well (after appropriate adjustments) on another log-log paper with the same scale as that used for the type curves.
- Follow the regular procedure for curve matching[1] and read the appropriate value of r/B by interpolating the position of the data curve among the type curves. Also read the dual coordinates of the matching point, s,t,1/u, and W(u,r/B).
- Calculate the hydraulic conductivity of the pumped aquifer from

$$K = \frac{Q}{4\pi bs} W(u,r/B) \qquad \text{(V-33)}$$

- Calculate the specific storage of the pumped aquifer from

$$S_s = \frac{4tK}{r^2(1/u)} \qquad \text{(V-34)}$$

- Finally, calculate the vertical conductivity of the aquitard from

$$K' = \frac{Kbb'}{r^2} \left(\frac{r}{B}\right)^2 . \qquad \text{(V-35)}$$

---

[1] A unique fitting position is difficult to obtain unless sufficient data are available from the period when the leakage effect is insignificant (Hantush, 1964).

U.S.B.R. Method

U.S. Bureau of Reclamation (1977) has published a groundwater manual as a guide for field personnel in groundwater investigation. Following is the method which that manual suggests for interpretation of pump test data of a leaky aquifer. Fig. V-10 shows a family of type curves prepared from Jacob's leaky aquifer solution (1946). As was discussed before, Jacob's solution was developed for a radially bounded aquifer. However, in developing Fig. V-10 the outer boundary was located at a sufficient distance that the effect of pumping never reached it (Glover, Moody, and Tapp, 1960). This approach permits the curves to be used for infinite aquifers. The steps to be used in applying the USBR method are as follows:

- Drawdown versus time from two or more observation wells (after appropriate corrections) located at different radial distances r from the pumped well should be plotted on a log-log paper with the same scale as Fig. V-10.

- Superimpose the field curve with those of Fig. V-10.

- After obtaining the best match read the dual coordinates of a match point (s,t, u and $\eta$), and the x value of the best fitting type curve. Interpolation may be required to find the x value.

- Calculate the hydraulic conductivity of the aquifer from

$$K = \frac{Qu}{2\pi Ms} \qquad \text{(V-36)}$$

- Calculate the hydraulic conductivity of the aquitard from

$$K' = KMM'\left(\frac{x}{r}\right)^2 \qquad \text{(V-37)}$$

- Finally, calculate the storage coefficient of the aquifer from

$$S = \frac{K't}{\eta M'} \qquad \text{(V-38)}$$

In the above equations M and M' indicate the thickness of the aquifer and the aquitard, respectively. The ratio r/x is the leakage factor B used in the development of the theory. The definitions of other terms are given in Fig. V-10.

The following is a quotation from the U.S.B.R. staff on the interpretation of leaky aquifer pump test data from the Missouri river basin project (Glover, Moody, and Tapp, 1960, p. 175).

> "When drawdown data from well tests are compared with drawdown curves computed for idealized conditions a lack of perfect agreement is generally evident".

Other methods of analysis of field data based on r/B solution have been suggested by Hantush (1964, p. 416-417), and Narasimhan (1968).

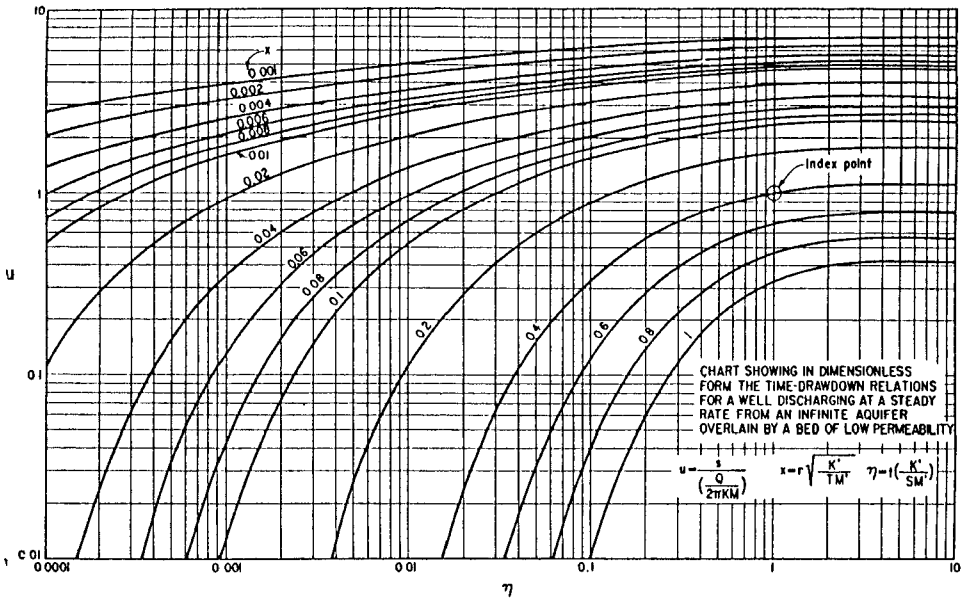


Figure V-10. Leaky aquifer type curves based on r/B approach (USBR, 1977).

Uncertainties

The problem of flow to a pumped well in a hydrologic system consisting of several aquifers separated by less pervious aquitards or aquicludes is in fact three dimensional. A rigorous approach to the solution of such a problem is analytically intractable. Therefore, it has been customary to simplify the problem by assuming that flow is essentially horizontal in the aquifers and vertical in the aquitards and aquicludes. The validity of this assumption which was used in the derivation of the r/B solution, was evaluated by Neuman and Witherspoon (1969). They noted that the errors introduced by this assumption are less than 5 percent provided that the conductivities of the aquifers are more than three orders of magnitude greater than that of the aquitards. These errors increase with time and decrease with radial distance from the pumping well. One should note that the 5 percent error given by Neuman and Witherspoon (1969) is the percentage difference between drawdowns calculated by the analytic solution based on the above assumption and drawdowns obtained by a finite-element numerical analysis without that assumption. The magnitude of the error which may result in the calculation of the hydraulic properties of the confining layer is not known.

Another assumption used in the derivation of the r/B solution is that no water is released from storage in the aquitard. Neuman and Witherspoon (1969) have found that this assumption tends to result in overestimating the permeability of the aquifer and underestimating the permeability of the aquitard.

An important uncertainty about the r/B solution is that it does not provide a means of distinguishing whether the leaking bed lies above or below the aquifer being pumped. In the case of leakage from both above and below the aquifer, this method does not provide a means for determining conductivities of individual aquitards. This becomes particularly important when one is looking for the hydraulic conductivity of a certain confining bed rather than that of the aquifer itself.

When the hydraulic conductivity of the confining bed becomes so small that the ratio of K'/K tends to zero, the drawdown distribution in the aquifer becomes essentially the same as would be predicted by the Theis solution for an aquifer without leakage. As a result, techniques based on observation in the aquifer alone fail to give the properties of the confining bed.

B) Hantush Modified Solution

In 1960 Hantush published another paper in which he introduced a new treatment of leaky aquifers which overcame some of the difficulties of the r/B solution.

Purpose

The Hantush modified solution provides a more accurate approach to the evaluation of the vertical hydraulic conductivity of less permeable layers which confine permeable aquifers.

Procedure

The test procedure again follows the same steps as a regular pump test. Needed for interpretation is a record of drawdown versus time in one or more observation wells around a pumping well.

Theory

In this development, in addition to assigning a storage capacity to the confining aquitard, Hantush (1960) solved the problem for two different cases: (1) an infinite horizontal aquifer overlain by an aquitard whose upper boundary does not experience any change in drawdown, and (2) the same situation but with an impermeable bed overlying the aquitard. Other assumptions applied in the development of the r/B solution, including vertical flow in the aquitard and horizontal flow in the aquifer, still hold. In this solution Hantush considered leakage into the aquifer from both above and below. He presented the solutions for two ranges of time t as indicated below.

Solutions for Small Values of Time

For t less than both b'S'/10K' and b"S"/10K", the solution for both cases is the same and is given by

$$S = \frac{Q}{4\pi Kb} H(u,\beta) \qquad \text{(V-39)}$$

where

$$H(u,\beta) = \int_u^\infty \frac{e^{-y}}{y} \operatorname{erfc}(\beta\sqrt{u}/\sqrt{y(y-u)})dy$$

$$\beta = (r\lambda)/4$$

$$\lambda = \sqrt{\frac{K}{Kb'}\frac{S'}{S}} + \sqrt{\frac{K''}{Kb''}\frac{S''}{S}}$$

$$u = \frac{r^2 S}{4tbK}$$

s = drawdown in the aquifer.

S",S' = storage coefficient of the lower and upper aquitards, respectively.

K",K' = hydraulic conductivity of the lower and upper aquitards, respectively.

r = radial distance of the observation well from the pumped well.

b",b' = thickness of aquitards below and above the aquifer, respectively.

$H(u,\beta)$ has been extensively tabulated (Hantush, 1960b). A short table of $H(u,\beta)$ is also available (Hantush, 1964).

Solution for Large Values of Time

Case 1.

In this case, t should be larger than both 5b'S'/K' and 5b"S"/K". The solution is then given by

$$s = \frac{Q}{4\pi bK} W(u\delta_1,\alpha) \qquad \text{(V-40)}$$

where

$$W(u\delta_1, \alpha) = \int_{u\delta_1}^{\infty} \frac{dy}{y} \exp(-y - \frac{\alpha^2}{4y})$$

is the well function for leaky aquifers which is tabulated by Hantush (1956);

$$\alpha = r\sqrt{\frac{K'}{bb'K} + \frac{K''}{bb''K}}$$

$$\delta_1 = 1 + \frac{S' + S''}{3S}$$

The other terms are the same as defined before.

Case 2.

For t greater than both 10b'S'/K' and 10b"S"/K" the expression for drawdown in the aquifer is

$$s = \frac{Q}{4\pi Kb} W(u\delta_2) \qquad \text{(V-41)}$$

where

$$W(u\delta_2) = \int_{u\delta_2}^{\infty} \frac{e^{-y}}{y} dy \quad \text{is the well function}$$

$$\delta_2 = \frac{S' + S''}{S} + 1$$

At this point, before describing the method of interpreting the pump test data, the applicability of the different operations given above will be reviewed. For large values of time, equation (V-40) indicates that, even when one considers the storage capacity of the confining bed, the r/B solution could be safely used for evaluation of the aquifer and aquitard, provided that $t > \frac{5b'S'}{K'}$. This solution may qualify at relatively small values of time when the aquitard is thin, when it has a relatively high hydraulic conductivity and is incompressible (i.e. very small S'). For example, if b' = 5m, K' = $2x10^{-7}$ m/s, and S' = $2x10^{-5}$, then the r/B solution is applicable after 2500 seconds, or approximately 41 minutes after the start of the test. In applying the simpler r/B solution, note that u should be replaced by $u(1 + \frac{S'}{3S})$. Also, the aquifer above the aquitard should not show any drawdown during the test. If the overlying aquifer does show some drawdown, then the r/B solution tends to underestimate the hydraulic conductivity of the aquitard. On the other hand, if the confining bed is relatively thick and elastic with low hydraulic conductivity, then the r/B solution is not applicable. For example, if b' = 50m, K' = $5x10^{-9}$ m/s and S' = $10^{-3}$, then the r/B solution is only applicable after $5x10^{7}$ seconds, or approximately 1.5 years after the test has started.

Equation (V-41) suggests that when the confining bed is thin, relatively permeable, and incompressible, and overlain by an impermeable layer which cannot supply water, the drawdown

data in the aquifer will follow the Theis solution at relatively small values of time. In applying the Theis solution, note that u should be replaced by $u(1 + \frac{S'}{S})$.

Equation (V-39) is the solution for small values of time. It can also be applied to relatively large values of time when the aquitard is thick, relatively impermeable and compressible. For example, if b' = 100m, K' = $10^{-9}$ m/s, and S' = $10^{-3}$, then equation (V-39) is applicable for $10^7$ seconds or the first 115 days of the test. Note that within this range of time the effect of pumping would not reach the upper boundary of the aquitard. Therefore, the assumption of a constant head boundary there does not introduce any error. The above discussion was made only with reference to the upper confining bed. In each case, however, both the upper and lower beds must meet the same criteria for these simplifications to apply.

Analysis of the Field Data

Figure V-11 shows a family of type curves on a log-log plot of $H(u,\beta)$ versus 1/u which can be used for the analysis of the Hantush modified solution.

- Plot the variation of drawdown versus time on a log-log paper with the same scale as that of the type curves.
- Use the superposition method to find the best match between the observed plot and the appropriate type curve.
- Read the value of $\beta$ from the type curve which matches the observed plot, and the dual coordinates $H(u,\beta)$, 1/u, t, and s of the match point.
- Calculate the hydraulic conductivity of the aquifer from

$$K = \frac{Q}{4\pi bs} H(u,\beta) \qquad \text{(V-42)}$$

- Calculate the storage coefficient of the aquifer from

$$S = \frac{4tbKu}{r^2} \qquad \text{(V-43)}$$

- Calculate $\lambda$ from

$$\lambda = \frac{4\beta}{r} \qquad \text{(V-44)}$$

- If we assumed that the lower layer is completely impermeable, then

$$K'S' = \lambda^2 Kbb'S$$

- If one can determine the magnitude of the storage coefficient of the aquitard S' from other methods, then the hydraulic conductivity of the aquitard may be obtained from

$$K' = \frac{\lambda^2 Kbb'S}{S'}$$

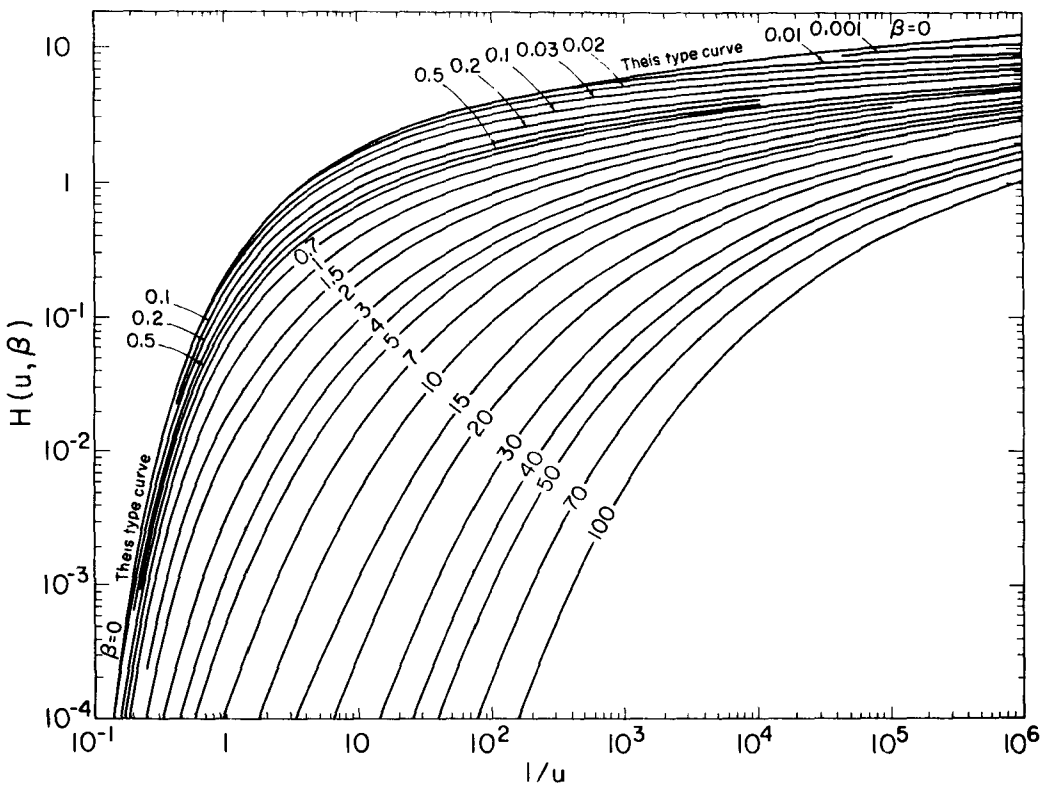


Figure V-11. Type curves of the function H(u,$\beta$) against 1/u, for various values of $\beta$ (after Lohman, 1972).

Uncertainties

Except for very large values of $\beta$, the type curves have shapes that are not too different from the Theis curve. Thus, it is difficult to decide which of the type curves to use in matching against field data. When b is very small, one may easily choose a $\beta$ which could be off by two orders of magnitude. Since $K'S' = (\beta^2)\frac{16Kbb'S}{r^2}$, an error in choosing $\beta$ would lead to a much larger error in the calculation of (K'S'). Thus, two orders of magnitude error in estimating $\beta$ would lead to four orders of magnitude error in (K'S').

In order to improve this problem, Weeks (1977) suggested that data from at least two observation wells at different distances from the pumping well should be used. A composite plot of the drawdown versus $t/r^2$ is made on a log-log paper with the same scale as that of the type curves. As a result, one should obtain two or more type curves each with different values of $\beta$ proportional to the value of r. A unique match may then be obtained by adding the extra constraint that r values for observation wells must fall on curves having proportional $\beta$ values (Weeks, 1977). This method could somewhat improve the results but, when $\beta<0.01$, type curves with different values for $\beta$ are so close together that a unique match is still next to impossible.

Very often both layers above and below an aquifer constitute leakage to the aquifer. If this is the case, one may not be able to find the properties of either of the confining layers. All this method can give is the value of $\lambda$ (equation V-44), which is a parameter depending on the properties of both confining layers and the aquifer. This method provides no means for independently determining the properties of both confining layers.

Even when leakage comes only from one of the confining layers, this method gives the product of the hydraulic conductivity and the storage coefficient of the aquitard. The value of the storage coefficient for the aquitard must be found by some other means before one can finally obtain the vertical hydraulic conductivity.

C) Witherspoon and Neuman Ratio Method

When the ratio of K'/K decreases, both r/B and $\beta$, as defined in previous methods, decrease and equations (V-32) and (V-39) will eventually reduce to the Theis solution. Therefore, it is obvious that determining the hydraulic conductivity of a tight confining layer by observations in the aquifer alone, if at all possible, is associated with a great many uncertainties. Witherspoon et al. (1962) suggested a method of calculating the permeability of the caprock of gas storage reservoirs which was based on using observations of drawdown in both the aquifer and the overlying aquiclude. Later, Witherspoon and Neuman (1967) presented as improvement over the previous method. This work, together with their more recent works (Neuman and Witherspoon, 1972), will be discussed here.

Purpose

The purpose of this section is to describe a method of determining the vertical hydraulic diffusivity of a low permeable layer overlying an aquifer.

Procedure

- Complete a pumping well through the total thickness of the aquifer.

- Construct an observation well in the aquifer at a distance r from the axis of the pumping well.

- Establish at least three transducers at three different elevations within the confining bed as shown in Fig. V-12. It is required that the radial distance of all three transducers from the pumping well be the same as that of the observation well. To avoid the effect of possible inhomogeneity of the media, it is preferred to have all the transducers in the same well close to the observation well.

- Start recording water levels in the observation well and values of pressure measured by the transducers long before the start of the pumping test. It is very important that the values of pressure measured by the transducers come to an equilibrium condition before the beginning of the test.

- Start producing from the pumping well with a constant rate Q. Pumping should continue until at least half a meter of drawdown is observed by the middle transducer in the aquiclude. Recently very accurate pressure-measurement instruments have been introduced to the market which are able to measure pressure changes equivalent to 1 cm or less of water. If such instruments are available for use, then 10 cm of drawdown would be sufficient. Recording of water level in the observation well and pressures measured by the transducers should continue at least a few days after pumping has stopped.

Theory

Let us first discuss the theory which was developed for evaluating a slightly permeable aquiclude. A review of more recent works from Neuman and Witherspoon will then follow.

Consider an aquifer of finite thickness overlain by a semi-infinite confining bed. When the ratio of K'/K is sufficiently small, then under the influence of pumping the aquifer, the flow in the confining bed is essentially vertical, and the drawdown in the aquifer can be closely approximated by the Theis solution. The term semi-infinite has been used to indicate that the aquiclude is so thick that the effect of pumping the aquifer does not reach the top of the aquiclude. With the above assumptions in mind, Witherspoon and Neuman (1967) derived the following expression which gives the drawdown in the aquiclude as a function of time t and elevation z above the top of the aquifer.

$$s' = \frac{Q}{2\pi^{3/2}Kb}\int_{1/4t_D'}^{\infty} - EI\left[-\frac{t_D'y^2}{t_D(4t_D'y^2 - 1)}\right] e^{-y^2}dy \qquad \text{(V-45)}$$

where

$$t_D' = \frac{K't}{S_s'z^2}$$

$$t_D = \frac{Kt}{S_s r^2}$$

$$-Ei(-x) = \int_x^{\infty} \frac{e^{-y}}{y}dy$$

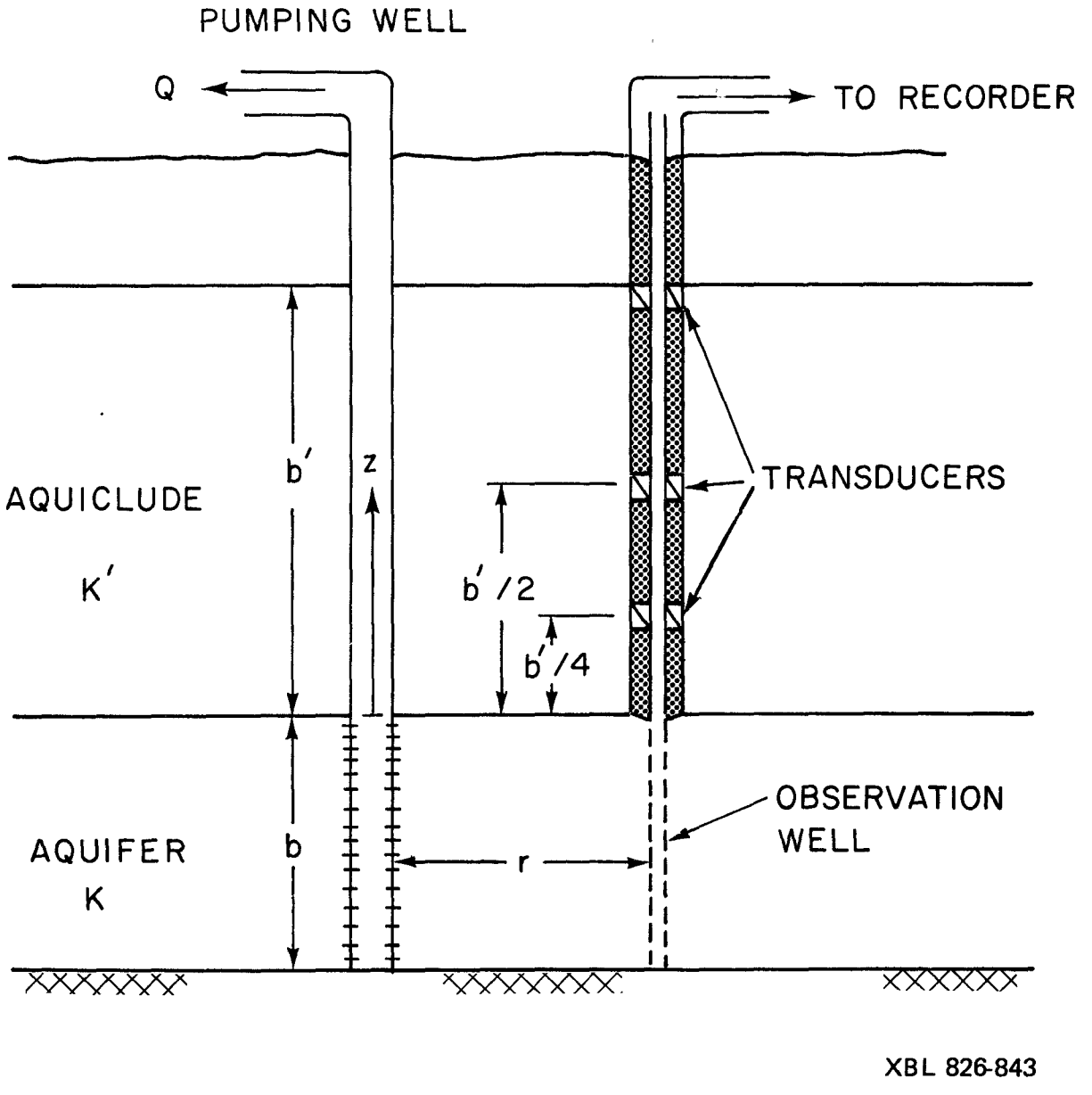


Figure V-12. A suggested arrangement for conducting a ratio-method test.

$z$ = vertical distance from the top of the aquifer

$S_s$, $S_s'$ = specific storage of the aquifer and the aquiclude, respectively.

Equation (V-45) has been evaluated over a practical range for the two parameters $t_D$ and $t_D'$. Calculated values of s' and s'/s for different $t_D$ and $t_D'$ have been tabulated in Appendix G of Witherspoon et al. (1967). Figure V-13 shows a family of curves presenting variation of s'/s versus $t_D'$ for different values of $t_D$.

A variation of the above problem, involving a finite thickness aquiclude, has also been solved by Neuman (1966). In this derivation the hydraulic head was assumed to be constant at the top of the aquiclude. This solution has been evaluated over a practical range of relevant dimensionless parameters and the results are tabulated in Appendix H of Witherspoon et al. (1967).

Later, Neuman and Witherspoon (1969a) developed a complete solution for the distribution of drawdown in a system consisting of an aquitard separated by two aquifers as shown on Fig. V-14. In each aquifer the solution depends on five dimensionless parameters, and in the aquitard six dimensionless parameters are involved. Consequently, Neuman and Witherspoon (1972) stated that "This large number of dimensionless parameters make it practically impossible to construct a sufficient number of type curves to cover the entire range of values necessary for field application." Hantush (1960) apparently had noticed this problem before as he stated that "It should be remarked that rigorous solutions can be obtained for the actual nonsteady three-dimensional flow in layered aquifers, as well as solutions for flow systems in which the condition of vertical leakage is removed. These solutions, however, are very difficult to evaluate numerically and are therefore not presented here."

As a result, in spite of the development of more sophisticated theories, because of the difficulties which appear in the process of their application in the field, authorities seem to go back and recommend the simpler approaches. For example, all the methods of analysis of the leaky-aquifer pump tests described by Hantush (1964), appearing four years after he introduced the modified theory (1960), are based on the r/B solution. Neuman and Witherspoon (1972), too, stated that "We therefore decided to adopt the ratio method as a standard tool for evaluating the properties of aquitards." This happened five years after their original introduction of the ratio method (1967).

Analysis of the Field Data

- Observe the pressure record of the transducer at the top of the confining bed. If it shows any drawdown beyond the error limits of the system, note the time of such observation and ignore all records of drawdown measured after that time.

- Calculate the hydraulic conductivity K, and the specific storage $S_s$ of the aquifer using Hantush's modified solution and the drawdown record from the observation well.

- Plot the values of drawdown, measured both in the aquifer and the aquiclude, on log-log paper and draw smooth curves through the data.

- Select several arbitrary values of time t. All values should be smaller than the time when drawdown was first noted at the top transducer.

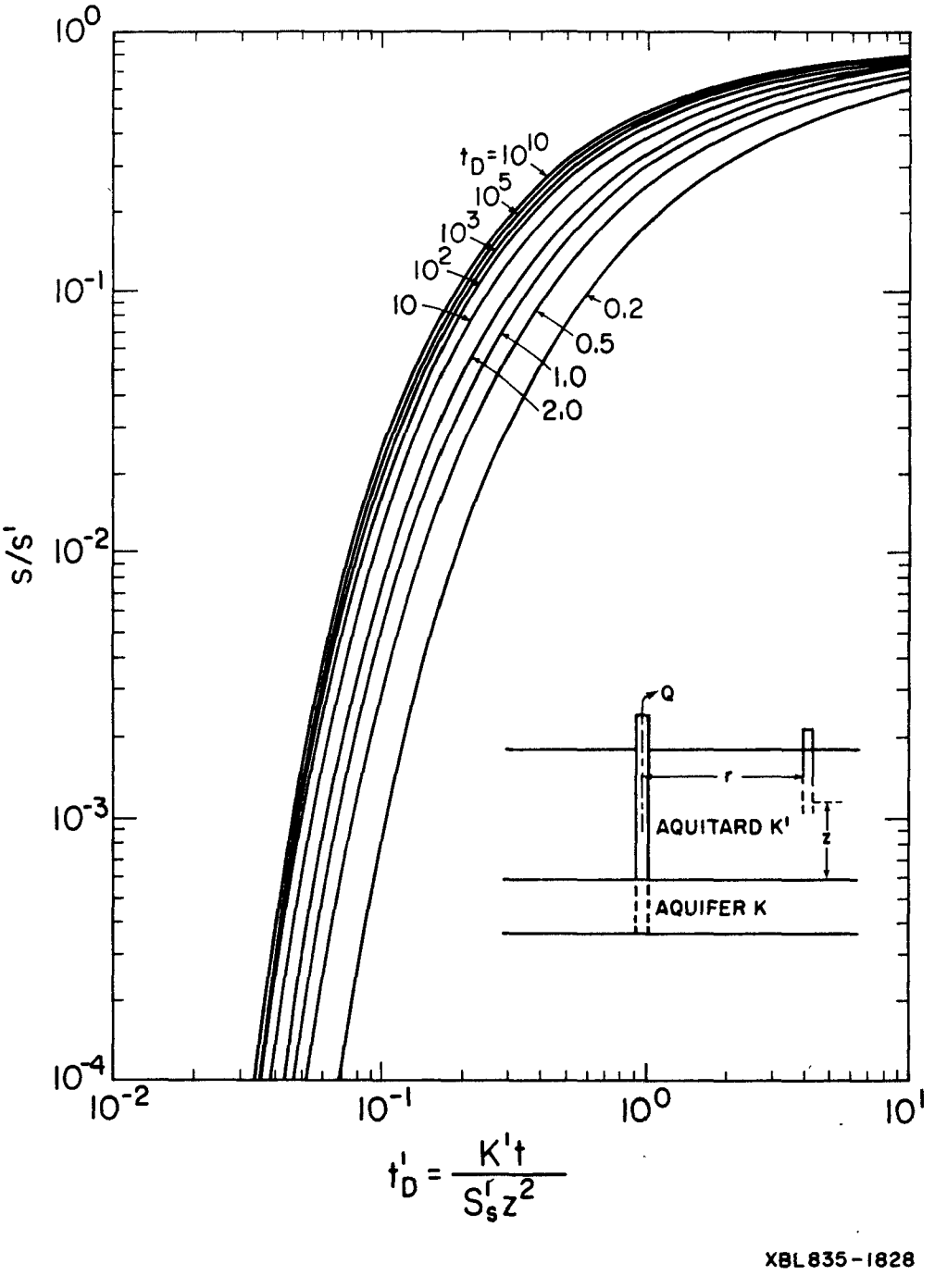


Figure V-13 The variation of s'/s with $t_D$' for a semi-infinite aquitard (modified from Witherspoon et al. 1967).

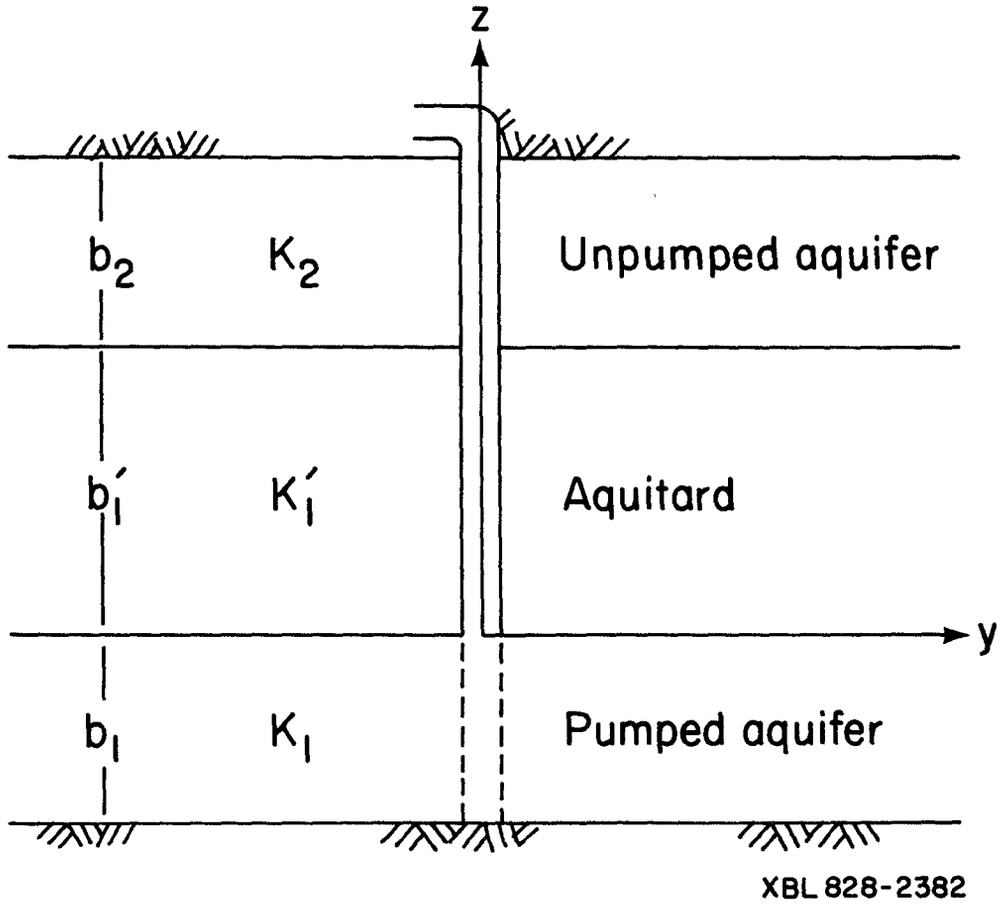


Figure V-14. Schematic diagram of two aquifer system.

- Calculate $t_D$ for each selected value of t from the following equation

$$t_D = \frac{Kt}{S_s r^2} \qquad \text{(V-46)}$$

- At each value of time select representative values of s and s' from the time drawdown plots.

- Using the appropriate curve corresponding to each value of $t_D$ from Fig. V-13, find $t_D'$ for each ratio of s'/s.

- Calculate the vertical hydraulic diffusivity of the confining bed for each value of t and z of a particular transducer from

$$\frac{K'}{S_s'} = \frac{z^2 t_D'}{t} \qquad \text{(V-47)}$$

- For each value of z find the average value of $K'/S_s'$ calculated for different selected times. The average value calculated for each z should represent the diffusivity of that part of the confining layer between the top of the aquifer and that particular elevation.

Advantages

As was noted before, if the aquifer received leakage from both above and below, then r/B and $\beta$ methods, which relied on the measurement of drawdowns in the aquifer alone, failed to lend themselves to calculation of the hydraulic conductivities of the confining layers. The ratio method, on the other hand, can provide a means of calculating hydraulic diffusivities of both upper and lower confining beds.

Uncertainties

- The ratio method can only lead to the calculation of the vertical diffusivity of the confining beds. If one can calculate the specific storage by other means, then the vertical hydraulic conductivity of those layers may be computed. Leahy (1976) has used the following approach to overcome the above difficulty. He used Hantush's (1960) $\beta$ solution to find the product of K' and $S_s'$, and the Witherspoon and Neuman (1967) ratio method to find the ratio of $K'/S_s'$. Then, he calculated the value of K' from

$$K' = \left(\left(\frac{K'}{S_s'}\right) \cdot (K' \cdot S_s')\right)^{1/2} \qquad \text{(V-48)}$$

- The method is based on the assumption that the hydraulic head remains constant at the top of the confining bed. Depending on the thickness and the hydraulic properties of the aquitard, this may or may not cause errors in the result. If the aquitard is thin with a small storage coefficient, the transient effect may completely penetrate it at relatively early stages of the pump test.

- Wolff (1970) reported that piezometers completed in the aquitard exhibit reverse water-level fluctuations, in that water levels rise for some period of time after the start of pumping from the aquifer. He relates these changes to radial and vertical deformation of the aquifer and aquitard resulting from their compressibility. Because the ratio method does not take such phenomena into account, Weeks (1977) warns the investigators against application of this method. This phenomenon has not been observed in other tests such as the ones reported by Leahy (1977), and Neuman and Witherspoon (1972).

## V-4 Conclusions

Vertical hydraulic conductivity of permeable formations can be easily obtained by the analysis of appropriate aquifer pump tests. For less permeable formations, two general types of field tests are available which could estimate vertical hydraulic conductivity. The first includes methods based on single well tests in the low permeability formation itself, while the second includes large scale multiple well pumping tests designed and interpreted based on the various theories of leaky aquifer systems.

The problem inherent in the first type of tests is that the measured hydraulic conductivity is normally only representative of a small zone around the testing interval. Hence, again, a large number of testing wells is required to give a clear picture of the distribution of the vertical hydraulic conductivity in the area of interest.

The most commonly used method among the second type of test is based on an early leaky aquifer solution of Hantush (1956). This solution ignores the storativity of the confining bed. Neuman and Witherspoon (1969) have noted that the application of this method tends to overestimate the hydraulic conductivity of the aquifer and underestimate that of the confining bed. When the confining layer is thin and relatively permeable and incompressible, however, this method could give useful results.

Hantush's (1960) modified method and the "ratio method" of Neuman and Witherspoon (1972) are two other techniques of the second type of tests which under certain circumstances could be used for determination of $(KS_s)$ and $(K/S_s)$, respectively. Unfortunately, neither of these two methods can yield vertical hydraulic conductivity unless the specific storage of the low permeability layer is independently identified (see Chapter VI). Furthermore, Hantush's method is unable to separately distinguish the contribution of leakage from upper and lower confining beds, thus introducing further difficulties in calculation of the vertical hydraulic conductivity of the individual confining layers.

# CHAPTER VI

# FIELD METHODS FOR THE MEASUREMENT OF EFFECTIVE POROSITY, HYDRAULIC HEAD, AND STORATIVITY*

## VI-1 Introduction

As the reader will have realized by now, most of this report is devoted to the measurement of hydraulic conductivity distributions and a brief discussion of how such distributions may be used in mathematical modeling. However, in a complete study of the hydraulics of contaminated ground water it is necessary to measure other hydrogeologic properties or parameters such as effective porosity, hydraulic head, and storativity. For this reason, and in the interest of completeness, Chapter VI will be devoted to a review of the definition and measurement of these three quantities.

While not nearly as important or variable as hydraulic conductivity, porosity of geologic materials plays an important role in controlling groundwater travel time and transport of hazardous substances between sources and the accessible environment. Therefore, determination of a representative value of porosity for a given volume of geologic materials, or a statistical distribution of this parameter, is of interest in predicting the transport of hazardous waste substances in projects such as radioactive waste isolation and underground injection of hazardous waste liquids. Another important area of such need is in projects related to groundwater contamination and remediation. In this chapter, some of the conventional methods used for the field measurement of porosity will be reviewed. The limitations and uncertainties related to each method will be discussed.

Hydraulic head measurements are fundamental to determining rates and directions of movement of contaminant plumes. Usually, such measurements are straightforward except for the case where multiple fluids of different densities, such as salt water and fresh water, are present. Therefore, an overview of hydraulic head measurement is presented with attempts to clarify the measurement of head in fluids having non-negligible density differences.

When contaminant transport in time varying flow fields is of interest, one may have the need to measure aquifer storativity or storage coefficient. Methods for accomplishing this are reviewed briefly.

## VI-2 Field Measurement of Effective Porosity

The porosity of a material is defined as the ratio of void space to total bulk volume. Sometimes some of the voids are isolated and do not play a role in transmitting fluid. This is the reason for introducing the concept of effective porosity, which is defined as the ratio of the volume of connected pores to the bulk volume of the material. Porosity is a scalar property of the rock, which means it is independent of direction.

---

* Material in this chapter has been taken from the Lawrence Berkeley Laboratory Report No. LBL-15050 entitled "Field Determination of the Hydrologic Properties and Parameters that Control the Vertical Component of Groundwater Movement" by Iraj Javandel, prepared under sponsorship of the U.S. Nuclear Regulatory Commission.

There are several methods which are commonly used in the laboratory to measure the porosity of a rock core sample. These techniques, including the direct method, mercury injection, gas expansion, and imbibition have been fully discussed in an American Petroleum Institute report (1960). Because laboratory techniques are not within the scope of this report, we shall not discuss them further.

In the field, porosity may be obtained by several methods including well logging and tracer tests. The following is a brief discussion of several of these techniques, such as Sonic, Formation Density, and Neutron Logs, and tracer tests. There are various private companies that perform porosity measurements as well as other types of geophysical measurement services.

VI-2.1 Sonic Log Method

A more detailed description of this method and additional references are given in Schlumberger (1972). Generally, for a given rock, when porosity increases the sonic velocity decreases. The Sonic Log is a recording of interval transit time ($\Delta t$) versus depth. The interval transit time is the time required for a compressional sound wave to traverse through one foot of formation. This transit time for a given formation is a function of its lithology and porosity. The Sonic Log is therefore a useful means for obtaining porosity, provided the lithology is known.

A) Theory and Procedure

A sonic tool, consisting of two transmitters and two pairs of receivers, is lowered into an uncased well filled with drilling mud or other fluid, (See Figure VI-1). A pulse is generated by each of the two transmitters and the difference between the arrival times of the first wave at the corresponding pair of receivers is measured. The $\Delta t$ from the two sets of receivers are averaged and recorded as a function of depth.

The wave generated by the transmitter will travel through different available media. However, since the speed of the wave in the formation is generally larger than that in the drilling fluid or the sonde itself, the wave which will first arrive at the receivers is the one which has traveled through the formation very close to the wall of the hole. As we measure the difference in travel time to the two receivers, the period of time corresponding to travel through the drilling fluid is cancelled out. As a result, knowing the constant of the instrument, the measured $\Delta t$ can be adjusted to show the reciprocal of the velocity in the formation. $\Delta t$ is generally recorded in microsecond/foot ($\mu$sec/ft) and it varies between about 44 $\mu$sec/ft (for dense, zero porosity dolomite) to about 190 $\mu$sec/ft for pure water.

Wyllie et al. (1956, 1958) have proposed the following empirical formula for determining the porosity $\phi$ of a consolidated formation with uniformly distributed pores:

$$\phi = \frac{\Delta t_{log} - \Delta t_{ma}}{\Delta t_f - \Delta t_{ma}} \qquad \text{(VI-1)}$$

where

$\Delta t_{log}$ = transit time reading on the Sonic Log, in $\mu$sec/ft

$\Delta t_{ma}$ = transit time for the rock matrix material (values for different rocks are given in Table VI-1)

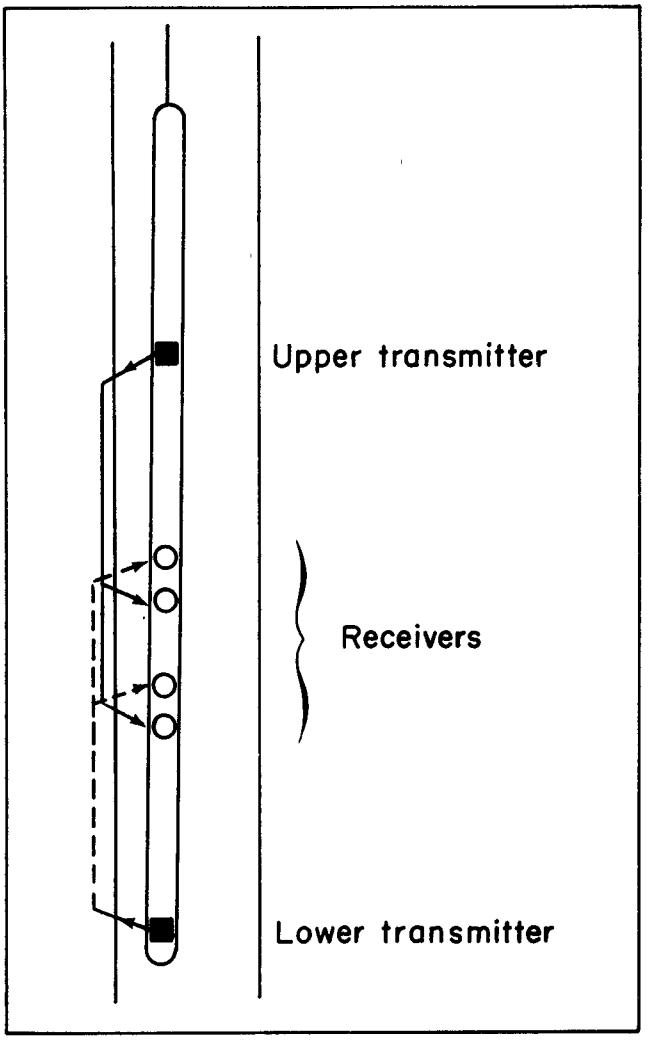


Figure VI-1. Sketch of a sonic tool, showing ray paths for transmitter receiver sets (modified from Kokesh et al., 1965).

$\Delta t_f$ = the inverse of the velocity of a Sonic Wave in the pore fluid (about 189 $\mu$sec/ft).

Table VI-1. Values of transit time for common rocks and casing (modified from Schlumberger, 1972).

| Rock | $\Delta t_{ma}$($\mu$sec/ft) |
|---|---|
| Sandstones | 51.0-55.5 |
| Limestones | 47.5 |
| Dolomites | 43.5 |
| Anhydrite | 50.0 |
| Salt | 67.0 |
| Casing (iron) | 57.0 |

To calculate porosity at a given depth, one should identify the type of rock from cores and/or cuttings and determine the value of $\Delta t_{ma}$ from Table VI-1, or other sources. $\Delta t_{log}$ from the Sonic Log is then measured for that particular depth. Equation VI-1 may then be used to calculate porosity at the depth under consideration.

B) Uncertainties

The depth of penetration of the recorded wave is only a few inches from the borehole wall. Thus, the value of porosity obtained by this method is limited to a very small zone around the well.

According to Wyllie et al. (1956, 1958), the sound velocity in vuggy materials (materials containing fractures or solution openings) depends mostly on the primary porosity. Therefore, the sonic method tends to ignore secondary porosity such as fractures. The Sonic Logs in comparison with the Density Logs and Neutron Logs could, however, give a measure or secondary porosity.

The method is not suitable for determining effective porosity if there is a significant volume of isolated pore space.

VI-2.2 Density Log Method

A downhole radioactive source, in contact with the borehole wall, emits medium-energy gamma rays into the surrounding formation. After colliding with electrons in the formation, the scattered gamma rays are counted by a detector placed at a fixed distance from the source. The response to such a bombardment is determined essentially by the electron density of the formation, which is a function of the true bulk density, $\rho_b$. Therefore, the porosity of the formation may be calculated if the densities of the rock matrix and the pore fluid are known.

A) Theory and Procedure

A formation density logging device, consisting of a source and one or two detectors attached to a skid, is lowered into an uncased well filled with drilling mud or other fluid. The

device is designed such that the source and detectors come in contact with the borehole wall. The variation of bulk density against depth is recorded. These tools are usually calibrated to indicate apparent bulk density. For some types of rock such as sandstone, limestone and dolomite, in the saturated zone the apparent bulk density is essentially equal to the bulk density itself. Other types of rock bulk density should be estimated from apparent values using available graphs (Schlumberger, 1972). The porosity, $\phi$, of the rock can be estimated from

$$\phi = \frac{\rho_{ma} - \rho_b}{\rho_{ma} - \rho_f} \qquad \text{(VI-2)}$$

where

$\rho_b$ = bulk density of the rock obtained from the log.

$\rho_f$ = the density of pore fluids close to the well.

$\rho_{ma}$ = rock matrix density.

B) Uncertainties

- This method determines total porosity. It does not differentiate between connected and isolated pore spaces within the formation.
- The presence of shale or clay in the formation introduces some errors into the results.

VI-2.3 Neutron Log Method

This method can determine the amount of in situ liquid-filled porosity of a given material. The technique is based essentially on a measurement of the amount of hydrogen present in the formation. If the pore space of the rock is filled with water, and no other source of hydrogen, such as the water in gypsum ($CaSO_4 + 2H_2O$), is present, then the response of this test is a measure of porosity.

A) Theory and Procedure

There are at least three different kinds of Neutron Logs which are currently available. Gamma Ray Neutron Tool (GNT), Sidewall Neutron Porosity (SNP), and Compensated Neutron Log (CNL) use plutonium-beryllium or americium-beryllium as sources of neutrons with initial energies of several million electron volts (Schlumberger, 1972). Here, we shall only address the SNP method. Information about other tools and additional references on those tools may be obtained from Schlumberger (1972).

In the SNP method, a neutron source and a detector are mounted on a skid which is lowered into an uncased well, preferably without fluid and drilling mud. This tool is designed such that it comes in contact with the borehole wall. The neutrons emitted by the source, after penetrating the formation and colliding with the nuclei of the formation materials are received by the detector. The response is measured against depth. A surface panel automatically makes necessary corrections for salinity, temperature, and hole diameter variations, and records the porosity directly. If the hole is filled with drilling mud, porosity values should be corrected for the mud-cake thickness, using available charts (Schlumberger, 1972).

Neutrons are electrically neutral particles, each with the mass of a hydrogen atom (Tittman, 1956). The source on the tool continuously emits fast neutrons. These neutrons collide with nuclei of the formation materials and lose some of their energy. The amount of energy which a neutron loses in each collision depends on the relative mass of the nucleus against which the neutron collides. Collision with a hydrogen nucleus causes the maximum energy loss. Thus, the slow-down of neutrons depends largely on the amount of hydrogen in the formation, which in turn is related to the amount of water in the formation. The SNP method has the advantages that borehole effects are minimized (Schlumberger, 1972) and that most of the corrections required are performed automatically in the panel.

B) Uncertainties

- This method can measure effective porosity only if the isolated pores are free of liquid, otherwise the method does not differentiate between connected and isolated pores.

- The tool responds to all the hydrogen atoms in the formation including those chemically bound to formation materials.

- In shaly formations the porosity derived from the neutron response will be greater than the effective porosity.

- The zone of influence of this method depends on the porosity of the formation, but generally it is limited to a short distance from the wall of the hole.

## VI-2.4 Tracer Techniques

There are several tracer methods for determination of aquifer properties such as effective porosity and dispersivity. The literature is replete with descriptions of theory and practice of tracer tests, see for example, Nir and Kirk (1982); Klett et al. (1981); Benson (1988); Fried (1975); Hoehn and Roberts (1982); Malaszowski and Zuber (1985); Lenda and Zuber (1970); Ivanovich and Smith (1978) and Güven et al. (1986). Many types of radioactive and nonradioactive tracers have been used. A list of some of the tracers which have been used in groundwater studies has been given by Davis et al. (1980) and Thompson (1981).

Unfortunately, most of the analyses of tracer tests for porosity computation are based on the assumption of a two-dimensional, vertically homogeneous aquifer. Thus unknown variations of hydraulic conductivity will lead one to compute porosity values or variations that may be erroneous. For this reason, the commonly used tracer based methods for measuring effective porosity are not discussed herein.

## VI-3 Definition of Hydraulic Head

An important parameter which controls the movement of groundwater is the hydraulic gradient. Distribution of hydraulic head within a given hydrologic system is generally controlled by the conditions at the boundaries of the system and the properties of the media.

The potential $\phi$ of a given fluid at any point in space is generally defined as the mechanical energy per unit mass of the fluid, which has three components

$$\phi = gz + \frac{v^2}{2} + \int_{P_o}^{P} \frac{dP}{\rho} \qquad \text{(VI-3)}$$

where

g = gravitational acceleration.

z = elevation of the point above the chosen datum.

v = velocity of fluid.

P = pore water pressure at the point of interest.

$\rho$ = density of fluid.

$P_o$ = atmospheric pressure.

The potential $\phi$ is the amount of work required to bring a unit mass of fluid from an arbitrary standard state to the point under consideration. The standard state is usually considered to be at elevation $z=0$, velocity $v=0$, and pressure $P=P_o$, atmospheric pressure. The first term of the right hand side of Equation (VI-3) represents the work against gravity necessary to bring a unit mass of fluid from the standard position to the elevation z. The second term is the work required to increase the velocity of the unit mass from zero to V. Finally, the third term is the work required to bring the pressure of the fluid from $P_o$ to P.

For the case of flow through porous media, where velocity is generally very small, the term $v^2/2$ may be ignored with respect to the other terms. In the case of slightly compressible fluids, where the dependence of $\rho$ on pressure can be ignored in computing potential, the third term may also be simplified and equation (VI-3) becomes

$$\phi = gz + \frac{P-P_o}{\rho} \qquad \text{(VI-4)}$$

One may note that in some cases, such as fracture flow close to a well or a shaft, where fluid velocity is relatively large, the term $v^2/2$ may not be so small as to be negligible.

If we refer to $P-P_o$ as gauge pressure, then the expression for potential becomes

$$\phi = gz + \frac{P}{\rho} \qquad \text{(VI-5)}$$

A term for potential which is commonly used in groundwater hydrology is hydraulic head which is defined as energy per unit weight of the fluid. Therefore,

$$h = \frac{\phi}{g} = z + \frac{P}{\rho g} \qquad \text{(VI-6)}$$

For a homogeneous fluid with constant $\rho$, Darcy's law states that fluid flows from regions of higher heads toward regions of lower heads, and that the flow velocity is proportional to the gradient of the hydraulic head. However, if we have more than one type of fluid or $\rho$ changes from one aquifer to the other, which could occur because of changes of temperature or salt concentration, then at each point in space one can define as many potentials as there are densities (Hubbert, 1940). For example, if we have three different densities such as $\rho_1$, $\rho_2$ and

$\rho_3$, then at any point in the space with elevation z and pore pressure P, regardless of which fluid occupies that space, we can write

$$\phi_1 = gz + \frac{P}{\rho_1} \qquad \text{(VI-7)}$$

$$\phi_2 = gz + \frac{P}{\rho_2} \qquad \text{(VI-8)}$$

$$\phi_3 = gz + \frac{P}{\rho_3} \qquad \text{(VI-9)}$$

In this case, according to Hubbert (1940), motion of fluid i with the density $\rho_i$ should be solely studied by the distribution of its own potential $\phi_i$ or head $h_i = \phi_i/g$. Let us emphasize that potential $\phi_i$ based on the density $\rho_i$ is defined everywhere in the space including the space occupied by fluids of other densities. This concept is very important when we are investigating flow between two aquifers of differing salinity separated by some low permeability layer.

To make this point clear let us consider the following example. A look at Fig VI-2 without attention to the quality of water of two aquifers makes one think that there is a drop of hydraulic head from the freshwater aquifer downward to the saline water, and thus flow is downward. However, the following calculations show that flow is actually occurring upward from the saline aquifer towards the fresh-water aquifer.

The values of potential of fresh water at points A and B, top and bottom of the aquitard, are

$$\phi_{f_A} = 160g + \frac{120\rho_f g}{\rho_f} = 280g \qquad \text{(VI-10)}$$

$$\phi_{f_B} = 100g + \frac{178\rho_s g}{\rho_f} = 284.5g \qquad \text{(VI-11)}$$

It is now apparent that the fresh-water potential at point B is larger than that at A, thus causing an upward flow from B to A. Assuming a linear variation of potential between A and B, salt-water potential gradient between B and A is

$$\frac{\phi_{s_B} - \phi_{s_A}}{60} = \frac{(278 - 275.77)}{60} g = 0.0371g$$

The vertical velocity component is upward with the magnitude of

$$v_z = -\frac{k_z}{\mu_s} \rho_s \frac{\partial \phi}{\partial z} = -\frac{k_z}{\mu_s} (0.0385g\rho_f) \qquad \text{(VI-12)}$$

In the above calculations the density of saline water $\rho_s$ is 1.036 g/cm$^3$.

For the study of groundwater movement in a porous medium containing fresh, diffused, and salt water, Lusczynski (1961) has introduced three different types of head at each point i within the medium: fresh-water head $h_{if}$, point-water head $h_{ip}$, and environmental-water head $h_{in}$, which are defined as follows.

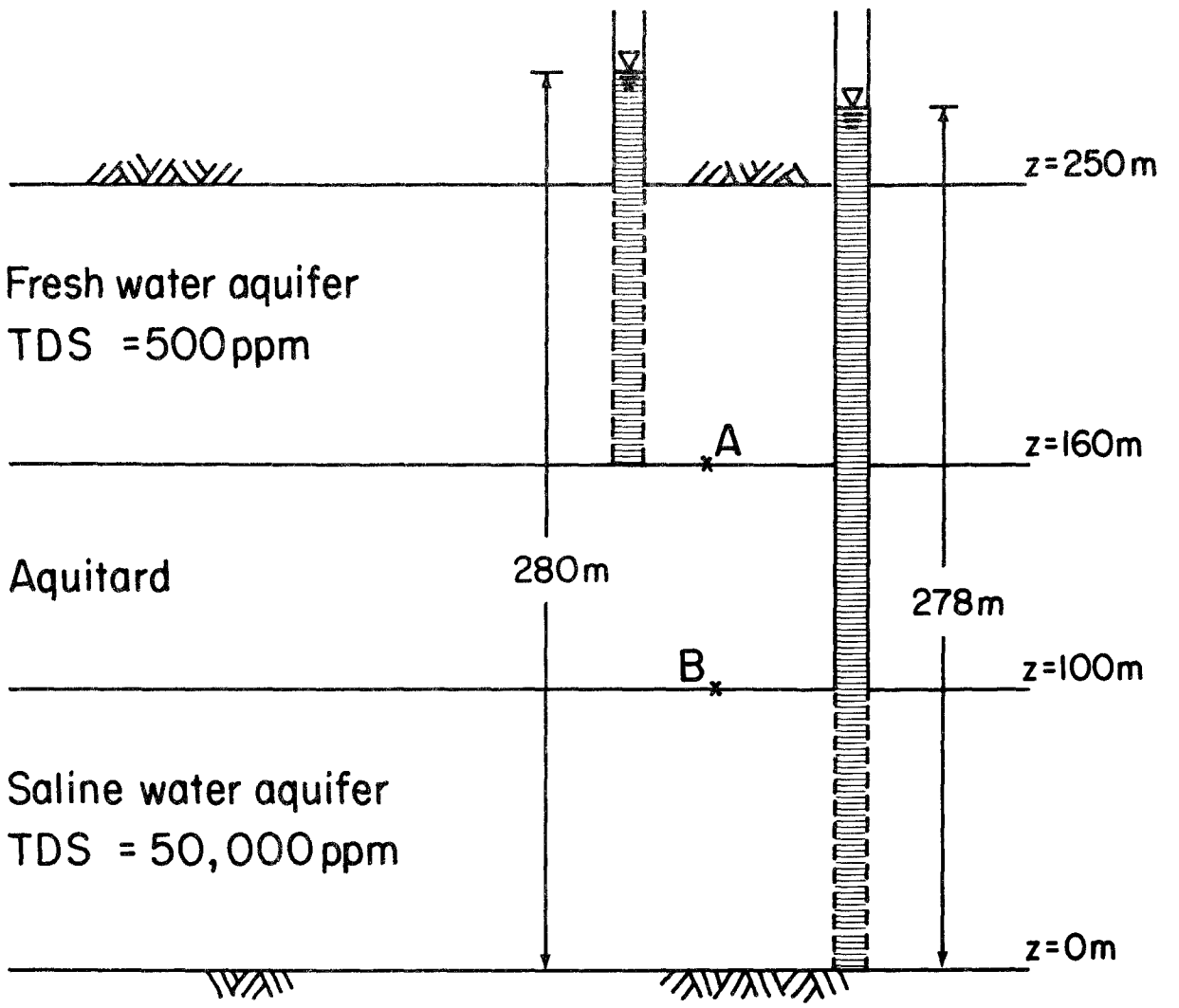


Figure VI-2. Schematic diagram showing two observation wells, one open in the top fresh-water aquifer and the other screened in the lower saline aquifer.

Fresh-water head at point i, Fig. VI-3.B, is defined as the height of the water above the datum in a well filled with fresh-water from point i to a level high enough to balance the existing pressure at point i. Based on this definition, fresh-water head at point i may be written as

$$h_{if} = z_i + \frac{P}{g\rho_f} \qquad \text{(VI-13)}$$

where

$h_{if}$ = fresh-water head at the point i.

$z_i$ = elevation of point i.

$P$ = gage pressure at point i.

$\rho_f$ = density of fresh-water.

As defined above, $h_{if}$ is the energy per unit weight of fresh water at the point i, as was defined by Hubbert (1940).

Point-water head at point i, Fig. VI-3, in groundwater of variable density, is defined as the water level above the datum in a well filled with water of the type found at point i to balance the existing pressure at point i. From this definition one can write

$$h_{ip} = z_i + \frac{P}{g\rho_i} \qquad \text{(VI-14)}$$

where

$h_{ip}$ = point-water head at point i.

$\rho_i$ = density of water at i.

Environmental-water head at a given point i, Fig. (VI-3), in groundwater of variable density is defined as the fresh-water head reduced by an amount corresponding to the difference of salt mass in fresh-water and the environmental water between point i and the top of the zone of saturation. Environmental water between point i and the top of the zone of saturation is herein defined to be the water of constant or variable density occurring in the environment along a vertical line between point i and the top of the zone of saturation.

Based on the above definition, environmental-water head at point i may be written as

$$h_{in} = \frac{P}{\rho_f g} - (z_r - z_i)\frac{\rho_a}{\rho_f} + z_r \qquad \text{(VI-15)}$$

or in terms of fresh-water head one can write

$$h_{in} = h_{if} - (z_r - z_i)\left(\frac{\rho_a}{\rho_f} - 1\right) \qquad \text{(VI-16)}$$

where

$h_{in}$ = environmental head at point i.

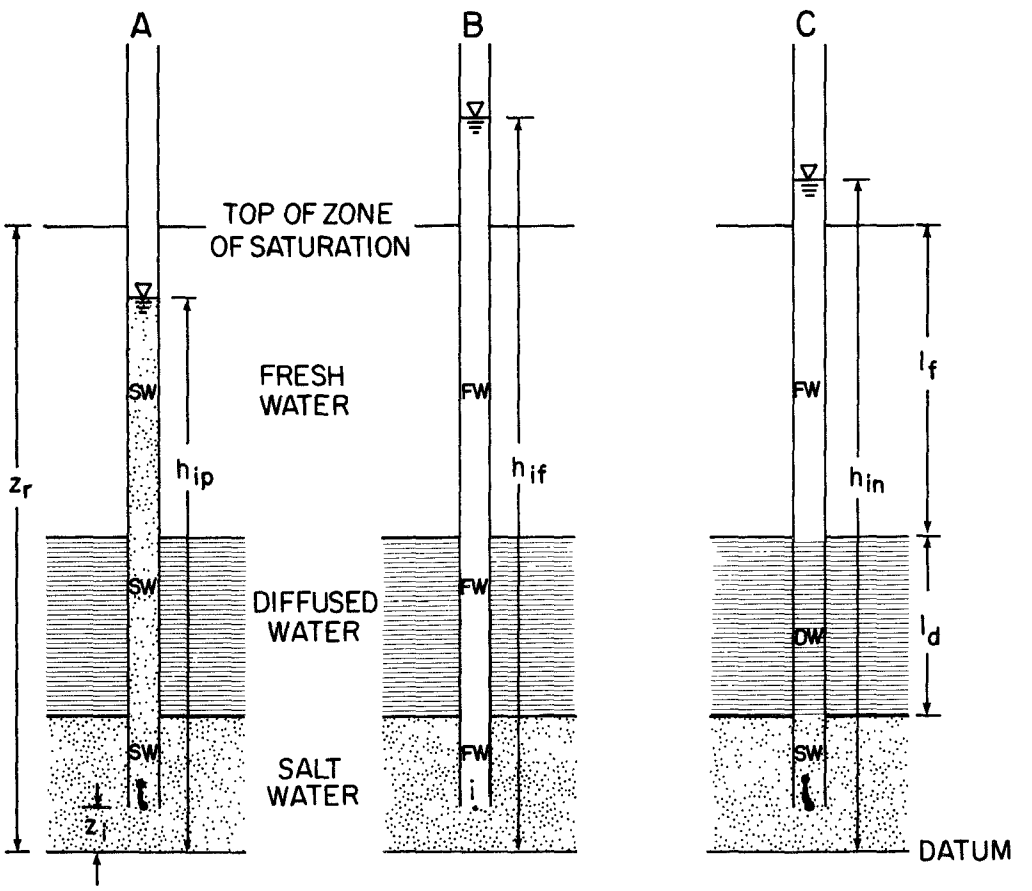


Figure VI-3. Heads in groundwater of variable density, (A) point-water head, (B) fresh-water head, and (C) environmental head, (modified from Lusczynski, 1961).

$z_r$ = vertical distance between datum and top of the zone of saturation.

$\rho_a$ = average density of water between point i and top of the zone of saturation.

$$\rho_a = \frac{1}{z_r - z_i} \int_{z_i}^{z_r} \rho(z)dz \qquad \text{(VI-17)}$$

Lusczynski (1961) states that "fresh-water heads define hydraulic gradients along a horizontal. However, along a vertical environmental-water heads should be used to define the hydraulic gradient". Although along a horizontal the Lusczynski and Hubbert theories match, in a vertical direction their theories lead to different values of gradients. Based on the Lusczynski approach, environmental head at point A of the example of Fig. (VI-2) is the same as the fresh-water head which is 280 m. The value of environmental head at point B may be calculated from equations (VI-1), (VI-16), and (VI-17). Assuming that the aquitard is occupied by saline water, the value of $\rho_a$ may be calculated from equation (VI-17) to be $1.0146\rho_f$. Substituting for $\rho_a$ and $h_{if}$ in equation (VI-16), one obtains the value of $h_{in}$ at B to be 282.31m. Therefore, Lusczynski's approach also gives the direction of flow from B to A. The magnitude of gradient is also the same as that obtained by the Hubbert approach for saline water. If the concentration of water in the aquitard is somewhere between fresh and saline water, then the environmental water head at point B would be larger than 282.31m leading to a gradient different from those obtained by the Hubbert approach.

Lusczynski (1961) has given the following formula for calculation of components of velocity in the horizontal and vertical directions at point i

$$v_h = -\frac{k_h g}{\mu_i}\left(\rho_f \frac{\partial h_{if}}{\partial x}\right) \qquad \text{(VI-18)}$$

$$v_z = -\frac{k_z g}{\mu_i}\left(\rho_f \frac{\partial h_{in}}{\partial z}\right) \qquad \text{(VI-19)}$$

Some authors believe that in dealing with problems in which density is a function of space, it is more convenient to formulate the groundwater flow equation in terms of pressure rather than head, because pressure head ($P/\rho g$) is dependent on fluid density which in turn is dependent on salt concentration (Anderson, 1979). In terms of pressure, Darcy's law at a point i in a groundwater system may be written as (Scheideger, 1960):

$$\vec{v}_i = -\frac{[k]}{\mu_i}\left(\nabla P_i - \rho_i \vec{g}\right) \qquad \text{(VI-20)}$$

where

$\vec{v}_i$ = Darcy's velocity vector.

$\nabla P_i$ = gradient of pressure at point i.

$\mu_i$ = viscosity of fluid at point i.

$[k]$ = permeability matrix.

$\rho_i$ = density of fluid at point i.

$\vec{g}$ = gravity vector.

Let us now examine the example in Fig. (VI-2) with the approach of equation (VI-20). Values of pressure at points A and B are $120\rho_f g$ and $184.5\rho_f g$, respectively. If we assume a linear variation of pressure between A and B, then the component of pressure gradient in the vertical direction becomes

$$\frac{\partial P}{\partial z} = \left(\frac{184.5-120}{60}\right)g\rho_f = 1.075g\rho_f \qquad \text{(VI-21)}$$

and

$$\frac{\partial P}{\partial z} - \rho_B g = (1.075-1.0365)g\rho_f = 0.0385g\rho_f \qquad \text{(VI-22)}$$

and the vertical velocity component at the point B is

$$v_{z_B} = -\frac{k_z}{\mu_s}(0.0385g\rho_f) \qquad \text{(VI-23)}$$

which is exactly the same magnitude as obtained from the Hubbert approach.

The above discussion was based on the gradient of hydraulic head alone. Other types of gradient such as chemical, electrical, and thermal are also effective in moving fluid, even in the absence of any hydraulic head gradient (Philip and de Vries, 1957; Casagrande, 1952). In particular, for a problem such as the above example, where one is dealing with a big contrast of concentration, a certain amount of solute moves from the higher concentration zone to the lower one with water moving in the opposite direction. The law governing this type of motion is called Fick's first law of diffusion which is

$$F = -D\frac{dC}{dx} \qquad \text{(VI-24)}$$

where

F = mass of solute passing through a unit area per unit time,.

D = diffusion coefficient.

C = concentration of solute.

Although the value of D is generally very small, over a long period of time this diffusion process could cause a considerable amount of contaminant transport. Note that in the above example the chemical gradient acts in the same direction as the hydraulic head gradient.

Clarification of one point seems to be in order here. A layer of compacted clay restricts the passage of ions while allowing relatively unrestricted passage of neutral species (Freeze and Cherry, 1979). Thus, salt may not easily move across a compacted clay layer while water may, if, of course, the hydraulic gradient allows.

## VI-4 Field Measurement of Hydraulic Head

Hydraulic head at a given point in a geological formation occupied by a fluid may be measured both directly and indirectly. Hydraulic head may be measured directly by a pipe with

one end open at the point of interest and the other end open to the atmosphere. This pipe is generally referred to as a piezometer. The elevation of fluid in this pipe at equilibrium relative to an arbitrary datum is the hydraulic head at the point of interest, where water is allowed to enter the pipe. The end of the pipe which allows water to enter is usually equipped with a small section of slotted pipe or a device called a well point. Hydraulic head may be obtained indirectly by measuring the pore water pressure at any point with the help of a transducer. Most commercially available transducers generate a voltage proportional to pressure which can be converted to the actual pressure of the water at the point. The value of pressure and the elevation of the point of measurement may be substituted into equation (VI-6) to give the hydraulic head at the point of interest.

Within a single-layer aquifer where flow is essentially horizontal and equipotential lines are vertical (hydraulic head remains constant with depth), water level in an observation well which is screened along all or part of the thickness of the aquifer would give the value of hydraulic head of the aquifer at the position of the well. If for some reason such as stratification of the aquifer, proximity to the zones of recharge or discharge, or change in water quality with depth, hydraulic head varies with depth, then the observation well can only give an average value of head of the aquifer for the screened interval. This head may not be accurate enough for a critical study of groundwater movement.

As we discussed above, an important parameter which one should always measure together with hydraulic head is the density of fluid at the point of measurement. Density varies with temperature and chemical properties. It is recommended that a water sample be taken from the point of interest for chemical analysis. If the medium is occupied by freshwater, i.e., total dissolved solid (TDS) less than 1000 mg/1, one can ignore the effect of density variation, and hydraulic head as defined by equation (VI-6) is adequate for calculation of the velocity components of groundwater movement. If, however, TDS is very high and its magnitude changes with position, then one must consider the density of water at each point where hydraulic head is measured. At 75°F and atmospheric pressure, the relation between NaC1 water salinity and water density may be approximated by

$$\rho = 1 + .73C \qquad \text{(VI-25)}$$

where C is NaC1 concentration is ppm x $10^{-6}$. A chart showing variation of water density with temperature and pressure at different NaC1 concentrations is given in page 47 of Schlumberger (1972).

The above methods of hydraulic head measurement are only practical when the formation is reasonably permeable such that height of water within the pipe comes to equilibrium with the formation pressure at the point within a reasonably short period of time. Measurement of hydraulic head in less permeable formations is quite involved. This is because of the long period of time required for water pressure in the pipe to come to equilibrium with the formation pressure. To overcome this difficulty one should pack off the test interval from the rest of the hole to minimize the volume of water needed to be produced by the formation. For further information about installation of piezometers in fine-textured soils and application of inflatable straddle packers for hydrologic testing, readers are referred to Johnson (1965) and Shuter and Pemberton (1978), respectively.

## VI-5 Storage Coefficient Definition and Measurement

The storage coefficient or the storativity S of a saturated confined geological bed of thickness b is defined as the volume of water that the bed releases from storage per unit surface

area of the bed per unit decline in the component of hydraulic head normal to that surface. This term has been commonly defined for aquifers (Freeze and Cherry, 1979, Hantush, 1964). However, storativity has been generally used for aquitards and aquicludes as well. Some authors have used the term storativity for both confined and unconfined aquifers (USBR, 1977). A particularly thorough discussion of storativity may be found in Narasimhan and Kanehiro (1980).

Note that in the above definition it is inherent that the hydraulic head is the same through the total thickness of the bed. This may not be a valid assumption for cases in which hydraulic head varies with elevation. Consequently, Hantush (1964) has used the term average hydraulic head in the definition of the storage coefficient in order to overcome the above problem. A more accurate term to use is the specific storage. The specific storage $S_s$ of a saturated confined geological bed is defined under a unit decline in hydraulic head. For cases where the hydraulic head remains constant throughout the total thickness b of the bed, then the following relation holds

$$S = bS_s \qquad \text{(VI-26)}$$

The storativity and the specific storage are scalar parameters. They may be space dependent, but they are independent of direction.

A decrease in hydraulic head leads to a decrease in fluid pressure and an increase in effective stress. Therefore, the volume of water that is released from storage due to decreasing the hydraulic head h is produced by two mechanisms: (1) the expansion of the water caused by decreasing the pore water pressure, and (2) the compaction of the skeleton of the medium caused by increasing the effective stress. The expansion of the water is controlled by its compressibility $\beta$ and the compaction of the medium by the matrix compressibility $\alpha$. Therefore, it can be shown that the specific storage $S_s$ is given by

$$S_s = \rho g(\alpha + \phi\beta) \qquad \text{(VI-27)}$$

where

$\rho$ = density of the water

g = acceleration of gravity

$\phi$ = porosity of the medium.

Equations (VI-26) and (VI-27) indicate that $S_s$ has the dimension of $(L)^{-1}$ and S is dimensionless.

## VI-5.1 Methods of Measurement

In general, methods of in-situ measurement of the storage coefficient fall into two categories: (1) methods which are based on well testing of aquifers, and (2) techniques which rely on the change of barometric pressure and earth tides. In addition, some indirect methods such as measurement of subsidence and consolidation have been used to obtain a rough estimate of the storativity of the shallower unconsolidated materials.

Average storativity of an aquifer can be determined by the common pump test technique. Some of these tests were discussed in Chapter V. Unfortunately, the suitability of the current pump test techniques to determine the storativity of less pervious confining beds is questionable. As we discussed before, the original leaky aquifer theory (r/B method) simply

ignores the storage capacity of the aquitard. The more recent theories such as the B solution of Hantush (1960) and the ratio method of Witherspoon and Neuman (1967) cannot single out the storativity of the aquitards. The Hantush solution could at best give the product of the specific storage and the hydraulic conductivity of the aquitard, and the ratio method yields the hydraulic diffusivity of the aquitard. In fact, we noticed that calculation of hydraulic conductivity was only possible if one could obtain the storativity from other sources.

Application of the B solution of Hantush combined with the ratio method of Witherspoon and Neuman has been reported (Leahy, 1977) to yield a value for the storativity of the aquitard. However, despite the fact that the B method cannot differentiate properties of the two confining layers above and below the aquifer, the procedure used by Leahy is suitable for cases where one is certain that leakage into the aquifer is from only one of the confining beds.

In regard to single well tests, the modified Burns' method as described in a previous section should give a value for the storativity of the layer being tested. Recalling the limitations of that test, the estimated value of storativity belongs to the materials very close to the well. Other single well tests are either unable to give $S_s$ or, if they do, the reliability of the calculated value is questionable (Papadopolus et al., 1973).

Barometric efficiency of a well can also be used to find the average storage coefficient of a confined aquifer (Jacob, 1940)

$$S = \frac{\phi \gamma b}{E_w B} \qquad \text{(VI-28)}$$

where

$S$ = storage coefficient.

$\phi$ = porosity.

$b$ = aquifer thickness.

$E_w$ = bulk modulus of elasticity of water.

$B$ = barometric efficiency.

$\gamma$ = specific weight of water.

Fluctuation of the water level in a well due to the earth tide has occasionally been used to estimate the storativity of deep confined aquifers (Kanehiro and Narasimhan, 1980). However, because of uncertainties in estimating input data this method is not commonly applied in the field.

# CHAPTER VII

# MATHEMATICAL MODELING OF ADVECTION-DOMINATED TRANSPORT IN AQUIFERS

## VII-1 Introduction

There are a variety of ways in which vertically-distributed hydraulic conductivity distributions can be used to understand and assess problems involving contaminated ground water. A significant amount of insight will be obtained simply by observing and discussing the implications of such information on patterns of contaminant migration. However, use of the three-dimensional vertically-distributed data in three-dimensional mathematical models will be a common procedure for developing quantitative assessments of a variety of possible activities such as evaluation of site remediation plans. Thus it is worthwhile to devote a chapter to a discussion of the relationship between vertically-distributed hydraulic conductivity data and mathematical modeling.

As pointed out in Chapter I, once one moves from the use of vertically-averaged aquifer properties in two-dimensional mathematical models to the use of vertically-distributed aquifer properties in three-dimensional models, the nature of the physical process represented by the model changes dramatically. In many situations, the model changes from one being largely dominated by dispersion (low Peclet number flows) to one largely dominated by advection (high Peclet number flows). Unfortunately, most of the standard finite-difference and finite-element algorithms for solving mathematical models do not work well when applied to advection-dominated flows, especially those that involve chemical or microbial reactions. The necessary evolution from dispersion-dominated to advection-dominated numerical algorithms for solving the flow and transport equations is far from trivial, so it is important to call attention to some of the newer numerical methods, particularly those that produce a minimum of numerical dispersion when used to solve the transport equation. Therefore, we will present a brief review of numerical methods, emphasize the approaches that work best for advection-dominated transport problems, and present several overviews of example applications developed by the authors during the past several years.

## VII-2 Governing Equations for Flow and Transport

In developing a model of contaminant migration in the subsurface, one usually must deal with the flow equation, the transport equation or both. As developed in Jacob (1940), Bear (1979) and numerous other sources, what we will refer to as the flow equation may be written as

$$S_s \frac{\partial h}{\partial t} - \nabla \cdot (\underline{\underline{K}} \cdot \nabla h) = \Sigma S_o - \Sigma S_i \qquad \text{(VII-1)}$$

where t is time, $S_s$ is the specific storage, which depends on the specific weight and compressibility of the water and compressibility of the porous matrix (see, e.g., Bear, 1979, sections 5-2 and 5-11), h is hydraulic head, $\underline{\underline{K}}$ is the hydraulic conductivity matrix, $\Sigma S_o$ is the sum of volumetric sources of water and $\Sigma S_i$ is the sum of volumetric sinks.

Equation (VII-1) may be solved, together with the appropriate initial and boundary conditions, for the head, h, provided that the hydraulic conductivity $\underline{\underline{K}}$ is known as a function of position ($\underline{x}$) in the medium and provided that information is available on the spatial distribution of the specific storage $S_s$ and the spatial and temporal variations of the source(s) and sink(s). It

is assumed that the relevant fluid properties such as density and viscosity are all known and nearly constant, independent of position or composition. Once the solution for the head is obtained, the flow field can be obtained using Darcy's law, which is given by

$$\underline{v}(\underline{x},t) = - \underline{\underline{K}} \cdot \nabla h/\theta \qquad \text{(VII-2)}$$

where $\underline{v}$ is the pore velocity vector and $\theta$ is the porosity.

If we are interested in the transport of a single species, and if it is assumed, for simplicity, that the reaction terms can be described by a first-order decay expression with the same decay rate constant $\lambda$ for both the solid phase and water phase components of the species, and that the linear Freundlich isotherm is applicable, then the solute transport equation may be written as

$$R_f\theta \frac{\partial C}{\partial t} + \nabla \cdot (\theta C \underline{v}) - \nabla \cdot (\theta \underline{\underline{D}} \cdot \nabla C) = - \lambda R_f \theta C + \Sigma S_o C_o - \Sigma S_i C_i \qquad \text{(VII-3)}$$

where $R_f$ is the retardation factor, C is solute concentration, $\underline{\underline{D}}$ is the dispersivity maxtrix and $C_o$ and $C_i$ are solute concentrations in the source(s) and sink(s) respectively. Given the flow field $\underline{v}$ and the spatial distribution of the medium parameters such as porosity, retardation factor, tortuosity and dispersivity and the other parameters such as the decay rate constant and molecular diffusion coefficient, the solute transport equation can be solved, together with the appropriate initial and boundary conditions, for the concentration C.

## VII-3 Numerical Solutions of Governing Equations

Several books are available in the hydrology literature which are devoted to the study of numerical solutions of subsurface flow and transport equations (e.g., Remson et al., 1971; Huyakorn and Pinder, 1983; Bear and Verruijt, 1987). A concise history of the applications of numerical methods to the solution of subsurface flow and transport problems can be found in the work by Huyakorn and Pinder (1983). Recently, a number of comprehensive reviews and state-of-the-art reports have been presented on the subject (Odeh, 1987; Allen, 1987; Cady and Neuman, 1987; Abriola, 1987; Pinder, 1988a,b).

A major step in the numerical solution of either the flow or the transport equation is the discretization of the solution domain and the governing equation. This may be accomplished in various ways including the finite difference method, the integrated finite difference method and the finite element method (see, e.g. Huyakorn and Pinder, 1983; Narasimhan and Witherspoon, 1976). The advantages and disadvantages of each of these methods are discussed briefly by Pinder (1988a). The discretization process leads to a set of algebraic equations in terms of the nodal values of head, h, or the concentration, C, over a numerical solution grid. These equations are linear in the case of the flow equation (VII-1) and the transport equation (VII-3). However, in general, in the case of unsaturated flow or multiphase flow and transport equations, the discretization results in a set of nonlinear equations which are often subjected to an intermediate linearization step to obtain a set of linear algebraic equations in terms of the independent variables (see, e.g., Odeh, 1987). Alternatively, an iterative nonlinear equation solver may be used (Remson et al., 1971).

The solution of the linear algebraic equations may be accomplished using either direct elimination or iterative methods (Odeh, 1987; Pinder, 1988a; Schmid and Braess, 1988; Lapidus and Pinder, 1982). While the direct elimination procedure is more reliable and the method of choice for systems involving less than a few hundred equations, iterative methods are preferred

in large three-dimensional flow and transport problems, as they require less computer storage and time (Odeh, 1987; Pinder, 1988a). Several iterative methods in current use are discussed briefly by Odeh (1987) and Allen (1987). These include the strongly implicit procedure, SIP, the successive over relaxation method, SOR, and the conjugate gradient method with matrix preconditioning, PCG. Another iterative method is the multigrid, MG, method which has been described by Brandt (1977) and originally suggested by Federenko (1961). The multigrid method appears to be very suitable for the solution of large equation systems associated with three-dimensional flow and transport modeling problems in heterogeneous media (see, e.g., Schmid and Braess, 1988; Cole and Foote, 1987,1988). A comparison of various solution methods for some two-dimensional groundwater flow problems, including the direct Choleski decomposition method and the iterative PCG and MG methods have been presented recently by Schmid and Braess (1988). More detailed discussions of various matrix solution methods and additional references can be found in the recent work by Oran and Boris (1987).

### VII-3.1 Flow Equation Solution

The solution of the flow equation (VII-1) together with the initial and boundary conditions is fairly straightforward (see, e.g., Huyakorn and Pinder, 1983). However, problems arise with respect to computer storage and time limitations when large scale three-dimensional flow problems in heterogeneous media are considered which require the solution of a large system of equations. As discussed briefly above, these problems may be alleviated greatly by the use of the multigrid iterative method, although multigrid solution methods are not yet widely used in three-dimensional subsurface flow applications. At the present time, most three-dimensional flow codes seem to favor the strongly implicit procedure (McDonald and Harbaugh, 1984; Ababou, Gelhar and McLaughlin, 1988), while the applications of the multigrid technique have been limited mostly to two-dimensional problems (Cole and Foote, 1987; Schmid and Braess, 1988). Applications of the MG methods to three-dimensional flow problems are just beginning to be made (e.g., Cole and Foote, 1988).

The use of the finite difference or the integrated finite difference methods with simple rectangular grids appear to be the most practical approach at present to three-dimensional flow problems in heterogeneous media (McDonald and Harbaugh, 1984; Ababou et al., 1988). It may be useful to mention also a versatile finite element approach, particularly suited to fractured media, described by Kiraly (1988) and Hufschmied (1989), which can incorporate one-dimensional and two-dimensional elements together with three-dimensional elements for the purpose of large scale groundwater flow modeling in highly heterogeneous media.

### VII-3.2 Transport Equation Solution

The solution of the transport equation (VII-3) is more complicated than the solution of the flow equation. This is primarily due to the existence of the advective transport term (second term on the left-hand side) in (VII-3) which gives the transport equation a hyperbolic character. Reviews of various techniques for the solution of the transport equation have been presented by Allen (1987), Cady and Neuman (1987), Farmer (1987), Hauguel (1985), and Baptista, Adams and Stolzenbach (1985). In general, these techniques can be grouped into three classes; namely, Eulerian, Lagrangian, and Eulerian-Lagrangian methods. Eulerian methods are more suited to dispersion dominated systems while Lagrangian methods are most suited to advection dominated systems. Eulerian-Lagrangian methods have been introduced to deal efficiently and accurately with situations in which both advection and dispersion are important.

A) Eulerian Methods

The Eulerian methods are based on the discretization of the transport equation on a numerical solution grid that is fixed in space, and all of the terms of the equation, including the advective transport term, are discretized together and the resulting algebraic equations are solved simultaneously in one solution step. As discussed by Cady and Neuman (1987), while Eulerian methods are fairly straightforward and generally perform well when dispersion dominates the problem and the concentration distribution is relatively smooth, they are usually constrained to small local grid Peclet numbers ($Pe = v\Delta s/D_{ss}$, where v is the magnitude of the seepage velocity, $\Delta s$ is the grid spacing along the flow direction, and $D_{ss}$ is the longitudinal component of the dispersion matrix along the flow direction), and to small grid Courant numbers ($Co = v_r \Delta t/\Delta s$, where $\Delta t$ is the time step and $v_r$ is the retarded seepage velocity = $v/R_f$). Daus and Frind (1985) describe an alternating-direction Galerkin finite element method for two-dimensional domains which is constrained to $Pe < 2$ and $Co < 1$. Burnett and Frind (1987a,b) present a similar method for three-dimensional domains. Frind, Sudicky, and Schaellenberg (1988) apply this method to study the detailed evolution of contaminant plumes in heterogeneous media. Another example of an Eulerian method applied to a three-dimensional domain is the curvilinear finite element method of Huyakorn et al. (1986a,b).

B) Lagrangian Methods

Methods which are based on solutions of the transport equation on a moving grid, or grids, defined by the advection field, or methods which do not rely on a direct solution of the Eulerian transport equation (VII-3) but which are based on an analysis of the transport, deformation and transformation of identified material volumes, surfaces, lines or particles by tracking their motion in the flow field are generally called Lagrangian methods (Cady and Neuman, 1987; Oran and Boris, 1987). Here, we will reserve this term only for methods which are based on tracking alone and will consider the moving-grid methods which have been called Lagrangian before by some authors simply as special cases of the Eulerian-Lagrangian methods.

It appears that the first applications of the Lagrangian method in groundwater solute transport problems are the immiscible front movement analyses of Muskat (1937). These analyses and other studies of immiscible front movements are described by Bear (1979). This approach is most suited to situations where advection is the dominant process and the effects of hydrodynamic dispersion and chemical reactions are negligible. Nelson (1978a,b,c,d) and Nelson et al. (1987) have used this approach to calculate arrival time distributions to evaluate the environmental consequences of groundwater contamination in various geological settings. Güven et al. (1986) have developed a simplified Lagrangian analysis of two-well tracer tests in stratified aquifers, neglecting the effects of hydrodynamic dispersion, and Molz, Güven and Melville (1983) have used a similar Lagrangian approach in their analysis of some of the single-well tracer test results of Pickens and Grisak (1981a,b).

If sorption can be approximated as an equilibrium process, the effects of sorption can be easily taken into account in a Lagrangian framework by advecting the tracked particles or the fronts with the retarded velocity $v_r$. First-order decay or degradation can also be simulated fairly easily in a number of ways (Prickett, Naymik, and Lonnquist, 1981; Kinzelbach, 1988).

The effects of hydrodynamic dispersion can be incorporated in a Lagrangian framework by introducing a large number of particles into the flow field, each with a specified quantity of solute mass associated with it, and adding a random-walk component to the motion of each particle as the particles are advected in the flow field. This method has been popularized by the

random-walk solute transport model of Prickett et al. (1981). Improvements to the basic random-walk model, to take into account the effects of nonzero spatial derivatives of the dispersion coefficients in flow fields with spatially variable dispersion coefficients, are discussed by Kinzelbach (1988), Uffink (1988) and Ackerer (1988). A discussion of the advantages and disadvantages of Lagrangian methods can be found in the work by Kinzelbach (1988). Lagrangian methods are described and discussed further in the recent book by Bear and Verruijt (1987).

C) Eulerian-Lagrangian Methods

Reviews of Eulerian-Lagrangian methods (ELM) have been presented recently by Cady and Neuman (1987) and others (e.g., Hauguel, 1985; Baptista, Adams and Stolzenbach, 1985). These methods combine the advantageous aspects of the Lagrangian and the Eulerian methods by treating the advective transport using a Lagrangian approach and the dispersive transport and chemical reactions using an Eulerian approach. According to how the advective transport is taken into account, these methods can be generally grouped into three classes; one class makes use of particle tracking and relates the concentration at a grid node to the solute mass associated with each particle and the particle density around that node, while the second class treats concentration directly as a primary variable throughout the calculations without resorting to the use of any particles, and the third class consists of models in which the first and second approaches are used together in an adaptive manner depending on the steepness of the concentration gradients. The first type of method, which was originally suggested by Garder, Peaceman and Pozzi (1964) according to Cady and Neuman (1987) and also applied by Konikow and Bredehoeft (1978), is often called the method of characteristics (MOC). This type of method which makes use of particles had been denoted as ELM/P by Baptista et al. (1985). The second type of method has been called the "single-step reverse particle tracking" method by Neuman (1984) and the "modified method of characteristics" by others (e.g., Ewing, Russell and Wheeler, 1984). Since the concentration, C, is used as the primary variable throughout the calculations without resorting to the use of any particles, Baptista et al. (1985) have denoted this method as ELM/C. The third method, developed by Neuman (1984), and Cady and Neuman (1987), is called the adaptive Eulerian-Lagrangian method; in keeping with the notation of Baptista et al. (1985), we may denote this method as ELM/A.

The ELM/C method has been used by a number of investigators including Baptista, Adams and Stolzenbach (1984), Cheng, Casulli and Milford (1984), Holly and Usseglio-Polatera (1984), Wang, Cofer-Shavica and Fatt (1988), Sorek (1988), Wheeler et al. (1987) and others (see, e.g., Cady and Neuman, 1987; Baptista, Adams and Stolzenbach, 1985; Hauguel, 1985).

A variation of the ELM, other than ELM/P, ELM/C or ELM/A methods, has been described by Doughty et al. (1982). The method of Doughty et al. (1982) has been applied by Güven et al. (1985) to the analysis of a single-well tracer test in a stratified aquifer and by Molz et al. (1986a) to a coupled transport problem involving biodegradation.

It may be useful to point out that Eulerian-Lagrangian methods have been developed extensively for the numerical modeling of complex three-dimensional industrial and environmental flows and for the solution of various fluid mechanics problems particularly over the last decade (see, e.g., Oran and Boris, 1987; Hauguel, 1985). These methods are now becoming popular also in the area of subsurface contaminant migration modeling.

## VII-3.3 Available Computer Codes

Several well documented computer codes for three-dimensional flow and solute transport modeling as well as parameter identification and uncertainty analysis are available in the public domain. These codes have been developed by universities, various government agencies and government supported laboratories. There are also several proprietary codes developed by private consulting firms and research organizations such as the Electric Power Research Institute. Many of these codes have been listed in the recent monographs by Javandel et al. (1984) and van der Heijde et al. (1985). In this regard, the International Ground Water Modeling Center (IGWMC) serves as an information, education, and research center for groundwater modeling with offices in Indianapolis, Indiana (IGWMC, Holcomb Research Institute, Butler University, 4600 Sunset Avenue, Indianapolis, Indiana 46208) and Delft, the Netherlands. IGWMC operates as a clearinghouse for groundwater modeling codes and organizes and annual series of short courses on the use of various codes. Similar specialized short courses are also organized by various universities as well as professional organizations such as the National Water Well Association (NWWA, 6375 Riverside Dr., Dublin, Ohio 43017). The aforementioned references and organizations may be consulted for the availability of various modeling codes.

## VII-4 Examples of Advection-Dominated Modeling

Much of this report is devoted to field methods for obtaining the vertical distribution of horizontal hydraulic conductivity. Such information obtained at an array of observation wells can serve, among other things, as a basis for the development of fully three-dimensional models or quasi-three-dimensional models of transport processes in aquifers. In order to represent the transport process in a manner that is realistic physically, such models must be advection-dominated and solved in such a way that significant amounts of numerical dispersion is not introduced.

The problem of developing numerical schemes that allow for the preservation of large gradients on grids of practical size has been with us ever since the development of modern numerical models. Such large persisting gradients can occur at the boundaries of contaminant plumes, at interfaces of fresh and salt water, and in various multiphase flows in oil reservoirs. Techniques that allow one to preserve large gradients in advection-dominated flows may be termed "front-tracking methods", and were discussed previously in this chapter. There are now a variety of such techniques that fall into the classification of Lagrangian methods or Eulerian-Lagrangian methods (Cady and Neuman, 1987). The remainder of this chapter will review and elaborate on some of the recent models and modeling applications of the Lagrangian or Eulerian-Lagrangian type. Specific applications will involve concentration measurements made during forced-gradient tracer experiments and measurements made in aquifer fluids supporting microbial activity.

## VII-4.1 Performance of Single-Well and Two-Well Tracer Experiments

The most common types of forced gradient tracer experiments are single-well experiments and two-well experiments. In the past, both types have been performed in Canada (Pickens and Grisak, 1981) and in the United States (Molz et al., 1985, 1986b). Shown in Figure VII-1 is a typical configuration for a single-well experiment. The term "single-well" represents the fact that only one pumping well is required in order to perform the experiment. As detailed in Güven et al. (1985), an observation well with multilevel samplers is required in order to obtain concentration versus time data at selected locations. One or more such

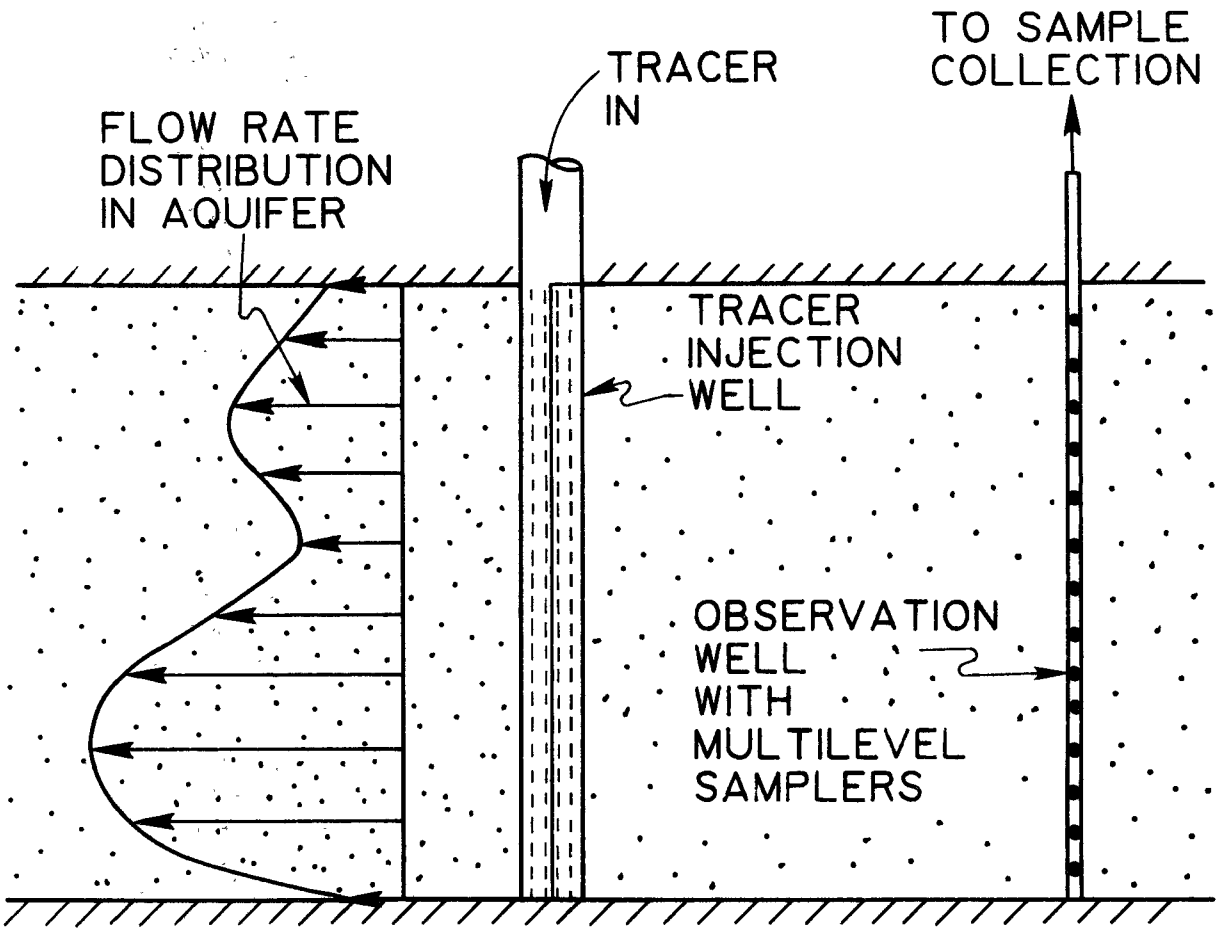


BASIC CONCEPT OF SINGLE-WELL
TRACER TEST

Figure VII-1. Vertical Cross-sectional diagram showing single-well test geometry.

observation/sampling wells may be used in any particular tracer study. Actual performance of the experiment involves the injection of water having a known concentration of tracer in a well which is fully penetrating (Fig. VII-1). After some time, the flow may be reversed and the tracer-labeled water removed from the same well.

A typical configuration and flow pattern for a two-well tracer experiment is illustrated in Fig. VII-2. Here there are two pumping wells because the experiment involves the simultaneous operation of an injection well and a withdrawal well, both of which are fully penetrating. Water is pumped into the injection well at a steady flow rate and is removed from the withdrawal well, usually at the same rate, although two-well tests have been performed in which the flow rates in the two pumping wells were not equal. A conservative tracer of known concentration is added at the injection well for a period of time and the concentration of tracer in the water leaving the withdrawal well is measured and recorded as a function of time to give a concentration versus time breakthrough curve. Multilevel sampling wells may be placed at various locations in the flow field (Molz et al., 1986b, 1988).

VII-4.2 Advection-Dominated Modeling of a Single-Well Tracer Experiment

A single-well tracer experiment was performed by Pickens and Grisak (1981a) in which K(z) was measured, and concentration vs. time breakthrough curves were recorded in several multilevel sampling wells. An Eulerian-Lagrangian numerical model called SWADM was developed by Güven et al. (1985) to simulate several of the experiments. This model took into account depth-dependent advection in the radial direction and local hydrodynamic dispersion in the vertical and radial directions (Güven et al. 1985). The model is based on the equation given by

$$\frac{\partial C}{\partial t} + v_r \frac{\partial C}{\partial r} = \frac{1}{r}\frac{\partial}{\partial r}\left(rD_r \frac{\partial C}{\partial r}\right) + \frac{\partial}{\partial z}\left(D_z \frac{\partial C}{\partial z}\right) \qquad \text{(VII-4)}$$

where r is the radial coordinate, $C = C(r,z,t)$ is the tracer concentration, $v_r = v_r(r,z)$ is the radial seepage velocity, $D_r = D_d + \alpha_r|v_r|$ is the radial (longitudinal) dispersion coefficient, $D_z = D_d + \alpha_v|v_r|$ is the vertical dispersion coefficient, $D_d$ is the effective molecular diffusion coefficient, and $\alpha_r$ and $\alpha_v$ are the radial and vertical local dispersivities.

The detailed single-well tracer dispersion experiment of interest was performed in a shallow unconfined aquifer. A volume of 95.6 cubic meters of tracer-labeled water was injected into an 8.2 m thick aquifer at a rate of 3.2 $m^3$/hr for a period of 30 hours and then withdrawn at the same rate. Withdrawal began immediately at the end of injection. Multi-level samplers were located in the aquifer at distances of 1, 2, 3, 4 and 6 m from the injection-withdrawal well. From the relative tracer arrival times at different elevations in the observation wells, a dimensionless radial hydraulic conductivity distribution in the vertical ($K/\overline{K}$) was calculated, where $\overline{K}$ is vertically averaged K. Additionally, Pickens and Grisak (1981a) determined that the effective porosity was 0.38 and found the values of local longitudinal dispersivity at each sampling point to be fairly constant with an average magnitude of about 0.007 m. The $K/\overline{K}$ distribution inferred from the breakthrough data at the observation well at a distance of 1 m from the injection-withdrawal well in test SW1 was used in the SWADM simulation. This profile is shown in Figure VII-3.

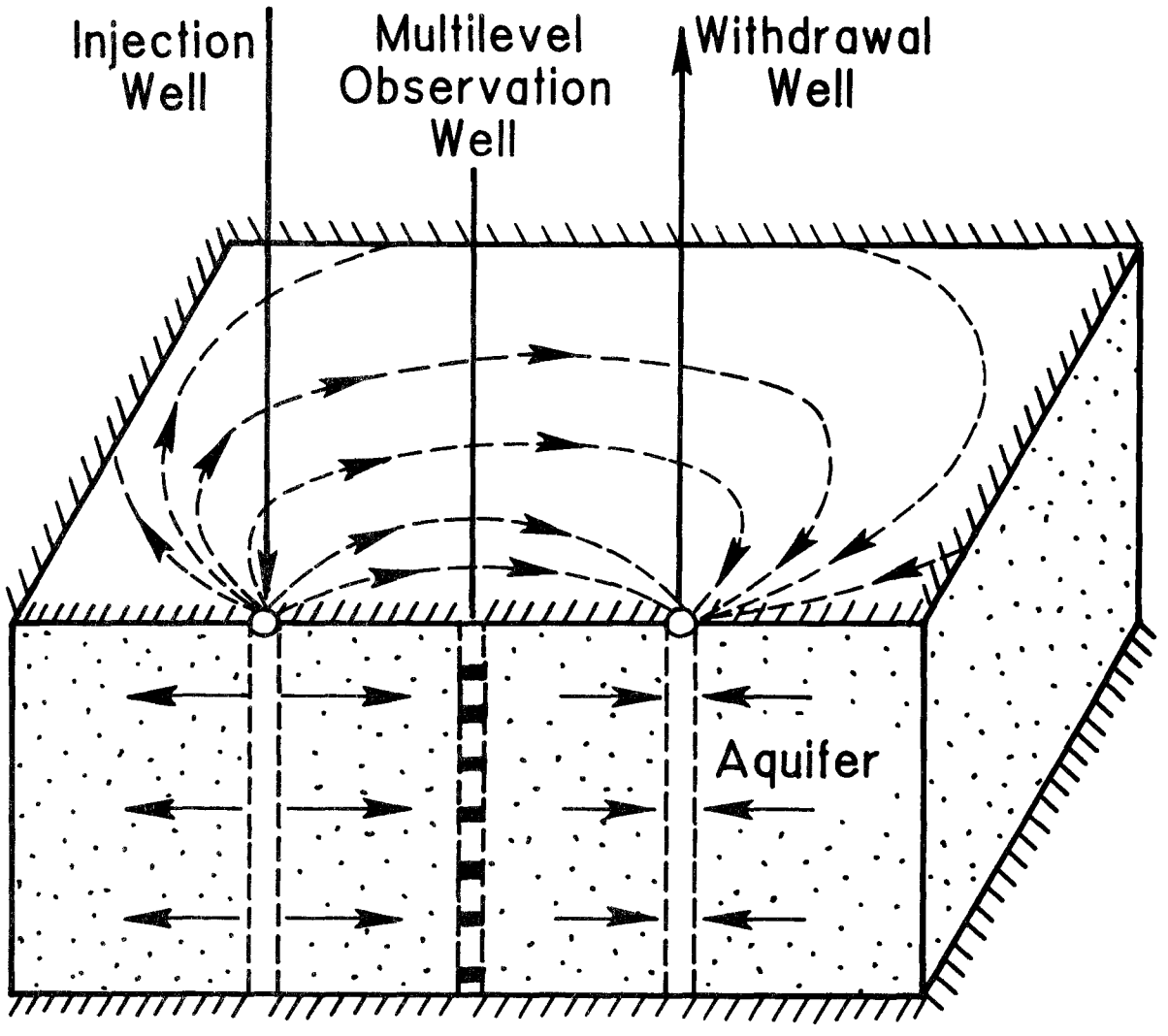


Figure VII-2. Geometry and flow field for a two-well tracer test.

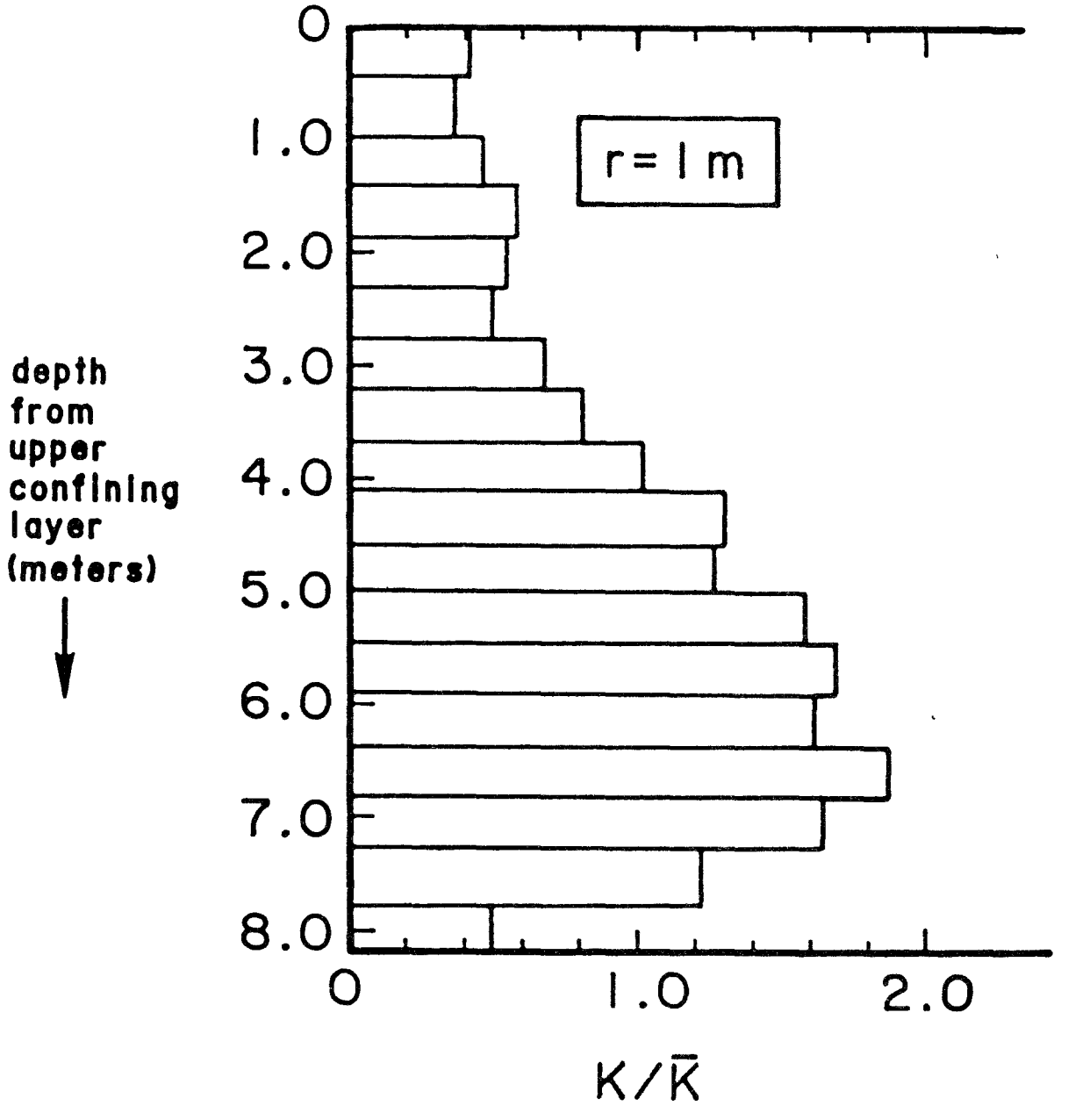


Figure VII-3. Hydraulic conductivity profile measured by Pickens and Grisak (1981) and used in the calculations by Güven et al. (1985).

In Figures VII-4 and VII-5, the flow-weighted concentration breakthrough curves from observation wells located 1 and 2 m from the injection-withdrawal well respectively (Pickens and Grisak, 1981b) are shown along with the corresponding breakthrough curves calculated by SWADM. The experimental concentration versus time data measured at the injection-withdrawal well are shown in Figure VII-6 along with the results of the SWADM simulation using the unsteady input concentrations. The early part of the experimental data seems to show a large amount of scatter, however, this part of the curve is closely modeled by SWADM using the actual unsteady injection concentration. The later part of the breakthrough curve is underestimated by SWADM, and this is discussed further in Güven et al. (1985). In obtaining the results shown in Figures VII-4 and VII-5, and VII-6, no "model calibration" of any type was performed. Only parameter values measured by Pickens and Grisak (1981a) were utilized. The resulting curves represent very accurate simulations which indicate an advection-dominated dispersion process with local dispersivities approaching those measured in the laboratory. As also discussed in more detail by Molz et al. (1983) and Güven et al (1984), it is clear that if a full-aquifer dispersivity were calculated from these data it would not represent a physical property of the aquifer.

VII-4.3 Advection-Dominated Modeling of Two-Well Tracer Experiments

Both fully Lagrangian and fully Eulerian models have been developed for simulating two-well tracer experiments. Güven et al. (1986) describe application of a Lagrangian-based analysis of the two-well tracer experiment performed by Pickens and Grisak (1981a). Theory and experiment matched well, indicating once again the advection domination of the transport process. Both Eulerian and Lagrangian models were used to simulate a two-well tracer experiment performed by Molz et al. (1986b,c). The comparison of the two numerical approaches is interesting and is described below.

Application of the two modeling approaches was done separately and independently. Under contract to Auburn University, Geotrans, Inc. developed a three-dimensional Eulerian advection-dispersion model that took advantage of the particular geometry of the experiment (Huyakorn et al., 1986a,b). The aquifer was divided vertically into 12 layers of varying thicknesses and flow between the injection and production wells was assumed to be stratified, steady and horizontal within each layer. The advection pattern for such a situation is well known, so the Darcy velocity, U, could be calculated at any particular point within the 12-layer system (Huyakorn et al., 1986a,b). Given the known velocity distribution, the advection-dispersion equation was solved using a finite element approach (Huyakorn et al., 1986b) with the governing equation written in three-dimensional curvilinear streamline coordinates (s,n,z) where s and n are the horizontal coordinate along and normal to a local streamline, and z is the vertical coordinate. This type of coordinate system minimizes numerical dispersion problems. The transformed advection-dispersion equation is given by

$$\frac{1}{h_2}\frac{\partial}{\partial s}\left(h_2 D_s \frac{\partial C}{\partial s}\right) + \frac{1}{h_1}\frac{\partial}{\partial n}\left(h_1 D_n \frac{\partial C}{\partial n}\right) + \frac{\partial}{\partial z}\left(D_z \frac{\partial C}{\partial z}\right) - \frac{U}{\theta}\frac{\partial C}{\partial s} - \frac{\partial C}{\partial t} = 0 \qquad \text{(VII-5)}$$

where $D_s$, $D_n$ and $D_z$ are principal components of the hydrodynamic dispersion matrix in the longitudinal, transverse and vertical directions, respectively, and $h_1$ and $h_2$ are the scale factors of the curvilinear coordinate system (Huyakorn et al., 1986a).

The second model used to simulate the two-well experiment is called the two-well advection model (TWAM) (Güven et al., 1986). A Lagrangian solution method is used in this model based on the travel times of tracer along various flow lines from one well to the other. In this model, it is assumed that the aquifer is horizontal, confined, of constant thickness and

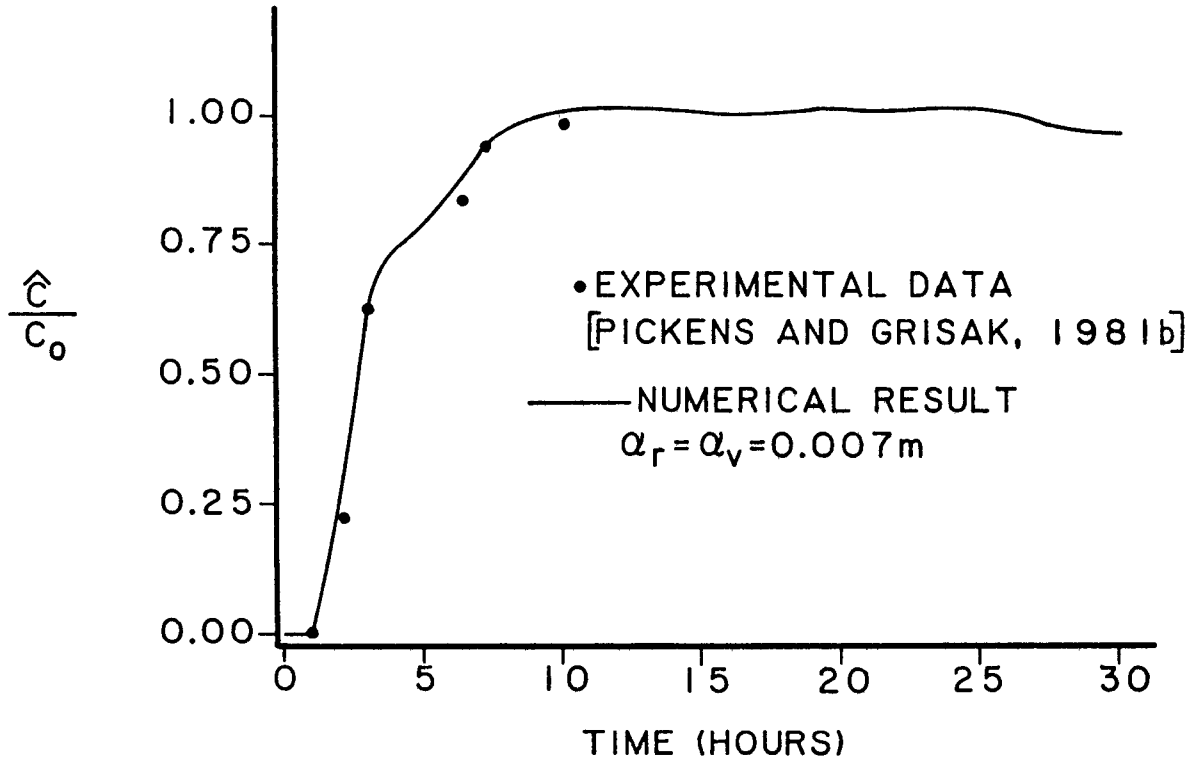


Figure VII-4. Comparison of SWADM results with field data for the flow-weighted concentration from an observation well one meter from the injection-withdrawal well. From Güven et al. (1985).

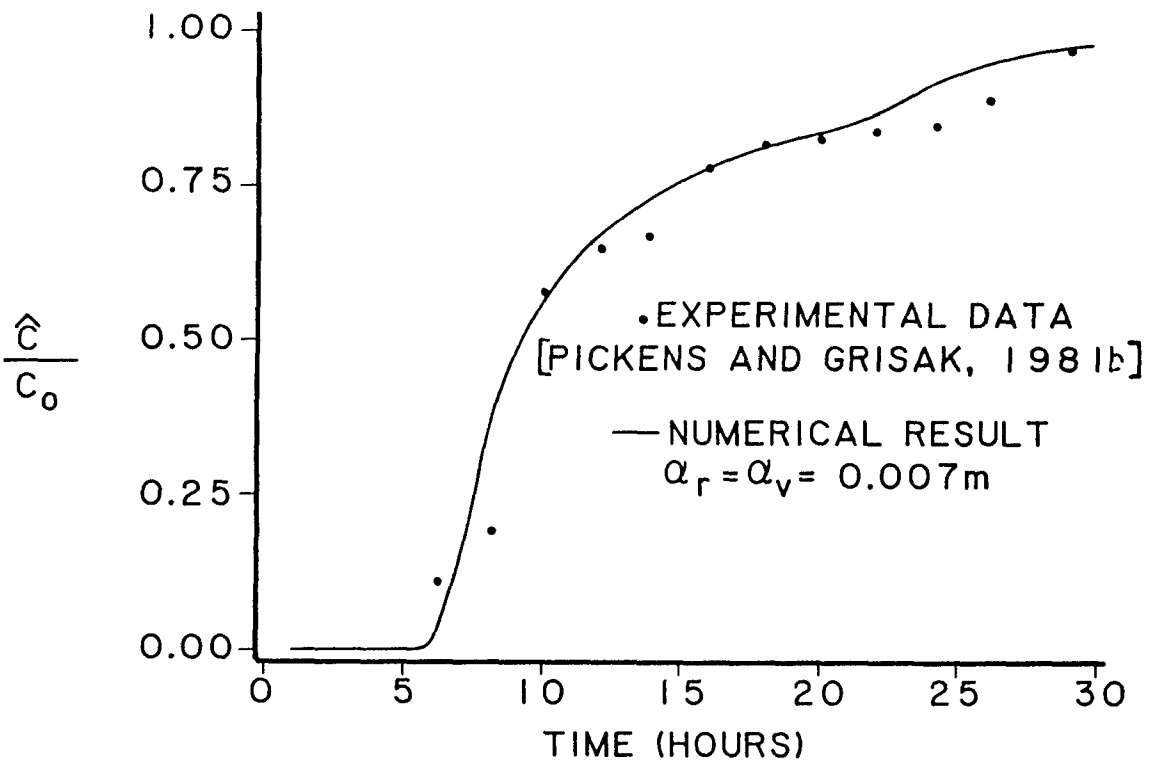


Figure VII-5. Comparisons of SWADM results with field data for the flow-weighted concentration from an observation well two meters from the injection-withdrawal well. From Güven et al. (1985).

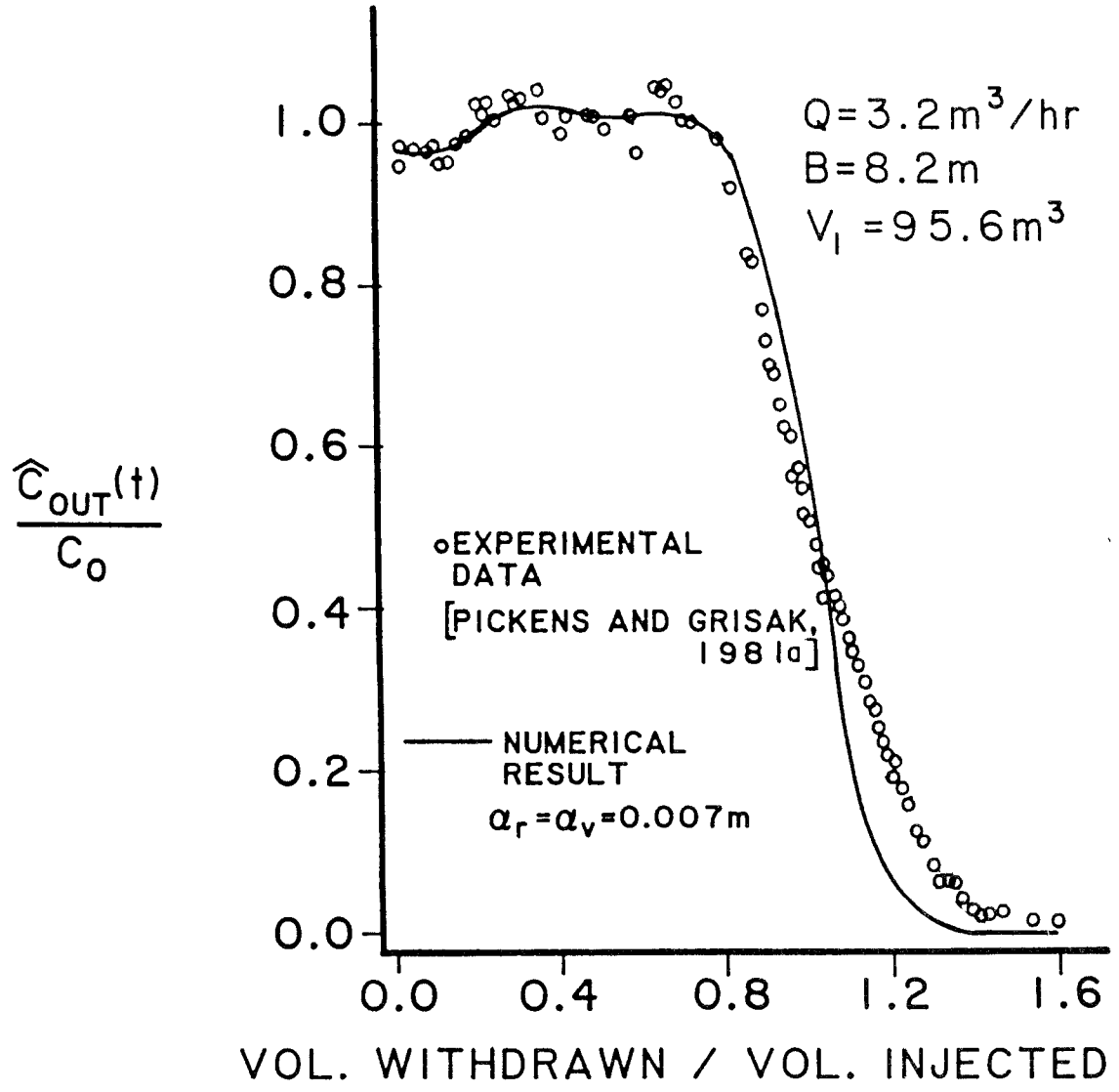


Figure VII-6. Comparison of SWADM results with field data for the concentration leaving the injection-withdrawal well. From Güven et al. (1985).

porosity, and perfectly stratified in the vicinity of the test wells. TWAM takes into account the depth-dependent advection in the horizontal planes, but neglects completely any local hydrodynamic dispersion. Thus any simulations resulting from application of TWAM will yield dispersed concentration distributions based solely on differential advection.

Shown in Figure VII-7 are the results of the three-dimensional dispersion simulation and the advection simulation using the model called TWAM (Güven et al., 1986). Both models do a good job of predicting the recovery concentrations during the two-well test, although the Lagrangian model ran in a small fraction of the time required by the Eulerian approach. The result of the Lagrangian analysis showed that local hydrodynamic dispersion played a very minor role in determining the time distribution of tracer concentration in the withdrawal well. The entire experiment, which involved estimated travel distances over individual flow paths ranging from 38.3 m to about 90 m in the most permeable layer, was highly advection-dominated.

If one assumed a homogeneous aquifer during the performance of the two-well experiment being analyzed, the tracer concentration versus time curve shown in Figure VII-8 would be predicted. One could make the theoretical curve fit the data well by using a scale-dependent longitudinal dispersivity that was about 4 m at the 38 m separation of the injection and production wells ((Huyakorn et al., 1986b). However, the previous results show that this traditional approach is purely curve-fitting.

During the summer of 1985 a second two-well tracer experiment was performed at the Mobile site in a different portion of the study aquifer (Molz et al., 1988). The same Lagrangian model (TWAM), but with a different hydraulic conductivity distribution, was used to simulate the tracer recovery concentration in the withdrawal well. The results shown in Figure VII-9 are again good. This decreases the probability that the relatively good comparison between theory and experiment at the Mobile site was simply fortuitous.

### VII-4.4 Advection-Dominated Modeling of Subsurface Transport Processes that Incorporate Chemical and Microbial Kinetics

Contaminant transport models that incorporate chemical or microbial reaction terms are, in many common situations, very sensitive to hydrodynamic dispersion, particularly vertical transverse dispersion (Molz and Widdowson, 1988). This stems from the fact that for such reactions to occur, it is necessary for a number of dissolved substances to come into intimate physical contact. Thus anything in a mathematical model that causes artificial mixing, like dispersion coefficients that are unrealistically large, will cause the model to overpredict the rates and distribution of possible chemical and microbial reactions.

In order to study such processes with a mathematical model relatively free from numerical dispersion, Molz et al. (1986a) developed an Eulerian-Lagrangian model for simulating microbial growth dynamics coupled to nutrient and oxygen transport in porous media. This model was based on the split-operator approach of Holly and Preissman (1977), and the microbial kinetics employed by Benefield and Molz (1983). A two-dimensional version of the model was used to explore the transport implications of large chemical concentration gradients that have been measured recently in natural aquifers by several research groups (Barker, Patrick and Major, 1987; Ronen et al., 1987a,b; Smith et al., 1987). The actual equations used have been described in detail previously (Molz et al., 1986a; Widdowson et al., 1988), and values selected for the various parameters may be found in Molz and Widdowson (1988). The overall model consists of two advection-dispersion-adsorption-consumption equations describing transport of substrate (organic carbon and energy source) and oxygen at the Darcy scale, two

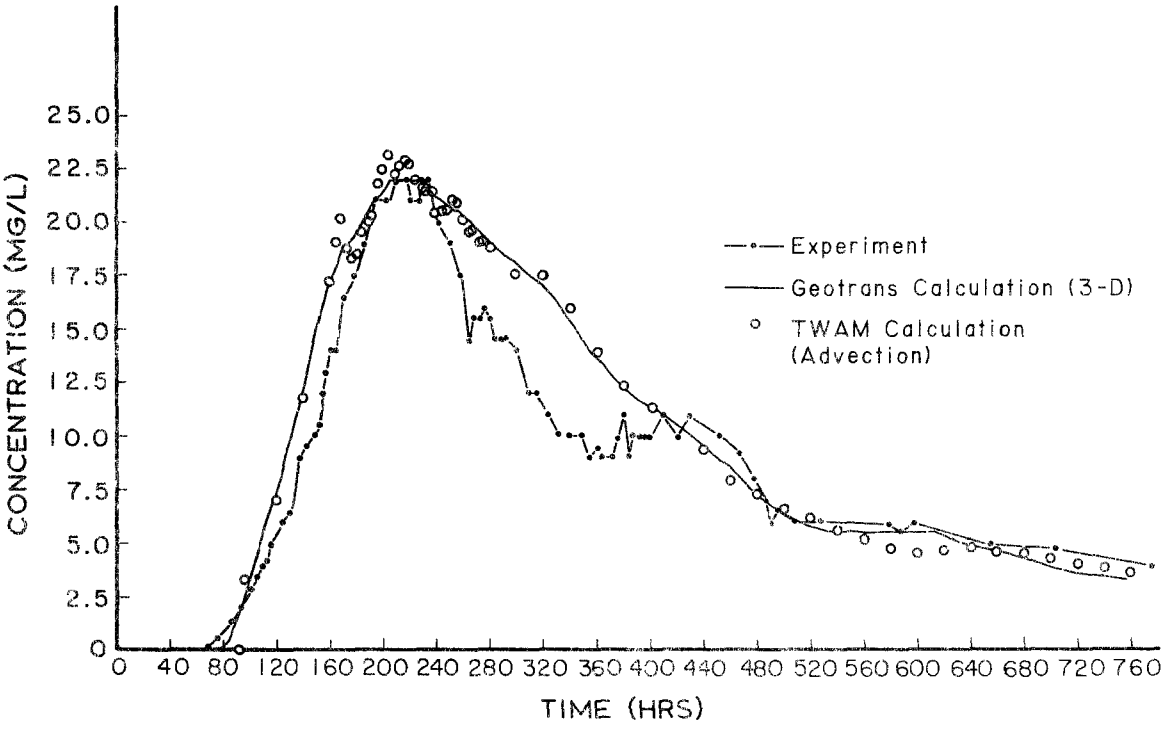


Figure VII-7. Results of various simulations of the first two-well tracer test conducted at the Mobile site. No "calibration" or curve-fitting of any type was used. From Molz et al. (1986a).

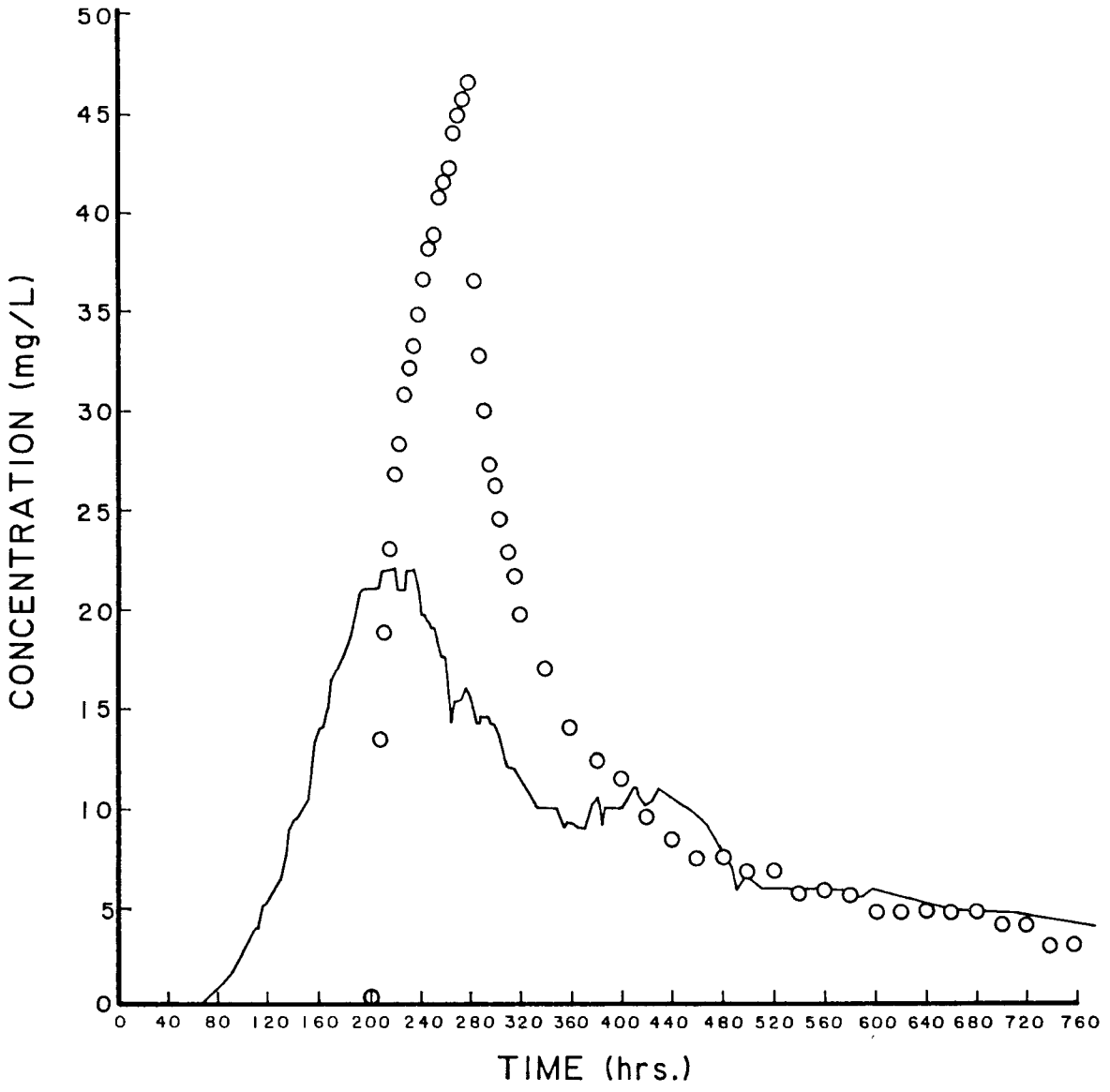


Figure VII-8. Calculated tracer concentration versus time in the withdrawal well based on an assumed homogeneous, isotropic aquifer with no local dispersion (circles) shown together with the results of the first two-well test (full line) at the Mobile site.

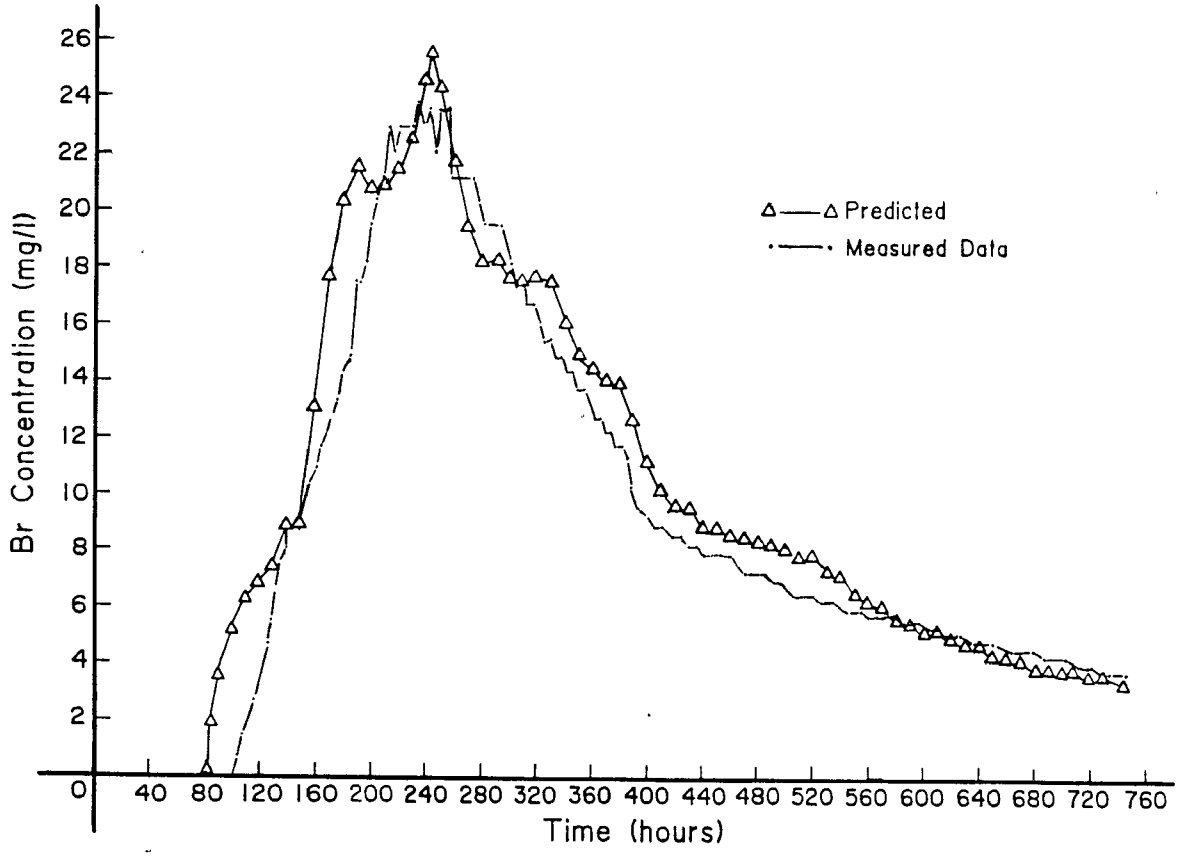


Figure VII-9. Measured and predicted Br concentration versus time in the withdrawal well during the second two-well tracer test at the Mobile site. From Molz et al. (1988).

algebraic chemical kinetic equations describing uptake of substrate and oxygen by microbes, and one additional kinetic equation describing growth or decay of the particle-bound microbial population. The flow direction is assumed to be horizontal, with flow magnitude varying only with vertical position. Diffusion/dispersion, however, is fully two dimensional.

Shown in Figure VII-10 is the hypothetical domain and velocity distribution that was selected as the basis for the generic modeling effort. Flow in a vertical cross section of the aquifer is assumed to be horizontal and perfectly stratified. However, both oxygen and substrate are allowed to move in the horizontal and vertical directions. Boundary conditions were selected to be compatible with a contaminant source in the upper left-hand region of the domain. Oxygen but not substrate (contaminant) was allowed to cross the water table.

Shown in Figure VII-11 is simulated oxygen concentration versus depth for two different values of vertical dispersivity. The profiles correspond to a travel distance of 62 m at an average horizontal seepage velocity of 10 cm/day. Indicated on the figure is the maximum value of oxygen concentration gradient. It is evident that to obtain a concentration gradient and overall oxygen distribution roughly similar to that measured by Barker et al. (1987), and shown in Figure VII-12, it is necessary to use a vertical transverse dispersivity of about 0.1 cm. This shows simultaneously the numerical capability of Eulerian-Lagrangian models and the necessity for using such models if one is to simulate accurately chemical/microbial processes that occur commonly in porous media.

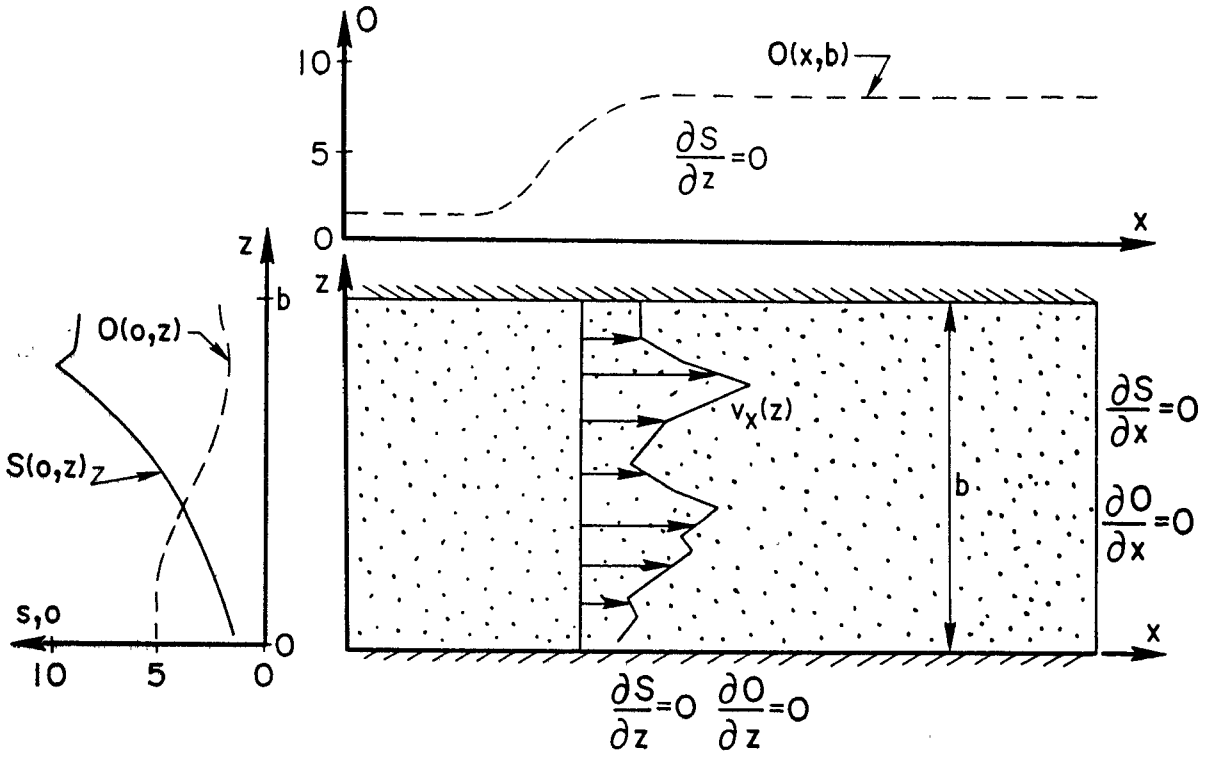


Figure VII-10. Schematic diagram of the hypothetical domain, velocity distribution and boundary conditions used in generic model simulations. O = oxygen concentration; S = substrate concentration. From Molz and Widdowson (1988).

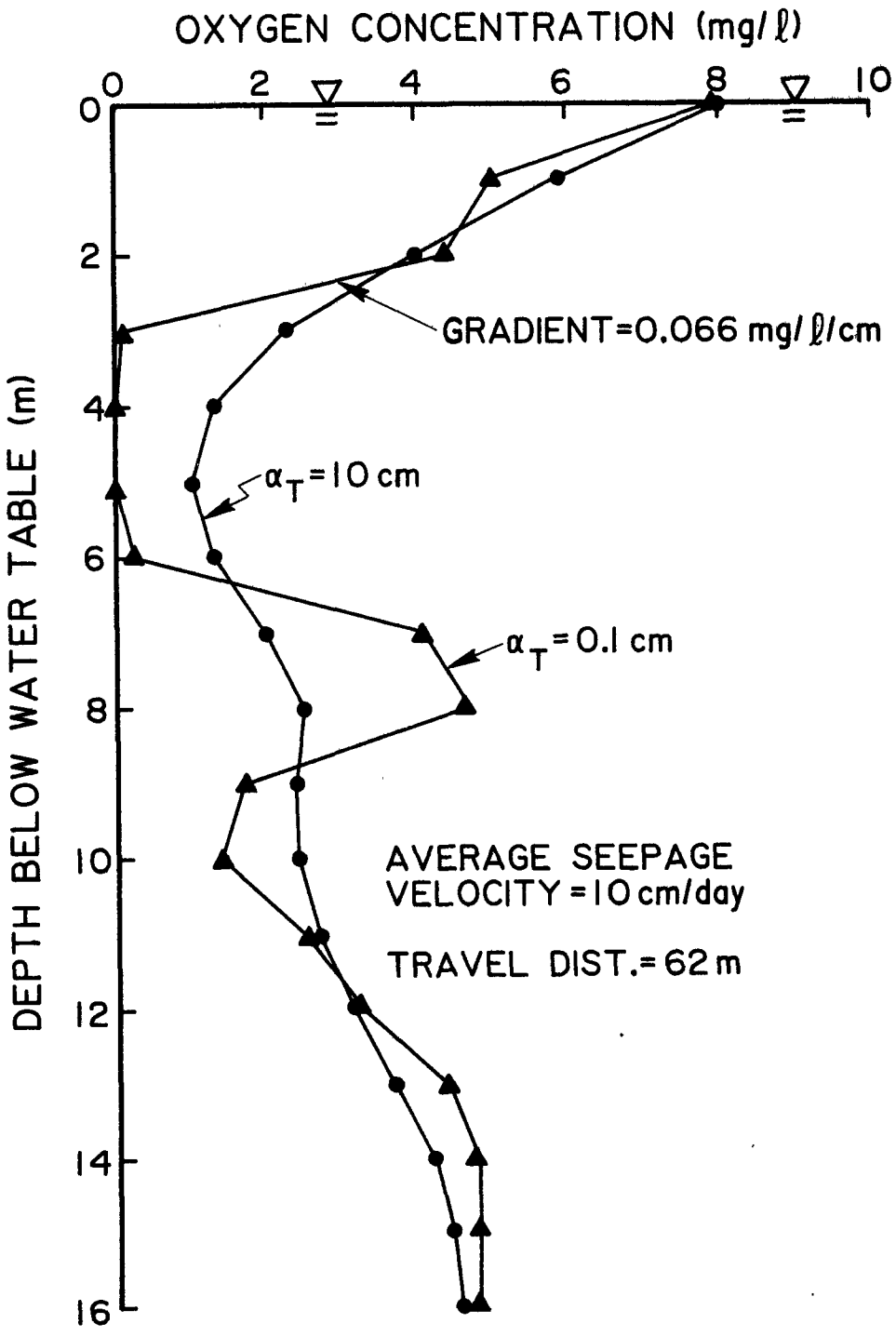


Figure VII-11. Simulated oxygen concentration versus depth below water table for two different values of vertical dispersivity and an average horizontal seepage velocity of 10 cm/day. From Molz and Widdowson (1988).

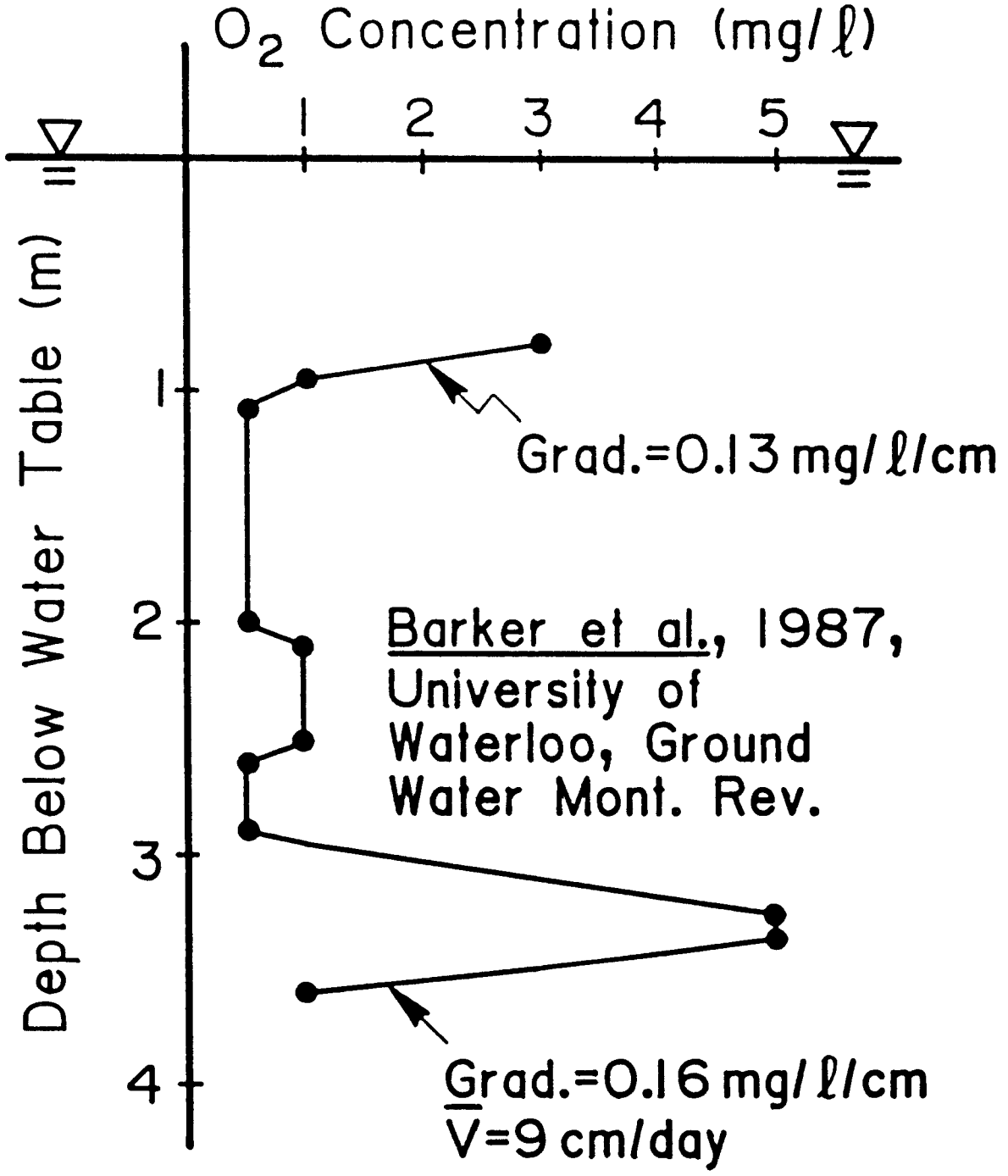


Figure VII-12. Plot of oxygen concentration versus depth below water table (After Barker et al., 1987). From Molz and Widdowson (1988).

# REFERENCES


Ababou, R., L.W. Gelhar, and D. McLaughlin. 1988. Three-dimensional flow in random porous media. Report No. 318, Ralph M. Parsons Laboratory, Department of Civil Engineering, Massachusetts Institute of Technology, Cambridge, Massachusetts.

Abriola, L.M. 1987. Modeling contaminant transport in the subsurface: An interdisciplinary challenge. Reviews of Geophysics, 25, 125-134.

Ackerer, P. 1988. Random-walk method to simulate pollutant transport in alluvial aquifers or fractured rocks. In: Groundwater Flow and Quality Modelling, edited by E. Custodio, A. Gurgui, and J.P Lobo Ferreira. NATO ASI Series C: Mathematical and Physical Sciences, Dordrecht, Holland: D. Reidel Publishing Co., Vol. 224, pp. 475-486.

Allen, M.B. 1987. Numerical modeling of multiphase flow in porous media. Advances in Transport Phenomena in Porous Media, edited by J. Bear and M.Y. Corapcioglu. NATO ASI Series E: Applied Sciences, No. 128. Dordrecht, The Netherlands: Martinus Nijhoff Publishers.

American Petroleum Institute. 1960. Recommended Practice for Core Analysis Procedure. API RP40, Washington, D.C., 55.

Anderson, M.P. 1979. Using models to simulate the movement of contaminants through groundwater flow systems. Critical Reviews in Environmental Control, 9, 97-156.

Anderson, M.P. 1984. Movement of Contaminants in Groundwater: Groundwater Transport Advection and Dispersion. In: Groundwater Contamination, National Academy Press. Washington, D.C., 37-45.

Arnold, D.M., and H.J. Paap. 1979. Quantitative monitoring of water flow behind and in wellbore casing. Transactions of American Institute of Mining Engineers, 267, 121-130.

Baptista, A.M., E.E. Adams, and K.D. Stolzenbach. 1985. Comparison of several Eulerian-Lagrangian models to solve the advection diffusion equation. Proceedings of the International Symposium on Refined Flow Modelling and Turbulence Measurements, Iowa Institute of Hydraulic Research, The University of Iowa, Iowa City, Iowa, 16-18 September, Vol 1, pp. B11.1-B11.9.

Barker, J.F., G.C. Patrick, and D. Major. 1987. Natural attenuation of aromatic hydrocarbons in a shallow sand aquifer. Ground Water Monitoring Rev., 7, 64-71.

Bear, J. 1979. Hydraulics of Groundwater. McGraw-Hill, New York.

Bear, J., and A. Verruijt. 1987. Modeling Groundwater Flow and Pollution. D. Reidel Publishing Co., Dordrecht, Holland.

Benefield, L.D., and F.J. Molz. 1983. A kinetic model for the activated sludge process which considers diffusion and reaction in the microbial floc. Biotechnology and Bioengineering, 25, 2591-2615.

Benson, S.M. 1988. Characterization of the hydrologic and transport properties of the shallow aquifer under Kesterson Reservoir. Ph.D. Dissertation, University of California, Berkeley.

Bird, J.R., and J.C. Dempsey. 1955. The use of radioactive tracer surveys in water-injection wells. Kentucky Geological Survey Special Publications, 8, 10.

Boast, C.W., and D. Kirkham. 1971. Auger hole seepage theory. Soil Science Society of America Journal, 35, 365-374.

Brandt, A. 1977. Multi-level adaptive solutions to boundary-value problems. Mathematics of Computation, 31, 333-390.

Bouwer, H. and R.C. Rice. 1976. A slug test for determining hydraulic conductivity of unconfined aquifers with completely or partially penetrating wells. Water Resources Research, 12, 423-428.

Braester, C., and R. Thunvik. 1984. Determination of formation permeability by double-packer tests. Journal of Hydrology, 72, 375-389.

Bredehoeft, J.D., and S.S. Papadopulos. 1980. A method for determining the hydraulic properties of tight formations. Water Resources Research, 16, 233-238.

Burnett, R.D., and E.O. Frind. 1987a. Simulation of contaminant transport in three dimensions, 1, The alternating direction Galerkin technique. Water Resources Research, 23, 683-694.

Burnett, R.D., and E.O. Frind. 1987b. Simulation of contaminant transport in three dimensions, 2, Dimensionality effects. Water Resources Research, 23, 695-705.

Burns, W.A., Jr. 1969. New single-well test for determining vertical permeability. Transactions American Institute of Mining Engineers, 246, 743-752.

Cady, R., and S.P. Neuman. 1987. Advection-dispersion with adaptive Eulerian-Lagrangian finite elements. In: Advances in Transport Phenomena in Porous Media, edited by J. Bear and M.Y. Corapcioglu. NATO ASI Series E: Applied Sciences, No. 128, Dordrecht, The Netherlands: Martinus Nijhoff Publishers.

Casagrande, A. 1949. Soil mechanics in the design and construction of the Logan International Airport. Journal Boston Society of Civil Engineers, 36, 192-221.

Casagrande, L. 1952. Electro-osmotic stabilization of soils. Boston Society of Civil Engineers Contri. Soil Mech. 1941-1953, 285.

Chapman, H.T., and A.E. Robinson. 1962. A thermal flowmeter for measuring velocity of flow in a well. U.S. Geological Survey Water-Supply Paper, 1544-E, 12.

Cheng, R.T., V. Casulli, and S.N. Milford. 1984. Eulerian-Lagrangian solution of the convection-dispersion equation in natural coordinates. Water Resources Research, 20, 944-952.

Cherry, J.A., R.W. Gillham and J.F. Pickens. 1975. Contaminant hydrogeology, I. Physical processes. Geoscience Canadian, 2, 76-84.

Chirlin, G.R. 1989. A critique of the Hvorslev method for slug test analysis: the fully penetrating well. Ground Water Monitoring Review, 9, 130-138.

Claasen, H.C., and E.H. Cordes. 1975. Two-well recirculating tracer test in fractured carbonate rock, Nevada. Hydrological Sciences Bulletin, 3, 367-382.

Cole, C.R., and H.P. Foote. 1987. Use of a multigrid technique to study effects of limited sampling of heterogeneity on transport prediction. Proceedings of the NWWA Conference on Solving Ground Water Problems with Models, Dublin, Ohio, National Water Well Association, pp. 355-380.

Cole, C.R., and H.P. Foote. 1988. Evaluation of a three-dimensional multigrid code for studying flow and transport in porous media with multiple scales of heterogeneity. EOS, Transactions of the American Geophysical Union, 69, 1192.

Cooper, H.H., J.D. Bredehoeft, and S.S. Papadopulos. 1967. Response of a finite diameter well to an instantaneous charge of water. Water Resources Research, 3, 263-269.

Cooper, H.H., and C.E. Jacob. 1946. A generalized graphical method for evaluating formation constants and summarizing well-field history. Transactions American Geophysical Union, 27, 526-534.

Dagan, G. 1978. A note on packer, slug, and recovery tests in unconfined aquifers. Water Resources Research, 14, 929-934.

Daus, A.D., and E.O. Frind. 1985. An alternating direction Galerkin technique for simulation of contaminant transport in complex groundwater systems. Water Resources Research, 21, 653-644.

Davis, S.N., G.M. Thompson, H.W. Bentley, and G. Stiles. 1980. Groundwater tracers - a short review. Ground Water, 18, 14-23.

Doughty, C., G. Hellstrom, C.F. Tsang, and J. Claesson. 1982. A dimensionless parameter approach to the thermal behavior of an aquifer thermal energy storage system. Water Resources Research, 18, 571-587.

Drost, W., D. Klotz, A. Koch, H. Moser, F. Neumaier, and W. Rauert. 1968. Point dilution methods of investigating groundwater flow by means of radioisotopes. Water Resources Research, 4, 125-146.

Dudgeon, C.R., M.J. Green, and W.J. Smedmore. 1975. Heat-pulse flowmeter for boreholes: Medmenham, Marlow, Bucks, England. Water Research Centre Technical Report TR-4, 69.

Earlougher, R.C., Jr. 1980. Analysis and design methods for vertical well testing. Journal of Petroleum Technology, 32, 505-514.

Edwards, J.M., and E.L. Holter. 1962. Applications of a subsurface solid-state isotope injector to nuclear-tracer survey methods. Journal of Petroleum Technology, 14, 121-124.

Ewing, R.E., T.F. Russell, and M.F. Wheeler. 1984. Convergence analysis of an approximation of miscible displacement in porous media by mixed finite elements and a modified method of characteristics. Computer Methods in Applied Mechanics and Engineering, 47, 73-94.

Fair, G.M., and L.P. Hatch. 1933. Fundamental factor governing the stream line flow of water through sands. Journal American Water Works Association, 25, 1551-1565.

Farmer, C.L. 1987. Moving point techniques. In: Advances in Transport Phenomena in Porous Media, edited by J. Bear and M.Y. Corapcioglu. NATO ASI Series E: Applied Sciences, Dordrecht, The Netherlands: Martinus Nijhoff Publishers, No. 128, pp. 955-100-4.

Federenko, R.P. 1961. A relaxation method for solving elliptic difference equations. Z. Vycisl. Mat. i., Mat. Fiz., 1, 922-927.

Fogg, G.E. 1986. Groundwater flow and sand body interconnectedness in a thick multiple-aquifer system. Water Resources Research, 22, 679-694.

Freeze, R.A., and J.A. Cherry. 1979. Groundwater. Prentice-Hall, Englewood Cliffs, New Jersey, 604.

Fried, J.J., and M.A. Combarnous. 1971. Dispersion in porous media. Advances in Hydrosciences, 7, Academic Press, N.Y., 169-282.

Fried, J.J. 1975. Groundwater Pollution, Developments in Water Science, No. 4, Elsevier, N.Y., 330 pp.

Frind, E.O., E.A. Sudicky, and S.L. Schellenberg. 1988. Micro-scale modelling in the study of plume evolution in heterogeneous media. In: Groundwater Flow and Quality Modelling, edited by E. Custodio, A. Gurgui, and J.P. Lobo Ferreira. NATO ASI Series C: Mathematical and Physical Sciences, Dordrecht, Holland: D. Reidel Publishing Co., Vol. 224, pp. 439-461.

Garder, A.O., D.W. Peaceman, and R.L. Pozzi, Jr. 1964. Numerical calculation of multidimensional miscible displacement by the method of characteristics. Society of Petroleum Engineers Journal, 4, 26-36.

Gelhar, L.W., A.L. Gutjahr, and R.L. Naff. 1979. Stochastic analysis of macrodispersion in a stratified aquifer. Water Resources Research, 15, 1387-1397.

Gelhar, L.W. 1982. Analysis of two-well tracer tests with a pulse input. Rockwell Hanford Operations, RHO-BW-CR-131P, Richland, WA.

Gelhar, L. and C.L. Axness. 1983. Three-dimensional stochastic analysis of macrodispersion in aquifers. Water Resources Research, 19, 161-180.

Gelhar, L.W. 1986. Stochastic subsurface hydrology from theory to applications. Water Resources Research, 22, 135-145.

Glover, R.E., W.T. Moody, and W.N. Tapp. 1960. Till permeabilities as estimated from the pump-test data obtained during the irrigation well investigations. Studies of Groundwater Movement, Bureau of Reclamation Tec. Memo 656.

Grove, D.B., and W.A. Beetem. 1971. Porosity and dispersion constant calculations for a fractured carbonate aquifer using the two well tracer method. Water Resources Research, 7, 128-134.

Güven, O., F.J. Molz and J.G. Melville. 1984. An analysis of dispersion in a stratified aquifer. Water Resources Research, 20, 1337-1354.

Güven, O., R.W. Falta, F.J. Molz, and J.G. Melville. 1985. Analysis and interpretation of single-well tracer tests in stratified aquifers. Water Resources Research, 21, 676-684.

Güven, O., R.W. Falta, F.J. Molz, and J.G. Melville. 1986. A simplified analysis of two-well tracer tests in stratified aquifers. Ground Water, 24, 63-71.

Güven, O., and F.J. Molz. 1986. Deterministic and stochastic analyses of dispersion in an unbounded stratified porous medium. Water Resources Research, 20, 1565-1574.

Guven, O., and F.J. Molz. 1988. A field study of scale-dependent dispersion in a sandy aquifer-comment. Journal of Hydrology, 101, 359-363.

Hada, S. 1977. Utilization and interpretation of micro flowmeter. Engineering Geology (Japan), 18, 26-37.

Hann, C.T. 1977. Statistical Methods in Hydrology. Iowa State University Press, Ames, Iowa, 378.

Hantush, M.S., and C.E. Jacob. 1955. Non-steady radial flow in an infinite leaky aquifer. Transactions American Geophysical Union, 36, 95-100.

Hantush, M.S. 1956. Analysis of data from pumping tests in leaky aquifers. Transactions American Geophysical Union, 37, 702-714.

Hantush, M.S. 1957. Nonsteady flow to a well partially penetrating an infinite leaky aquifer. Proceedings Iraqi Scientific Society, 1, 10.

Hantush, M.S. 1960a. Modification of the theory of leaky aquifers. Journal of Geophysical Research, 65, 3713-3726.

Hantush, M.S. 1960b. Tables of the function H(u,$\beta$), Document 6427, U.S. Library of Congress, Washington, D.C.

Hantush, M.S. 1961. Drawdown around a partially penetrating well. ASCE Journal of Hydraulics Division, HY4, 83-98.

Hantush, M.S. 1964. Advances in Hydroscience, Ven Te Chow, Ed. Academic Press, New York, Vol. 1.

Hauguel, A. 1985. Numerical modelling of complex industrial and environmental flows. Proceedings of the International Symposium on Refined Flow Modelling and Turbulence Measurements. Iowa Institute of Hydraulic Research, The University of Iowa, Iowa City,. Iowa, 16-18 September, Vol. 1, pp. K1.1-K1.25.

Hess, A.E. 1982. A heat-pulse flowmeter for measuring low velocities in boreholes. U.S. Geological Survey Open File Report 82-699, 40 pp.

Hess, A.E. 1986. Identifying hydraulically conductive fractures with a slow-velocity borehole flowmeter. Canadian Geotechnical Journal, 23, 69-78.

Hess, A.E. 1988. Characterizing fractured hydrology using a sensitive borehole flowmeter with a wire-line powered packer. International Conference on Fluid Flow in Fractured Rock, Proceedings, May, Atlanta, GA (in press).

Hess, A.E., and F.L. Paillet. 1989. Characterizing flow paths and permeability distribution in fractured rock aquifers using a sensitive thermal borehole flowmeter. Proceedings of the Conference on New Field Techniques for Quantifying the Physical and Chemical Properties of Heterogeneous Aquifers. Dallas, Texas.

Hirasaki, G.J. 1974. Pulse tests and other early transient pressure analyses for in-situ estimation of vertical permeability. Transactions American Institute of Mining Engineers, 257, 75-90.

Hoehn, E., and P.V. Roberts. 1982. Advection dispersion interpretation of tracer observations in an aquifer. Ground Water, 20, 457-465.

Holly, F.M., Jr., and A. Preissman. 1977. Accurate calculation of transport in two dimensions. Journal of the Hydraulic Division, ASCE, 103, 1259-1277.

Holly, F.M., Jr., and J. Usseglio-Polatera. 1984. Dispersion simulation in two-dimensional tidal flow. Journal of Hydraulic Engineering, ASCE, 110, 905-926.

Hooper, J.A., and D.R.F. Harleman. 1967. Dispersion in radial flow from a recharge well. Journal of Geophysical Research, 72, 3595-3607.

Hubbert, M.K. 1940. The theory of groundwater motion. Journal of Geology, 48, 785-944. Also in Theory of Groundwater Motion and Related Papers, Hafner, New York, 1969.

Hufschmied, P. 1983. Ermittlung der Durchlassigkeit von Lockergesteins- Grundwasserleitern, eine vergleichende Untersuchung verschiedener Feldmethoden. Doctoral Dissertation No. 7397, ETH Zurich, Switzerland.

Hufschmied, P. 1989. Treatment of uncertainties in ground-water flow modeling in the Swiss radioactive waste program. In: Proceedings of the Conference in Geostatistical, Sensitivity, and Uncertainty Methods for Ground-Water Flow and Transport Modeling, edited by B.E. Buxton, Columbus, Ohio: Battelle Press, pp. 63-87.

Huntley, D. 1986. Relations between permeability and electrical resistivity in granular aquifers. Ground Water, 24, 466-474.

Huyakorn, P.S., and G.F. Pinder. 1983. Computational Methods in Subsurface Flow. Academic Press, New York.

Huyakorn, P.S., P.F. Andersen, O. Güven, and F.J. Molz. 1986a. A curvilinear finite element model for simulating two-well tracer tests and transport in stratified aquifers. Water Resources Research, 22, 663-678.

Huyakorn, P.S., P.F. Andersen, F.J. Molz, O. Güven, and J.G. Melville. 1986b. Simulations of two-well tracer tests in stratified aquifers at the Chalk River and the Mobile sites. Water Resources Research, 22, 1016-1030.

Hvorslev, H.J. 1951. Time lag and soil permeability in ground-water observations. Bulletin 36, Waterways Experiment Station, Corps of Engineers, U.S. Army, Vicksburg, MS.

Ivanovich, M., and D.B. Smith. 1978. Determination of aquifer parameters by a two-well pulsed method using radioactive tracers. Journal of Hydrology, 36, 35-45.

Jacob, C.E. 1940. On the flow of water in an elastic artesian aquifer. American Geophysical Union Transactions, 2, 574-586.

Jacob, C.E. 1946. Radial flow in a leaky artesian aquifer. Transactions American Geophysical Union, 27, 198-205.

Javandel, I., and P.A. Witherspoon. 1969. A method of analyzing transient fluid flow in multilayered aquifers. Water Resources Research, 5, 856-869.

Javandel, I., C. Doughty, and C.F. Tsang. 1984. Groundwater Transport: Handbook of Mathematical Models, American Geophysical Union, Washington, DC, 228 pp.

Johnson, A.I. 1965. Piezometers for pore-pressure measurement in fine-textured soils. U.S. Geological Survey, Open-file report.

Kanehiro, B.Y., and T.N. Narasimhan. 1980. Aquifer response to earth tides. Proceedings of the 3rd Invitational Well-Testing Symposium, Lawrence Berkeley Laboratory, 120-129.

Keller, G.V., and F.C. Frischknecht. 1966. Electrical methods in geophysical prospecting. Pergamon Press, 519 pp.

Keys, W.S., and L.M. MacCary. 1971. Application of borehole geophysics to water resources investigations. Techniques of water-resources investigations of the United States Geological Survey, NTIS, Washington, DC, Book 2, Chapt. E1, 109-114.

Keys, W.S., and R.F. Brown. 1978. The use of temperature logs to trace the movement of injected water. Ground Water, 16, 32-48.

Keys, W.S., and J.K. Sullivan. 1978. Role of borehole geophysics in defining the physical characteristics of the Raft River geothermal reservoir. Idaho Geophysics, 44, 1116-1141.

Kinzelbach, W. 1988. The random walk method in pollutant transport simulation. In: Groundwater Flow and Quality Modelling, edited by E. Custodio, A. Gurgui, and J.P. Lobo Ferreira, NATO ASI Series C: Mathematical and Physical Sciences, Dordrecht, Holland: D. Reidel Publishing Co., Vol. 224, pp. 227-245.

Kiraly, L. 1988. Large scale 3-D groundwater flow modeling in highly heterogeneous porous medium. In: Groundwater Flow and Quality Modelling, edited by E. Custodio, A. Gurgui, J.P. Lobo Ferreira, NATO ASI Series, Series C: Mathematical and Physical Sciences, Dordrecht, Holland; D. Reidel Publishing Co., Vol. 224, pp. 761-775.

Klett, R.D., C.E. Tyner, and E.S. Hertel. 1981. Geologic flow characterization using tracer techniques. Sandia National Laboratory Report SAND80-0454, 84 pp.

Kokesh, F.P., R.J. Schwartz, W.B. Wall, and R.L. Morris. 1965. A new approach to sonic logging and other acoustic measurements. Journal of Petroleum Technology, 17, 3-12.

Konikow, L.F., and J.D. Bredehoeft. 1978. Computer model of two-dimensional solute transport and dispersion in groundwater. Techniques of Water Resources Investigations of the United States Geological Survey, NTIS, Washington, D.C., Book 7, Chapter C2.

Kwader, T. 1985. Estimating aquifer permeability from formation resistivity factors. Ground Water, 23, 762-766.

Lapidus, L., and G.F. Pinder. 1982. Numerical Solution of Partial Differential Equations in Science and Engineering, John Wiley, New York.

Leahy, P.P. 1977. Hydraulic characteristics of the piney point aquifer and overlying bed near Dover, Delware. Delaware Geological Survey Report of Investiation, No 9., 26, 24 pp.

Lehr, J.H. 1988. An irreverent view of contaminant dispersion. Ground Water Monitoring Review, 8, 4-6.

Lenda, A., and A. Zuber. 1970. Tracer dispersion in groundwater experiments. Isotope Hydrology, International, Atomic Energy Agency, Vienna, 619-641.

Leonhart, L.S., R.L. Jackson, D.L. Graham, L.W. Gelhar, G.M. Thompson, B.Y. Kanehiro, and C.R. Wilson. 1985. Analysis and interpretation of a recirculating tracer experiment performed on a deep basalt flow top. Bulletin of the Association of Engineering Geologists, 22, 3, 259-274.

Lohman, S.W. 1972. Groundwater Hydraulics, USGS Professional paper 708, 70 pp.

Lusczynski, N.J. 1961. Head and flow of groundwater of variable density. Journal of Geophysical Research, 66, 4247-4256.

Maloszewski, P. and A. Zuber. 1985. On the theory of tracer experiments in fissured rocks with a porous matrix. Journal of Hydrology, 22, 259-274.

Masch, F.D., and K.J. Denny. 1966. Grain size distribution and its effect on the permeability of unconsolidated sands. Water Resources Research, 2, 665-677.

Matheron, G. and F. DeMarsily. 1980. Is transport in porous media always diffusive? A counter example. Water Resources Research, 16, 901-917.

Mazac, O., W.E. Kelly, and I. Landa. 1985. A hydrogeological model for relations between electrical and hydraulic properties of aquifers. Journal of Hydrology, 79, 1-19.

McDonald, M.G., and A.W. Harbaugh. 1984. A modular three-dimensional finite difference groundwater flow model. U.S. Department of the Interior, U.S. Geological Survey, National Center, Reston, Virginia.

McLinn, E.L., and C.D. Palmer. 1989. Laboratory testing and comparison of specific conductance and electrical resistivity borehole dilution devices. Proceedings, Conference of New Field Techniques for Quantifying the Physical and Chemical Properties of Heterogeneous Aquifers. Dallas, Texas.

Melville, J.G., F.J. Molz, and O. Güven. 1985. Laboratory investigation and analysis of a ground-water flow meter. Ground Water, 23, 486-495.

Melville, J.G., F.J. Molz, O. Güven and M.A. Widdowson. 1989. Multi-level slug tests with comparisons to tracer data. Ground Water, submitted for publication.

Mercado, A., and E. Halvey. 1966. Determining the average porosity and permeability of a stratified aquifer with the aid of radioactive tracers. Water Resources Research, 2, 525-531.

Moench, A.F., and A. Ogata. 1981. A numerical inversion of the Laplace transform solution to radial dispersion in a porous medium. Water Resources Research, 17, 250-252.

Moltyaner. G.L. 1987. Mixing cup and through-the-wall measurements in field-scale tracer tests and their related scales of averaging. Journal of Hydrology, 89, 281-302.

Moltyaner, G.L., and R.W.D. Killey. 1988a. The Twin Lake tracer tests: longitudinal dispersion. Water Resources Research, 24, 1613-1627.

Moltyaner, G.L., and R.W.D. Killey. 1988b. Twin Lake tracer tests: transverse dispersion. Water Resources Research, 24, 1628-1637.

Molz, F.J., O. Güven, and J.G. Melville., 1983. An examination of scale-dependent dispersion coefficients. Ground Water, 21, 715-725.

Molz, F.J., J.G. Melville, O. Güven, R.C. Crocker, and K.T. Matteson. 1985. Design and performance of single-well tracer tests at the Mobile site. Water Resources Research, 21, 1497-1502.

Molz, F.J., O. Güven, J.G. Melville, R.D. Crocker, and K.T. Matteson. 1986a. Performance, analysis, and simulation of a two-well tracer test at the Mobile site. Water Resources Research, 22, 1031-1037.

Molz, F.J., O. Güven, J.G. Melville, and J.F. Keely. 1986b. Performance and analysis of aquifer tracer tests with implications for contaminant transport modeling. USEPA, R.S. Kerr Environmental Research Laboratory, Ada, OK 74820, EPA/600/2-86/062.

Molz, F.J., M. Widdowson, and L.D. Benefield. 1986c. Simulation of microbial growth dynamics coupled to nutrient and oxygen transport in porous media. Water Resources Research, 22, 1207-1216.

Molz, F.J., and M.A. Widdowson. 1988. Internal inconsistencies in dispersion-dominated models that incorporate chemical and microbial kinetics. Water Resources Research, 24, 615-619.

Molz, F.J., O. Güven, J.G. Melville, J.S. Nohrstedt, and J.K. Overholtzer. 1988. Forced gradient tracer tests and inferred hydraulic conductivity distributions at the Mobile site. Ground Water, 26, 570-579.

Molz, F.J., R.H. Morin, A.E. Hess, J.G. Melville, and O. Güven. 1989a. The impeller meter for measuring aquifer permeability variations: evaluation and comparison with other tests. Water Resources Research, 25, 1677-1683.

Molz, F.J., O. Güven, J.G. Melville, and C. Cardone. 1989b. Hydraulic conductivity measurement at different scales and contaminant transport modeling. In: Dynamics of Fluids in Hierarchical Porous Media, edited by J.H. Cushman. New York, Academic Press, in press.

Morin, R.H., A.E. Hess, and F.L. Paillet. 1988a. Determining the distribution of hydraulic conductivity in a fractured limestone aquifer by simultaneous injection and geophysical logging. Ground Water, 26, 587-595.

Morin, R.H., D.R. LeBlanc, and W.E. Teasdale. 1988b. A statistical evaluation of formation disturbance produced by well-casing installation methods. Ground Water, 26, 207-217.

Morrow, T.B., and S.J. Kline. 1971. The evaluation and use of hot-wire and hot-film anemometers in liquids. Stanford University, Department of Mechanical Engineering, Thermosciences Division, Report MD-25, 187 pp.

Muscat, M. 1937. The Flow of Homogeneous Fluids Through Porous Media. McGraw-Hill, New York.

Narasimhan, T.N. 1968. Ratio method for determining characteristics of ideal, leaky and bounded aquifers. Bulletin of International Association of Scientific Hydrology, 13, 70-83.

Narasimhan, T.N., and P.A. Witherspoon. 1976. An integrated finite difference method for analyzing fluid flow in porous media. Water Resources Research, 12, 57-64.

Narasimhan, T.N., and B.Y. Kanehiro. 1980. A note on the meaning of storage coefficient. Water Resources Research, 16, 423-429.

Nelson, R.W. 1978a. Evaluating the environmental consequences of groundwater contamination, 1, An overview of contaminant arrival distributions as general evaluation requirements. Water Resources Research, 14, 408-415.

Nelson, R.W. 1978b. Evaluating the environmental consequences of groundwater contamination, 2, Obtaining location/arrival time and location/outflow quantity distribution for steady flow systems. Water Resources Research, 14, 416-428.

Nelson, R.W. 1978c. Evaluating the environmental consequences of groundwater contamination, 3, Obtaining contaminant arrival distributions in transient flow systems. Water Resources Research, 14, 429-440.

Nelson, R.W. 1978d. Evaluating the environmental consequences of groundwater contamination, 4, Obtaining and utilizing contaminant arrival distributions in transient flow systems. Water Resources Research, 14, 441-450.

Nelson, R.W., E.A. Jacobson, and W. Conbere. 1987. Uncertainty assessment for fluid flow and contaminant transport modeling in heterogeneous groundwater systems. In: Advances in Transport Phenomena in Porous Media, edited by J. Bear and M.Y. Corapcioglu. NATO ASI Series E: Dordrecht, The Netherlands: Martinus Nijhoff Publishers, Applied Sciences, 128, pp. 703-726.

Neuman. S.P. 1966. Transient Behavior of an Aquifer with a Slightly Leaky Caprock, M.S. Thesis, University of California, Berkeley.

Neuman, S.P. and P.A. Witherspoon. 1968. Theory of flow in aquicludes adjacent to slightly leaky aquifers. Water Resources Research, 4, 103-112.

Neuman, S.P. and P.A. Witherspoon. 1969. Applicability of current theories of flow in leaky aquifers. Water Resources Research, 5, 817-829.

Neuman, S.P., and P.A. Witherspoon. 1972. Field determination of the hydraulic properties of leaky multiple aquifer systems, Water Resources Research, 8, 1284-1298.

Neuman, S.P. 1984. Adaptive Eulerian-Lagrangian finite element method for advection-dispersion. International Journal for Numerical Methods in Engineering, 20, 321-337.

Neuzil, C.E. 1982. On conducting the modified 'slug' test in tight formations, Water Resources Research, 18, 439-441.

Nir, A., and B.L. Kirk. 1982. Tracer theory with applications in geosciences, Oak Ridge National Laboratory Report, ORNL-5695/P1 Publication No. 1964, 83 pp.

Nisle, R.G. 1958. The effect of partial penetration on pressure build-up in oil wells. Transactions American Institute of Mining Engineers, 213, 85-90.

Odeh, A.S. 1987. Mathematical modeling of the behavior of hydrocarbon reservoirs - The present and the future. In: Advances in Transport Phenomena in Porous Media, edited by J. Bear and Y. Corapcioglu. NATO ASI Series E: Dordrecht, The Netherlands: Martinus Nijhoff Publishers, Applied Sciences, 128, pp. 821-848.

Ogata, A. 1958. Dispersion in porous media, Ph.D. dissertation, Northwestern University, Evanston, Illinois, 121 pp.

Oran, E.S., and J.P. Boris. 1987. Numerical Simulation of Reactive Flow. Elsevier, New York.

Osiensky, J.L., G.V. Winter, and R.E. Williams. 1984. Monitoring and mathematical modeling of contaminated ground-water plumes in fluvial environments. Ground Water, 22, 298-306.

Paillet, F.L., W.S. Keys, and A.E. Hess. 1985. Effects of lithology on televiewer-log quality and fracture interpretation. Society of Professional Well Log Analysis Logging Symposium, 26th, Dallas, TX, Transactions, JJJ1-JJJ30.

Paillet, F.L., A.E. Hess, C.H. Cheng, and E.L. Hardin. 1987. Characterization of fracture permeability with high-resolution vertical flow measurements during borehole pumping. Ground Water, 25, 28-40.

Paillet, F.L., and A.E. Hess. 1987. Geophysical well log analysis of fractured granitic rocks at Atikokan, Ontario, Canada. U.S. Geological Survey Water Resources Investigations Report 87-4154, 36 pp.

Papadopulos, S.S., J.D. Bredehoeft, and H.H. Cooper, Jr. 1973. On the analysis of "slug test" data. Water Resources Research, 9, 1087-1089.

Parr, A.D., F.J. Molz, and J.G. Melville. 1983. Field determination of aquifer thermal energy storage parameters. Ground Water, 21, 22-35.

Patten, E.R., and G.D. Bennett. 1962. Methods of flow measurement in well bores. U.S. Geological Survey Water-Supply Paper 1554-C, 28 pp.

Philip, J.R., and D.A. deVries. 1957. Moisture movement in porous materials under temperature gradients. Transactions American Geophysical Union, 38, 222-232.

Pickens, J.F., and G.E. Grisak. 1981a. Scale-dependent dispersion in a stratified granular aquifer. Water Resources Research, 17, 1191-1211.

Pickens, J.F., and G.E. Grisak. 1981b. Modeling of scale-dependent dispersion in hydrogeologic systems. Water Resources Research, 17, 1701-1711.

Pinder, G.F. 1988a. An overview of groundwater modeling. In: Groundwater Flow and Quality Modeling, edited by E. Custodio, A. Gurgui, J.P. Lobo Ferreira. NATO ASI Series C: Mathematical and Physical Sciences, Dordrecht, Holland: D. Reidel Publishing Co., Vol. 224, pp. 119-134.

Pinder, G.F. 1988b. Solution methods in groundwater flow and transport. In: Groundwater Flow and Quality Modelling, edited by E. Custodio, A. Gurgui, J.P. Lobo Ferreira. NATO ASI Series C: Mathematical and Physical Sciences, Dordrecht, Holland: D. Reidel Publishing Co., Vol. 224, pp. 815-817.

Prickett, T.A., T.G. Naymik, and C.G. Lonnquist. 1981. A random-walk solute transport model for selected groundwater quality evaluations. Bulletin 65, Illinois State Water Survey, Champaign, Illinois.

Prats, M. 1970. A method for determining the net vertical permeability near a well from in-situ measurements. Transactions American Institute of Mining Engineers, 249, 637-643.

Rehfeldt, K.R., P. Hufschmied, L.W. Gelhar, and M.E. Schaefer. 1988. The borehole flowmeter technique for measuring hydraulic conductivity variability. Report #_____, Electric Power Research Institute, 3412 Hillview Ave., Palo Alto, CA.

Remson, I., G.M. Hornberger, and F.J. Molz. 1971. Numerical Methods in Subsurface Hydrology with an Introduction to the Finite Elements Method. Wiley (Interscience), New York.

Rijnders, J.P. 1973. Application of pulse-test methods in Oman. Journal of Petroleum Technology, 25, pp. 1025-1032.

Robson, S.G. 1974. Feasibility of digital water quality modeling illustrated by application at Barstow, CA. U.S. Geological Survey Water Research Investigation Report 46-73, 66 pp.

Ronen, D., M. Magaritz, N. Paldor, and Y. Backmat. 1986. The behavior of groundwater in the vicinity of the watertable evidenced by specific discharge profiles. Water Resources Research, 22, 1217-1224.

Ronen, D., M. Magaritz, E. Almon, and A.J. Amiel. 1987a. Anthropogenic anoxification ("eutrophication") of the water table region of a deep phreatic aquifer. Water Resources Research, 23, 1554-1560.

Ronen, D., M. Magaritz, H. Gvirtzman, and W. Garner. 1987b. Microscale chemical heterogeneity in groundwater. Journal of Hydrology, 92, 173-178.

Russo, D., and W.A. Jury. 1987a. A theoretical study of the estimation of the correlation scale in spatially variable fields, 1. stationary fields. Water Resources Research, 23, 1257-1268.

Russo, D., and W.A. Jury. 1987b. A theoretical study of the estimation of the correlation scale in spatially variable fields, 2. nonstationary fields. Water Resources Research, 23, 1269-1279.

Saad, K.F. 1967. Determination of the vertical and horizontal permeabilities of fractured water-bearing formations. Bulletin International Association of Scientific Hydrology, 3, 23-26.

Sauty, J.P. 1980. An analysis of hydrodispersive transfer in aquifers. Water Resources Research, 16, 145-158.

Scheidegger, A.E. 1960. The Physics of Flow Through Porous Media, The MacMillan Company, New York.

Schimschal, U. 1981. Flowmeter Analysis at Raft River, Idaho. Ground Water, 19, 93-97.

Schmid, G., and D. Braess. 1988. Comparison of fast equation solvers for groundwater flow problems. In: Groundwater Flow and Quality Modelling, edited by E. Custodio, A. Gurgui, J.P. Lobo Ferreira. NATO ASI Series C: Mathematical and Physical Sciences, Dordrecht, Holland: D. Reidel Publishing Co., Vol. 2242, pp. 173-188.

Schlumberger. 1972. Log interpretation, Vol. 1. Principles, Houston, Texas, 112 pp.

Shutter, E., and R.R. Pemberton. 1978. Inflatable straddle packers and associated equipment for hydraulic fracturing and hydrologic testing, U.S. Geol. Survey, Water Resources Investigation, 55-78.

Smith, R.L., R.W. Harvey, J.H. Duff, and D.R. LeBlanc. 1987. Importance of close-interval vertical sampling in delineating chemical and microbial gradients in ground-water studies. In: B.J. Franks, ed., USGS Open-File Report 87-109, U.S. Geological Survey, Books and Open-File Reports Section, Federal Center, Box 254425, Denver, Colorado 80225, pp. B35-B38.

Sorek, S.P. 1988. Eulerian-Lagrangian method for solving transport in aquifers. In: Groundwater Flow and Quality Modelling, edited by E. Custodio, A. Gurgui, and J.P. Lobo Ferreira. NATO ASI Series C: Mathematical and Physical Sciences, Dordrecht, Holland:D. Reidel Publishing Co., Vol. 224, pp. 201-214.

Stallman, R.W. 1971. Aquifer-test design, observation and data analysis, Book 3, Chapter B1 of Techniques of Water-Resources Investigations of the United States Geological Survey.

Taylor, T.A., and J.A. Dey. 1985. Bibliography of borehole geophysics as applied to groundwater hydrology. Geological Survey Circular 926, #1985-576-049/20,029, U.S. Government Printing Office, Washington, DC.

Taylor, S.R., and K.W.F. Howard. 1987. A field study of scale-dependent dispersion in a sandy aquifer, Journal of Hydrology, 90, 11-17.

Taylor, S.R., and K.W.F. Howard. 1988. A field study of scale-dependent dispersion in a sandy aquifer-reply. Journal of Hydrology, 101, 363-365.

Taylor, K., F.J. Molz, and J. Hayworth. 1988. A single well electrical tracer test for the determination of hydraulic conductivity and porosity as a function of depth. Proceedings of the Second National Outdoor Action Conference, Las Vegas, NV. May 23-26.

Taylor, K. 1989. Review of borehole methods for characterizing the heterogeneity of aquifer hydraulic properties. Proceedings of the Conference on New Field Techniques for Quantifying the Physical and Chemical Properties of Heterogeneous Aquifers. Dallas, Texas.

Taylor, K., S.W. Wheatcraft, J. Hess, J.S. Hayworth, and F.J. Molz. 1989. Evaluation of methods for determining the vertical distribution of hydraulic conductivity. Ground Water, 27, in press.

Thompson, G. 1981. Some considerations for tracer tests in low permeability formations, Proc. of 3rd Invitational Well Testing Symposium, March 26-28, 1980. Lawrence Berkeley Laboratory Report 12076, Berkeley, CA, 67-73.

Tittman, J. 1956. Radiation Logging. In: Fundamentals of Logging, University of Kansas, Report #722.

Uffink, G.J.M. 1988. Modeling of solute transport with the random walk method. In: Groundwater Flow and Quality Modelling, edited by E. Custodio, A. Gurgui, and J.P. Lobo Ferreira. NATO ASI Series C: Mathematical and Physical Sciences, Dordrecht, Holland:D. Reidel Publishing Co., Vol. 224, pp. 247-265.

Urish, D.W. 1981. Electrical resistivity-hydraulic conductivity relationships in glacial outwash aquifers. Water Resources Research, 17, 401-408.

U.S. Bureau of Reclamation. 1977. Groundwater Manual. Water resources technical publication, # 480.

U.S. Congress, Office of Technology Assessment. 1988. Are We Cleaning Up? 10 Superfund Case Studies - Special Report. OTA-ITE-362 Washington, D.C.: U.S. Government Printing Office. 76 pp.

van der Heijde, P., Y. Bachmat, J. Bredehoeft, B. Andrews, D. Holtsz, and S. Sebastian. 1985. Groundwater Management: The Use of Numerical Models, 2nd ed. American Geophysical Union, Washington, D.C.

Wang, J.D., S.V. Cofer-Shabica, and J.C. Fatt. 1988. Finite element characteristic advection model. Journal of Hydraulic Engineering, ASCE, 114, 1098-1114.

Webster, D.S., J.F. Proctor and I.W. Marine. 1970. Two-well tracer test in fractured crystalline rock. Water Supply paper, 1544-I, 22 pp.

Weeks, E.P. 1964. Field methods for determining vertical permeability and aquifer anisotrophy. Professional paper 501-D, 193-198.

Weeks, E.P. 1969. Determining the ratio of horizontal to vertical permeability by aquifer-test analysis. Water Resources Research, 5, 196-214.

Weeks, E.P. 1977. Aquifer tests - The state of the art in hydrology. Proceedings of Invitational Well-Testing Symposium, October 19-21, Berkeley, California, Lawrence Berkeley Laboratory, LBL-7027, 14-26.

Wheeler, M.F., C. Dawson, and P.B. Bedient. 1987. Numerical modeling of subsurface contaminant transport with biodegradation kinetics. Proceedings of the NWWA/API Conference on Petroleum Hydrocarbons and Organic Chemicals in Ground Water: Prevention, Detection and Restoration, Dublin, Ohio: National Water Well Association, pp. 471-490.

Widdowson, M.A., F.J. Molz, and L.D. Benefield. 1988. A numerical transport model for oxygen- and nitrate-based respiration linked to substrate and nutrient availability in porous media. Water Resources Research, 24, 1553-1565.

Widdowson, M.A., F.J. Molz, and J.G. Melville. 1989. Development and application of a model for simulating microbial gorwth dynamics coupled to nutrient and oxygen transport in porous media. Proceedings, Solving Ground Water Problems with Models, Vol. 1, 28-51. National Water Well Assoc., Columbus, OH.

Witherspoon, P.A., T.D. Mueller, and R.W. Danovan. 1962. Evaluation of underground gas-storage conditions in aquifers through investigations of groundwater hydrology. Transactions American Institute of Mining Engineers, 225, 555-561.

Witherspoon, P.A., I. Javandel, S.P. Neuman, and R.A. Freeze. 1967. Interpretation of Aquifer Gas Storage Conditions from Water Pumping Tests. American Gas Association, Inc., New York, NY, 273 pp.

Witherspoon, P.A., and S.P. Neuman. 1967. Evaluating a slightly permeable caprock in aquifer gas storage, I. caprock of infinite thickness. Journal of Petroleum Technology, 19, 949-955.

Wolff, R.G. 1970. Relationship between horizontal strain near a well and reverse water level fluctuation. Water Resources Research, 6, 1721-1728.

Wyllie, M.R.J., A.R. Gregory, and G.H.F. Gardner. 1956. Elastic wave velocities in heterogeneous and porous media. Geophysics, 21, 41-70.

Wyllie, M.R.J., A.R. Gregory, and G.H.F. Gardner. 1958. An experimental investigation of factors affecting elastic wave velocities in porous media. Geophysics, 23(3).

Young, S.C., and W.R. Waldrop. 1989. An electromagnetic borehole flowmeter for measuring hydraulic conductivity variability. Proceedings of the Conference on New Field Techniques for Quantifying the Physical and Chemical Properties of Heterogeneous Aquifers. Dallas, Texas.

Zemanek, J., E.E. Glenn, L.J. Norton, and R.L. Caldwell. 1970. Formation evaluation by inspection with the borehole televiewer. Geophysics, 35, 254-269.

# APPENDIX I

# OVERVIEW AND EVALUATION OF METHODS FOR DETERMINING THE DISTRIBUTION OF HORIZONTAL HYDRAULIC CONDUCTIVITY IN THE VERTICAL DIMENSION

## AI-1 Introduction

This appendix will start with an overview of several techniques for measuring K(z), the vertical distribution of horizontal hydraulic conductivity. It is based largely on a paper by Taylor et al. (1989) published in Ground Water. Therefore, much of the credit for the overview portion of Appendix I should be given to the major authors (K. Taylor, S. Wheatcraft, J. Hess and J. Hayworth) of the Taylor et al. (1989) paper. This reference should be consulted for a more in-depth evaluation of those techniques not emphasized in this report.

As discussed in more detail in Chapter I of this report, application of the advection-based modeling approach requires measurement of hydraulic conductivity distributions. This has been done previously using forced-gradient tracer techniques (Molz et al., 1988, 1989b), but in the authors' opinion, tracer technology is expensive and time-consuming and can only be justified in granular aquifers for exceptional situations. Therefore, tracer methodology will not be discussed further. The remainder of this appendix will be devoted to tests designed to be performed in boreholes. We will assume that the holes are screened wells because most past applications have been in granular aquifers. Undisturbed cores are also difficult to obtain in such formations and are of limited use.

An important general consideration when making measurements of hydraulic conductivity is the volume over which the measurement is averaged. This volume spans the range of a few tenths of a liter for core studies to hundreds or thousands of cubic meters for hydraulic testing of aquifers. Depending on the intended use of the hydraulic conductivity data, the volume over which the measurement is made may be significant. When the measured volume is too large, important small scale features may be ignored. When the measured volume is small, there is a tendency to undersample, which can also result in missing significant features. The exact definition of large or small depends on the local variability of the hydraulic properties and the intended application of the data.

Another important consideration is that most natural formations have a strong horizontal to vertical anisotropy ratio with respect to hydraulic conductivity. Anisotropy ratios on the order of 10:1 or more are common [Freeze and Cherry, 1979]. In such situations, measurements of hydraulic conductivity made in one direction are of limited use when modeling fluid movement that is occurring in another direction. When hydraulic conductivity is treated as a scalar or a diagonalized matrix, which for convenience it usually is, it is important to be sure that the fluid movement that is being modeled is consistent with the directions in which the scalar values of hydraulic conductivity are measured.

All borehole methods sense the properties of the formation immediately surrounding the well. The distance into the formation away from the well for which the measurement is representative is referred to as the radius of investigation. Depending on the method, the radius of investigation can range from about 0.05 to 5 m. It is important to ensure that this zone is not disturbed significantly by the presence of the borehole or drilling effects such as drilling mud forced

into the formation. Morin et al. (1988b) discuss the effects of various drilling methods on the development of the disturbed zone.

## AI-2 Straddle Packer Tests

One of the most common methods for determination of the vertical distribution of average horizontal hydraulic conductivity is to perform hydraulic testing over short intervals of a borehole. The section of the borehole that is of interest is commonly isolated from the rest of the borehole by a straddle packer (Fig. AI-1). There are several variations of straddle packer tests. For example, one can pump at a constant rate from or into the packed-off section while measuring head, or inject at a constant head while measuring flow. A common method is to change the head suddenly in the packed-off section by adding or displacing a volume of water, and then monitoring the return to equilibrium by recording head vs time. This latter procedure may be called a multi-level slug test. In any case, these methods are accurate only if the packer is effective in hydraulically isolating the segment of the borehole. If channels exist around the well screen, it will not be possible to obtain a good seal with the packer. Channels may be present in the structure of a well screen or can be caused by the failure of the formation or backfill material to fill the annulus between the casing and the borehole wall. A similar problem may occur if a gravel pack is installed that has a greater hydraulic conductivity than the formation. In this case, fluid will preferentially flow along the well, bypassing the packer, instead of flowing radially toward, or outward, from the well as is desired. Ideally, the well is constructed with short screened intervals that are isolated from one another by grouting between the intervals. However, this type of construction is expensive.

If leakage around the packers exist, results obtained with a straddle packer test will indicate a hydraulic conductivity that is erroneously high. To test if this is occurring, it is desirable to monitor the head in the zones that are hydraulically isolated from the packed off interval. Typically, this would require a pressure transducer above and below the packed off interval. However, if the transmissivity of the segments of the well that are not packed-off is larger than the transmissivity of the segment of the well that is packed-off, leakage of fluid around the straddle packer will not cause a detectable change in head outside the packed off interval. To identify this problem, it is necessary to install a second set of packers (Fig. AI-1). The hydraulic head in the segments of the well that are between the two sets of packers will now be sensitive to leakage around the first set of packers that are isolating the segment that is being tested.

If the hydraulic head in the segments between the two sets of packers is influenced significantly by the hydraulic testing in the packed-off interval, it is then known that the straddle packer is not isolating the segment of the well and, hence, the results are not valid. If this situation occurs, it is usually not possible to correct and the straddle packer method cannot be used. Because of the need for four packers and three transducers, it can be a cumbersome arrangement to operate in the field. Nevertheless, based on comparisons with other test results, the straddle packer technique worked well at the Mobile site and, therefore, was selected for detailed study.

The straddle packer method can be used to measure hydraulic conductivity over well segments that range from centimeters to hundreds of meters in length. However, the data must be analyzed carefully for small test intervals because the flow can have significant vertical components (Dagan, 1978; Melville et al., 1989). The calculated hydraulic conductivity reflects that of the formation material within 25 to 35 well radii for a typical 2 in (5 cm) well (Braester and Thunvik, 1984).

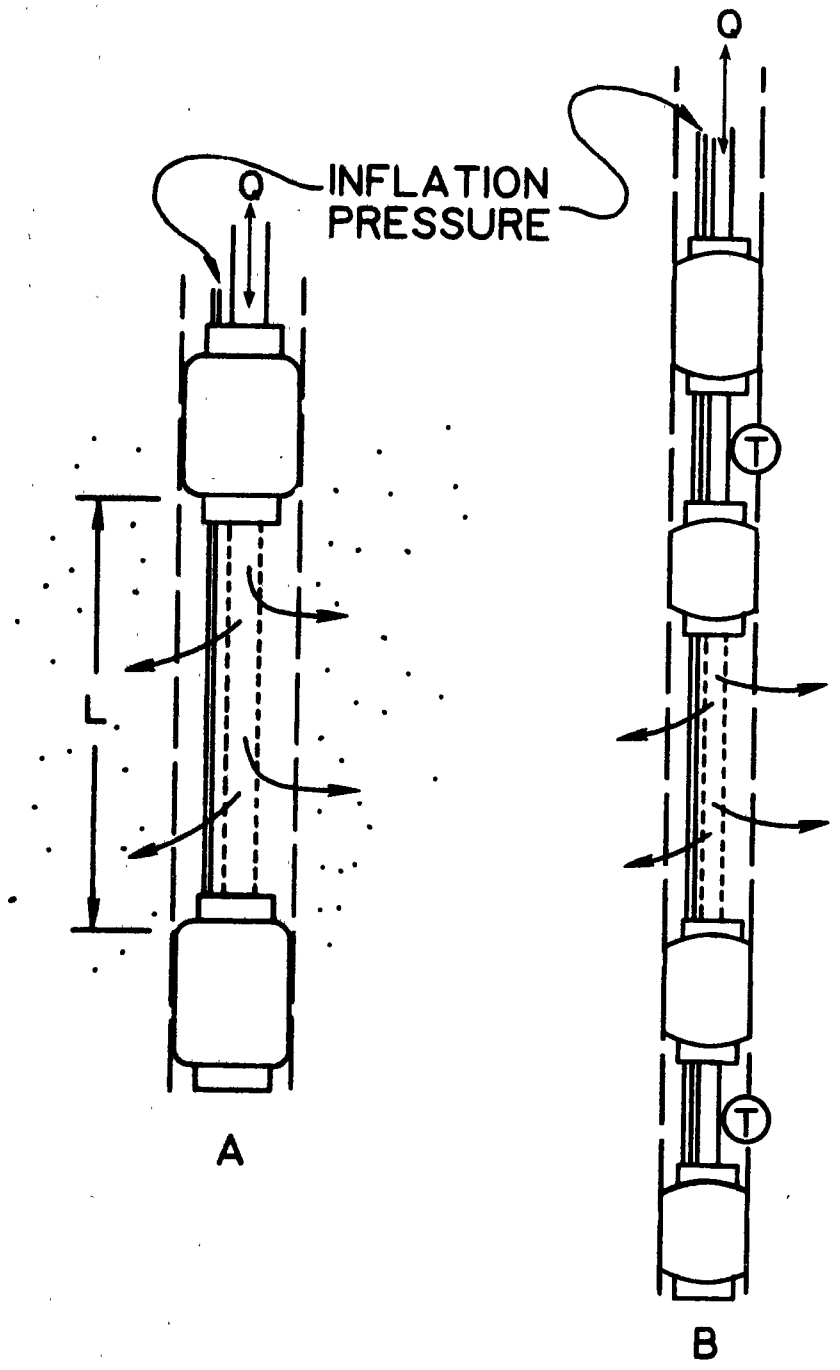


Figure AI-1. Details of an inflatable straddle packer design.

## AI-3 Particle Size Methods

In a material consisting of unconsolidated particles, the hydraulic conductivity is controlled, in part, by the size and distribution of the pores. In an effort to quantify this, Fair and Hatch (1933) and Masch and Denny (1966) have developed analytical approaches to estimate hydraulic conductivity from a description of the formation grains. The model proposed by Fair and Hatch requires that the distribution of grain sizes be known. The model proposed by Masch and Denny requires that the mean and standard deviation of the grain size be known.

Both of these methods suffer from several of the fundamental problems listed below.

1. Samples must be collected during drilling. This is not always done, hence for many if not most existing wells, these methods cannot be used.

2. To determine the grain-size statistics required for the analysis, the formation must be sieved. Obviously, features such as small scale layering, compaction, and sorting are destroyed by this process. If these features exist, which is usually the case, then the material which is evaluated will not be representative of the formation.

3. Sampling bias may be introduced by the sampling method. The sampling method may be unable to collect large material such as gravel or may not adequately sample fine particles.

4. The methods are limited to clean formations with sand-size particles (greater than 0.06 mm). Formations that have silt or clay-size material cannot be accurately analyzed with these methods.

Because of these problems, grain-size analysis methods have a restricted application and should be considered as approximate. They are unlikely to be suitable for characterization of aquifers for detailed contaminant transport modeling.

## AI-4 Empirical Relationships Between Electrical and Hydraulic Conductivity

The electrical conductivity of a porous medium is a measure of the ability of the medium to conduct electrical current. In natural formations, electrical conduction occurs along two paths. The first path is by ionic conduction through the pore fluid. This is controlled by the electrical conductivity of the pore fluid, the volume of the pore fluid, and the manner in which the pores are connected. The size of individual pores does not influence the electrical conductivity of the fluid. The second path for electrical conduction is along the surface of the formation matrix. This path is a function of the type and distribution of the matrix mineralogy, particularly clay minerals. In clay-free formations, with a constant pore fluid electrical conductivity, the formation electrical conductivity is usually found to be a function of porosity. Archie's rule is a frequently used relationship relating electrical conductivity and porosity in clay-free formations (Keller and Frischknecht, 1966).

The hydraulic conductivity of a porous medium is a function of the size of the pores and the manner in which they are connected. Two formations with the same pore fluid that have the same pore volume (porosity), but have different size pores, will have the same electrical conductivity and porosity, but different hydraulic conductivities. Hence, in general, there is not a unique relationship between electrical and hydraulic properties. The situation is further complicated when anisotropic effects are considered, because the axis of anisotropy for electrical and hydraulic

conductivity may not coincide. The presence of clays will further complicate any relationship between electrical and hydraulic conductivity.

Despite these problems, there exist numerous examples in the literature of empirical relationships that have been developed between electrical and hydraulic properties (Mazac et al., 1985; Kwader, 1985; Huntley, 1986; Urish, 1981). These relationships were developed in clay-free formations where electrical conduction by the matrix was not a significant factor. It is also necessary for the formation to have a relationship between porosity and hydraulic conductivity and to have a pore fluid of constant and known electrical conductivity. Depending on the formation and the methods used to measure the properties, both positive and negative correlations between the two properties have been observed. These empirical relationships are only applicable over limited areas of a specific formation. Such restrictions, and the need to measure the hydraulic conductivities at numerous locations first to define the relationship, severely limit the utility of this approach. However, if a relationship can be defined, the electrical measurements can be made rapidly and a large number of hydraulic conductivity determinations can be made with little additional effort.

The radius of investigation of this method is dependent on the process that is used to determine the electrical and hydraulic conductivities. The hydraulic conductivities are usually measured with hydraulic testing and, hence, typically have a radius of investigation of several meters. The radius of investigation of the electrical measurements is controlled by the instrumentation used to make the measurement and should be comparable to the radius of investigation of the hydraulic measurements.

### AI-5 Measurements Based on Natural Flow Through a Well

There are several techniques whereby one can obtain information about the hydraulic conductivity distribution surrounding a well by measuring the natural fluid velocity distribution through the well. These methods work best when the fluid velocity is horizontal. The basic idea of these methods is illustrated in Figure AI-2. They differ mainly in how the velocity measurement is made within the packed-off section of the well. There are heat-pulse devices for making the measurement (Melville et al., 1985) and various types of point-dilution approaches (Drost et al., 1968; McLinn and Palmer, 1989; Taylor et al., 1989). In this latter approach, a tracer is injected into the segment of the well of interest and must be kept well mixed. The tracer is removed from the segment by diffusion and by advection of the fluid moving horizontally through the well. Vertical fluid movement is blocked by packers. If the fluid velocity is high, the tracer concentration, which must be recorded, will decrease more rapidly than if the fluid velocity is low. Because the decay is exponential, the slope of the tracer decay curve on a semi-log plot is a function of the horizontal fluid velocity.

A new type of point-dilution apparatus based on an arrangement of dialysis cells is illustrated in Figure AI-3. Glass cylinders having selected types of semipermeable membranes as their ends are mounted along a positioning rod. Each cell, which has a flexible rubber seal above and below, is filled with water that is depleted in the isotope oxygen-18, i.e. the $O_{18}/O_{16}$ ratio is different for the water within the cell compared to the natural groundwater (Alternatively, some other tracer may be used.). The entire apparatus, which may contain something like 20 or more dialysis cells spaced at equal intervals along the rod, is then lowered into the well and positioned within the screen. Immediately after positioning, oxygen-18 begins to diffuse into each cell, and the rate of diffusion depends on the groundwater flow velocity in the immediate cell vicinity. By measuring $O_{18}/O_{16}$ ratios in each cell before and after a test period, the groundwater flow velocity as a function of cell position can be calculated. The calculation procedure is only moderately

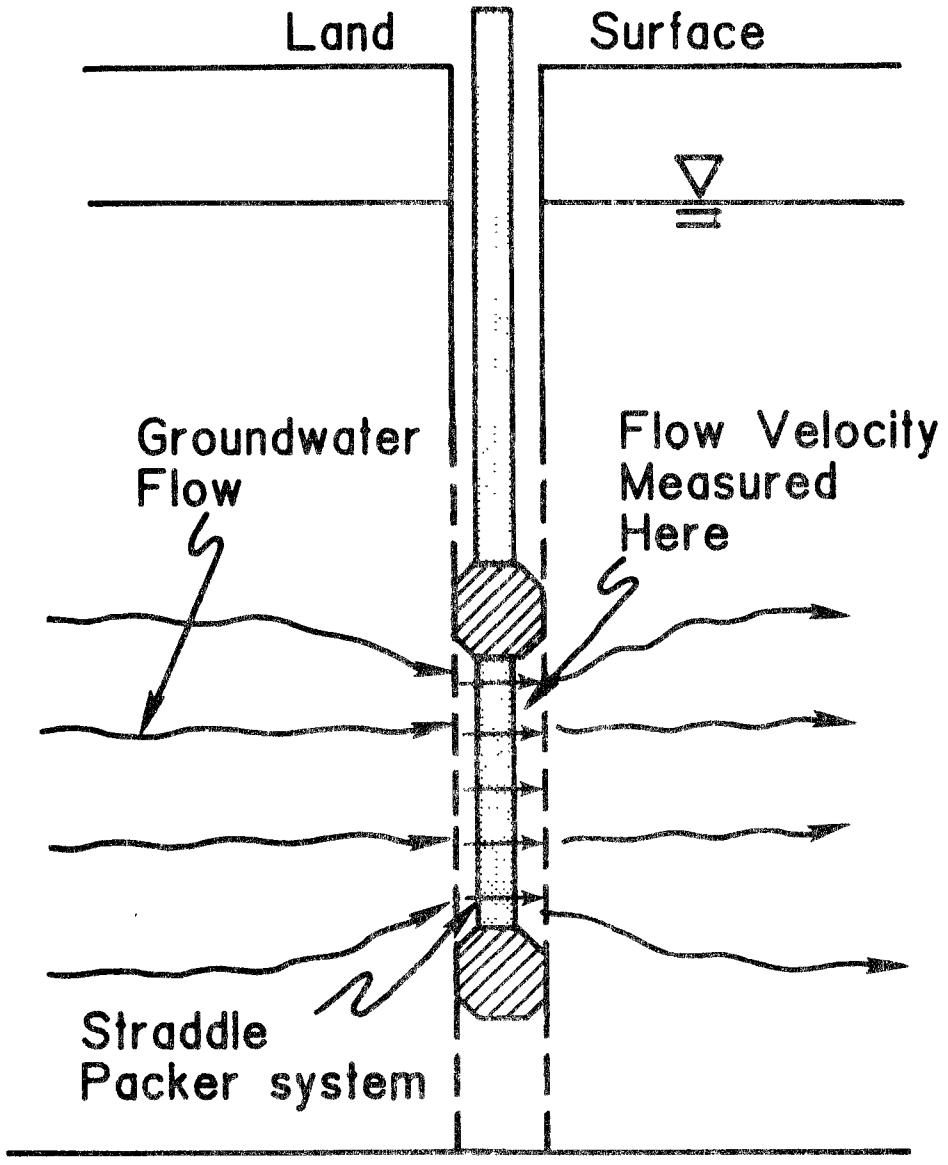


Figure AI-2. Schematic diagram illustrating a natural flow field in the vicinity of a well.

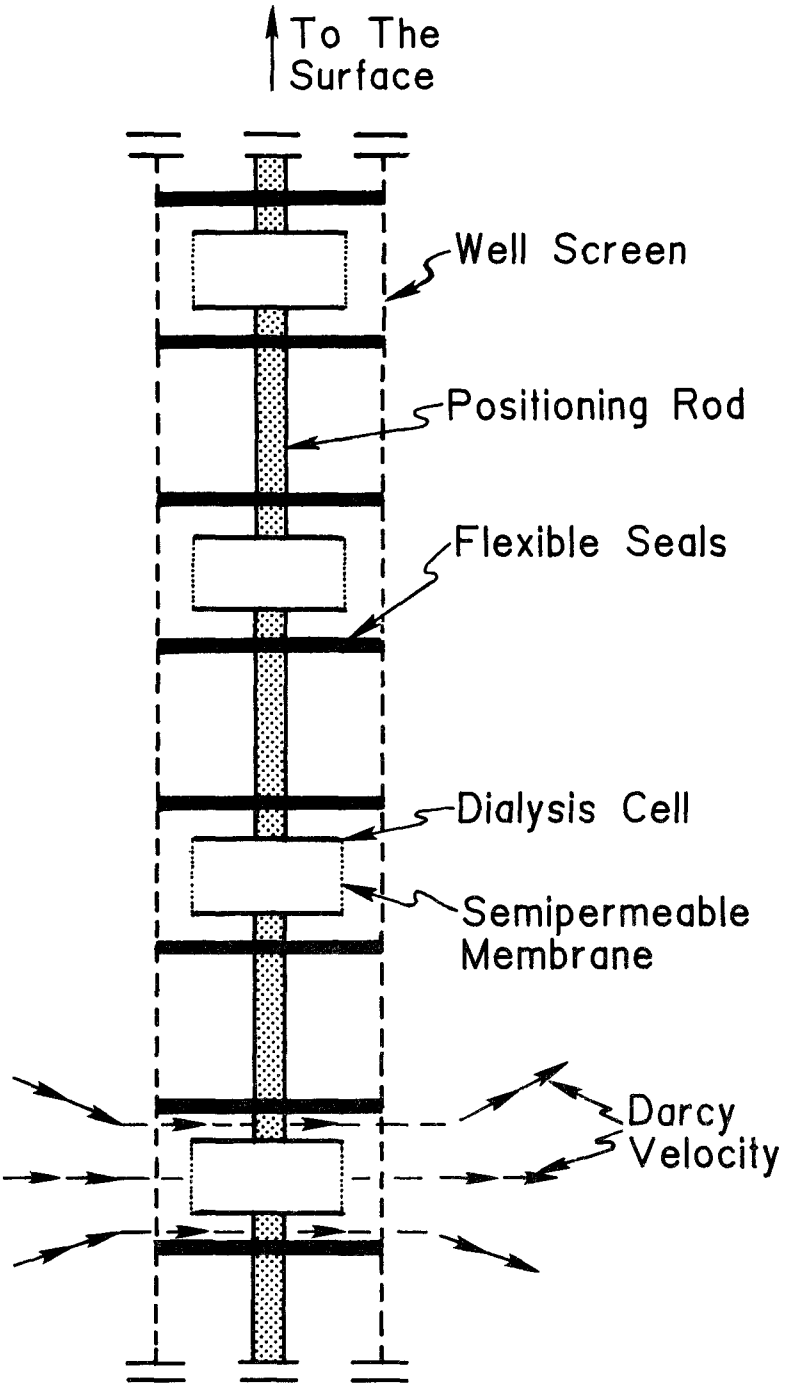


Figure AI-3. Geometry and instrumentation associated with the dialysis cell method for measurement of Darcy velocity.

involved and is described in Ronen et al., 1986, who developed and applied the technique in an unconfined aquifer. The method was also applied with apparent success at the Mobile site. Once the cells and cell holders/isolators are available in large quantities, many measurements can be made fairly efficiently.

As the title of this section implies, the natural flow methods result in a velocity measurement not a hydraulic conductivity measurement. If one assumes that the head gradient is predominantly in the horizontal direction, constant with depth and the formation has a constant porosity, then K(z) will be proportional to the fluid velocity distribution v(z). An approach that results in a more direct calculation of K is described by Taylor et al., 1989.

All of the natural flow methods are relatively difficult to apply and the resulting data difficult to interpret. Due to a variety of factors, a complex flow pattern develops around a well screen that is sensitive to near-hole disturbances. Some methods require that the packed-off section be filled with glass beads, and it is difficult or impossible to achieve the same bead packing in all the measurement sections.

### AI-6 Single Well Electrical Tracer (SWET) Test

In the single well electrical tracer (SWET) method (Taylor et al., 1988), salt water is injected under steady-state conditions into a well. While injection of the tracer continues, the radius of invasion of the tracer is determined with a borehole induction tool (Figure AI-4). By repeatedly measuring the depth of invasion at different times, the rate of invasion can be determined. The hydraulic head, which is a measure of the driving force required to inject the fluid, is also noted. The tracer will invade different intervals of the formation at different rates depending on the hydraulic properties of each interval of the formation. This information can be used to calculate a hydraulic conductivity log of the formation. Because multiple induction logs are run, the rate of invasion can be determined at several different radii of invasion. Hence, the hydraulic conductivity log of the formation can be calculated at several different radii of invasion. A porosity log can also be calculated by using a model of formation electrical conductivity that accounts for variations in matrix conductivity and porosity. The SWET test procedure was field-tested for the first time at the Mobile site during the summer of 1987.

The hydraulic conductivities calculated by the SWET test are representative of the formation for a radius around the well that is roughly equivalent to the radius of effect of the well. This radius is larger than the radius of invasion because the rate of invasion is not only influenced by the hydraulic properties of the portion of the formation that is invaded, but is also influenced by the portion of the formation into which the displaced native fluid is forced. At the Mobile site, this was on the order of 4 m. Because most wells have a disturbed zone around them, techniques that have a shallow radius of investigation will be inaccurate; the SWET test minimizes these problems. Another advantage of the SWET test is that the entire well is subjected to the same hydraulic head. Straddle packer tests pressurize only a portion of the well and will be in error if there is leakage around the packer.

A disadvantage of the SWET test is that the method requires the careful injection of a large volume of electrolyte. At some locations this may not be allowed. However, in the author's opinion further study of the SWET test is warranted.

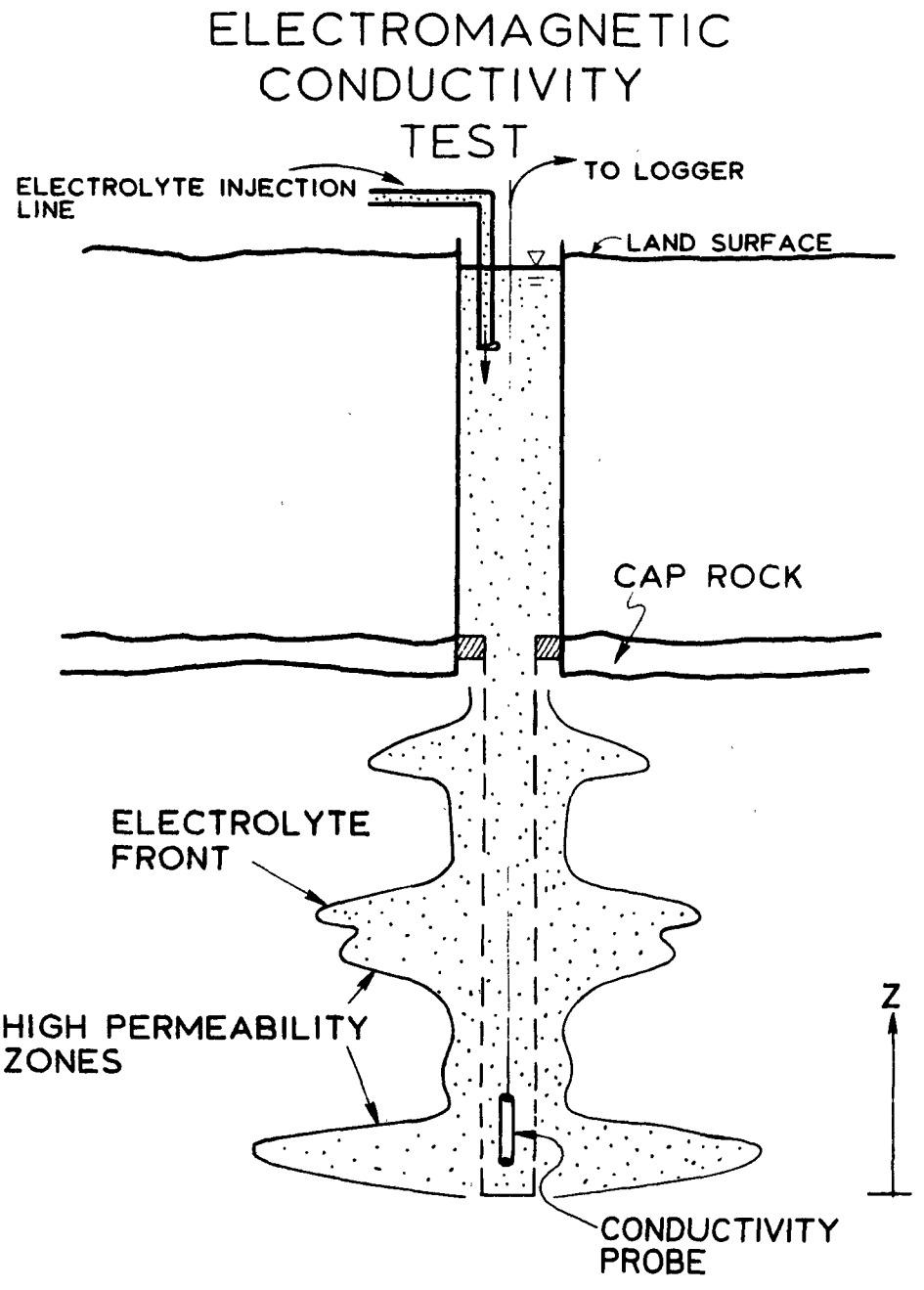


Figure AI-4. Apparatus and geometry associated with the SWET test.

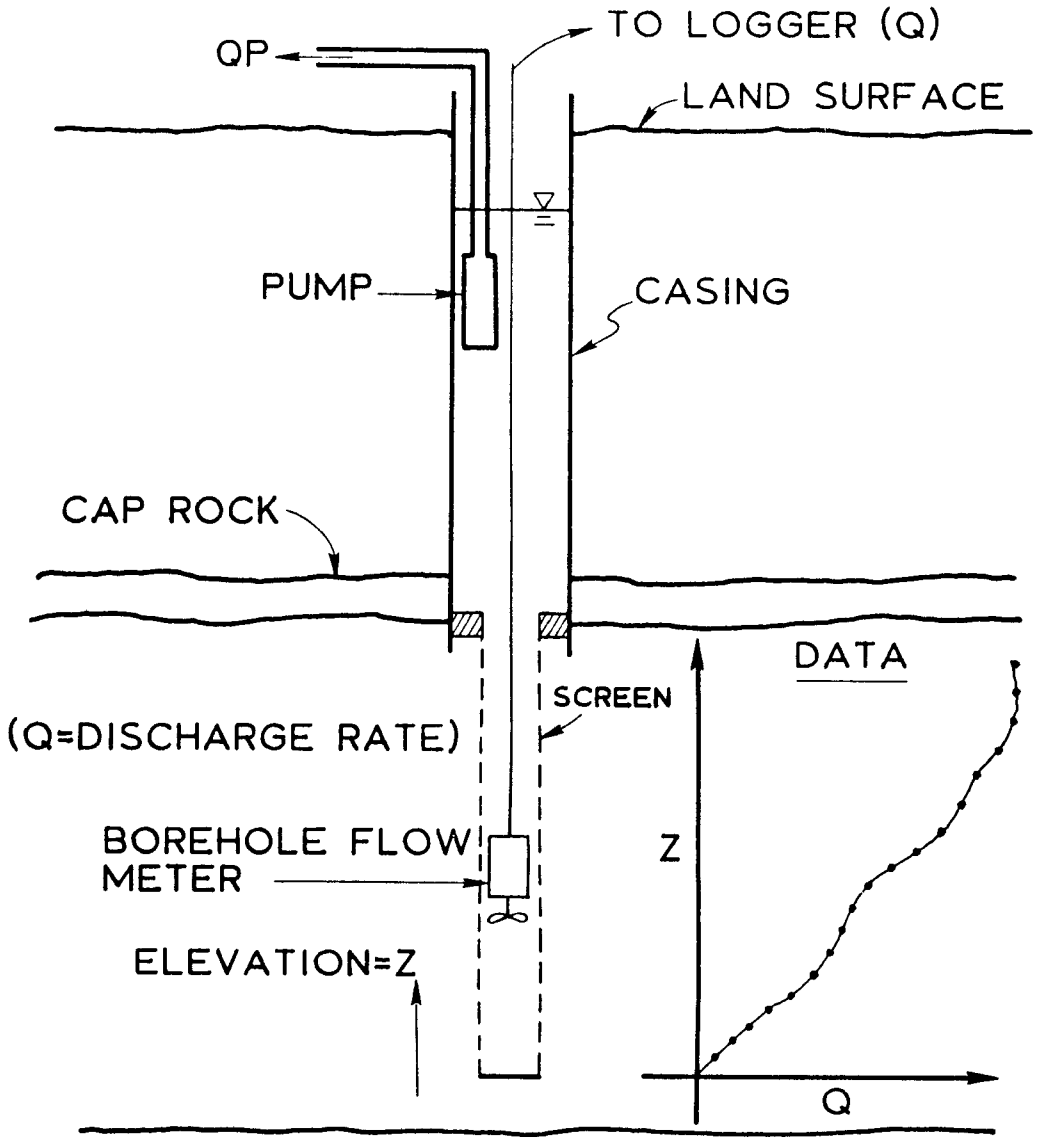


Figure AI-5. Apparatus and geometry associated with a borehole flowmeter test.

## AI-7 Borehole Flowmeter Tests

The idea behind this test is illustrated in Figure AI-5. A small pump is placed in a well and operated at a constant flow rate, Q. After something near steady-state behavior is obtained, the flowmeter, which measures vertical flow, is lowered to near the bottom of the well and a reading taken. The meter is then raised a few feet, another reading taken, raised another few feet - and so on. As illustrated in the lower portion of Figure AI-5, the result is a series of data points giving vertical discharge within the well screen as a function of position. Just above the top of the screen the meter reading should be equal to Q, the steady pumping rate that is measured independently on the surface.

The basic data analysis procedure is quite easy. One simply takes the difference between two successive meter readings, which yields the net flow entering the screen segment between the elevations where the readings were taken. This information may be analyzed in several ways to obtain a K(z) value. Along with the multi-level slug test, the flowmeter test was selected for detailed study at the Mobile site.

The flowmeter test suffers from the lack of ready availability of impeller meters designed for water well applications. Also, other types of promising technologies for flowmeter applications, such as heat-pulse (Hess and Paillet, 1989) and electromagnetic (Young and Waldrop, 1989) techniques, are not fully developed. However, it does appear that some types of heat-pulse (Hess and Paillet, 1989) and electromagnetic (Young and Waldrop, 1989) water well flow meters will be available in the very near future.

## AI-8 The Role of Geophysical Logging

The more traditional geophysical logging methods such as gamma logs, electric logs of various types, nuclear logs, etc., can be used to help identify the overall stratigraphy and geological setting of a site. They can also provide information of a general nature concerning hydraulic conductivity distributions. Applicable techniques are reviewed by Taylor (1989), and an approach to application and interpretation is provided by Paillet (1989) for groundwater investigations. Detailed descriptions of methodology may be found in Keys and MacCary (1971), and a bibliography of borehole geophysics as applied to groundwater hydrology has been developed by Taylor and Dey (1985).

# APPENDIX II

## ANALYSIS OF PARTIALLY PENETRATING SLUG TESTS CONSIDERING RADIAL AND VERTICAL FLOW AND ANISOTROPY

### AII-1 Introduction

The authors are aware of three approaches or techniques for analyzing partially penetrating slug tests that allow for both radial and vertical flow in an aquifer that is assumed to be locally homogeneous and isotropic for the purpose of test analysis (Boast and Kirkham, 1971; Bouwer and Rice, 1976; Dagan, 1978). None of these approaches are entirely satisfactory, especially for test sections that have relatively large diameter to length ratios (Melville et al., 1989; Widdowson et al., 1989). Therefore, there is a need for a more general approach that is reasonably accurate, free from limiting assumptions and easy to use. In addition, it is desirable to have a procedure that includes the effect of anisotropy in the test aquifer, since this physical phenomenon is so common.

The purpose of Appendix II is to present the details of a procedure for analyzing slug test data that was developed recently at Auburn University and which considers radial and vertical, anisotropic, axi-symmetric flow to or from the test interval. This procedure was used as one of the 3 analysis techniques in Chapter III dealing with multi-level slug tests. It is based on a finite element model called EFLOW that was licensed through the Electric Power Research Institute and modified at Auburn University for partially penetrating slug test analysis.

### AII-2 Mathematical Model Development

Diagrams of the two-dimensional geometry within which the mathematical model is applied are shown in Figure AII-1. Diagram (A) applies specifically to the case of a confined aquifer, while diagram (B) applies to the unconfined case. When analyzing a partially penetrating slug test in an unconfined aquifer one assumes that the water table stays at a constant elevation throughout the test (Dagan, 1978).

In a homogeneous, anisotropic aquifer, the equation governing transient, axi-symmetric flow is given by

$$S_s \frac{\partial h}{\partial t} = K\left(\frac{\partial^2 h}{\partial r^2} + \frac{1}{r}\frac{\partial h}{\partial r}\right) + K_z \frac{\partial^2 h}{\partial z^2} \qquad \text{(AII-1)}$$

where $S_s$ is specific storage, h is hydraulic head, t is time, r is radial distance, z is vertical distance, and K and $K_z$ are hydraulic conductivities in the radial and vertical directions respectively. The initial and boundary conditions for simulating a slug test within the geometry of Figure AII-1 are:

I.C.) $$h(r, z, 0) = h_o \qquad \text{(AII-2)}$$

B.C.) $$h(r_w, z, t) = h_o - y(t), \text{ for } (D-H) \le z \le (D-H+L) \qquad \text{(AII-3)}$$

$$\frac{\partial h}{\partial z}(r, 0, t) = \frac{\partial h}{\partial z}(r, D, t) = 0, \text{ for } r_w < r < R_e \qquad \text{(AII-4)}$$

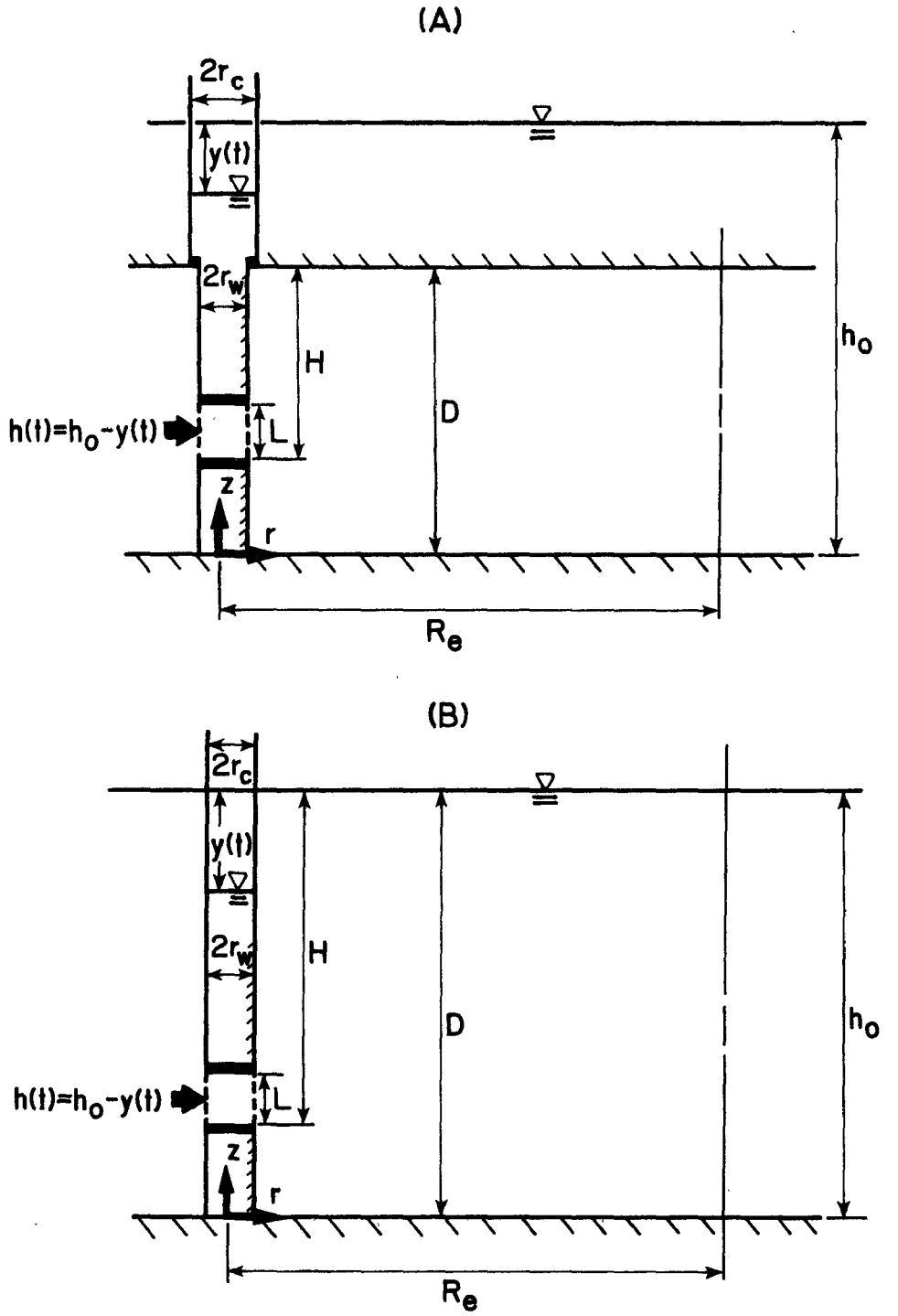


Figure AII-1. Diagram illustrating the geometry within which a partially penetrating slug test is analyzed. Diagram (A) is for the confined case and diagram (B) is for the unconfined case.

$$\frac{\partial h}{\partial r}(r_w, z, t) = 0, \text{ for } 0 \leq z < (D-H) \text{ and } (D-H+L) < z < D \qquad \text{(AII-5)}$$

$$h(R_e, z, t) = h_o, \text{ for } 0 \leq z \leq D \qquad \text{(AII-6)}$$

For simulating a partially penetrating slug test in an unconfined aquifer, all boundary and initial conditions remain the same except condition (AII-4) which is changed to

$$\frac{\partial h}{\partial z}(r, 0, t) = 0; \; h(r, D, t) = h_o, \text{ for } r_w < r < R_e \qquad \text{(AII-7)}$$

It is generally assumed in the analysis of slug tests that storage effects are small because of the small volumes of water that are involved (Dagan, 1978). Moreover, the analysis procedure being developed uses as input the slope of the straight-line portion of a plot of log (y(t)) vs t, and the slope will be constant only after transient storage effects have died out. Since the value of this slope will be independent of $S_s$, it is sufficient to solve the mathematical model given by

$$0 = K\left(\frac{\partial^2 h}{\partial r^2} + \frac{1}{r}\frac{\partial h}{\partial r}\right) + K_z \frac{\partial^2 h}{\partial z^2} \qquad \text{(AII-8)}$$

and subject to the boundary conditions presented previously. This is called a quasi-steady state model because even though time does not appear explicitly in equation (AII-8), it enters the overall problem because of the time-dependent boundary condition given by (AII-3).

## AII-3 Model Solution and Parametric Study

For a variety of specific geometries that are members of the class represented by Figure AII-1, the quasi-steady flow model was solved using EFLOW. A representative set of solutions was obtained for each anisotropy ratio of interest and for both confined and unconfined conditions. The dependence of each solution set on the various parameters, such as K, H, L, and $r_w$, was summarized using the dimensionless variable plots suggested by Dagan (1978). The possible dependence of the solution on $R_e$ was removed by choosing a sufficiently large value so that large perturbations about this value had a negligible effect on the numerical solution. The reasoning behind the parametric study is given below.

By conservation, the rate of change of the water level in the test well casing (Fig. AII-1) with respect to time, dy/dt, is related to the volumetric flow rate into the aquifer, Q, by

$$Q = -A_c(dy/dt) \qquad \text{(AII-9)}$$

where $A_c$ is the open cross-sectional area of the casing. $A_c$ will depend on the radius of the casing and the cross-sectional area of anything within the casing that is displacing water.

For the succession of steady states and a given aquifer geometry, the flow into the aquifer at any instant of time is proportional to y, that is, because of the steady-state flow distribution at each time instant, doubling y will double the flow into the aquifer. More precisely,

$$Q = \beta y \qquad \text{(AII-10)}$$

where $\beta$ is the constant of proportionality. Combining equations (AII-9) and (AII-10) and rearranging yields

$$(1/y)dy/dt = d(\ln(y))/dt = -\beta/A_c \qquad \text{(AII-11)}$$

Since the right-hand side of (AII-11) is constant, this shows that a plot of ln(y) versus t will yield a straight line.

Through the use of Darcy's law the flow into the aquifer may also be written as

$$Q = 2\pi r_w K \int_{D-H}^{D-H+L} \frac{\partial h}{\partial r}(r_w,z)dz \qquad \text{(AII-12)}$$

One may now define a dimensionless flow parameter, P, given by

$$P = \frac{Q}{2\pi KLy} = \frac{r_w}{Ly} \int_{D-H}^{D-H+L} \frac{\partial h}{\partial r}(r_w,z)dz \qquad \text{(AII-13)}$$

The parameter, P, depends only on the geometry of a particular slug test. From numerical solutions of equation (AII-8) for different geometries and using equation (AII-13), Figures AII-2 and AII-3 were generated for the confined and unconfined cases respectively, showing the dependence of P on H/L and $L/r_w$ for isotropic conditions. Dimensionless curves for $K/K_z$ of 1, 0.2 and 0.1 are also presented in tabular form in Tables AII-1 through AII-6. From this data it is possible for an individual to develop his own detailed figures, or interpolate directly from the tables.

Once the various figures or tables are developed for a given anisotropy ratio, they may be used in combination with a semi-log plot of slug test data to calculate the hydraulic conductivity in the radial direction. For example, assume one is working with Fig. AII-2. The procedure is to enter the figure with the appropriate values of H/L, and $L/r_w$, and obtain the corresponding number for P (call it $P_n$). Then using equation (AII-9) one notes that

$$Q = 2\pi KLyP_n = -A_c(dy/dt) \qquad \text{(AII-14)}$$

Employing the fact that $(1/y)dy/dt = d(\ln(y))/dt$ and solving equation (AII-14) for K yields

$$K = -\frac{A_c}{2\pi LP_n}\frac{d(\ln(y))}{dt} = -\frac{A_c}{2\pi LP_n}(2.3B) \qquad \text{(AII-15)}$$

where B is the slope of a semi-log plot (base 10 logs) of y vs. t, with the y vs. t values obtained from an actual slug test. B should always be considered a negative number regardless of whether y is above or below the reference level during the slug test.

## AII-4 Numerical Example

Multi-level slug test data from the Mobile site has been analyzed using the method presented here (Melville et al., 1989). Data from eleven levels in a test well are shown in Figure AII-4 along with straight line representations using linear regression. The following, which applies specifically to the data centered at z=11.2 ft in Figure AII-4, is an outline of the procedure by which the individual hydraulic conductivity values were calculated:

1. Obtain a measurement or estimate of aquifer anisotropy ratio.

   $K_r:K_z$ = 6.7:1. (Parr et al., 1983)

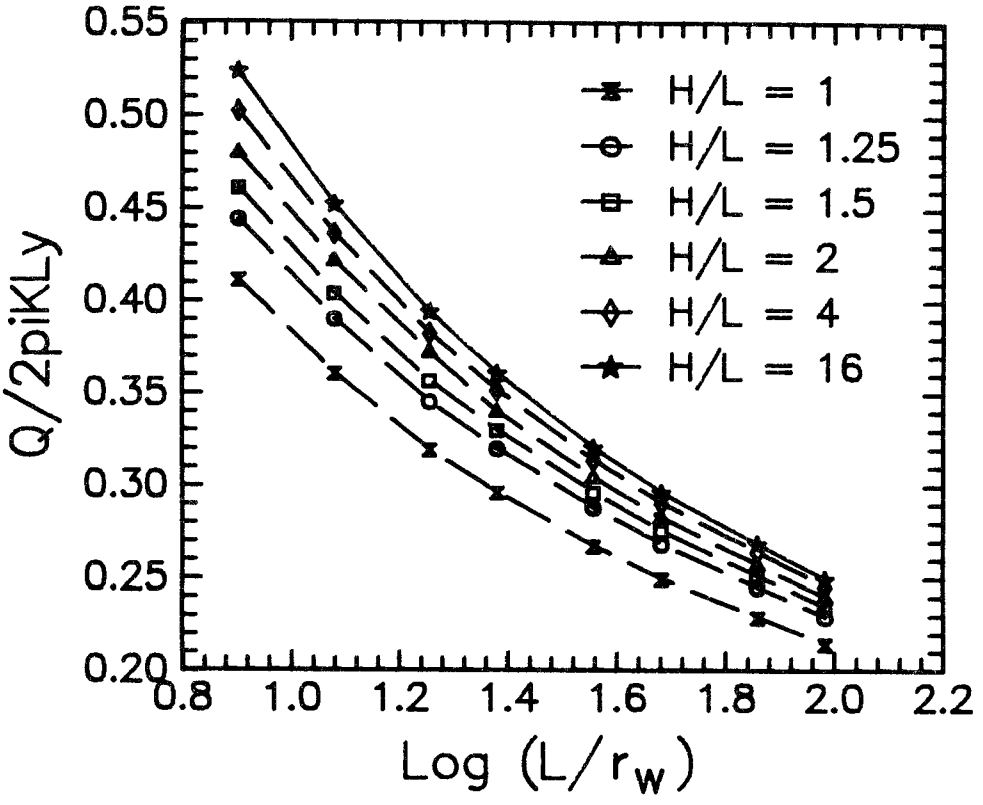


Figure AII-2. Plots of dimensionless discharge, P = Q/2πKLy, for the isotropic, confined aquifer problem as a function of $L/r_w$ and H/L.

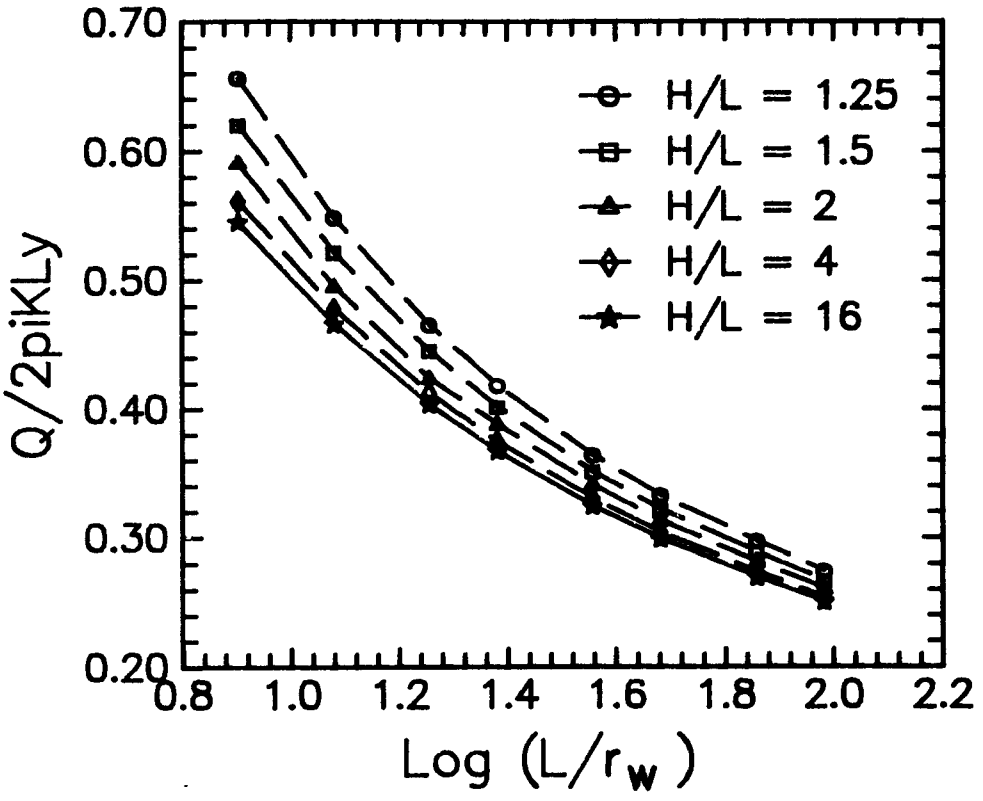


Figure AII-3. Plots of dimensionless discharge, $P = Q/2\pi KLy$, for the isotropic, unconfined aquifer problem as a function of $L/r_w$ and H/L.

Table AII-1. Dimensionless discharge, P, as a function of H/L and $L/r_w$ for the confined case with $K/K_z$ = 1.0.

| | $L/r_w$ = | 8 | 12 | 18 | 24 | 36 | 48 | 72 | 96 |
|---|---|---|---|---|---|---|---|---|---|
| H/L | | | | | | | | | |
| 1 | | .4117 | .3610 | .3196 | .2964 | .2675 | .2497 | .2293 | .2147 |
| 1.25 | | .4448 | .3905 | .3456 | .3202 | .2882 | .2685 | .2455 | .2295 |
| 1.5 | | .4617 | .4045 | .3570 | .3303 | .2965 | .2757 | .2515 | .2348 |
| 2 | | .4805 | .4219 | .3725 | .3402 | .3045 | .2828 | .2575 | .2400 |
| 4 | | .5029 | .4370 | .3829 | .3519 | .3140 | .2908 | .2645 | .2459 |
| 8 | | .5155 | .4463 | .3898 | .3576 | .3183 | .2945 | .2674 | .2484 |
| 16 | | .5243 | .4526 | .3945 | .3610 | .3207 | .2964 | .2687 | .2496 |

Table AII-2. Dimensionless discharge, P, as a function of H/L and $L/r_w$ for the confined case with $K/K_z$ = 0.2.

| $L/r_w$ = | 8 | 12 | 18 | 24 | 36 | 48 | 72 | 96 |
|---|---|---|---|---|---|---|---|---|
| H/L | | | | | | | | |
| 1 | .3205 | .2874 | .2597 | .2434 | .2230 | .2102 | .1955 | .1847 |
| 1.25 | .3428 | .3076 | .2778 | .2601 | .2377 | .2238 | .2078 | .1957 |
| 1.5 | .3533 | .3165 | .2852 | .2667 | .2434 | .2288 | .2124 | .1997 |
| 2 | .3660 | .3279 | .2950 | .2741 | .2487 | .2336 | .2168 | .2034 |
| 4 | .3771 | .3360 | .3013 | .2806 | .2551 | .2392 | .2215 | .2076 |
| 8 | .3837 | .3411 | .3053 | .2840 | .2577 | .2415 | .2232 | .2092 |
| 16 | .3878 | .3442 | .3076 | .2858 | .2589 | .2424 | .2237 | .2096 |

Table AII-3. Dimensionless discharge, P, as a function of H/L and $L/r_w$ for the confined case with $K/K_z = 0.1$.

| $L/r_w$ = | 8 | 12 | 18 | 24 | 36 | 48 | 72 | 96 |
|---|---|---|---|---|---|---|---|---|
| H/L | | | | | | | | |
| 1 | .2914 | .2634 | .2398 | .2256 | .2078 | .1966 | .1839 | .1742 |
| 1.25 | .3121 | .2821 | .2567 | .2410 | .2207 | .2085 | .1949 | .1840 |
| 1.5 | .3209 | .2894 | .2630 | .2457 | .2255 | .2129 | .1990 | .1876 |
| 2 | .3295 | .2979 | .2701 | .2523 | .2302 | .2172 | .2028 | .1909 |
| 4 | .3401 | .3055 | .2765 | .2588 | .2357 | .2219 | .2068 | .1945 |
| 8 | .3453 | .3096 | .2798 | .2615 | .2378 | .2238 | .2081 | .1958 |
| 16 | .3463 | .3105 | .2800 | .2616 | .2387 | .2245 | .2083 | .1960 |

Table AII-4. Dimensionless discharge, P, as a function of H/L and $L/r_w$ for the unconfined case with $K/K_z$ = 1.0.

| $L/r_w$ = | 8 | 12 | 18 | 24 | 36 | 48 | 72 | 96 |
|---|---|---|---|---|---|---|---|---|
| H/L | | | | | | | | |
| 1.25 | .6564 | .5487 | .4658 | .4186 | .3644 | .3329 | .2973 | .2742 |
| 1.5 | .6207 | .5219 | .4455 | .4018 | .3515 | .3220 | .2887 | .2667 |
| 2 | .5912 | .4955 | .4241 | .3883 | .3410 | .3132 | .2813 | .2605 |
| 4 | .5616 | .4783 | .4129 | .3748 | .3305 | .3042 | .2736 | .2540 |
| 8 | .5505 | .4701 | .4066 | .3697 | .3264 | .3007 | .2707 | .2516 |
| 16 | .5453 | .4662 | .4036 | .3672 | .3244 | .2990 | .2695 | .2505 |

Table AII-5. Dimensionless discharge, P, as a function of H/L and $L/r_w$ for the unconfined case with $K/K_z$ = 0.2.

| $L/r_w$ = | 8 | 12 | 18 | 24 | 36 | 48 | 72 | 96 |
|---|---|---|---|---|---|---|---|---|
| H/L | | | | | | | | |
| 1.25 | .4528 | .3944 | .3469 | .3187 | .2853 | .2651 | .2423 | .2258 |
| 1.5 | .4351 | .3802 | .3356 | .3090 | .2774 | .2582 | .2362 | .2206 |
| 2 | .4201 | .3683 | .3256 | .3018 | .2708 | .2524 | .2311 | .2162 |
| 4 | .4047 | .3564 | .3166 | .2926 | .2639 | .2463 | .2259 | .2117 |
| 8 | .3988 | .3517 | .3128 | .2894 | .2612 | .2441 | .2242 | .2102 |
| 16 | .3960 | .3494 | .3110 | .2879 | .2601 | .2431 | .2238 | .2097 |

Table AII-6. Dimensionless discharge, P, as a function of H/L and $L/r_w$ for the unconfined case with $K/K_z = 0.1$.

| $L/r_w$ = | 8 | 12 | 18 | 24 | 36 | 48 | 72 | 96 |
|---|---|---|---|---|---|---|---|---|
| H/L | | | | | | | | |
| 1.25 | .3960 | .3498 | .3114 | .2883 | .2605 | .2434 | .2237 | .2096 |
| 1.5 | .3824 | .3386 | .3023 | .2804 | .2539 | .2376 | .2185 | .2051 |
| 2 | .3724 | .3292 | .2946 | .2737 | .2482 | .2326 | .2141 | .2012 |
| 4 | .3587 | .3195 | .2867 | .2667 | .2424 | .2274 | .2098 | .1974 |
| 8 | .3540 | .3157 | .2835 | .2640 | .2402 | .2255 | .2085 | .1962 |
| 16 | .3517 | .3139 | .2821 | .2628 | .2393 | .2248 | .2083 | .1960 |

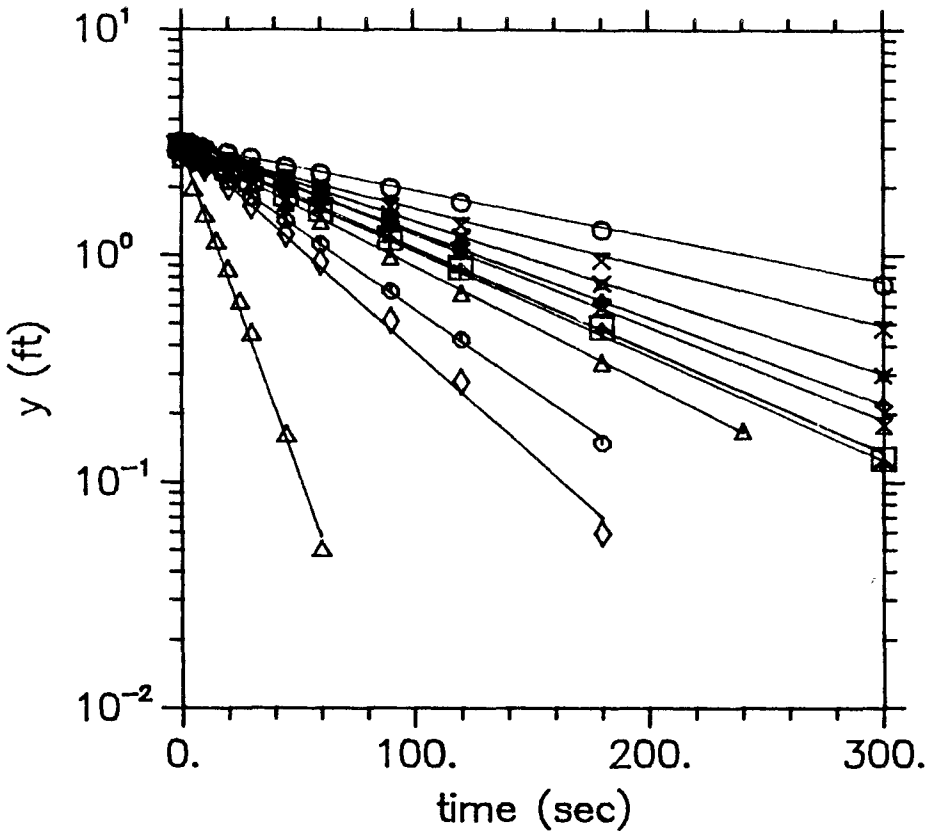


| | | |
|---|---|---|
| log(y)=−0.0280t+0.47 | Z=11.2 ft |
| log(y)=−0.0045t+0.49 | Z=17.2 ft |
| log(y)=−0.0020t+0.50 | Z=23.2 ft |
| log(y)=−0.0038t+0.49 | Z= 5.2 ft |
| log(y)=−0.0041t+0.51 | Z=29.2 ft |
| log(y)=−0.0034t+0.49 | Z=35.2 ft |
| log(y)=−0.0026t+0.47 | Z=41.2 ft |
| log(y)=−0.0046t+0.48 | Z=47.2 ft |
| log(y)=−0.0053t+0.48 | Z=53.2 ft |
| log(y)=−0.0071t+0.47 | Z=59.2 ft |
| log(y)=−0.0092t+0.50 | Z=65.2 ft |

Figure AII-4. Multilevel slug test data from well E6, $B=\log(y_1/y_2)/(t_2-t_1)$ = magnitude of the slope of the log(y(t)) response.

2. Calculate H/L and $\log(L/r_w)$ from experimental geometry.

   Aquifer thickness, D = 70 ft

   Packer separation length, L = 3.63 ft

   Distance (H) to closest boundary = 13.01 ft

   Radius of screen = 0.167 ft

   H/L= 3.58

   $L/r_w$ = 21.8; $\log_{10}(L/r_w)$ = 1.34

3. Select dimensionless discharge by interpolating between 1:5 and 1:10 anisotropy values in Tables AII-2 and AII-3.

   $P_n$ = 0.277

4. Determine slope of semi-log data plot (Figure AII-4).

   B = 0.028 $sec^{-1}$

5. Calculate hydraulic conductivity from equation (AII-15).

   With $A_c$ = 0.180 $ft^2$, K = 0.00183 ft/sec = 158 ft/day

# APPENDIX III

# THE PHYSICAL PROCESSES OF ADVECTION AND HYDRODYNAMIC DISPERSION

## AIII-1 Introduction

Most individuals have an intuitive understanding for what is meant by molecular diffusion. Molecular diffusion of a solute (such as salt) is caused by the random thermal motions (Brownian motion) of the water and solute molecules. In a solution undergoing perfect laminar flow, the Brownian motion will cause an irreversible mixing of the solute and water molecules, so that solute will slowly migrate from zones of higher concentrations to zones of lower concentrations. If allowed to proceed for a sufficiently long time, the solute and water molecules will ultimately become uniformly mixed. Molecular diffusion is a relatively simple process to visualize and represent mathematically, even though the motions involved on the molecular scale are very complex. This is because the scale of mixing due to Brownian motion is very small compared to the size of a container or flow regime within which the fluid/solute mixture is confined.

If one wanted to increase the rate of mixing in a fluid/solute mixture undergoing perfect laminar flow, one could, in principle, cause some type of mixing process in the mixture as it moved along. If this mixing process, whatever it might be, caused random mixing on a scale that was larger than the diffusion scale but still relatively small compared to the size of the container or flow regime, then to a good approximation it could be visualized and represented mathematically as a diffusion-like process with a "diffusion" coefficient having a larger value than the coefficient of molecular diffusion. In fact, given the appropriate conditions, the combined mixing process could be represented as a diffusion-like process with a diffusion coefficient given by $D_d + D_m$, where $D_d$ is the coefficient of molecular diffusion and $D_m$ could be called the coefficient of mechanical dispersion in recognition of whatever mechanical process caused the additional small-scale mixing.

When a solution moves in perfect laminar flow through a porous medium, the irregular and tortuous structure of the pore space and the velocity gradients below the Darcy scale cause a type of mixing on a scale of many pores that is small compared to the size of the problem of interest which is defined by the overall Darcy flow field. This pore-scale mixing is analogous to the hypothetical "mechanical dispersion" discussed in the previous paragraph and, in fact, is called mechanical dispersion. In a porous medium, diffusion and mechanical dispersion take place simultaneously, and the sum of the two processes at each point of the medium is called local hydrodynamic dispersion. These concepts will be elaborated further in the next section. Additional discussion may also be found in Bear (1979).

## AIII-2 The Mechanisms of Dispersion

In order to improve our capability of modeling solute transport, it is important to understand the major physical mechanisms which affect the evolution of an existing groundwater contamination plume or the future course of an anticipated plume. The catch-all name given to the spreading of a contaminant in groundwater is dispersion, a term which is familiar to almost everyone. However, as illustrated in Figure AIII-1, many different phenomena contribute to the dispersion process in aquifers. At the stage of development of the hypothetical tracer plume in Figure AIII-1, the extent of horizontal spreading is determined mainly by the elapsed travel time

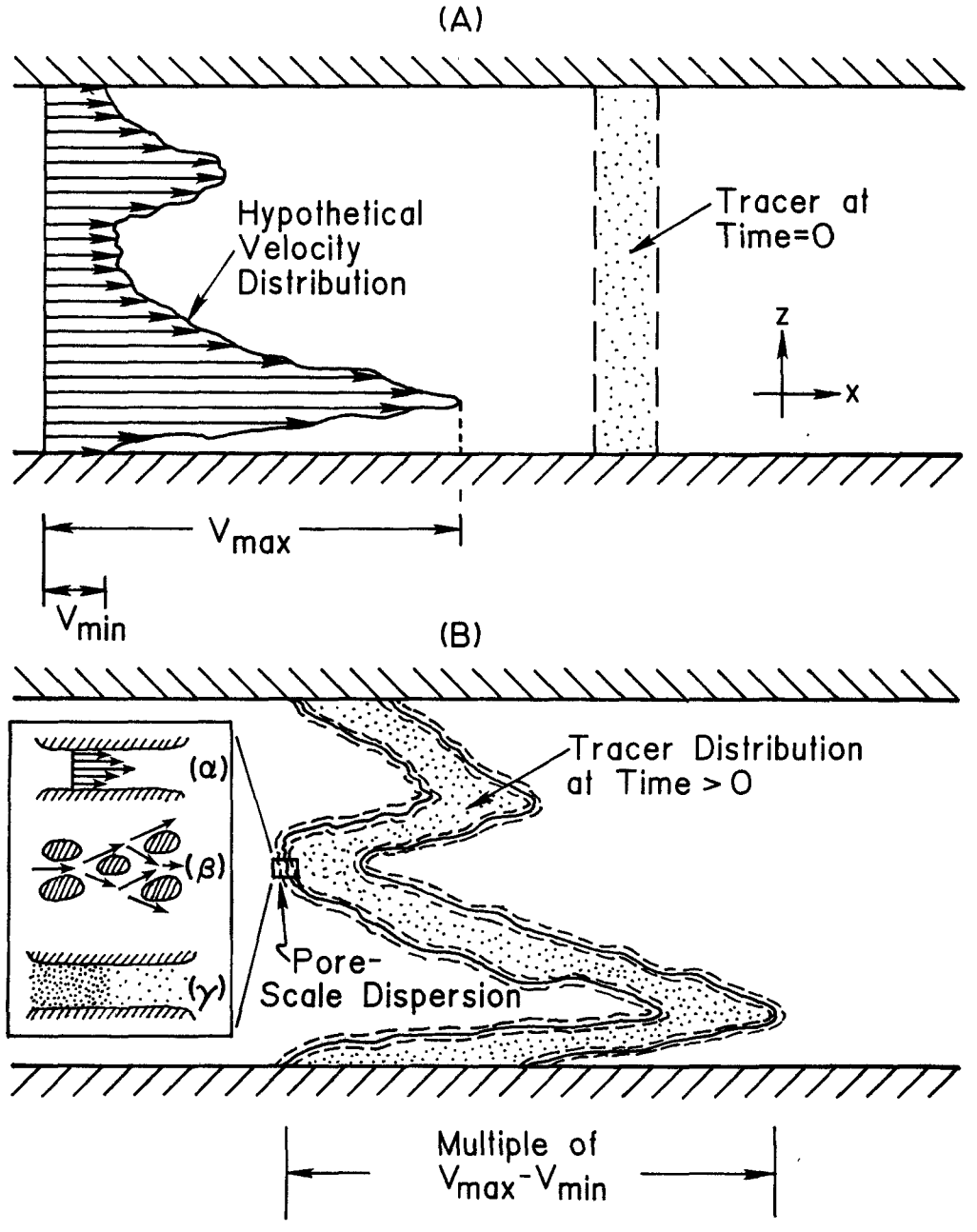


Figure AIII-1. Part (A) shows a hypothetical velocity distribution and an initial distribution of tracer while part (B) shows how the tracer would be dispersed by the moving groundwater at several different scales. Three common mechanisms of pore scale dispersion (velocity variation within a pore ($\alpha$); flow path tortuosity ($\beta$), and molecular diffusion due to concentration differences ($\gamma$)) are illustrated also.

and the difference between the maximum and minimum values of the horizontal advective velocities. These velocity variations result primarily from the larger-scale variations of hydraulic conductivity. This type of plume dispersion is due to the fact that the solute is simply carried along with the moving ground water at different fluid velocities depending on position. Such dispersion may be called advective dispersion or shear-flow dispersion. Considered alone, advective dispersion causes spreading but no irreversible mixing of the tracer with water. Much of this report is devoted to methods for measuring the hydraulic conductivity variations that give rise to advective dispersion.

To get irreversible mixing, one must, as a minimum, consider the dilution within the plume and along the plume boundaries that is caused by pore-scale mixing (the local hydrodynamic dispersion discussed previously) due in part to molecular diffusion, velocity variations within each pore, and the overall tortuosity of the flow path. Mixing due to local hydrodynamic dispersion is relatively large at plume boundaries where concentration variations with distance (gradients) are largest. It is evident, therefore, that advective dispersion and hydrodynamic dispersion act synergistically to increase irreversible mixing. Advective dispersion tends to increase the surface area of a plume where the concentration gradients are largest, and this promotes increased mixing due to local hydrodynamic dispersion.

Some researchers have suggested that random, diffusion-like mixing on a scale much larger than the pore-scale (the scale of local hydrodynamic dispersion) can be conceptualized. Depending on the scale being considered, names for these hypothesized mixing processes include field-scale dispersion, macro-dispersion and, when the mixing scale is across the entire vertical dimension of an aquifer, full-aquifer dispersion. These concepts are somewhat controversial at the present time, and the present authors are of the opinion that their practical use in field hydrology is limited. Out viewpoint is presented in Chapter I, and further discussion may be found in Güven and Molz (1988).

APPENDIX IV

TABLE OF CONTENTS FOR THE PROCEEDINGS ENTITLED "NEW FIELD TECHNIQUES FOR QUANTIFYING THE PHYSICAL AND CHEMICAL PROPERTIES OF HETEROGENEOUS AQUIFERS"*

## Session 1
## Geology-Intensive Approaches to Property Measurements



## Session 2
## Property Measurement Using Borehole Geophysics and Log Analysis

**A Direct Integral Method for the Analysis of Borehole Fluid Conductivity Logs to Determine Fracture Inflow Parameters** by Chin-Fu Tsang and Frank V. Hale (Earth Sciences Division, Lawrence Berkeley Laboratory, 1 Cyclotron Road, University of California, Berkeley, CA 94720).

**On the Field Determination of Effective Porosity** by Iraj Javandel (Earth Sciences Division, Lawrence Berkeley Laboratory, 1 Cyclotron Road, Berkeley, CA 94720).

## Session 3
## Measurement of Vertically-Averaged Aquifer Properties

**Application of Interference Testing to Characterize Three Coal Seam Aquifers Near Birmingham, Alabama** by Robert A. Koenig (In-Situ, Inc., P.O. Box I, Laramie, WY 82070-0920).

**Analysis of Early-Time Oscillatory Aquifer Response** by Daniel A. Giffin and David S. Ward (GeoTrans, Inc., 250 Exchange Place, Suite A, Herndon, VA 22070).

**Delineating Geometry of Unconfined Aquifer Heterogeneities with Microgravity Surveys During Aquifer Testing** by Eileen P. Poeter (Department of Geological Engineering, Colorado School of Mines, Golden, CO 80401).

**A New and Comprehensive Method for the Characterization of Horizontally Anisotropic Aquifers Through the Analysis of Data from Pumped Wells** by Garry Grimestad (Hydralogic, P.O. Box 4722, Missoula, MT 59806).

**Conductive Slug Tracing as a Single-Well Test Technique for Heterogeneous and Fractured Formations** by Andrew Michalski (TRC Environmental Consultants, Inc., 18 Worlds Fair Drive, Somerset, NJ 08873).

## Session 4
## Tracer Techniques and Flow Regime Characterization

**Ground Water Flow Regime Characterization, Columbia Plateau Physiographic Province, Arlington, North Central Oregon** by Ching-Pi Wang (Washington Department of Ecology, 4350 150th Avenue NE, Redmond, WA 98052-5301) and Stephen M. Testa (Engineering Enterprises, Inc., 21818 South Wilmington Avenue, Long Beach, CA 90810).

**A Downhole Column Technique for Field Measurement of Transport Parameters** by Douglas R. Champ and Grigory L. Moltyaner (Chalk River Nuclear Laboratories, Chalk River, Ontario, Canada KOJ 1JO).

**Application of Data-Logger/Pressure-Transmitter/Conductivity-Probe Instrumentation in Long-Term Salt-Tracer Studies in a Fractured, Saturated Geologic Medium** by J.A. Paschis, R.A. Koenig and J.E. Benedik (In-Situ, Inc., P.O. Box I, Laramie, WY 82070).

**Quantifying the Nature and Degree of Heterogeneity Using Concepts of Non-Linear Dynamics and Fractals** by Stephen W. Wheatcraft, Scott W. Tyler and Michael J. Nicholl (Desert Research Institute, University of Nevada, P.O. Box 60220, Reno, NV 89506).

## Session 5
## Regulatory Problems and Multi-Level Measurement of Aquifer Properties

**Hydrochemical Monitoring and Hydrogeologic Characterization: Conflict and Resolution** by Ronald Schalla, Stuart P. Luttrell and Ronald M. Smith (Site Characterization and Assessment Section, Geoscience Department, Battelle Pacific Northwest Labs, P.O. Box 999, Richland, WA 99352).

**Ground-Water Monitoring at Hazardous Waste Facilities: Regulatory Changes that Consider Site-Specific Subsurface Characteristics** by Joseph M. Abe, James R. Brown and Vernon B. Myers (Waste Management Division, Office of Solid Waste, U.S. Environmental Protection Agency, 401 M Street, SW, Washington, DC 20460).

**Scale of Measurements, REV and Heterogeneities** by Arthur W. Warrick and T-C. Jim Yeh (The University of Arizona, Department of Soil and Water Science, 429 Shantz Building #38, Tucson, AZ 85721).

**Characterization of the Hydrogeologic Properties of Aquifers: The Next Step** by Fred J. Molz, Oktay Güven and Joel G. Melville (Civil Engineering Department, 238 Harbert Engineering Center, Auburn University, AL 36849-5337).

**Application of the Borehole Flowmeter Method to Measure The Spatially Variable Hydraulic Conductivity at the Macro-Dispersion Experiment (MADE) Site** by Kenneth R. Rehfeldt (Illinois State Water Survey, Ground-Water Section, 2204 Griffith Drive, Champaign, IL 61820-7495).

**Characterizing Flow Paths and Permeability Distribution in Fractured Rock Aquifers Using a Sensitive, Thermal Borehole Flowmeter** by Alfred E. Hess and Frederick L. Paillet (U.S. Department of Interior, U.S. Geological Survey, Box 25046, MS 403, Denver Federal Center, Denver, CO 80225).

**An Electromagnetic Borehole Flowmeter for Measuring Hydraulic Conductivity Variability** by Steven C. Young and William R. Waldrop (TVA Engineering Laboratory, P.O. Drawer E, Norris, TN 37828).

**Laboratory Testing and Comparison of Specific-Conductance and Electrical-Resistivity Borehole-Dilution Devices** by Eugene L. McLinn (Residuals Management Technology, Inc., Suite 124, 1406 East Washington Avenue, Madison, WI 53705) and Carl D. Palmer (Department of Environmental Science and Engineering, Oregon Graduate Center, 19600 von Neumann Drive, Beaverton, OR 97006-1999).

**Use of a Borehole Flowmeter to Determine Spatial Heterogeneity of Hydraulic Conductivity and Macrodispersion in a Sand and Gravel Aquifer Cape Cod, Massachusetts** by Kathryn M. Hess (U.S. Geological Survey, WRD, 28 Lord Road, Suite 200, Marlboro, MA 01752).

**Aquifer Parameter Estimation with the Aid of Radioactive Tracers** by Grigory S. Moltyaner (Atomic Energy of Canada Limited, Environmental Research Branch, Chalk River Nuclear Laboratories, Chalk River, Ontario, Canada KOJ 1JO).

**Measuring Hydraulic Conductivity in a Steep Appalachian Watershed** by Gary C. Pasquarell and Douglas G. Boyer (USDA/Agricultural Research Service, Appalachian Soil and Water Conservation Research Laboratory, Box 867, Airport Road, Beckley, WVA 25802-0867).

**Patterns of Groundwater Movement in Water Wells East Salt River Valley, Arizona** by Errol L. Montgomery, Andrew A. Messer and Ronald H. DeWitt (Errol L. Montgomery & Associates, Inc., 1075 East Fort Lowell Road, Suite B, Tucson, AZ 85719).

**A Direct-Reading Borehole Flowmeter** by William B. Kerfoot and Lawrence Kiely (K-V Associates, Inc., 281 Main Street, Falmouth, MA 02540).

**An Analytic Solution Relating Wellbore and Formation Velocities with Application to Tracer Dilution Problem** by Pascal Bidaux (CNRS Laboratoire d'Hydrogeologie, Universite des Sciences et Techniques, Pl. E. Bataillon, 34060 Montpellier Cedex, France) and Chin-Fu Tsang (Lawrence Berkeley Laboratory, University of California, Berkeley, CA 94720).

**An Advanced Technology for the In-Situ Measurements of Heterogeneous Aquifers** by Julie M. Smythe and Philip B. Bedient (Rice University, Department of Environmental Science and Engineering, P.O. Box 1892, Houston, TX 77251), Rick A. Klopp (Terra Technologies, Houston, TX 77099) and Chen Y. Chiang (Shell Development Company, Houston, TX 77001).

**The Hydrogeological Properties of the Gulf Coast Upper Chicot Aquifer Near Port Arthur, Texas** by Andreas Haug, R. Harold Petrini, and Gerald E. Grisak (Intera Technologies, Inc., Suite 300, 6850 Austin Center Blvd., Austin, TX 78731) and Kim Klahsen (Chemical Waste Management, Inc., P. O. Box 2563, Port Arthur, TX 77640).

**A Three-Dimensional Lagrangian Numerical Model of Two-Well Tracer Tests in Confined Aquifers** by Oktay Güven, Fred J. Molz and Joel G. Melville (Department of Civil Engineering, Harbert Engineering Center, Auburn University, AL 36849-5337).

**Free Gasoline Thickness in Monitoring Wells Related to Ground Water Elevation Change** by William T. Hunt, Jeffrey W. Wiegand and John D. Trompeter (Alton Geosciences, Inc., 16510 Aston Street, Irvine, CA 92714).

**Multilevel Slug Tests: Performance and Analysis** by Joel G. Melville, Fred J. Molz and Oktay Güven (Department of Civil Engineering, Harbert Engineering Center Auburn University, AL 36849-5337).

**Quantitation of Aviation Fuel Contaminant Levels in Sandy Subsurface Core Material by Gas Chromatography** by Steve A. Vandegrift (NSI Technology Services Corporation, Ada, OK) and Don H. Kampbell, (EPA Robert S. Kerr Environmental Laboratory, P.O. Box 1198, Ada, OK 74820).

**Cone Penetrometer Tests and Hydropunch[tm] Sampling: An Alternative to Monitoring Wells for Plume Definition** by Mark Smolley and Janet C. Kappmeyer (EMCON Associates, 1921 Ringwood Avenue, San Jose, CA 95131).

U. S. GOVERNMENT PRINTING OFFICE 1990/748-159/00381

## Session 6
## Measurement of Chemical and Biochemical Aquifer Properties

**In-Situ Methods for Evaluating Retardation Factors and Biotransformation Parameters** by Robert W. Gillham (Waterloo Centre for Groundwater Research, University of Waterloo, Waterloo, Ontario, Canada, N2L 3G1).

**Subsurface Microbiota as Monitors of Contaminant Migration and Mitigation** by David C. White (Institute for Applied Microbiology, University of Tennessee, 10515 Research Drive, Suite 300, Knoxville, TN 37932-2567) and John T. Wilson (R.S. Kerr Environmental Research Laboratory, USEPA, P.O. Box 1198, Ada, OK 74820).

**A Multi-Layer Sampler for Groundwater: New Field Technique to Study Chemical Processes and Transport Phenomena in Aquifers** by Daniel Ronen and Mordeckai Magaritz (Isotope Department, The Weizmann Institute of Science, 76 100, Rehovot, Israel).

**Measurement of Volatile and Aqueous Geochemical Properties in Shallow and Deep Groundwaters: Two Innovative Sampling Devices** by Barbara Sherwood Lollar and Shaun K. Frape, et al (Department of Earth Sciences, University of Waterloo, Waterloo, Ontario, Canada, N2L 3G1).

**Leaky Microcosms are Representative of BTX Biodegradation in the Borden Sand Aquifer** by J.F. Barker, G.C. Patrick, D.J. Berwanger and E.A. Sudicky (Waterloo Centre for Groundwater Research, University of Waterloo, Waterloo, Ontario, Canada N2L 3G1).

**Geochemical Evaluation of Reduced Subsurface Environments** by Dhanpat Rai and John M. Zachara (Battelle Pacific Northwest Laboratories, P.O. Box 999, Richland, WA 99352).

## Session 7
## Measurement in the Unsaturated Zone

**Vertical Profiles and Near Surface Traps for Field Measurement of Volatile Pollution in the Subsurface Environment** by David W. Ostendorf and Don H. Kampbell (Robert S. Kerr Environmental Research Laboratory, USEPA, P.O. Box 1198, Ada, OK 74820).

**Evaluation of Ceramic Vacuum Soil Solution Samplers in Sandy Soils Overlying Aquifers** by Nathaniel O. Bailey, Tammo S. Steenhuis and Jean Y. Parlange (Cornell University, Department of Agricultural and Biological Engineering, Riley-Robb #30, Cornell, Ithaca, NY 14853).

**Methods of Estimating Hydraulic and Transport Parameters for the Unsaturated Zone** by Jack C. Parker and Srikanta Mishra (Center for Environmental and Hazardous Materials Studies, Virginia Polytechnic Institute and State University, 332 Smythe Hall, Blacksburg, VA 24061).

---

* For a copy of the proceedings contact:
Water Resources Research Institute
202 Hargis Hall
Auburn University, AL 36849